NIKHEF

NATIONAL INSTITUTE FOR NUCLEAR PHYSICS AND HIGH-ENERGY PHYSICS

ANNUAL REPORT

1998

Kruislaan 409, 1098 SJ Amsterdam
P.O. Box 41882, 1009 DB Amsterdam

Colofon

Publication edited for NIKHEF:

Address:	Postbus 41882, 1009 DB Amsterdam Kruislaan 409, 1098 SJ Amsterdam
Phone:	+31 20 592.2000
Fax:	+31 20 592.5155
E-mail:	directie@nikhef.nl
Editors:	Hans de Vries, Bert Koene
Layout & art-work:	Kees Huyser
Organisation:	Marieke Wielenga
Printed version by:	Ponsen & Looijen BV, Wageningen
Cover Photograph:	Installation of the Atomic Beam Source (Photo: NIKHEF)

The National Institute for Nuclear Physics and High-Energy Physics (NIKHEF) is a joint venture of the Stichting voor Fundamenteel Onderzoek der Materie (FOM), the Universiteit van Amsterdam (UVA), the Katholieke Universiteit Nijmegen (KUN), the Vrije Universiteit Amsterdam (VUA) and the Universiteit Utrecht (UU). The NIKHEF laboratory with its accelerator facility (AmPS) is located at the Science Research Centre Watergraafsmeer (WCW) in Amsterdam.

The activities in experimental subatomic physics are coordinated and supported by NIKHEF with locations at Amsterdam, Nijmegen and Utrecht. The scientific programme is carried out by FOM, UVA, KUN, VUA and UU staff. Experiments are done at the European accelerator centre CERN in Geneva, where NIKHEF participates in two LEP experiments (L3 and DELPHI), in a neutrino experiment (CHORUS) and in a SPS heavy ion experiment (NA57). NIKHEF recently joined the Tevatron experiment D0 at Fermilab, Chicago. At DESY in Hamburg NIKHEF participates in the ZEUS, HERMES and HERA-B experiments. Research and development activities are in progress for the future experiments ATLAS, ALICE and LHCb with the Large Hadron Collider (LHC) at CERN.

The subatomic physics programme with intermediate energy electromagnetic probes is carried out with the electron accelerator, delivering a continuous high intensity beam with the Amsterdam Pulse Stretcher and Storage ring (AmPS). The scientific programme with AmPS is carried out in collaboration with several visiting teams from abroad. Research is concentrated on experiments with (polarised) internal targets.

NIKHEF is closely cooperating with the University of Twente. Training and education of students are vital elements in the research climate of the laboratory.

Contents

Preface

The sudden death of Jankarel Gevers, the chairman of the NIKHEF Board, on August 5th came as a great shock to our community. We remember him as a powerful governor and an enthusiastic supporter of NIKHEF.

The past year was the last in which our electron linear accelerator MEA and storage ring AmPS were operational. Already at the time of construction of AmPS it had been decided by FOM that the facility was to deliver its last electrons in the year 1998. Notwithstanding attempts 'to make the month of December last longer', inspired by our Scientific Advisory Committee which recommended a two months extension into 1999, the machine was 'switched off' from its standby position on December 26th at 7 o'clock in the morning by a short-circuit in a 10 kV power line.

Although the damage done to equipment turned out to be relatively modest, it was decided to not restart operation for physics. The main reason was to not delay any further the dismantling of the facility in view of its projected transfer to the Joint Institute of Nuclear Research at Dubna (Russian Federation) where MEA and AmPS will be reshaped into a synchrotron radiation source.

The majority of the 3390 hours of electron beam on target in 1998 were devoted to the study of spin-correlation observables with polarised internal gas targets. In part of these experiments also the stored electron beam was - longitudinally - polarised. In this way the spin structure of ^{3}He was extensively studied. One data point for the charge form factor of the neutron was obtained - with unprecedented precision - from experiments on polarised deuterons. This target was obtained from an atomic beam source, presently the most intense source of polarised protons and deuterons in the world.

With such experiments as highlights, many years of operation of MEA and of AmPS were terminated. This was a sad event not only for NIKHEF's physicists and technicians but also for the 30 groups from abroad that have participated in the in-house research programme. The termination of MEA-AmPS operation also marks the end of 30 years of electron scattering experiments at Amsterdam.

Part of the Dutch ATLAS team has joined past summer the D0 collaboration at Fermilab's Tevatron. The aim is to participate in Run II of this 2 TeV proton-proton collider prior to the LHC experiment ATLAS at a much higher energy. Whether the Higgs particle will be found remains to be seen. Certain is that better precision on the mass of the top quark together with that of the W boson will further limit - within the Standard Model - the possible mass range of the Higgs. At LEP, which is still increasing its energy towards 200 GeV and maybe slightly beyond, possible Higgs events are scrutinised, the present lower limit in mass being 95.2 GeV/c^2.

The past year also saw the approval by CERN of the fourth major future detector at the LHC: the CP violation experiment LHCb. NIKHEF is planning a relatively large participation aiming at responsibilities for the Outer Tracker and part of the vertex detector. The B physics programme at NIKHEF was approved. With this, a large fraction of NIKHEF's resources is now committed to three LHC experiments: ATLAS (Memorandum of Understanding signed), ALICE (Interim MoU signed) and LHCb.

The disappointing decision by the Netherlands' Science Organisation NWO to not fund the R&D project for GRAIL, a spherical gravitational wave detector, caused the end of an active collaboration between several non-partner universities and NIKHEF.

The Neutrino Oscillation Workshop (NOW98) organised by NIKHEF, initially only meant to discuss options for neutrino physics at the institute, grew into a major event also stimulated by the recent Super Kamiokande results.

At the end of the past year, dr. Jan Langelaar stepped down as the managing director of NIKHEF. The institute owes him much after his almost 15 years of service in this important post.

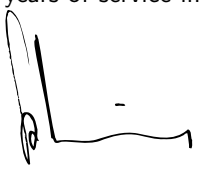

Ger van Middelkoop

One of the sections of the AmPS stretcher ring (photo: NIKHEF)

A Experiments in Progress

1 Electron Scattering

1.1 Introduction

The results of the experiments, performed with the extracted beam in the EMIN facility during the foregoing years, were further analysed. In the past years many publications about this work appeared in the refereed literature, with many more in preparation. Especially the two-nucleon knock-out studies and the observation of high-missing momentum components in the nuclear wave functions, attracted much international attention.

The analysis of the reaction ^{3}He$(e, e'pp)$ has shown large excess strength compared to state-of-the-art Faddeev calculations. A complete picture can only be obtained by measuring the isospin analogue reaction ^{3}He$(e, e'pn)$. For that purpose a proposal has been submitted to and approved by the Mainz PAC. The experiment will be carried out by a collaboration of physicists from Mainz, Glasgow, Edinburgh, Tübingen and NIKHEF with the 850 MeV MAMI beam in the A1-hall. Electrons will be detected in one of the Mainz magnetic spectrometers, the HADRON3 detector and its associated electronics will be shipped from NIKHEF to Mainz in order to serve as a proton detector, while the Tübingen and Scotland groups will build a 9 m^2 scintillator wall for neutron detection.

The experimental program was, during this last year of operation of the AmPS facility, completely devoted to experiments in the internal target facility. After the successful commissioning of the AmPS storage ring for polarised electrons - including the repair of the Siberian Snake - the experimental conditions were improved such that a large fraction of the experimental program could be finished before the end of the year.

In total 3390 hours of beam time were used for the internal target experiments. The first two months were used to study quasi-free pion production by electrons on a ^{4}He target. In this experiment the scattered electron was observed in the BigBite detector, the knocked-out protons in the HADRON4 large-acceptance scintillator array and the recoiling ^{3}H and ^{3}He nuclei in the recoil detector.

After completion of this experiment, the remaining part of the experimental program was completely dedicated to the study of spin-correlation observables from polarised internal gas targets.

To complete the research program on the spin structure of ^{3}He, the polarised ^{3}He target was installed, and proposal 94-05 took the floor until the summer shut down. BigBite was used for detection of the scattered electron, while the large scintillator bars from the HARP detector were used for the detection of the knock-out particles. Large amounts of knocked-out neutrons, protons and deuterons have been observed. The analysis is in progress.

The summer period was used to install the upgraded atomic beam source (ABS). New sextupole magnets, modified RF transition units and a new dissociator system make this ABS the most intense source of polarised ^{1}H and ^{2}H nuclei in the world. With an improved system of vacuum pumps the whole atomic beam source could be installed vertically, allowing the use of the horizontal plane as the reaction plane. This simplified the detector set-up compared to the old 91-12 configuration (see Ann. Rep. 1995). In spite of the fact that the amount of beam time was quite limited, the experiment with polarised ^{2}H has resulted in a data point for the charge form factor on the neutron with unprecedented accuracy. The polarised ^{1}H experiment yields information on the deformation of baryons.

To completely finish the required experimental program an additional beam period was foreseen for the first two months of 1999, but the collapse of a 10 kV transformer in the power system of the ring caused an unexpected early end to the successful period of AmPS operations.

Many parts of the experimental set-up will have a second life at other nuclear physics facilities. The ABS will be shipped to the MIT/BATES laboratory and will be used, starting from the fall of 1999, as a polarised ^{1}H/^{2}H internal target for the BLAST spectrometer facility. Also the Compton backscattering polarimeter will be used at MIT/BATES. The BigBite magnetic spectrometer will go to TJNAF to be used as a photon tagger in Hall-A. The two spectrometers of EMIN will be shipped to IASA in Athens.

At TJNAF the measurements on electroproduction of pions on ^{1,2}H were completed. Analysis of the calibration runs and part of the data has been finished.

About 25 groups from abroad participated in the research program with the beams from AmPS. Part of

this work took place within the framework of European network collaborations. The experimental program was performed by NIKHEF physicists and technicians in collaboration with the following institutes and research physicists:

Argonne National Laboratory, Argonne, IL 60439, USA
R.B. Wiringa
Arizona State University, Tempe, AZ, USA
R. Alarcon, E. Six
Budker Institute for Nuclear Physics, Novosibirsk, Russian Federation
D. Nikolenko, I. Rachek
DAPNIA/SPhN, CEA Saclay, Gif-sur-Yvette, France
J.E. Ducret, J.M. Laget, C. Marchand, R. Medaglia
ECT*, Villazzano (Trento), Italy
W. Leidemann
ETH, Zürich, Switzerland
J. Lang, D. Szczerba
Hampton University, Newport News, VA, USA
R. Ent, M. Harvey
INFN-Bari and Bari University, Bari, Italy
R. De Leo
INFN-Lecce, Italy
R. Perrino
INFN-Sezione Sanità, Rome, Italy
O. Benhar, E. Cisbani, S. Frullani, F. Garibaldi, M. Iodice, G-M. Urciuoli
Jagellonian University, Cracow, Poland
J. Golak, H. Witała
Johannes Gutenberg Universität, Mainz, Germany
H. Arenhövel
KVI, Groningen
N. Kalantar-Nayestanaki
MIT, Cambridge, Mass., USA
Z.L. Zhou
Old Dominion University, Norfolk, VA, USA
G.E. Dodge, L. Weinstein
Ruhr Universität, Bochum, Germany
W. Glöckle H. Kamada
TJNAF, Newport News, VA, USA
C.W. de Jager, D. Mack
University of Edinburgh, Scotland
J. Arneil, D. Branford, T. Davinson, M. Liang, J. Mackenzie, S.A. Morrow
University of Gent, Belgium
E.C. Aschenauer, G. De Meyer
University of Glasgow, Scotland
D.G. Ireland, A. Scott
University of Ohio, Athens, OH, USA
K. Hicks
University of Regina, Canada
G.J. Lolos
University of Virginia, Charlottesville, VA, USA
D.W. Higinbotham, B.E. Norum, K. Wang
Vrije Universiteit Amsterdam
W.J.W. Geurts, F.A. Mul.

1.2 Physics with the extracted beam of AmPS

Two-proton knockout from ^3He
(Prop. 94-05; with Bochum, Cracow, Glasgow, INFN-Rome, INFN-Bari, INFN-Lecce, ODU, Regina)

The electron-induced two-nucleon knockout reaction is well suited for the study of short-range nucleon-nucleon correlations. However, this reaction is not only driven by one-body currents, where the virtual photon couples to only one of the nucleons of a correlated pair, but also two-body currents, due to Δ excitation or the exchange of a meson (MEC), contribute to the cross section.

The ^{3}He system offers the opportunity to compare exclusive measurements of the three-body breakup process with continuum Faddeev calculations based on realistic *NN* potentials. By varying the energy and momentum of the transferred virtual photon, the relative importance of the competing mechanisms can be investigated.

Data were collected at three values of the three-momentum transfer q of 305, 375 and 445 MeV/c at an energy transfer of $\omega = 220$ MeV. At the central q value the ω dependence of the cross section between 170 and 290 MeV was investigated. The scattered electron was detected in the QDQ spectrometer and the two knocked-out protons were detected in the large-solid-angle HADRON detectors.

The missing-momentum (p_m) or neutron-momentum distribution as determined in one of the kinematic settings is shown in Fig. 1.1 together with the results of the continuum Faddeev calculations by Golak *et al.* Rescattering effects are included up to all orders, but only a one-body current operator is used.

At low values of the neutron momentum, the calculated cross section agrees quite well with the data, whereas at high p_m differences up to a factor of five are observed. In this region contributions from MEC and the excitation of the Δ resonance will play a significant role. The data collected at different values of ω, together with calculations that include two-body currents, are especially suited to investigate these contributions.

At low neutron momenta the dependence of the measured cross section on the momentum transfer q is sim-

ilar to that of the elementary one-body electron-proton cross section. This behaviour is also exhibited by the Faddeev calculations. This suggests that at low p_m the coupling mechanism is predominantly of single-nucleon character.

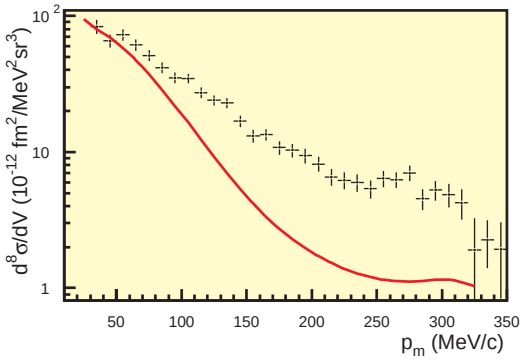

Figure 1.1: *Missing-momentum distribution for the* $^3He(e,e'pp)$ *reaction for the kinematic setting q=305 MeV/c, ω=220 MeV.*

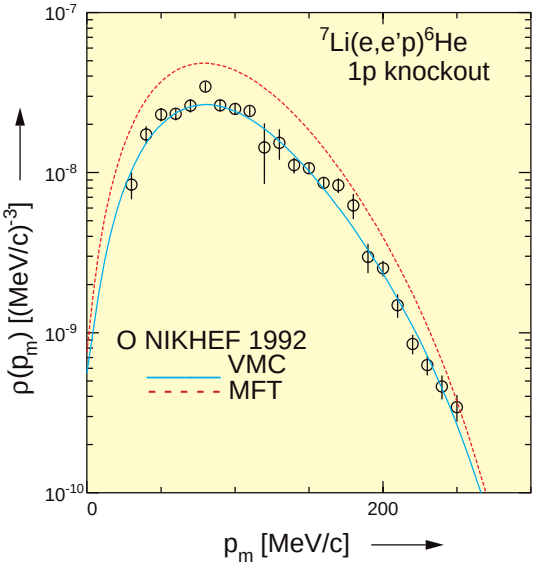

Figure 1.2: *Experimental momentum distribution for the summed transitions to the ground state and first excited state in the reaction* $^7Li(e,e'p)^6He$*, compared to CDWIA calculations with MFT (dashed) and VMC (solid) wave functions.*

Correlations in the ground-state wave function of ^7Li (with Argonne)

The effect of including short-range correlations, based on realistic *NN* interactions, in the calculation of nuclear structure has been studied in detail for few-body systems. The results agree well with experimental momentum distributions deduced from the reaction $(e,e'p)$. Experiments on complex (A>4) nuclei have been performed abundantly, but the comparison to theory hitherto suffered from the absence of calculations based on realistic interactions. Hence, these data were commonly compared to mean-field theory (MFT) analyses that did not include (short-range) correlations. As a result the calculated momentum distributions in general showed more strength than the experimental ones, and the normalisation (about 60-65% for nuclei ranging from A=6 to 209) required to bring theory and data into agreement, was interpreted as evidence for the presence of correlations. A quenching of this kind was predicted for infinite nuclear matter but the extension of this result to finite nuclei is not straightforward due to the coupling to surface vibrations, which affects the strength for transitions near the Fermi edge.

Recent *ab initio* calculations [Phys. Rev. C **56**, 1720 (1997)] via the variational Monte Carlo (VMC) technique, employing the Argonne v_{18} two-nucleon and Urbana IX three-nucleon potentials, now enable for the first time the comparison of ^{7}Li$(e,e'p)$ data directly with a parameter-free realistic theory. The experimental data were obtained in 1990 with the MEA facility of NIKHEF but so far remained unpublished. The results are shown in Fig. 1.2, where the experimental momentum distribution for 1p proton knockout from ^{7}Li leading to the ground state and first excited state in ^{6}He, is compared to CDWIA (Coulomb Distorted Wave Impulse Approximation) calculations with MFT and VMC wave functions. The 1p spectroscopic factor for the MFT calculation is unity, whereas that of the VMC calculation is 0.60. Scaling the MFT curve to the experimental data results in an experimental 1p spectroscopic factor of 0.58±0.05, where experimental systematic errors and uncertainties due to the calculation of the final-state interaction have been included. The experimental spectroscopic factor is in perfect agreement with the VMC value, thus unambiguously demonstrating the necessity to include short-range correlations based on realistic interactions in nuclear-structure calculations.

Electron-induced proton knockout from ^{12}C

Electron-induced proton knockout experiments in the quasi-elastic domain are commonly used to determine spectroscopic factors for proton removal from nuclei. As the spectroscopic factors enter directly into the

determination of the nuclear transparency for protons, which was recently studied at SLAC on ^{12}C in the (squared) four-momentum transfer (Q^2) range 1-6 $(\mathrm{GeV}/c)^2$, we have re-analysed all existing $^{12}\mathrm{C}(e,e'p)$ data for knockout from the $1p$ and $1s$-shell for $Q^2 < 0.4$ $(\mathrm{GeV}/c)^2$, in one consistent approach. The $1p$ results (world average S_{1p}=2.23±0.07) were reported before [Ann. Rep. 1995].

Since the existing data for $1s$ knockout from ^{12}C cover different ranges in missing energy (E_m) and the experimental $1s$ missing-energy distribution extends over a range of about 25-80 MeV a special procedure was followed to extract the $1s$-strength. Because the maximum of the $1s$ missing-energy distribution is located at about 40 MeV we first fitted CDWIA (Coulomb Distorted Wave Impulse Approximation) calculations to data from Saclay and Tokyo that cover the E_m range 30-54 MeV. From these fits the geometry of the Woods-Saxon well, used to generate the bound-state wave function, was determined and subsequently used to calculate all other reduced cross sections for $1s$-removal with wave functions that have the appropriate binding energy.

Next, the normalisation of these calculated $1s$ reduced cross sections was fitted to each data set to obtain the spectroscopic factor for $1s$ knockout in the particular E_m interval. From the obtained normalisations we deduced the $1s$ strength $S_{1s}(E_m^{up})$ integrated to an upper limit E_m^{up} in missing energy. These values have been plotted in Fig. 1.3, where the errors include statistical and systematic uncertainties. The $1s$ strength at any value of E_m^{up} can now easily be deduced from a fit to the data with an integral of a Lorentzian energy distribution with an energy-dependent width (solid curve). For the analysis of the $1s$ SLAC data in the interval E_m=30-80 MeV we derive the value $S_{1s}(80)$-$S_{1s}(30)$=1.18±0.07.

Using the precisely determined values of S_{1p} and S_{1s} we have reconsidered the interpretation of the $^{12}\mathrm{C}(e,e'p)$ experiment performed at SLAC at Q^2=1.1 $(\mathrm{GeV}/c)^2$. In this experiment the nuclear transparency for protons was measured with the aim of searching for colour-transparency effects, i.e. the predicted increase of the nuclear transparency due to the proposed reduced interaction probability of small colour neutral objects with the surrounding medium.

The nuclear transparency T_α ($\alpha = 1s, 1p$) is derived from the data (see Fig. 1.4) by fitting a PWIA curve, calculated with the above quoted values of S_α, to the data using T_α as a free parameter. The PWIA curves are close to the data, immediately suggesting a relatively large value of T. The obtained transparency values T_{1p}=0.86±0.05 and T_{1s}=0.71±0.06 are different for the two shells.

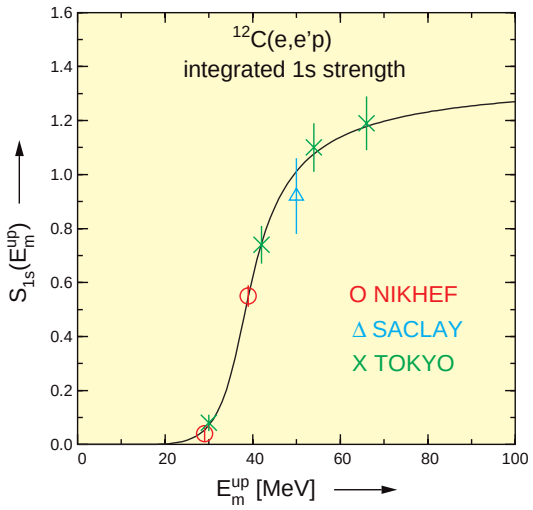

Figure 1.3: *Integrated $1s$-knockout strength obtained with the reaction $^{12}C(e,e'p)$ as a function of the upper integration limit in missing energy. The data points are from Tokyo, Saclay and NIKHEF. The curve represents a fit with an integrated Lorentzian as described in the text.*

Combining the two results we evaluated the average transparency (weighed by S_α) of nucleons removed from ^{12}C, yielding $T_{^{12}C}$=0.81±0.04, which is considerably larger than the value 0.65±0.05 obtained in the analysis of the same data presented in Ref. [Phys. Rev. Lett. **72** (1994) 1986]. The present value of $T_{^{12}C}$ is also significantly larger than the value $T_{^{12}C}$=0.61 (0.62) deduced from a Glauber calculation by Zhalov *et al.* without (with) Colour Transparency effects. At present we investigate whether a possible breakdown of the quasi-particle concept that underlies the analysis of the $(e,e'p)$ data at lower energies, may be at the origin of this discrepancy.

L/T separation in $^{12}C(e,e'p)$ at large p_m
(Prop. 91-E14; with KVI, Edinburgh, Gent, Glasgow, Ohio, Saclay)

The strong excitation of a triplet at an excitation energy of 7 MeV in the reaction $^{12}\mathrm{C}(\gamma,p)^{11}\mathrm{B}$, which was not observed in the analogous $^{12}\mathrm{C}(e,e'p)$ reaction, has given rise to various speculations concerning the origin of this strong excitation. As it has been suggested that the excitation of the triplet can be either be caused by

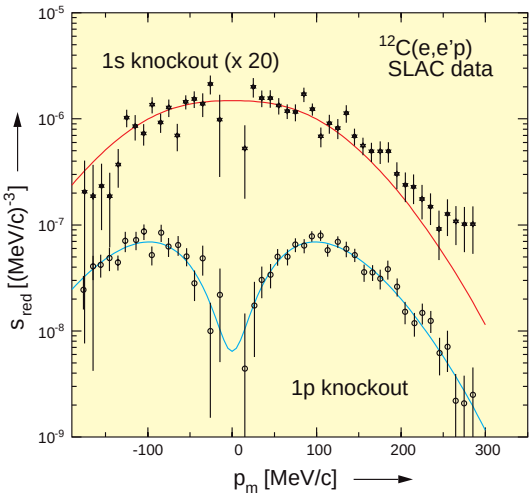

Figure 1.4: *Reduced cross section for 1p (circles) and 1s (crosses) proton knockout in the reaction $^{12}C(e,e'p)$ as obtained in a recent SLAC experiment at $Q^2 = 1.1$ $(GeV/c)^2$. The curves represent PWIA calculations normalised with the spectroscopic factors $S_{1p} = 2.23$ and $S_{1s} = 1.18$ and transparencies T_{1p} and T_{1s} fitted to the data.*

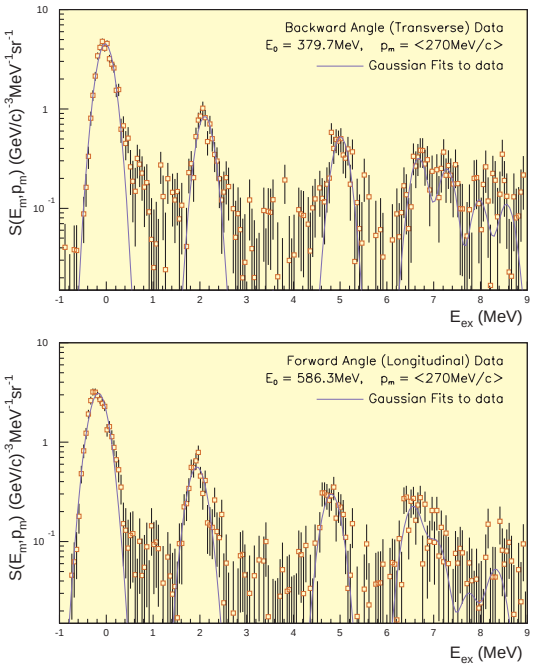

Figure 1.5: *Missing energy spectrum for the reaction $^{12}C(e,e'p)$ at two different values of the incident energy. The data are corrected for radiative effects. The separate contribution of the $(7/2^-,1/2^+)$ doublet at 6.8 MeV and the $5/2^+$ state at 7.3 MeV are seen in both spectra.*

some particular $2p1h$-configuration in the ^{12}C ground state wave function or by MEC-effects, a dedicated $(e,e'p)$ experiment has been performed to resolve this issue. As MEC effects will cause a transverse enhancement of the cross section, a separation of the longitudinal and transverse response functions, W_L and W_T, has been carried out in a missing momentum range similar to that probed in the $^{12}C(\gamma,p)$ reaction.

To accomplish a longitudinal-transverse separation, data have been collected at two beam energies. A missing-energy resolution of about 400 keV was obtained, which is enough to separate the $(7/2^-,1/2^+)$ doublet and the $5/2^+$ state, which together form the triplet at $E_x = 7$ MeV (see Fig. 1.5). The structure functions W_L and W_T have been determined for all states up to 9 MeV. At present, the systematic uncertainties involved in such an analysis are being studied.

Study of short-range correlations with the reaction $^{16}O(e,e'pp)^{14}C$
(Prop. 94-01; with INFN-Rome, INFN-Lecce, INFN-Bari, ODU and MIT)

Short-range correlations (SRC) in ^{16}O have been studied with the reaction $^{16}O(e,e'pp)^{14}C$, which is sensitive to such correlations via the one-body current in the interaction. However, also two-body currents like the excitation and subsequent decay of the Δ resonance into a proton pair contribute to the reaction yield. The latter process is expected to be strongly dependent on the energy transferred by the virtual photon. To investigate the relative strength of both processes, data were taken at three different values of the transferred energy ω: 180, 210 and 240 MeV.

The cross sections measured for the three values of ω as a function of the missing energy and the missing momentum, were compared to each other and to the results of calculations. These calculations were performed with a microscopic model developed by the theory group at Pavia. This model contains a thorough description of the reaction mechanism, which includes one-body (SRC) and two-body (Δ excitation) hadronic currents. The nuclear structure of the ^{16}O nucleus was taken from a DRPA calculation. Short-range correlations were incorporated via defect functions, which were derived from a realistic nucleon-nucleon potential.

The missing-momentum distributions for two intervals in excitation energy, which roughly correspond to the transitions to the ground state and the lowest excited 2^+ state of ^{14}C, respectively, are presented in Fig. 1.6. The cross section for the transition to the ground state is found to be hardly dependent on the transferred energy. These data are well described by the calculations, which indicate that SRC dominate the reaction at ω=180 and 210 MeV. The cross sections measured for the transition to the 2^+ state decrease strongly for increasing values of ω. This trend is not reproduced by the calculations. However, the shapes of the data and the calculations at ω=180 MeV are similar and hint at the dominance of SRC. The observed discrepancy is likely to be caused by an incomplete description of the nuclear structure.

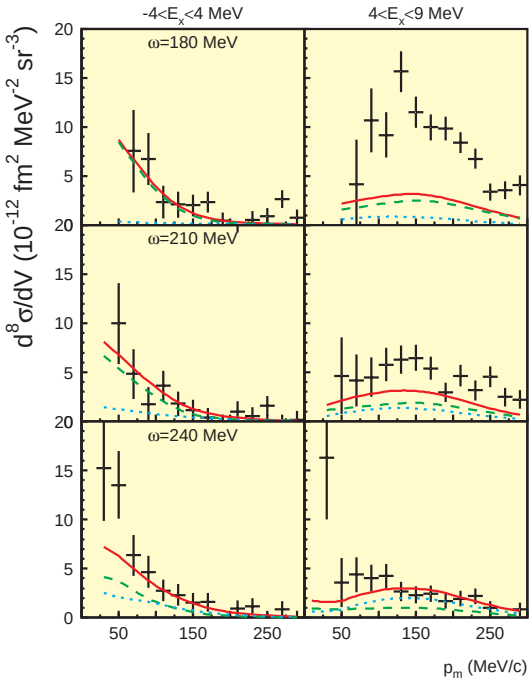

Figure 1.6: *Missing-momentum distributions for the three values of the transferred energy 180, 210 and 240 MeV for the transitions to the ground state (left) and the 2^+ state (right). The solid, dashed and dotted curves represent the total cross section and the components from SRC and Δ excitation, respectively.*

$^{208}Pb(e,e'p)^{207}Tl$ at high momentum transfer in transverse kinematics
(Prop. 91-E19; with Saclay, INFN-Lecce, INFN-Rome, Bari, Glasgow)

We have measured the missing momentum dependence of the reduced ^{208}Pb$(e,e'p)$ cross section at two momentum transfers (q) : 572 and 750 MeV/c to determine the spectroscopic factors of the valence shells of ^{208}Pb. Our kinematics were quasi-elastic and transverse: the electron was scattered at 100° so that the polarisation of the exchanged photon was predominantly transverse. The motivation for this experiment was based on observations made in the separation of longitudinal (W_L) and transverse (W_T) structure functions in $(e,e'p)$ quasi-elastic cross-sections performed at Saclay on light nuclei and on ^{40}Ca. From these experiments it was concluded that W_L, especially at low momentum transfer, was not well described by calculations including Coulomb distortion of the electron waves and final-state interaction between the ejected proton and the residual nucleus. Moreover, W_T did not show this behaviour and was more in agreement with theoretical predictions. As the previous measurement of the reaction ^{208}Pb$(e,e'p)$ at NIKHEF by Quint *et al.* was performed in kinematics with a dominant contribution of W_L and at low momentum transfer (200$<q<$ 500 MeV/c), we wanted to investigate how the response evolved at different four-momentum and polarisation of the exchanged photon.

The measured missing-momentum dependencies for proton knockout from the valence shells agree within the error bars for the two momentum-transfer values of our experiment. This is in agreement with earlier measurements at Saclay for lighter nuclei. Furthermore, the spectroscopic factors extracted from the high-q data depend only slightly on the momentum transfer and are significantly higher than those determined at low q by Quint *et al.* First calculations of the contribution of meson-exchange currents by the Gent group indicate that these are on the level of 10% or less. At q=750 MeV/c we observe differences between a relativistic and a non-relativistic description of the momentum distributions. In order to arrive at a reliable comparison between experimental spectroscopic factors determined from the reaction $(e,e'p)$ with those of many-body calculations, we presently investigate reaction mechanisms that allow for a consistent description of the response under all employed kinematic conditions.

The $^{208}Pb(e,e'p)$ reaction at high missing energy
(Prop. 94-13; with Glasgow, Saclay, INFN-Rome and INFN-Lecce)

We measured cross sections for the reaction ^{208}Pb$(e,e'p)$ up to a missing energy (E_m) of 100 MeV, in order to determine the proton spectroscopic

strength residing in deeply bound orbitals. The experimental cross sections may contain substantial contributions from multi-nucleon knockout processes, which are predominantly of transverse character. We performed a Rosenbluth separation to extract the longitudinal response, to which such processes hardly contribute. The preliminary results for the separated responses are shown in Fig. 1.7.

At high E_m the measured longitudinal and transversal cross sections may also contain contributions from the rescattering process $(e, e'N)(N, p)$. We evaluated the importance of the rescattering to the cross section in a model that includes a realistic approach to medium effects in ^{208}Pb. The shaded areas in Fig. 1.7 indicate the results obtained using this model. They show that rescattering processes contribute less than one percent to the measured strength.

The measured longitudinal and transverse responses have been compared to calculations based on a mean-field model using spectral factors measured previously in dedicated experiments. The calculated strength underestimates the transverse response extracted from the data, most notably beyond 50 MeV. This may be due to contributions from multi-nucleon knockout processes. The longitudinal response is described well for $E_m \leq 50$ MeV. The discrepancy observed for larger E_m is caused by the absence of correlations in the model. In order to estimate the effect of such correlations, we also compare the data to a nuclear-matter calculation based on a realistic interaction. As shown in Fig. 1.7 the results of this calculation describe the data at high E_m rather well.

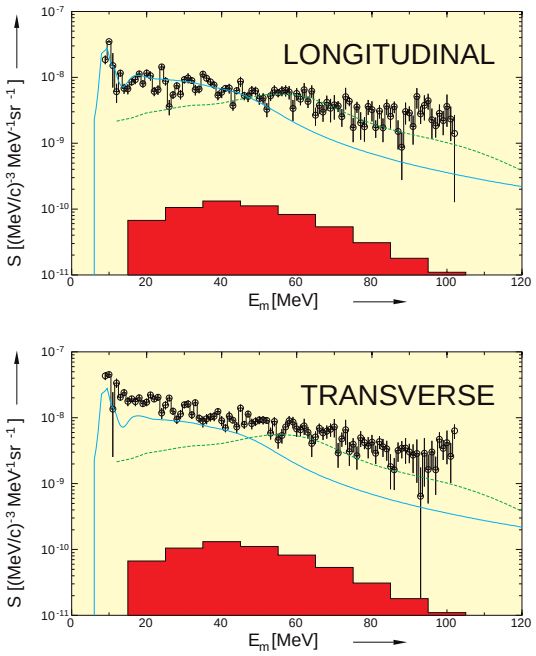

Figure 1.7: *Preliminary separated responses for the reaction $^{208}Pb(e, e'p)$ as a function of E_m. The solid and dashed lines represent the results obtained using the mean-field and nuclear-matter calculations, respectively. The shaded areas denote the rescattering contribution.*

1.3 Internal target facility

Introduction

In the scattering of leptons from hadronic targets the leptonic part of the interaction is presumably well understood. Therefore studies can be focused on the strong-interaction vertex and the underlying structure and dynamics of the nucleus. The ultimate probe consists of fully spin-dependent scattering with polarised leptons and polarised targets, and the last decade has seen a large effort devoted to the realisation of such experiments, with NIKHEF playing a leading role. Although relatively low in luminosity, spin-dependent electron scattering experiments from polarised gas targets internal to storage rings have the advantage that (i) they can be well matched with the application of large-acceptance detectors; (ii) rapid polarisation reversal and flexible orientation of the nuclear target spin can be obtained, reducing systematic uncertainties; and (iii) low-energy recoiling particles can escape the ultra-thin targets and be detected.

Instrumentation

In order to achieve sufficient luminosity and polarisation for the spin-dependent experiments of proposal 97-01, the atomic beam source (ABS) was upgraded at the Vrije Universiteit in collaboration with NIKHEF and ETH-Zürich. State-of-the-art permanent sextupole magnets were designed and implemented. This resulted in an increase of injected atomic beam flux by more than a factor of 2.5. The required high-frequency transition units were designed and tested. In order to allow the use of the BigBite magnetic spectrometer in the internal target hall (ITH), the necessary modifications were carried out for a vertical implementation of the ABS. The polarised internal target performance was further improved by doubling the pumping speed on the target chamber (less unpolarised molecular background), by using a longer storage cell (600 mm) cooled to 75 K, and by providing a stronger target guide field

over the storage cell. Compared to our previous experiments with tensor-polarised deuterium, this target setup resulted in an increase in figure of merit by more than an order of magnitude, with a typical target thickness of $\sim 1 \times 10^{14}$ atoms/cm^2 and polarisations up to $P_z \simeq 0.8$.

Experiments

Quasi-free pion electroproduction on ^{4}He
(Prop. 91-08; with Old Dominion and Virginia)

The reactions ^{4}He$(e, e'p\,^3$H$)\pi^0$ and ^{4}He$(e, e'p\,^3$He$)\pi^-$ were studied at invariant energies ranging from the pion production threshold to the delta resonance region. Comparison of the cross sections with those of pion production on the proton will provide information on ΔN and πN dynamics inside the ^{4}He nucleus.

The measurements were carried out with a 670 MeV electron beam and a 15 mm diameter open-ended storage cell of 40 cm length, cooled to 27 K and in which a target thickness of 10^{15} atoms/cm^2 was obtained. The average beam current was 80 mA. The scattered electrons were detected in the BigBite large-acceptance magnetic spectrometer, the knocked out protons in the HADRON4 large-acceptance plastic scintillator array, which has an energy acceptance of 30–250 MeV. Simultaneous measurement of both reaction channels was achieved by detecting the recoiling nuclei in the VUA Recoil Detector positioned opposite to the 3-momentum transfer. In this way the detection of the neutral pion was avoided. To accept recoil particles with energies as low as 1 MeV, the detector was separated from the scattering chamber vacuum only by a 0.9 μm thick mylar foil.

For each pion production reaction channel about 1200 events were collected. The missing mass spectrum for the reaction ^{4}He$(e, e'p\,^3$He$)\pi^-$ is shown in Fig. 1.8.

Also abundant ^{4}He$(e, e'p\,^3$H$)$ coincidences have been obtained, which serve as an independent normalisation and provide additional information on possible systematic errors.

Coherent π^0 electroproduction on ^{4}He in the Δ region
(Prop. 94-06; with Old Dominion and Virginia)

Coherent π^0 electroproduction on a composite nucleus is an excellent testing ground for theories of resonance propagation in the nuclear medium. At energy transfers of 200-400 MeV, the properties of the $\Delta(1232)$ resonance are expected to be effectively modified by interactions with the nucleons. Coherent π^0 electroproduction was studied on ^{4}He by scattering electrons

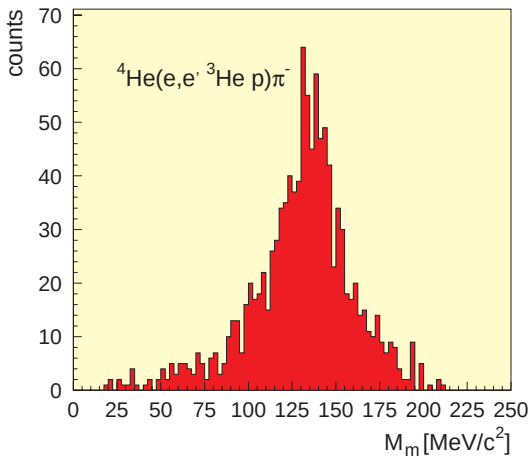

Figure 1.8: *Missing mass spectrum for the reaction $^4He(e, e'p\,^3He)\pi^-$.*

of 677 MeV from ^{4}He atoms, stored in a 15 mm diameter open-ended storage cell cooled to 77 K inside the ring vacuum.

The detection of neutral pions was avoided by making use of a dedicated recoil detector for the recoiling ^{4}He nuclei (1-95 MeV), placed at 17 cm from the target cell, with a solid angle of 250 msr. The scattered electrons were detected in the BigBite large-acceptance magnetic spectrometer.

Data were collected in March 1997 at two spectrometer angles, thus allowing the most complete study of the coherent reaction so far.

The coincidence setup was calibrated with ^{4}He$(e, e')^4$He elastic scattering events. For the analysis a separation of coherent events against a background of low-energy α particles coming from so-called radiative elastic scattering (in which a photon was also emitted either prior or after the nuclear reaction) must be achieved. This was done via a detailed Monte-Carlo simulation of both coherent and radiative events.

In Fig. 1.9 we show a typical missing-mass spectrum. The peak to the right is due to pion events: the dashed line is the Monte-Carlo result for the pions, which uses the cross sections calculated in DWIA by Kamalov. The peak to the left is due to radiative elastic scattering. The dotted line is the result of our Monte-Carlo model. The final cross section results will be compared to DWIA and Δ-hole type models.

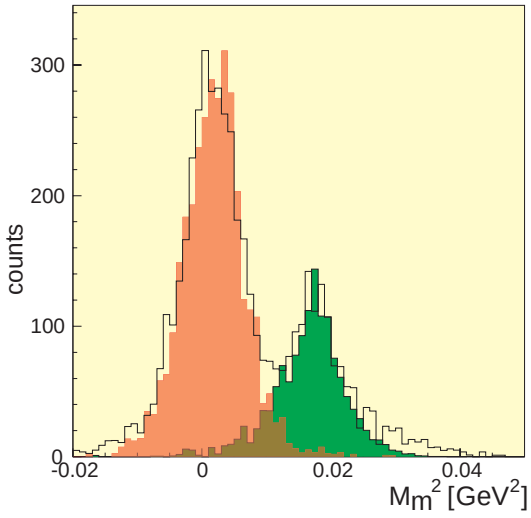

Figure 1.9: *Missing-mass spectrum for the* $^4He(e,e'^4He)$ *reaction showing elastic scattering events* ($M_m^2 = 0$) *and events in which a* π^0 *was produced* ($M_m^2 = M_\pi^2$).

While the study of the forward-peaked centre-of-mass angular distributions for the pion gives insight on the properties of the Δ-resonance propagation, the cross section at very large angles is rather sensitive to the reaction mechanism. Deviations from the coherent response in this region may give indications about two-body effects in pion production.

The spin structure of ^3He
(Prop. 94-05; with Arizona, Hampton, Virginia, Wisconsin)

This experiment aims to study the spin structure of ^{3}He by spin-dependent electron scattering from a polarised ^{3}He target internal to the AmPS polarised electron ring. Last year, a pilot experiment was performed, where a partial snake was used (see Ann. Rep. 1997). By repairing the Siberian Snake, increasing the energy to 720 MeV, and increasing the polarisation and target thickness of the ^{3}He target to the nominal values of the proposal, this year an increase in the figure of merit of three orders of magnitude was obtained.

Spin-dependent electron-scattering data were obtained in a wide range of kinematics with an average four-momentum transfer squared (Q^2) of about 0.21 GeV^2. About 40,000 neutrons were measured in the quasi-elastic region in kinematics with the target spins in the direction that is optimally sensitive to the determination of the charge distribution of the neutrons. Relatively clean neutron detection was obtained, with a background of accidental particles of the order of 10% and a background of misidentified hadrons of the order of 2%. It is expected that a statistical error in the deduced neutron electric form factor of ΔG_E^n of about 0.015 will be obtained. The extraction of G_E^n is complicated by final-state interaction effects and the presence of reaction tails from proton knockout in the neutron sample.

In addition to the neutrons, more than a million protons were detected for the spin correlation asymmetry A'_x and about 50,000 for A'_z. In part of the data also the recoiling system was detected with the VUA recoil detector. Furthermore about 30,000 coincident knocked-out deuterons were obtained. These combined data will enable a careful study of the spin structure of the ^{3}He ground-state wave function, especially the S'-component, which arises from the spin-isospin dependence of the nuclear interaction.

The 1997 data set was used to probe the reaction mechanism effects by measuring the induced asymmetry A_y^0 at $Q^2 = 0.17$ GeV^2. Deviations from zero of this time-reversal odd asymmetry are due to interferences of separate scattering amplitudes, due to the Fermi-Watson theorem. Therefore this asymmetry is strictly zero in the absence of final-state interaction or meson-exchange current effects. This asymmetry is very well suited to evaluate the accuracy of the theoretical models that are applied to extract G_E^n.

The experimental results have been compared with three state-of-the-art models for a subset of our kinematic acceptance. The model of Laget includes meson-exchange currents and single rescattering in the final state in a non-relativistic framework. The wave functions are calculated with the Paris potential. Nagorny provided a manifestly current conserving relativistic model with nucleons as the only degree of freedom and single rescattering effects taken into account (with the Reid soft core potential). Finally, Golak *et al.* performed calculations with their non-relativistic continuum-wave Faddeev model (where rescattering is taken into account to all orders). From Fig. 1.10 it appears that the final-state interaction is very important (the asymmetry is huge) and that the data are well described by the Faddeev calculations but not by the models with only one rescattering taken into account, even for kinematics close to the quasi-elastic peak at $Q^2 = 0.17$ GeV^2. Not the total phase space has been covered by these calculations (the average result of about 60 different kinematic configurations

was considered), and the models are in development as well (Golak will include meson-exchange diagrams and Nagorny is providing diagrams with double rescattering). Therefore the theoretical results in Fig. 1.10 are preliminary.

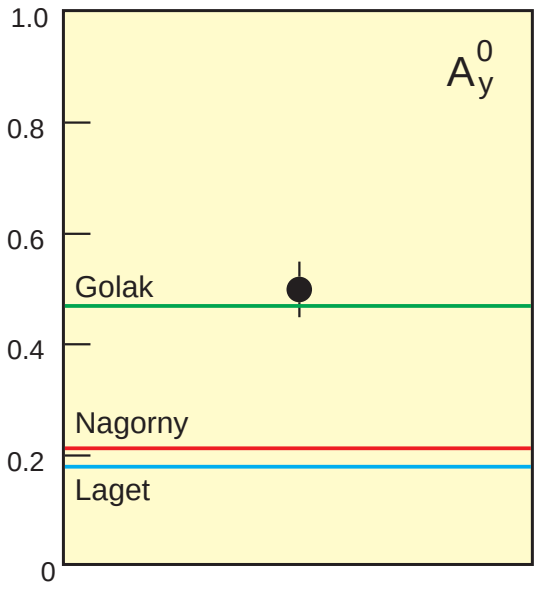

Figure 1.10: *Target asymmetry A_y^0 for the reaction $^3\vec{H}e(e,e'n)$ at $Q^2 = 0.17$ GeV^2. The target spin is oriented normal to the electron scattering plane. The curves represent the average results of Golak, Nagorny, and Laget, respectively.*

Tensor Analysing Powers with Deuterium
(Prop. 91-12; with BINP, ASU, Hampton, ETH, TJNAF and Virginia)

In the past few years we have obtained accurate measurements of T_{20} for elastic e-^{2}H scattering in the four-momentum transfer range $1 < Q < 3$ fm^{-1}. These precise polarisation data, in combination with the structure functions A and B (from cross-section measurements), allow the determination of the three electromagnetic form factors of the deuteron, which place strong constraints on models of the nuclear interaction. Alternatively, the *spin-dependent* density distribution can be probed by quasi-elastic electron scattering from tensor-polarised ^{2}H targets, which yields data complementary to the elastic channel where the *total* nuclear current (i.e. nucleon and meson contributions) is probed. In PWIA, a non-zero tensor analysing power (A_d^T) arises directly from the difference in the "shape" of a deuteron prepared in the spin substate ± 1 compared to that of a deuteron in spin substate 0, i.e. it is a direct consequence of a D-state admixture to the ground-state wave function.

Simultaneous to our T_{20} elastic scattering experiment we measured tensor asymmetries for quasi-elastic scattering. The experimental setup was discussed in previous Annual Reports. The data analysis has now been completed and we present here the final results. Figure 1.11 shows the measured analysing power A_d^T as a function of the cosine of the angle θ_s between the polarisation axis and the missing momentum $\mathbf{p}_m$, and as a function of p_m in approximately parallel kinematics, i.e. the centre-of-mass angle between the momentum of the knocked-out proton and the 3-momentum transfer has been restricted ($\theta_{pq}^{cm} < 13^\circ$). The data are compared to predictions for the Paris potential. The dashed curve represents the results for the plane-wave Born approximation (PWBA), which includes the coupling to the neutron. In the long-dashed curve, effects of final-state interaction (FSI) are included, whereas the solid curve represents the full calculation, i.e. with inclusion of FSI, meson-exchange currents (MEC), Δ-isobar currents, and relativistic corrections. In PWIA the asymmetry is proportional to the rotation function $d_{0,0}^2$. Therefore, the zero crossings of the asymmetry are predicted to be at $\cos\theta_s = \pm\sqrt{1/3}$ ($\approx \pm 0.58$) (see Fig. 1.11). Without a D-state component in the ground-state wave function the asymmetry vanishes. The results of the full calculation describe the data well. The inclusion of spin-dependent rescattering effects improves the description at the lowest missing momenta ($p_m \simeq 50$ MeV/c), where D-state contributions are small. Note that the tensor analysing power is sizeable, even at the relatively small missing momenta addressed in the present experiment. This is due to the fact that an interference between the small D-state amplitude and the dominant S-state amplitude is probed, whereas in the unpolarised cross section only the sum of the squares of the S-state and D-state amplitudes enter.

In this experiment, a first accurate measurement of a tensor polarisation observable in quasi-free electron scattering from deuterium was obtained. In future experiments, data taking should be extended to higher missing momenta, in the region where the tensor analysing powers are predicted to strongly depend on the details of the deuteron spin structure.

G_E^n with vector polarised deuterium
(Prop. 97-01; with ETH, Virginia, Arizona, TJNAF, MIT, Hampton, Novosibirsk)

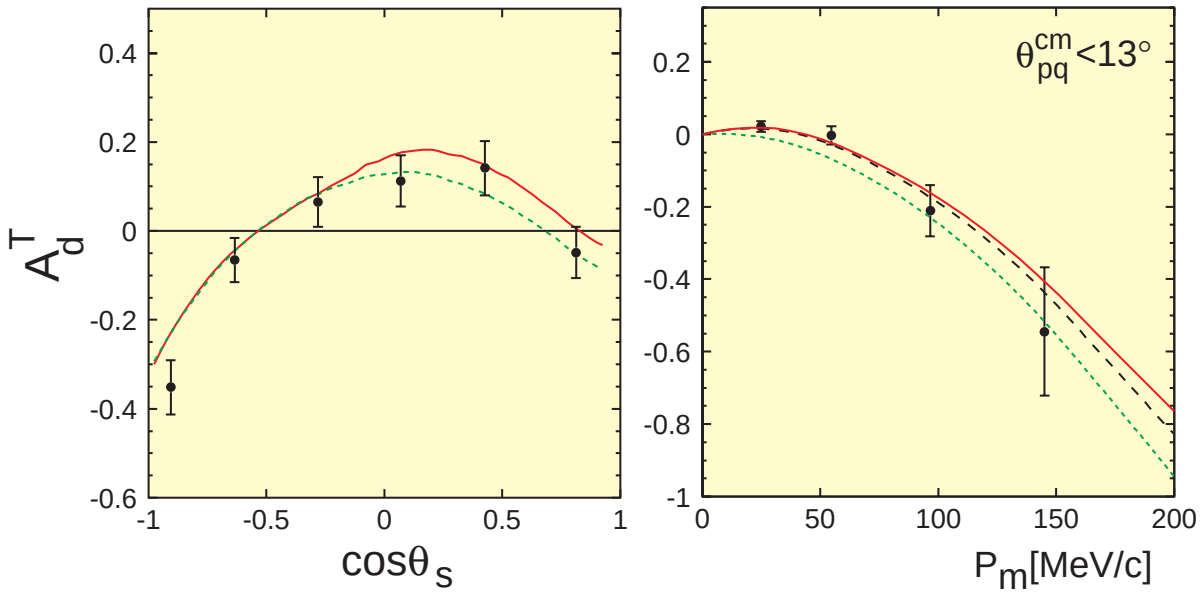

Figure 1.11: A_d^T *as a function of* $\cos\theta_s$ *and of* p_m *for parallel kinematics (i.e.* $\theta_{pq}^{cm} < 13°$*). The curves are explained in the text.*

Although the neutron has no net electric charge, it does exhibit a charge distribution. Precise measurements with thermal neutrons scattering from atomic electrons show that it has a positive core surrounded by a region of negative charge, the exact distribution being described by the charge form factor $G_E^n(Q^2)$. Since stable free neutron targets are not readily available, experimentalists mostly resorted (e.g. at Saclay) to precise unpolarised elastic e-^{2}H scattering measurements to determine this form factor. However, the G_E^n results of these experiments are flawed by large model-related uncertainties; they constrain the shape of $G_E^n(Q^2)$, while the scale remains poorly known. There is a worldwide effort (Mainz, TJNAF, MIT, and NIKHEF) to constrain G_E^n by scattering polarised electrons from neutrons bound in deuterium and ^{3}He nuclei, where either the target is polarised, or the polarisation of the knocked-out neutron is measured. Here, the measured sideways asymmetry A'_x (or recoil polarisation) arises from an interference of the small charge form factor with the dominant magnetic form factor G_M^n. Such spin observables are predicted to be considerably less sensitive to the details of the nuclear wave function. We show here the preliminary results of a measurement utilising a polarised electron beam and a vector-polarised deuterium target.

A stored polarised electron beam of 720 MeV was used, with beam currents of more than 100 mA and life times in excess of 15 minutes. With the Compton backscattering polarimeter the longitudinal polarisation at the interaction point was measured to be up to 65%. The $e'n/e'p$ trigger was formed by a coincidence between the electron arm trigger and a hit in any one of the eight time-of-flight bars. By simultaneously detecting both protons and neutrons in the same detector, one can construct asymmetry ratios for the two reaction channels $^2\vec{\mathrm{H}}(\vec{e}, e'p)n$ and $^2\vec{\mathrm{H}}(\vec{e}, e'n)p$, in this way minimising systematic uncertainties associated with the deuteron ground-state wave function, absolute beam and target polarisations, and possible dilution by cell-wall background.

We performed the measurement at $Q^2 = 0.21$ (GeV/c)^2, i.e. at the maximum of $G_E^n(Q^2)$ determined from the analysis of existing Saclay data. Combination of these data with our result and the known slope at $Q^2 = 0$ puts strong constraints on G_E^n up to $Q^2 = 0.6$ (GeV/c)^2. By comparison of the experimental data with the predictions of the model of Arenhövel averaged over the detector acceptance for various values of G_E^n (see Fig. 1.13), we extract $G_E^n(Q^2 = 0.21$ (GeV/c)^2 with an overall accuracy of about 23%. Although the focus of the experiment was on G_E^n, we simultaneously accumulated large amounts of data for the $^2\vec{\mathrm{H}}(\vec{e}, e'p)n$ reaction covering p_m up

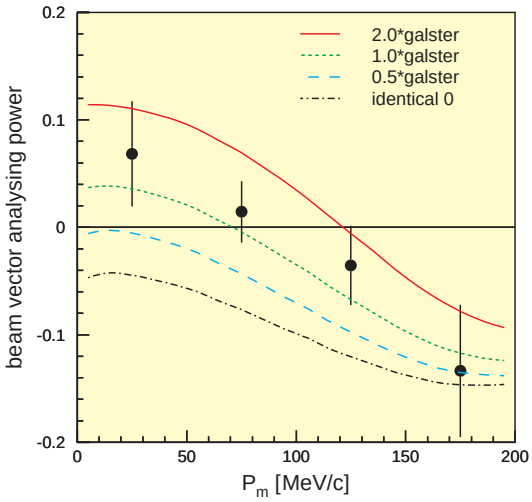

Figure 1.12: *Data and theoretical predictions for the sideways asymmetry A'_x versus missing momentum for the $^2\vec{H}(\vec{e},e'n)$ reaction. The curves represent the results of the full calculations of Arenhövel et al., for various values of G_E^n.*

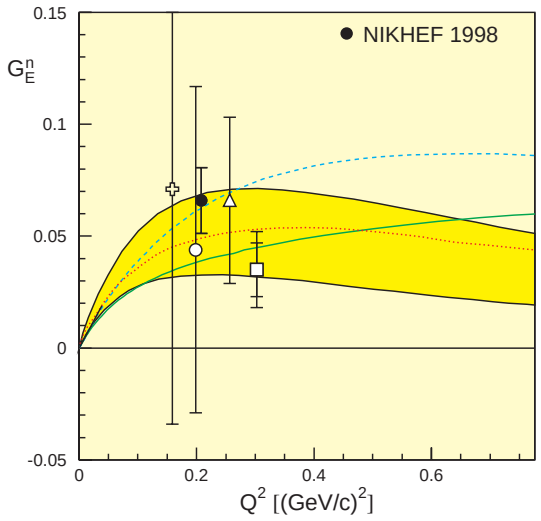

Figure 1.13: *Polarisation data (from MIT-Bates and Mainz) and theoretical predictions for G_E^n as a function of four-momentum transfer. The shaded area indicates the model uncertainty from the unpolarised Saclay data by Platchkov et al. The dotted curve shows the Galster parameterisation, while the solid and dashed curves represent the theoretical predictions of Gari and Krümpelmann with and without inclusion of the ϕ meson, respectively.*

to 350 MeV/c, and in the Δ resonance region (both inclusive and exclusive channels).

$N-\Delta$ Excitation with Polarised Hydrogen
(Prop. 97-01; with ETH, Virginia, Arizona, TJNAF, MIT, Hampton, Novosibirsk)

Information on the wave function of the nucleon, its resonances and the transition currents between them may be obtained by measuring electromagnetic response functions. Specifically, a D-state admixture can induce a non-zero electromagnetic $E2$ or $C2$ amplitude. A quadrupole deformation of the nucleon cannot be determined by elastic scattering, since the spin 1/2 of the nucleon forbids the $E2$ and $C2$ electromagnetic multipoles. The logical place to search for these contributions is in the $N-\Delta$ transition for a number of reasons: the Δ-resonance is the lowest lying resonance and decays purely into two-body final states, which considerably simplifies theoretical calculations of the cross section. It is well separated from other resonances and it dominates in excitation strength at low momentum transfer.

To obtain sensitivity to the quadrupole transition $C2$ ($E2$), it was suggested to measure the spin correlation parameter $A_{TL'}$ ($A_{T'}$) for which the $C2$ ($E2$) amplitude interferes with the dominant magnetic "spin-flip" amplitude $M1$. In December we performed an experiment with polarised electrons and polarised hydrogen. Both asymmetries were measured with equal statistics. Simultaneously, the beam-target polarisation product was obtained from the precisely known elastic scattering asymmetries. The measurements were performed at $Q^2 \simeq 0.11$ (GeV/c)^2 (for the Δ region) with a broad coverage in invariant mass, an important feature for disentangling the role of non-resonant amplitudes. These data for spin correlation parameters in the $^1\vec{H}(\vec{e},e')$ reaction will put constraints on treatment of the $N-\Delta$ excitation. Although our interest was focused on the inclusive channel, we have collected at the same time data for the exclusive channels $^1\vec{H}(\vec{e},e'n)\pi^+$ and $^1\vec{H}(\vec{e},e'p)\pi^0$.

1.4 Experiments abroad

Study of the Charged Pion Form Factor
(with the TJNAF E93-021/E96-007 collaboration)

The charge form factor of the pion will be determined by scattering electrons from a virtual pion in the proton. Pion electroproduction data on ^{1}H as well as ^{2}H, plus extensive calibration data for the optics of the Short Orbit Spectrometer and the new small

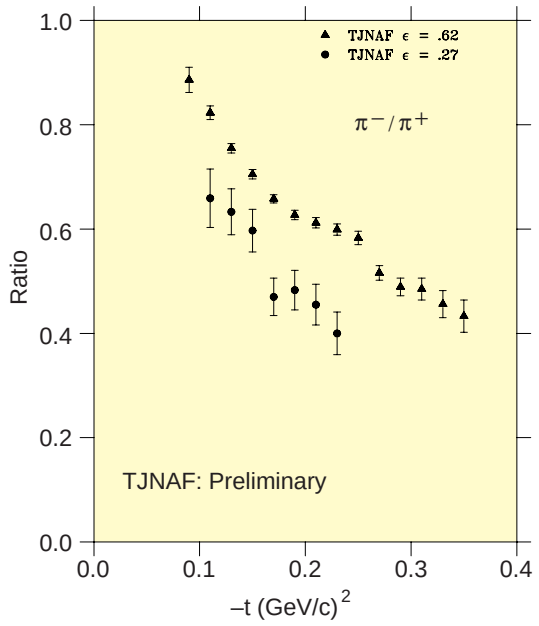

Figure 1.14: *Ratio of π^- to π^+ production on deuterium at a momentum transfer value of $Q^2 = 1.6$ (GeV/c)^2. The systematic errors are approximately 10%*

.

angle tune of the High Momentum Spectrometer were taken in Hall C at TJNAF in the fall of 1997. The optics data are fully analysed. The analysis of the pion data is well underway. Systematic studies of detector inefficiencies have been done for the most part.

Preliminary separated cross sections for the ^{1}H$(e, e'\pi^+)n$ reaction were obtained for the $Q^2 = 1.6$ (GeV/c)^2 point, the longitudinal cross section clearly showing a t-pole behaviour. Isoscalar background contributions have been studied in the ratio between π^- and π^+ production on deuterium.

The unseparated data show a tendency towards unity at low $-t$ (see Fig. 1.14), indicating that these background contributions vanish in very forward kinematics, as expected when the t-pole mechanism is dominant. At larger values of $-t$ one observes a decrease, which can be globally understood as due to the coupling of the virtual photon to the relevant valence quark. This will be studied further by also determining π^-/π^+ ratios for the separated response functions.

The MEA/AmPS control room (photo: NIKHEF)

2 HERMES

2.1 Introduction

This year the HERMES experiment at DESY has taken several important steps towards its prime scientific goal, the understanding of the spin structure of the nucleon. The long HERA shut-down was used to improve the HERMES spectrometer by installing new detection equipment. These improvements enhance the prospects for measurements of the amount of spin carried by the strange quarks and the gluons inside the nucleon in the coming years. The period without regular data taking was also exploited to finalise part of the analysis of data collected in previous years. This has resulted in a series of (draft) publications including a first result on the flavour decomposition of the nucleon spin.

For the NIKHEF/VU group in HERMES 1998 was also of particular importance with the successful defence of the first two PhD-theses that were based on HERMES data, and the achieved proof-of-principle for usage of silicon strip detectors inside the vacuum near a deep-inelastic scattering target. Moreover, the VU-group in HERMES has taken up a new responsibility, now that it participates in the development and maintenance of the Atomic Beam Source internal polarised target system.

As the HERA electron beam became available only late in the year, little data have been collected by HERMES in 1998. It is expected that the long 1999 run will make up for this.

2.2 Instrumentation

During the 1998 shut down the following detector components were added to the HERMES spectrometer: (i) a Ring-Imaging Cherenkov (RICH) detector in order to extend the particle identification properties of HERMES such that kaons and protons can be discriminated against electrons and pions; (ii) an iron wall with a scintillator hodoscope behind to identify muons; (iii) a forward quadrupole spectrometer (FQS) to detect scattered electrons under very small angles; and (iv) a silicon test counter (STC) below the storage cell to identify low-energy particles. The FQS and the STC were prototypes only, which were installed to demonstrate the feasibility of a new detection technique. In both cases the proof of principle has been given. The STC is part of the larger HERMES Silicon Detector Project, which is led by the NIKHEF group. More details on this project are presented as the last item of this report.

The new RICH detector at HERMES is the first to make use of clear aerogel (developed by KEK, Japan) as one of the radiators. The other radiator is the more commonly used C_4F_{10} gas which, in combination with the aerogel, provides hadron identification from 2 to about 16 GeV. An example of actual Cherenkov rings produced by the new RICH is shown in Fig. 2.1. These calibration data were obtained in the fall of 1998.

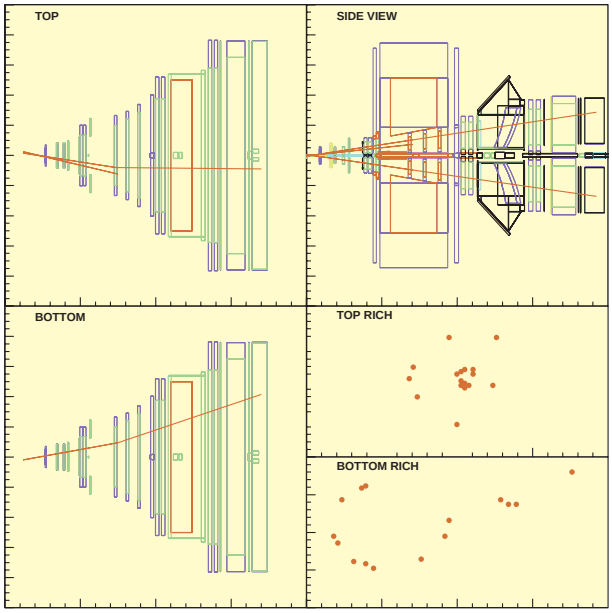

Figure 2.1: *HERMES on-line event display showing an event from various sides. In the lower right corner the rings observed with the new dual-radiator RICH detector are shown.*

The most forward component of the HERMES tracking system is the vertex chamber (VC), which was built by NIKHEF. While this multi-strip gas chamber system worked very reliably in 1997, some damage to the APC readout chips was observed in the second half of 1998. The origin of the problem is presently being investigated.

2.3 Physics analysis

The spin structure of the nucleon

The proton spin structure function $g_1^p(x)$ was extracted from deep-inelastic scattering data collected on a polarised ^{1}H target in 1997. In Fig. 2.2 the (published) HERMES data are compared to the results of similar experiments carried out at SLAC (left panel) and CERN (right panel). Correcting the data for Q^2 differences

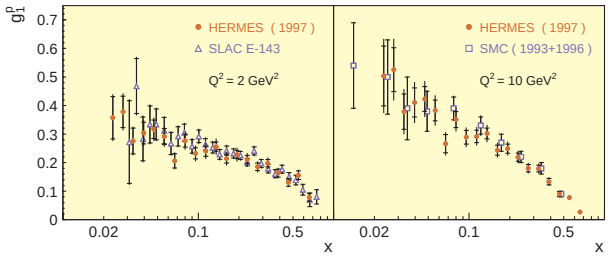

Figure 2.2: *The spin structure function g_1^p of the proton as a function of x. The HERMES data are evolved to $Q_0^2 = 2$ GeV^2 (left panel) and 10 GeV^2 (right panel). The data are compared to measurements from E-143 and SMC (shown for $x > 0.01$ only). The outer error bars represent the quadratic sum of the statistical and systematic uncertainties.*

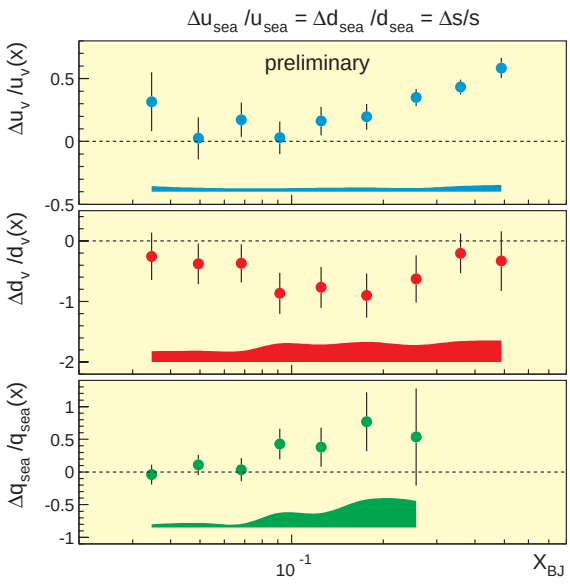

Figure 2.3: *Preliminary results of the flavour decomposition of the nucleon spin. The results are derived from the 1995 and 1996 HERMES data on polarised ^1H and ^3He targets. The enclosed areas near the bottom of each panel represent the systematic uncertainty of the data.*

using QCD evolution equations yields good agreement between the various data sets.

Using the inclusive and semi-inclusive asymmetries obtained on polarised ^{1}H (1996) and ^{3}He (1995) targets, the first (preliminary) result for the polarisation of the u, d and sea quark distributions was obtained. From the data (shown in Fig. 2.3) it is seen that the u quarks are polarised parallel to the spin of the proton, which is partially cancelled by the negative polarisation of the d quarks. The polarisation of the sea quarks is –given the size of the uncertainties involved– consistent with zero. The precision of the data displayed in Fig. 2.3 is expected to improve considerably over the next years if the full (available) polarised ^{1}H data set is analysed, and new polarised ^{2}H data will be collected.

Charm production

As the spin of the quarks cannot account for the spin of the nucleon, it has been suggested that the gluons carry a significant fraction of the proton spin. As there are no charmed quarks in the nucleon, the production of a meson containing a charmed quark involves a gluon through the photon-gluon fusion process. Hence, the polarisation of gluons inside the proton can be studied by measuring the asymmetry of charm production with respect to the spin orientation of the target.

In order to exploit this idea we investigated whether charmed mesons can be identified in the HERMES data. For that reason searches for various charmed particles have been started. In Fig. 2.4 the results are displayed of a search for D^* mesons in the 1996 and 1997 data. As the branching ratio of $D^* \rightarrow D^0\pi^+$ is large (68.1 %), the mass difference between the observed $K^-\pi^+\pi^+$ system and the corresponding $K^-\pi^+$ system should centre at $M_{D^*} - M_{D^0} = 0.145$ GeV. The data show a clear peak at the expected value of the mass difference, indicating the production of charmed D^* mesons at HERMES.

The various upgrades mentioned above will increase the acceptance for charmed meson production such that the signals can be used to extract a value of the gluon polarisation in the nucleon.

The hadronic structure of the photon

The duration or - equivalently - the distance traversed by a hadronic $q\bar{q}$-fluctuation of the photon depends on the energy of the photon and on the mass of the fluctuation. At HERMES the fluctuation (or 'coherence') length l_c ranges from 1 to 6 fm, which happens to be commensurate with nuclear dimensions. As a result the hadronic structure of the photon can be probed by comparing data collected on a nuclear target and a hydrogen target.

The observable which has been measured as a function of l_c is the transparency of the nucleus T_A for ρ^0 me-

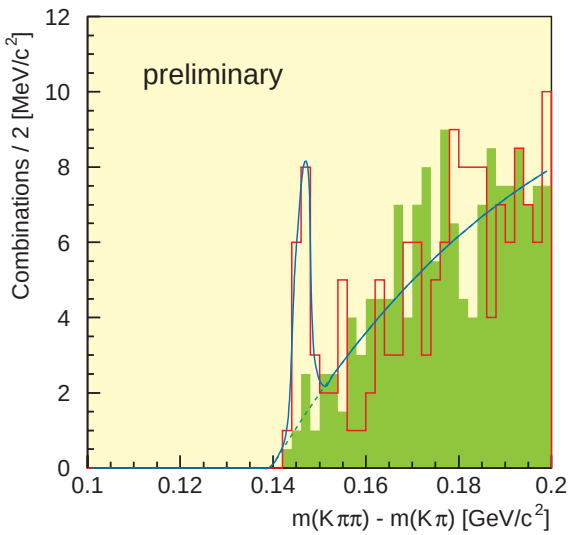

Figure 2.4: *The mass difference spectrum for D^* production at HERMES. The preliminary data are plotted as function of the difference between the mass of the observed $K^-\pi^+\pi^+$ system and the corresponding $K^-\pi^+$ system. The shaded area represents the background based on the same analysis using the wrong sign combination.*

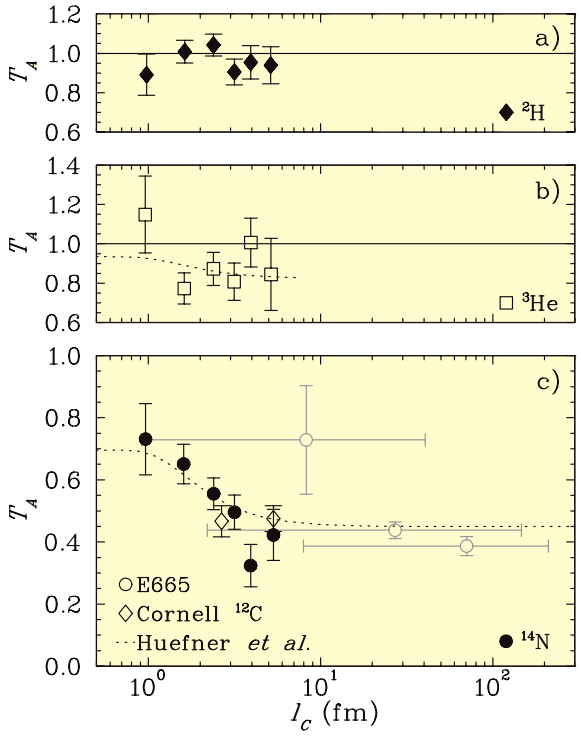

Figure 2.5: *Nuclear transparency T_A as a function of l_c for a) ^2H (filled diamonds); b) ^3He (open squares), and c) ^{14}N (filled circles) targets. The error bars include statistical and systematic uncertainties. Panel c) includes the data of previous experiments using photon (open diamonds) and muon (open circles) beams. The dashed curves represent Glauber calculations of Huefner and Kopeliovich for ^3He and ^{14}N.*

son production. The quantity T_A is obtained from the data by dividing the ρ^0 production cross section on nucleus A by A times the corresponding cross section for producing a ρ^0 meson on a nucleon.

The results, displayed in Fig. 2.5, show T_A measurements for ^{2}H, ^{3}He and ^{14}N. As expected the transparency for ρ^0 mesons decreases with increasing A. More importantly, T_A is seen to decrease with l_c. At $l_c \approx 1$ fm the transparency is only affected by the usual ρ^0-nucleus rescattering processes. At larger values of l_c the interaction between the $q\bar{q}$ fluctuation and the nucleus causes a substantial additional reduction of T_A, which saturates when l_c is about equal to the nuclear diameter (≈ 5 fm for ^{14}N). This qualitative interpretation of the data is quantitatively confirmed by a calculation of Huefner and Kopeliovich, shown as the dotted curve in Fig. 2.5.

Hadronisation in nuclei

In the hard scattering process of virtual photons from quarks inside the proton hadrons are formed. This hadronisation or fragmentation process can be studied by observing hadrons produced in deep-inelastic scattering on nuclear targets. The conditions for such studies are particularly favourable at HERMES, as the relevant length and time scales are commensurate with nuclear dimensions if the incident electron energies are near 25 GeV.

The attenuation of pions in nitrogen relative to deuterium has been measured at HERMES as a function of the energy transfer (ν) and the fractional energy transferred to the pion ($z = E_\pi/\nu$). The preliminary results are shown in Fig. 2.6 for two different ranges of z. The attenuation ratio R_A hardly depends on z, while it increases smoothly with ν. The dependence on ν is expected due to the Lorentz boost of the formation time. At large values of ν the formation occurs largely outside the nucleus, and therefore R_A approaches unity.

At small values of ν the influence of the nuclear medium is largest, and the data can be used to determine val-

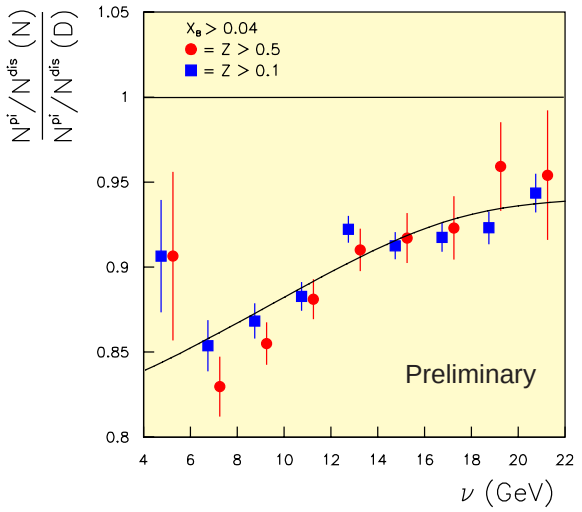

Figure 2.6: *Pion attenuation ratio R_A for semi-inclusive pion production on ^{14}N as a function of the energy transfer ν for two different cuts on z, the fractional energy carried by the pion. The curve represents a fit using a phenomenological formation time model.*

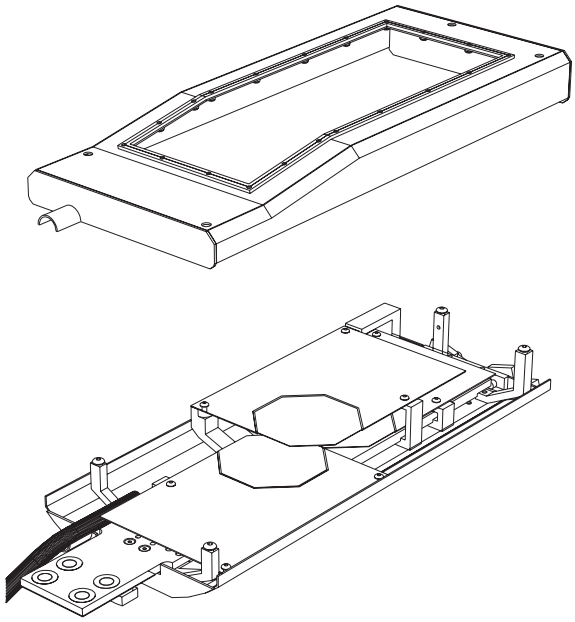

Figure 2.7: *Silicon test detector. The detector consists of three octagonal double-sided silicon detectors housed in a metal case to shield against RF effects. The cover plate (separately shown) has a fine mesh through which the particles pass on their way to the silicon detectors.*

ues of the hadron formation time τ_F using phenomenological models to describe the data in which τ_F is a free parameter. An example of such a fit is shown in Fig. 2.6.

2.4 The silicon detector project

The HERMES silicon detector project comprises three systems: (i) a Silicon test counter (STC), which was installed below the HERMES storage cell this spring; (ii) the Lambda Wheels (LW), which are presently under construction, and which will be installed in the spring of 1999; and (iii) the Recoil Detector (RD), of which the construction will start in the course of 1999. NIKHEF is responsible for both the STC and LW projects, which are described in more detail below. Other participants in the project are groups from Erlangen and St. Petersburg.

The Silicon Test Detector

In order to demonstrate the feasibility of silicon detection close to a high-intensity electron beam under ultra-high vacuum (UHV) conditions a test detector was built. A drawing of the system is shown in Fig. 2.7. The detector is made out of three octagonal silicon counters with 1 mm wide strips on each side. The strips are readout using an APC64 chip. Special care was needed to ensure that all materials used are UHV compatible. For that reason a special type of hybrid was developed consisting out of oxygen-free copper with a layer of kapton glued to each side. The copper ensures a good heat conduction which is important for cooling purposes, while the kapton layer is used for the electronic circuitry. The solution, which was shown to satisfy our vacuum requirements, has raised interest in the semi-conductor industry.

The individual silicon detectors were tested at the Erlangen Tandem accelerator, which provided low-intensity proton beams up to 8 MeV. The detectors and the readout system were shown to be operational, and the data could be used to calibrate the analogue output against the energy deposition.

Following the installation of the system below the HERMES storage cell the system has been operational for most of the remaining 1998 run. The break down of several APC readout chips due to electrostatic discharges made it impossible to use all detector planes. Nevertheless the remaining parts of detector gave sufficient information on the performance of the system to be able to conclude that it is possible to operate a silicon detector under these conditions.

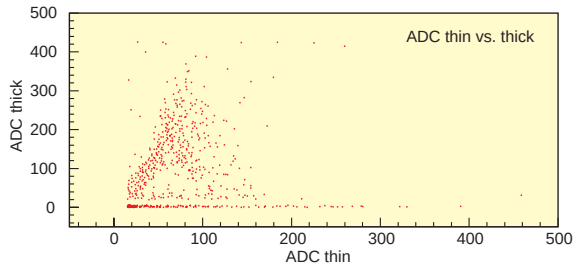

Figure 2.8: *Correlation between the analogue output of a thin and thick silicon counter of the STC. Three branches are observed, corresponding to particles stopping in the first layer (lower horizontal branch), particles stopping in the second layer (curved branch on the right) and particles passing both layers (straight branch on the left).*

An example of a $dE - E$ spectrum based on the output of a thin (140 μm) and thick (300 μm) silicon counter is shown in Fig. 2.8. The spectrum has the well-known triangular shape corresponding to particles stopping and/or passing in either detector. Although the final energy calibration is not yet available, a rough estimate shows that the observed signals correspond to recoil protons with momenta between 100 and 300 MeV/c. As the readout of the STC was triggered by a DIS event in the HERMES spectrometer, the data correspond to the first observation of slow recoil protons in deep inelastic scattering.

The Lambda Wheels

The Lambda Wheels are two wheel-shaped arrays of silicon strip counters which will be mounted inside the HERA electron beam vacuum approximately 50 cm downstream of the HERMES internal target. The Lambda Wheels will enlarge the acceptance for various semi-inclusive reaction channels by a factor of 2 - 4. Moreover, the precision of measurements of the Λ^0 polarisation will be greatly improved as the false asymmetries (which are large if the standard HERMES acceptance is used) essentially vanish with the Lambda Wheels.

The detector is made out of 12 modules, and has a outer diameter of about 35 cm. Each module (see Fig. 2.9) comprises 2 double-sided wedge-shaped silicon counters with the accompanying readout electronics. A computer aided drawing of the final design of the system is shown in Fig. 2.10.

In order to obtain the largest possible acceptance with minimal interference from support structures and readout electronics, the silicon counters are cut out of 6" wafers (while 4" is considered to be standard technology). The readout is based on the HELIX128 (v2.2) chip, which is also used in the ZEUS microvertex project. Apart from the cooling system (which is largely built by the St. Petersburg group) most of the components are under construction at NIKHEF.

In the spring of 1998 a technical design review (TDR) committee approved the design of the Lambda Wheels. Since then the basic design work has been finalised and the construction of the Lambda Wheels has started. By the end of 1998 many components had been manufactured, waiting for a complete assembly of the system in early spring 1999 at NIKHEF. Following several mounting and vacuum tests the installation is scheduled for May 1999.

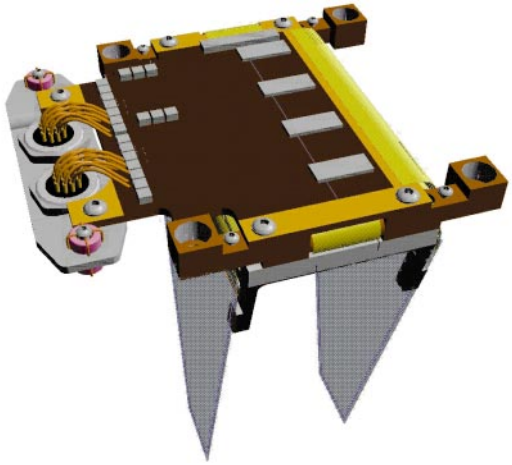

Figure 2.9: *Computer aided drawing of a single silicon module of the HERMES Lambda Wheels. As opposed to Fig. 2.10 the plate protecting the electronics on the hybrid is not shown. The curved kapton foils connecting the silicon counters themselves and the hybrid are visible on each side of the module.*

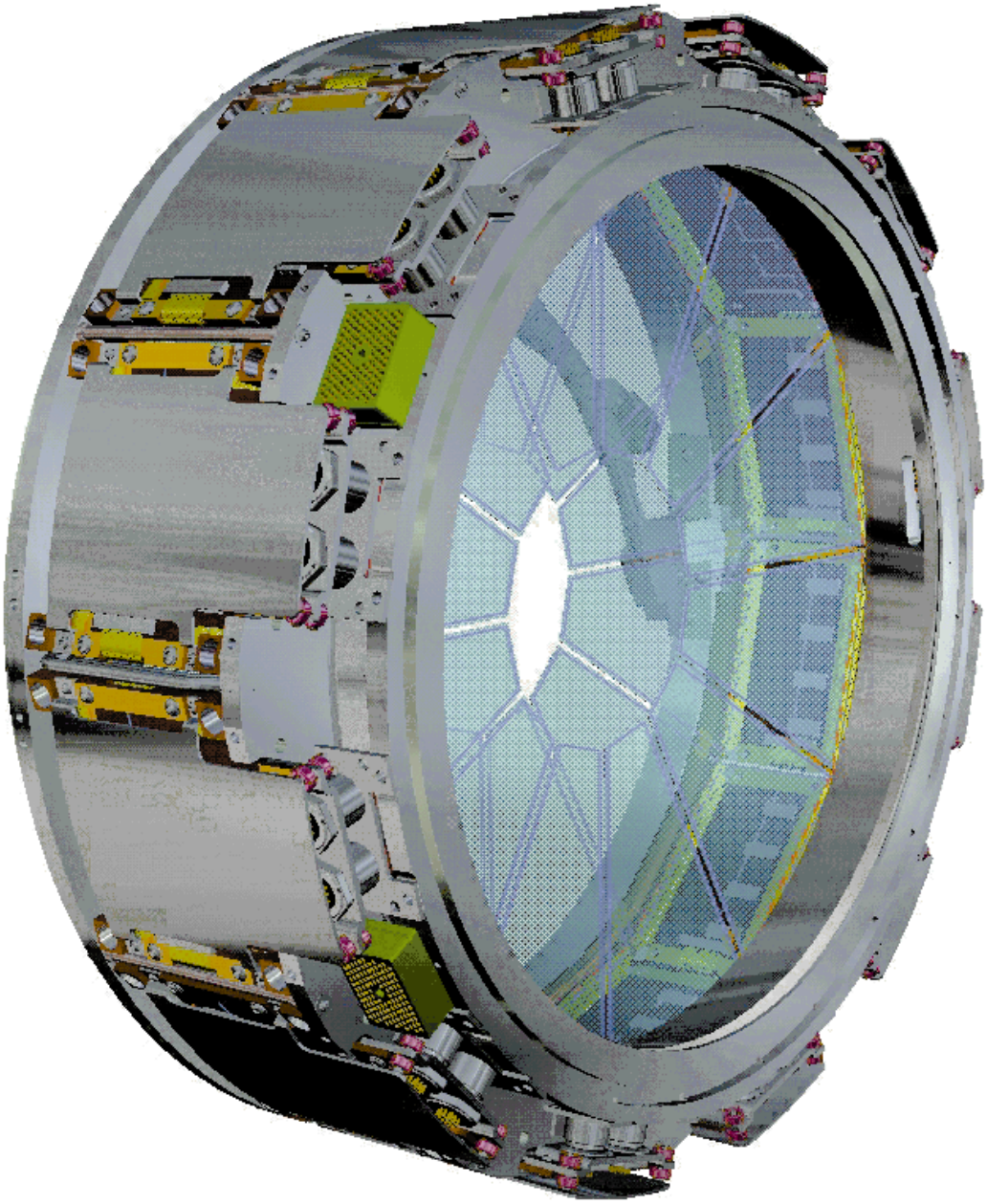

Figure 2.10: *The HERMES Lambda Wheels. The system consists of 12 wedge-shaped silicon modules, each comprising 2 silicon counters of 300 μm thickness with double sided readout. All support materials and readout electronics are located at the outer diameter of the system such as to stay clear of the standard HERMES spectrometer acceptance.*

3 ZEUS

3.1 Accelerator and Detector Operation

For the 1998 running period the HERA accelerator has resumed electron-proton operation. In 1994 it had been recognised that the beam lifetime for positrons was substantially better than for electrons. Since then, HERA has been operated with positrons. During the long winter shutdown 1997/1998 the integrated ion getter pumps in the dipole magnets were replaced by non-evaporating getter pumps in order to ensure a lifetime for electrons similar to that for positrons. Another important and successful modification affected the proton beam: the beam energy was increased from 820 to 920 GeV leading to higher cross sections for rare processes. Although the electron beam lifetime has reached the nominal value, the experiments have been suffering from background problems generated by HERA. Therefore, data taking efficiency is still somewhat lower than expected. The 1998 run lasted four months. HERA delivered an integrated luminosity of 8 pb^{-1}, of which 4.4 pb^{-1} was useful for data taking. A total of 8.2 million triggers were collected.

3.2 Physics Analysis

Deep Inelastic Scattering

The study of deep inelastic scattering (DIS) and the measurement of the proton structure functions in a new kinematic domain has contributed new and unique knowledge about parton momentum densities in the proton and their dynamical evolution.

More data and better understanding of the systematics allow a further refinement and extension of these measurements.

Low Q^2 Deep Inelastic Scattering

During 1998 the measurement of the proton structure function F_2 at relatively low Q^2 was finalised. The relevant kinematical variables for this study are the four momentum transfer Q^2 mediated by the exchanged boson and x, the fraction of the four momentum of the proton carried by the struck quark or gluon.

The main interest of the measurement in this kinematical domain is the study of the transition from a region in Q^2 where perturbation theory applies to a region where that might not be the case. The analysis of these data show that the NLO QCD fits give a good description of the F_2 data down to Q^2 values of 1 GeV^2 (see Fig. 3.1).

As a result of a full NLO DGLAP QCD fit to these

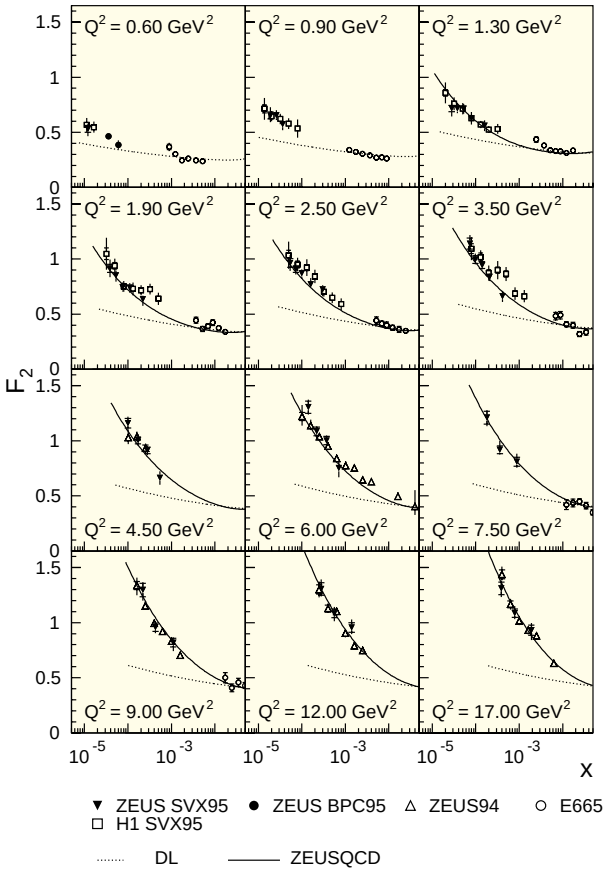

Figure 3.1: *Low Q^2 data samples plotted for different Q^2 bins as a function of x. The curves shown are (dotted) the Donnachie-Landshoff (DL) Regge model and (full) the ZEUS NLO QCD fit.*

data it is found that at the lower Q^2 limit of the fit the $q\overline{q}$ sea distribution is still rising towards small x values, whereas the gluon distribution is strongly suppressed (see Fig. 3.2). From the standard ZEUS QCD fits we also obtain a much improved determination of the gluon momentum density compared to previous measurements by ZEUS. As shown in Fig. 3.3 the total fractional error on the gluon density for Q^2=20 GeV^2 and x=5.10^{-5} is only 10%.

e^+p scattering at high x and Q^2

The high Q^2 kinematical region allows precision measurements of electron-quark interactions in a new domain and constitutes a new challenge to the Standard Model (SM). The data collected during the years 1994-

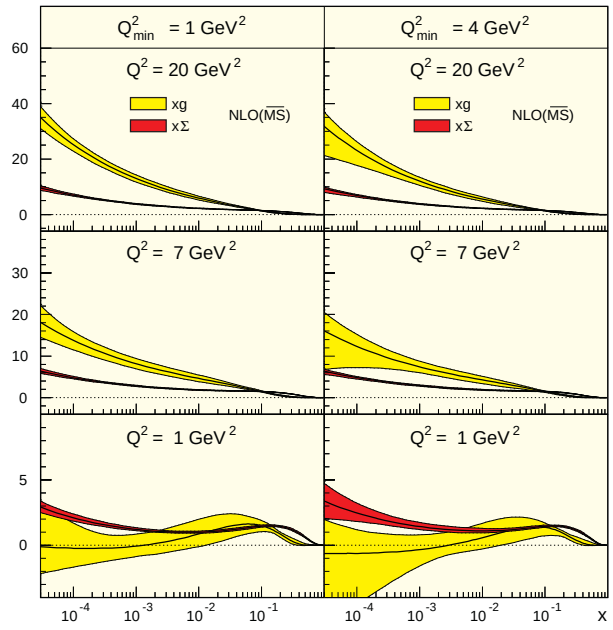

Figure 3.2: *The quark singlet momentum distribution (sum over all quark and anti-quark distributions), $x\Sigma$ (dark shaded), and the gluon momentum distribution, $xg(x)$(light shaded) as function of x for three Q^2 values. The three left hand plots show the results from the NLO QCD fits including data with Q^2 >1 GeV^2; the three right hand plots the corresponding results including data from Q^2 >4 GeV^2 onwards.*

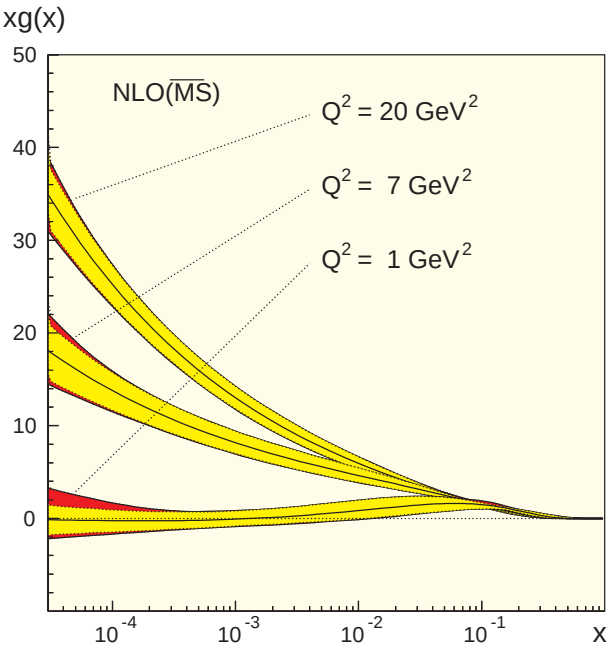

Figure 3.3: *The gluon momentum distribution $xg(x)$ as a function of x at fixed values of Q^2. The light shaded area represents the error on the data and input parameters, the dark shaded bands include the parametrisation errors.*

1996 showed more events than expected from the SM at high Q^2 and high x values, a phenomenon observed both by ZEUS and by the counterpart experiment H1. The statistical significance of the excess was, however, not very big. The data of the 1997 run have now been added, doubling the available statistics, which now corresponds to an integrated luminosity of 46.5 pb^{-1}. For the neutral current (NC) interaction ($e^+p \rightarrow e^+ + X$) about 500 events are observed with Q^2> 5000 GeV^2, and about 150 for the charged current (CC) interaction ($e^+p \rightarrow \overline{\nu}_e + X$). Figure 3.4 [A] shows the differential cross section for the CC events and Fig. 3.4 [B] for the NC events, both as a function of Q^2 integrated over all x. Also the results of the calculations based on the Standard Model are shown. The uncertainties in the predicted cross section originating from the parton momentum distributions have been studied in great detail and result in an error of less than 10% for Q^2 > 400 GeV^2. The data agree very well with the Standard Model predictions based on parton densities extracted at low Q^2 and do not leave much room for speculations on the validity of the model.

3.3 Photon structure

Dijet photoproduction at HERA provides information on the structure of the photon. Dijets are produced via the interaction of a photon with a constituent of the proton. HERA data have confirmed the QCD prediction that one clearly can distinguish the production of dijets either by a pointlike photon or by a resolved photon. For this purpose the quantity x_γ, the energy fraction of the photon which participates in the interaction, is calculated from the kinematics of the dijet event. We have measured the dijet cross section as a function of the transverse energy and pseudorapidity of the jets, demanding a transverse energy for the first jet bigger than 14 GeV and for the second bigger than 11 GeV.

The cross sections are very sensitive to the precise knowledge of the jet energy. A detailed study of data and Monte Carlo events has provided a correction procedure of the hadronic energy measurement which results in an error of less than 3% of the jet energy. Because of the high cut on E_t we expect a good description of the data by NLO QCD calculations. Input to

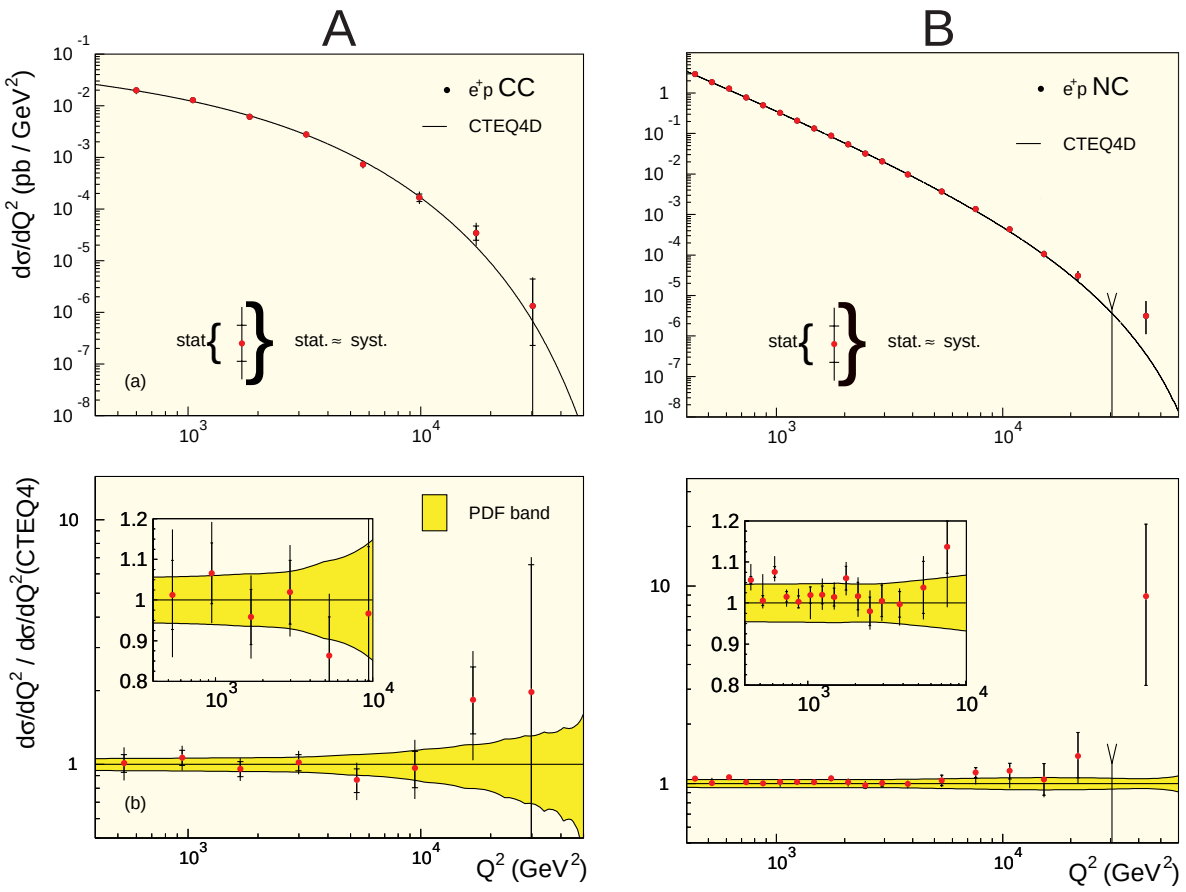

Figure 3.4: *The high Q^2 e^+p charged [A] and neutral [B] current DIS differential cross section as a function of Q^2, compared with the Standard Model expectation evaluated using the CTEQ4D parton density functions. The plot below shows the deviation between data and model; the shaded area indicates the uncertainty in the model expectation.*

these calculations are the parton densities in the proton (measured by HERA) and the parton densities in the photon, the knowledge of which is mainly based on data obtained with e^+e^- colliders at low x_γ values. Figure 3.5 shows the result for the angular correlation of the jets for a subset of the events for which the γp centre of mass energy is in the range 212-277 GeV, a region where the sensitivity to the photon structure is large. A clear disagreement between data and calculation is observed. The disagreement is seen for the full x_γ region and to a lesser extent in the high x_γ region. Parametrisations of the quark and gluon densities in the photon have to be updated to fit the data to the NLO QCD calculations.

3.4 ZEUS MicroVertex Detector project

The Zeus experiment will be upgraded with a new vertex detector (MVD) during the year 2000, when the HERA accelerator will be partly modified to increase the luminosity by a factor of five. The detector will allow the reconstruction of secondary vertices originating from the decay of long lived particles (charm, beauty) and will improve considerably the pattern recognition and momentum measurement of charged particles produced at the primary interaction point.

Support structure

NIKHEF has finished the design of the support structure and the prototyping of carbon fibre construction

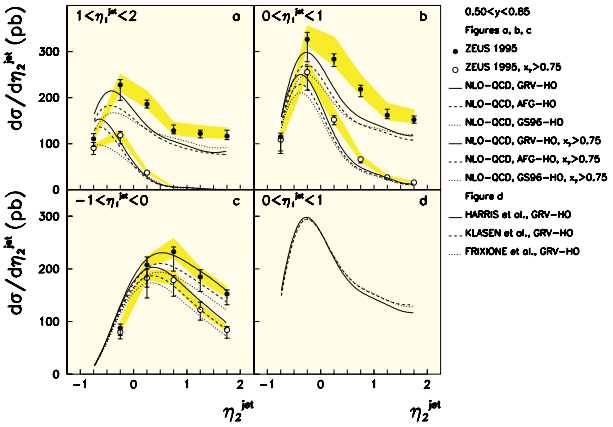

Figure 3.5: *Inclusive dijet cross section as function of the pseudorapidity of the two jets. Data are compared with NLO QCD calculations. Figure d shows the result of the calculation by three different groups using the same parametrisation for the photon structure.*

elements. Crucial for the performance of a vertex detector is the minimisation of construction material ensuring at the same time a rigid support structure to profit optimally from the precise position information provided by the silicon detectors.

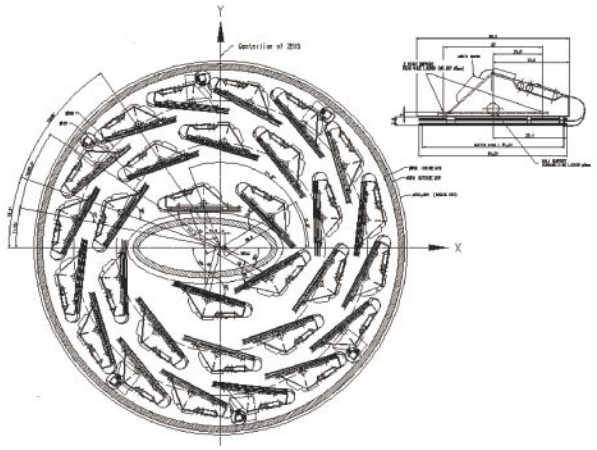

Figure 3.6: *Cross-sectional view of the layout of the silicon detectors in the barrel region; support structures and beampipe are also shown; the diameter of the outer cylinder support structure is 320 mm.*

Figure 3.6 shows the layout of the central barrel region of the MVD in cross section. Note also the elliptical beampipe with the asymmetric position of the beam in order to keep the synchrotron radiation inside the beampipe. Three double layers of single-sided silicon

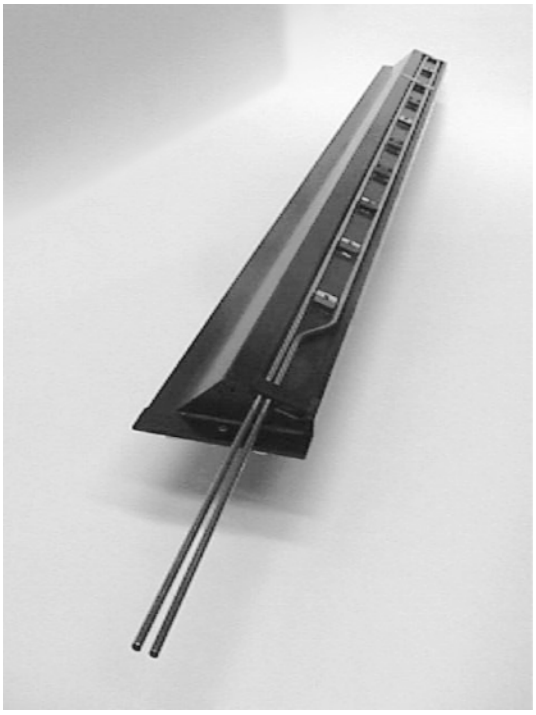

Figure 3.7: *Carbon fibre structure to support silicon detectors. Water cooling for the electronics is provided via the tube.*

strip detectors surround the interaction point. In addition, four double layers arranged in circles perpendicular to the interacting beams are mounted in the proton direction. Each layer in the barrel region is supported by a carbon fibre ladder structure; Fig. 3.7 shows an example. The overall support for the ladders (30 in total) is a cylindrical carbon fibre shell. A prototype of one half is shown in Fig. 3.8.

Silicon detectors and readout

The silicon strip detectors (64 mm x 64 mm) are single sided and have integrating coupling capacitors. The readout pitch is 120 μm and the intermediate strip pitch is 20 μm. Figure 3.9 shows about 1 x 1 mm^2 of the edge of a detector where many of the elements of the detector layout can be recognised. A first batch of twenty prototype detectors has recently been received. First (beam) tests have shown that the design specifications are met and that a 10 μm position resolution can be obtained. The development of high leakage currents in some of the detectors is still a worry and requires clarification before the production can start.

The detector signals are read out by HELIX, an analog

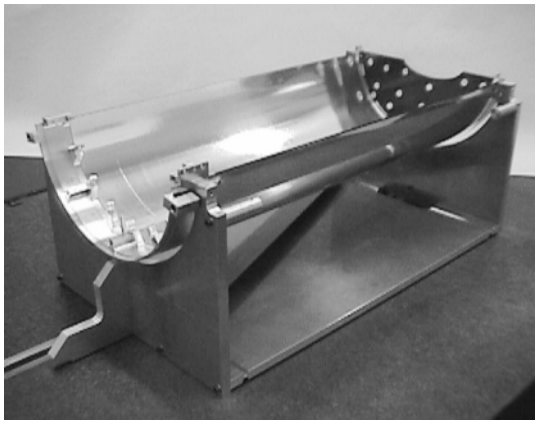

Figure 3.8: *Half of the barrel carbon fibre sandwich structure to support the MVD.*

chip initially designed by ASIC laboratories in Heidelberg and manufactured in the 0.8 μm CMOS process by the company AMS. The NIKHEF electronics department has contributed to the debugging of the chip and has implemented a fail-safe token feature which allows the exclusion of a bad chip in the readout chain without perturbing the functioning of the remaining chips in the chain. The final chip layout, HELIX 3.0, was submitted for a prototype production run in December.

Pattern recognition

A first version of a stand alone reconstruction program for the MVD has been produced. It has been coded in C++ and uses the Kalman filtering technique of combined track finding and track fitting.

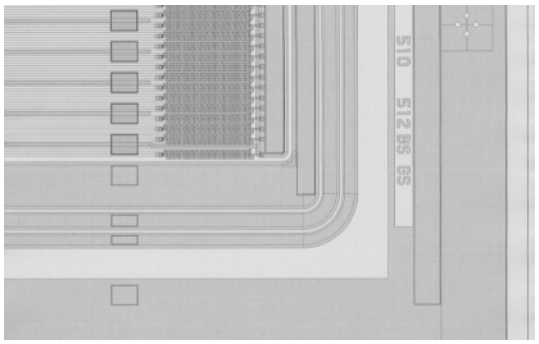

Figure 3.9: *Layout of a corner of a silicon detector; visible are the guard rings, probe pads on the readout strips and the bias line connected to the strips via polysilicon resistors.*

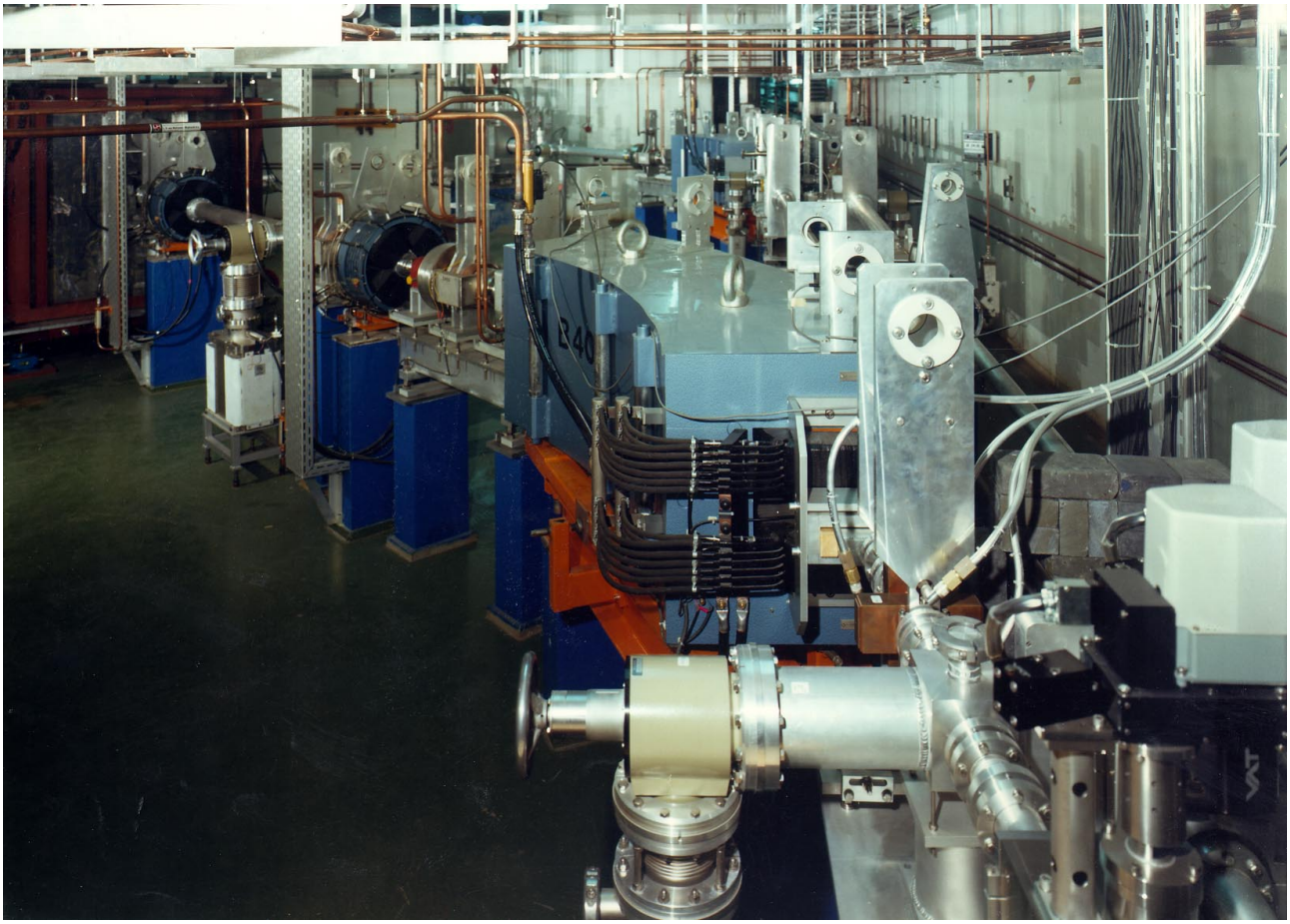

Overview of the deflection system AFBU (photo: NIKHEF)

4 SMC

4.1 Introduction

The Spin Muon Collaboration (SMC) studied the spin structure of the nucleon in deep inelastic scattering of high energy muons of 100 and 190 GeV in the experiment NA47 at CERN. The measurements by the SMC started in 1991 and were completed in the fall of 1996.

In 1998 we finished a next-to-leading order QCD analysis of the structure functions g_1^p and g_1^d for the world data including those of SMC. A new analysis of the spin asymmetries A_1^p and A_1^d for very small values of the Bjorken scaling parameter x, in the range of 10^{-4} to 10^{-3}, was performed. Final results for the beam polarisation measurements by means of (a) the positron spectrum from muon decay, and (b) the muon scattering from polarised electrons in a magnetised foil, were obtained. Our experience with the SMC polarised target, the worlds largest polarised proton and deuteron target, was documented in a comprehensive report. With the work reported here the activities in the frame of the SMC have come to an end.

4.2 Results

Spin dependent structure functions

The spin dependent structure function $g_1(x, Q^2)$ was determined from the measured spin asymmetry $A_1(x, Q^2)$ and a parameterisation of the structure functions F_2 and R. Fig. 4.1 shows the world data of $g_1(x, Q^2)$ for proton, deuteron, and neutron, and the results of our next-to-leading order QCD analysis of these data using two computer programs based on the $\overline{\text{MS}}$ factorisation scheme.

First moments and sum rules

The first moments $\Gamma_1 = \int_0^1 g_1(x)\mathrm{d}x$ were determined at the average Q^2 of the SMC measurements, $Q_0^2 = 10$ GeV^2. The measured contributions to the first moment of g_1 for the proton and the deuteron in the range $0.003 < x < 0.7$ were found to be $I_m^p = 0.131 \pm 0.005 \pm 0.006 \pm 0.004$ and $I_m^d = 0.037 \pm 0.006 \pm 0.003 \pm 0.003$, where the errors are statistical, systematic, and due to the QCD evolution, respectively.

The contributions of the unmeasured ranges were obtained by the parton distributions resulting from the QCD analysis. The results for the first moments are $\Gamma_1^p = 0.120 \pm 0.005 \pm 0.006 \pm 0.014$ and $\Gamma_1^d = 0.019 \pm 0.006 \pm 0.003 \pm 0.013$. Both values violate the Ellis-Jaffe predictions. Taking into account the D-state of the deuteron $\Gamma_1^p + \Gamma_1^n = 2\Gamma_1^d/(1 - \frac{3}{2}\omega_D)$, where $\omega_D = 0.05 \pm 0.01$, we find $\Gamma_1^p - \Gamma_1^n = 0.198 \pm 0.023$, in agreement with the theoretical value of the Bjorken sum rule 0.183 ± 0.003 at $Q_0^2 = 10$ GeV^2.

In Fig. 4.2 the first moments of proton, deuteron, and neutron are shown together with the Ellis-Jaffe and Bjorken sum rule predictions. The largest contribution to the uncertainties of the first moments is due to the extrapolation for the unmeasured low x region. This contribution and the different values of Q_0^2 account for the appearance of slightly smaller error bars for the SMC data alone, despite the superior statistics of the SLAC experiments at large values of x.

Spin asymmetries at small x

New results were obtained from an analysis of data obtained with a dedicated trigger involving a hadron requirement which strongly reduces the background at low x. The results are presented in Fig.4.3. In the overlap region of the low x trigger the results are consistent with those for the standard inclusive triggers. In the newly accessed low x and low Q^2 region the asymmetries A_1^p and A_1^d are consistent with zero.

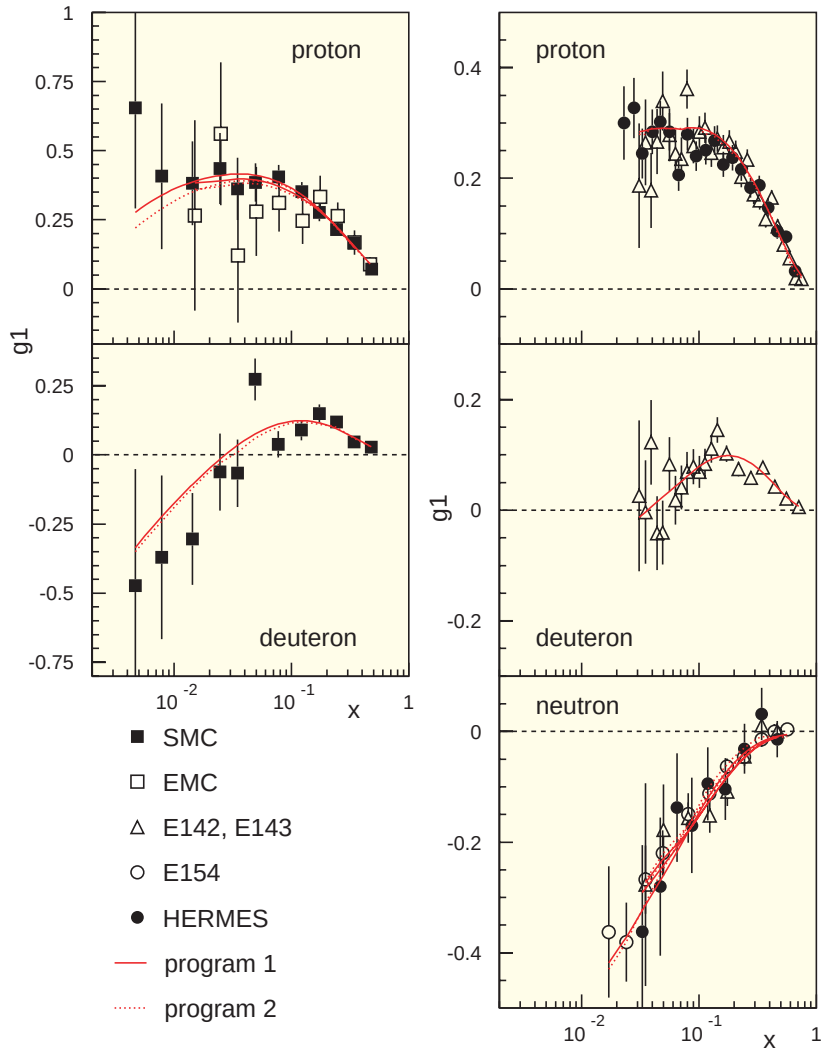

Figure 4.1: *The structure function $g_1(x)$ for the proton, deuteron, and neutron, obtained in the EMC and SMC experiments at a typical beam energy of 200 GeV, and in the SLAC and HERMES experiments at beam energies between 20 and 50 GeV. For the corresponding regions in x and Q^2 of the experiments the results of two QCD-fit programs are shown by the solid and dotted curves.*

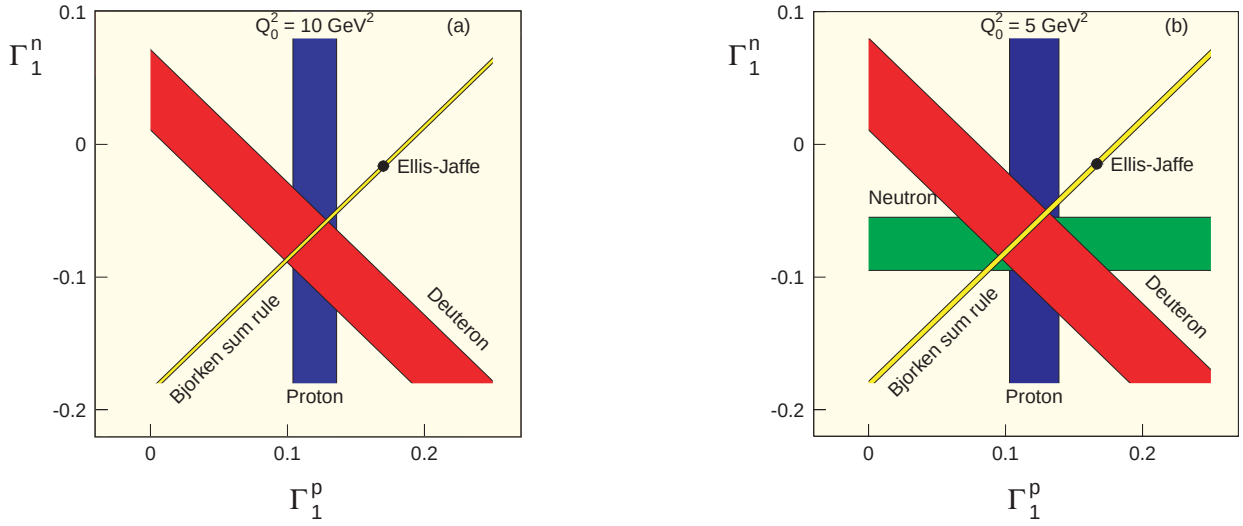

Figure 4.2: *The first moments Γ_1 for the proton and deuteron of (a) the SMC data at $Q_0^2 = 10$ GeV^2 and (b) the world data at $Q_0^2 = 5$ GeV^2 compared with the Bjorken, and Ellis-Jaffe predictions. The parallel lines enclose the regions of the measurements and the predictions within one standard deviation of their total errors.*

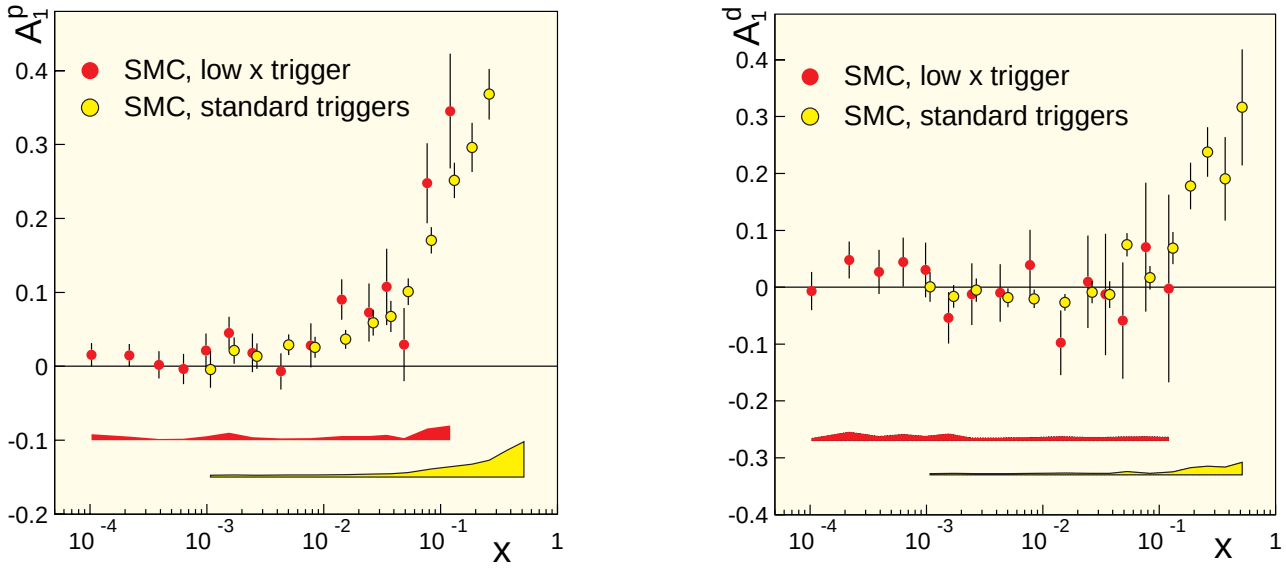

Figure 4.3: *The preliminary asymmetry A_1 for the proton and for the deuteron as a function of x at the measured Q^2 obtained with the low x trigger (filled circles) and with the standard triggers (open circles). The shaded bands indicate the size of the respective systematic errors.*

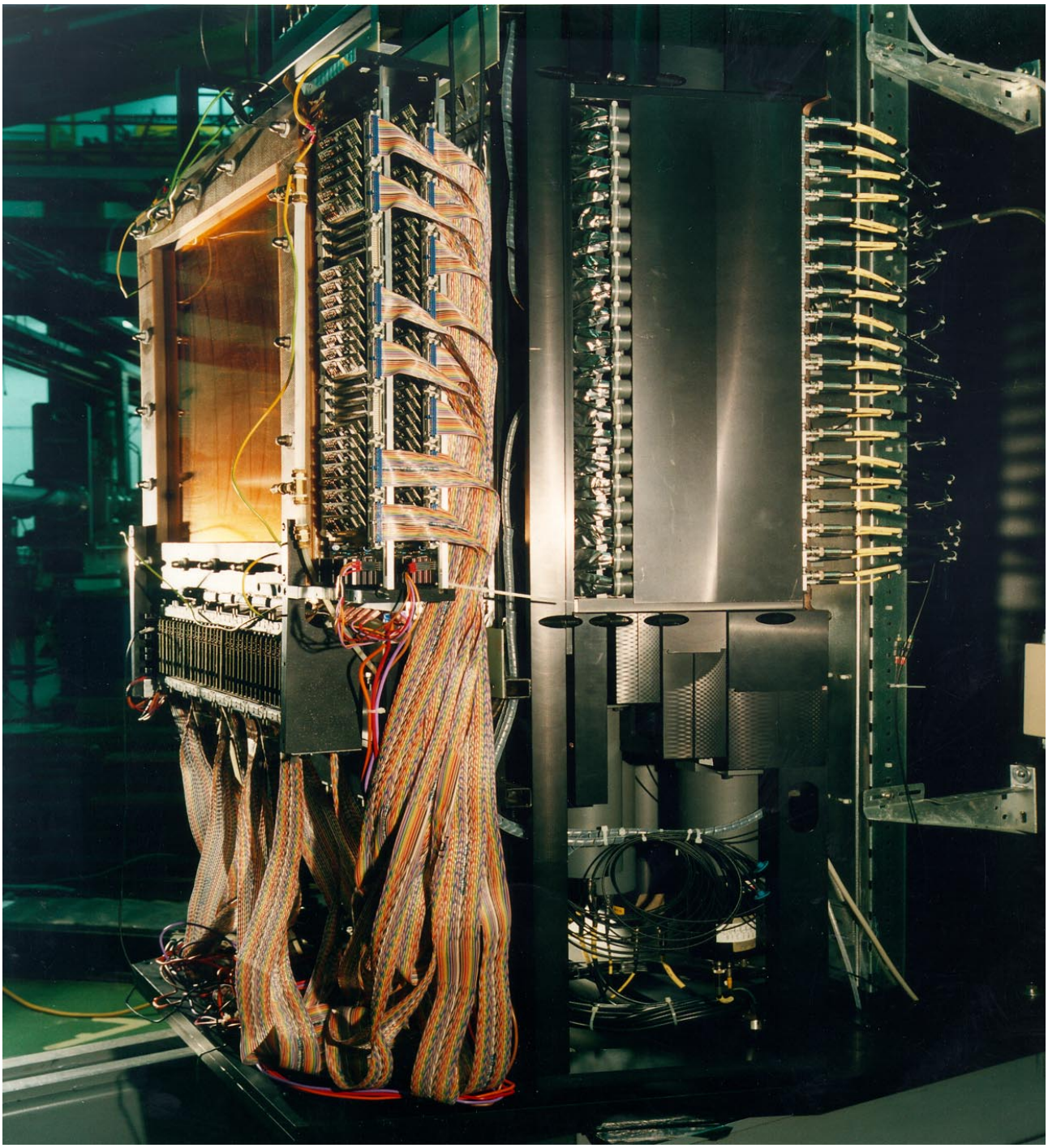

The HADRON detector (photo: Han Singels)

5 DELPHI

5.1 Data taking and detector status

LEP had a very successful year of running. After the installation of an additional 32 superconducting RF cavities, bringing the total to 272, the total energy of LEP could be raised to 189 GeV. LEP delivered record luminosities: peak values up to 10^{32} cm^{-2}s^{-1}, an average integrated luminosity of 196 pb^{-1} at 189 GeV and an additional 3 pb^{-1} at the Z^0 energy for detector calibration/alignment. There was some imbalance in the luminosities delivered to the 4 experiments. DELPHI collected a total of 158 pb^{-1} with an average data taking efficiency of 85%.

No major intervention was done on the DELPHI detector during the 1997/98 winter shutdown. A very good alignment of the Silicon Vertex Detector was therefore already available soon after the 2.5 pb^{-1} of Z^0 data taken in May. This alignment remained very stable over the year. New, improved tracking in the forward direction was available, with single points from the Very Forward Tracker included in the track search. The reprocessing of the 1998 data was completed beginning of December, with the corresponding production of Monte Carlo data samples arriving shortly after.

During the 1998/99 shutdown, a last set of 16 superconducting cavities (288 in total) has been installed, giving a 'design' maximum of 3060 MV of acceleration voltage. This will raise the LEP energy to 192 GeV, operating the superconducting cavities at the nominal value of 6 MV/m. The plan is to push the operating voltage to 7 MV/m, which would bring the total energy to 200 GeV.

5.2 Selected research topics

19 papers were published in physics journals by the DELPHI Collaboration in 1998, 10 of which were based on data collected at LEP II energies. A similar ratio between LEP I and LEP II results could still be seen in the 80 contributed papers to the Vancouver ICHEP98 conference. A few recent subjects, with contributions from our NIKHEF group, will be mentioned here.

The measurement of the W pair production cross section continued for the data taken at 183 GeV and 189 GeV. At 183 GeV a total of 408 events in the fully-hadronic, 303 events in the semi-leptonic and 59 events in the fully-leptonic final state were selected. The data are in agreement with lepton universality and the leptonic branching fraction Br($W \to \ell\nu$) is measured to be $0.1076 \pm 0.0052(stat) \pm 0.0017(syst)$, in agreement

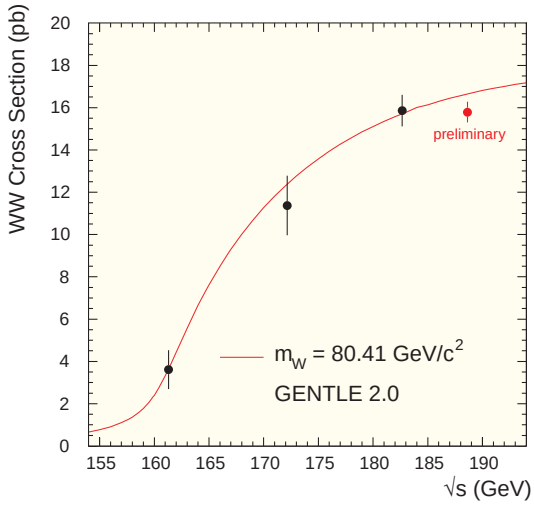

Figure 5.1: *W^+W^- cross section as a function of the centre-of-mass energy. The curve is the Standard Model prediction for $m_W = 80.41$ GeV/c^2.*

with the Standard Model expectation of 0.108. The total cross section for WW production at 183 GeV is determined to be $15.86 \pm 0.69(stat) \pm 0.26(syst)$ pb. This result is plotted in Fig. 5.1, together with a preliminary value for the cross section at 189 GeV (1998 data), based on a sample of 2434 events. The measurements at 183 GeV and lower energies agree well with the Standard Model prediction. If one takes into account a 2% theoretical error on the prediction, the 189 GeV data point agrees within 1.5 standard deviation with the Standard Model value.

The measurement of the leptonic W branching ratio, i.e. the corresponding hadronic branching ratio, can be used to extract the element $|V_{cs}|$ of the Cabibbo-Kobayashi-Maskawa (CKM) matrix. Using the 183 GeV data and the world average of the measurements of the other CKM matrix elements, this gives $|V_{cs}| = 0.985 \pm 0.073(stat) \pm 0.025(syst)$, which is already a big improvement with respect to existing measurements based on the $D \to \bar{K} e^+ \nu_e$ decay. A more independent value of $|V_{cs}|$ can be obtained by measuring directly the branching fraction Br($W \to c\bar{s}$). DELPHI is well suited for this measurement, as the c quarks are tagged with a precise measurement of non-zero impact parameters of tracks and the s quark is tagged, using the RICH detectors, through the presence of kaons in the s quark jets. Using the flavour tagging in all W pairs collected

in 1996 and 1997 at energies 161-183 GeV yielded a value $|V_{cs}| = 1.01^{+0.12}_{-0.10}(stat) \pm 0.010(syst)$.

The measurement of the W mass from direct reconstruction of the invariant mass of its decay products continued using the data collected at 183 GeV in 1997. The analysis in the semi-leptonic final states is similar as done last year for the 172 GeV data. The mass distributions for the $WW \to q\bar{q}e\nu$ and $WW \to q\bar{q}\mu\nu$ final states are shown in Fig. 5.2. The W mass itself is extracted from a combined likelihood fit, taking for each event into account the mass and error obtained from a constrained fit imposing momentum and energy conservation and equal masses for the two W's. The equal-mass distribution for the fully-hadronic events is also shown in Fig. 5.2. The analysis method in this final state (the *ideogram* method) however, has been further developed in two dimensions. The two W's are no longer constraint to have equal mass. For each event and every possible jet pairing, a two-dimensional probability is calculated that this particular pairing corresponds to two objects with mass m_1 and m_2, taking again the event mass errors into account, as well as the measured jet charges and W production angles and, in case of the 3-jet pairing in a 5-jet event, the transverse momentum of the third jet with respect to the other two. This procedure was then applied using three different jet clustering algorithms and the resulting ideograms added with equal weights. Examples of such a two-dimensional probability ideogram for a 4-jet and a 5-jet event are shown in Fig. 5.3. The final event likelihood is obtained by convoluting the two-dimensional ideogram with the product of two relativistic Breit-Wigner distributions.

An important point in the fully-hadronic events is the possibility of final state interactions: Bose-Einstein correlations among identical bosons in the final state and Colour Reconnection effects among the partons from the two colour-singlet systems. Both of these effects might shift the apparent W mass and have been extensively studied by doing the full W mass analysis on event samples generated with a number of Bose-Einstein and Colour Reconnection models incorporated in the DELPHI simulations.
The analysis on 183 GeV data (1997) is completed and a journal paper is in preparation. No significant difference is observed in the resulting m_W obtained from the semi-leptonic and fully-hadronic final states. The combined result from the semi-leptonic and fully-hadronic final states is $m_W = 80.27 \pm 0.15(stat) \pm 0.05(syst)$ GeV/c^2, almost a factor 3 improvement with respect to the result obtained from the data at 172 GeV in

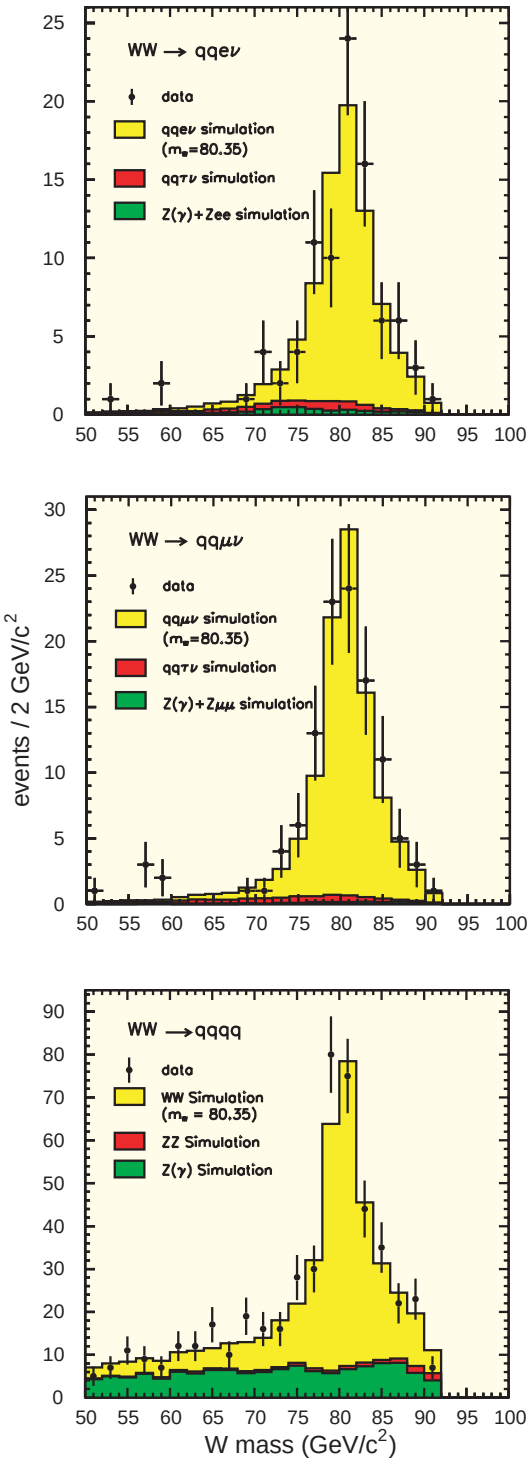

Figure 5.2: *The distributions of the reconstructed masses for the semi-leptonic (top and centre) and fully-hadronic (bottom) channels.*

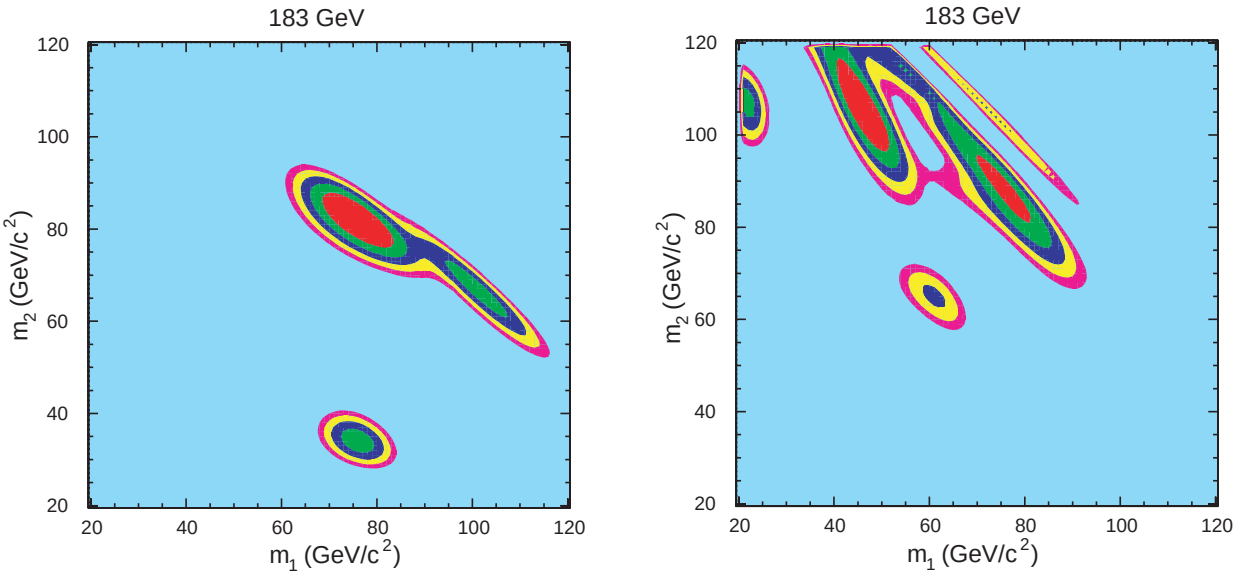

Figure 5.3: *Examples of two-dimensional probability ideograms for a 4-jet (left) and a 5-jet (right) fully-hadronic event. The first five sigma contours are given.*

1996. Also the W width has been measured in the two different final states and the combined result is $\Gamma_W = 2.33 \pm 0.47(stat) \pm 0.14(syst)$ GeV/c^2. The analysis of the 189 GeV data (1998) is in progress. The expected (statistical) error on the W mass from these data is 0.09 GeV/c^2.

The cross section for $e^+e^- \rightarrow ZZ$ production is expected to rise from 0.3 pb at 183 GeV to 0.7 pb at 189 GeV and is therefore an important background for Higgs production $e^+e^- \rightarrow HZ$ (or hA). One of the possible final states is 4-jets, where in the case of HZ production preferentially two of the jets are from the b-quarks of the Higgs decay. However, also the Z decays into $b\bar{b}$. The search and analysis for HZ and ZZ production therefore proceeds along the same line and depends crucially on b quark tagging in order to suppress the 4-jet WW background. An analysis for $ZZ \rightarrow q\bar{q}q\bar{q}$ uses the same two-dimensional ideogram probability as used in the 4-jet W mass analysis, calculating for each event the probability that the event is WW, ZZ or a 4-jet QCD event. The calculation of these probabilities uses the relative production cross sections, the jet-jet invariant mass information and their compatibility with the W or Z mass, and the b-tag probabilities. The normalised ZZ probability distribution is shown in figure 5.4. A rather pure sample of ZZ candidates can be selected by demanding this ZZ probability to be greater than 0.55. The equal-mass distribution of these events is also shown in Fig. 5.4.

The Standard Model Higgs is searched for in channels with 4 jets, 2 jets + 2 leptons and 2 jets + missing energy (where the Z decays into a pair of neutrinos). The reconstructed mass of the Higgs candidates is obtained from constrained fits. The final 95% CL lower limit on the SM Higgs mass obtained from the 183 GeV data is 85.7 GeV/c^2. Fig. 5.5 shows the distribution of the reconstructed mass from the 189 GeV data, compared to the sum of the expectations for all channels. Also shown is the expected contribution (dashed histogram) from HZ production for a Higgs mass of 95 GeV/c^2. The data are still in good agreement with the SM expectation *without* production of HZ. The preliminary value of the 95% CL lower limit on the Higgs mass from the 189 GeV data is 95.2 GeV/c^2.

The measurement of the forward-backward asymmetry of the strange-quark decays of the Z^0 (see also the 1997 Annual Report) has now been completed using all data from the years 1992-1995. The results were reported in a contributed paper to the Vancouver conference and the final journal paper is in preparation. The s quark pole asymmetry (see Fig. 5.6) is measured to be $A^0_{s\bar{s}} = 0.108 \pm 0.015(stat) \pm 0.007(syst)$. The corresponding value for the effective weak mixing angle is $\sin^2\theta^{lept}_{eff} = 0.2307 \pm 0.0029$. The s quark asymmetry value is in agreement with the measured pole asymme-

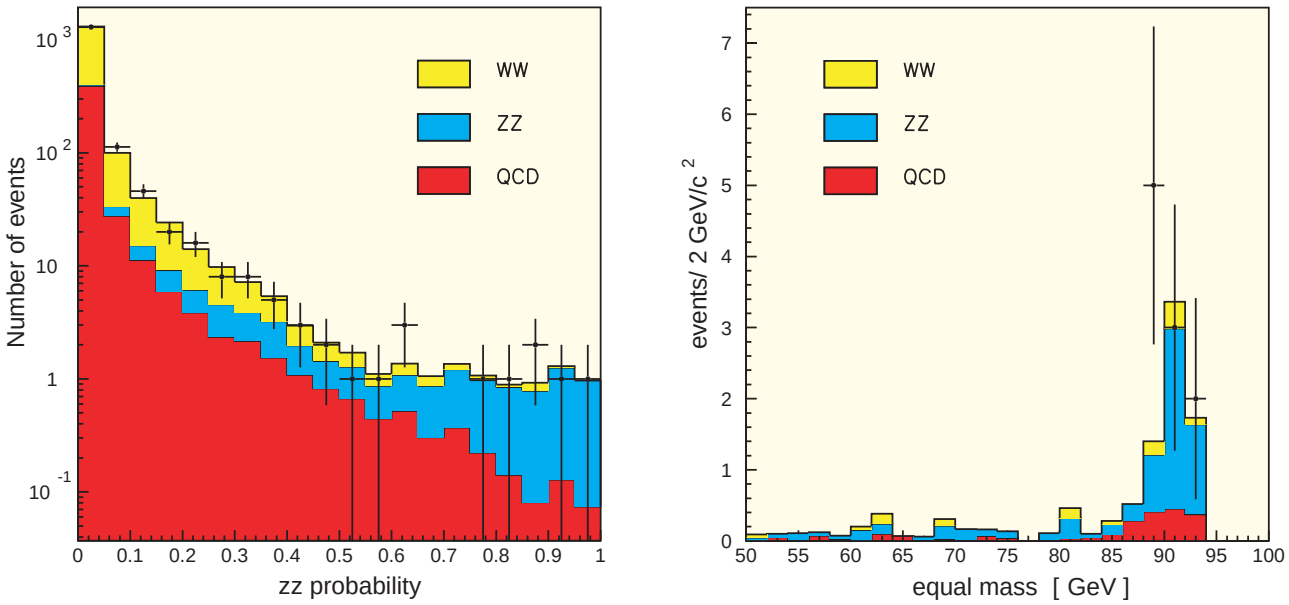

Figure 5.4: *Distribution of the ZZ probability in 4-jet events at 189 GeV (left) and of the equal-mass distribution (right) of the events with ZZ probability greater than 0.55.*

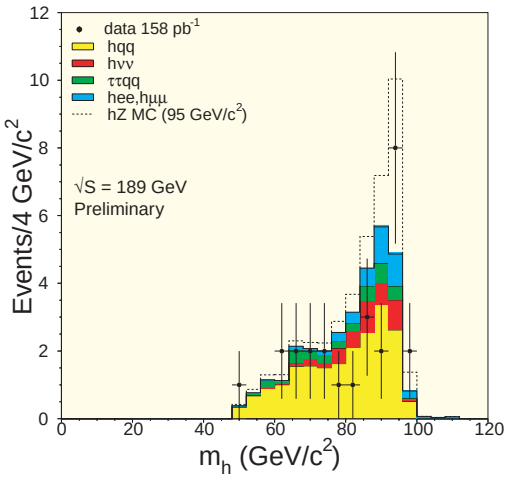

Figure 5.5: *Reconstructed mass spectrum of Higgs candidates in the 189 GeV data (1998).*

try for b quarks, supporting the hypothesis of flavour independence of the asymmetry for bottom and strange quarks.

The most precise measurement of the CKM matrix element $|V_{ub}|$ can be obtained from the measured branching ratio for the decay $b \to u\ell\nu$. Earlier measurements of $|V_{ub}|$ have been done using the rate of leptonic B decays with lepton momentum above the kinematic endpoint for $b \to c\ell\nu$ decays and also from exclusive branching ratio measurements of $B \to \pi\ell\nu$ and $B \to \rho\ell\nu$ decays. There is however a significant model dependence in these extractions of $|V_{ub}|$. Another possibility, with less model dependence, is to measure $|V_{ub}|$ from the shape of the invariant mass spectrum of the hadronic system recoiling against the lepton in $b \to u\ell\nu$ transitions. Using data collected at the Z^0 pole between 1993 and 1995, DELPHI has measured the ratio $|V_{ub}|/|V_{cb}|$ from a fit to the shape of the full spectrum of the lepton energy E_ℓ^* in the B rest frame for semi-leptonic B decays with a reconstructed hadronic invariant mass M_X smaller than the D mass. Using the secondary vertex topology and identified kaons in the final state, it was possible to define samples enriched and depleted in $b \to u$ transitions. The result of a simultaneous fit to the E_ℓ^* distributions for the 4 event classes enriched/depleted $b \to u$ for $M_X < 1.6$ and $M_X > 1.6$ GeV$/c^2$ is $|V_{ub}|/|V_{cb}| = 0.104 \pm 0.012(stat.) \pm 0.015(syst.) \pm 0.009(model)$. The distribution of the lepton energy E_ℓ^* for $M_X < 1.6$ GeV$/c^2$ is shown in Fig. 5.7.

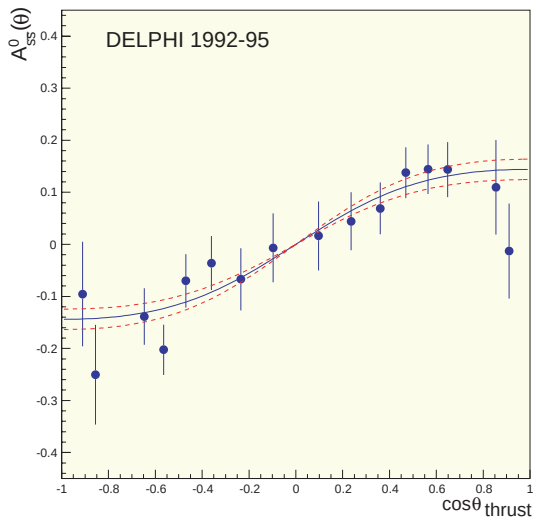

Figure 5.6: *The s quark pole asymmetry distribution as a function of* $\cos\theta_{thrust}$. *The data points are the values computed from the measured kaon asymmetry, the errors are statistical only. The superimposed curve represents the result of the measurement, the dashed curves correspond to one standard deviation.*

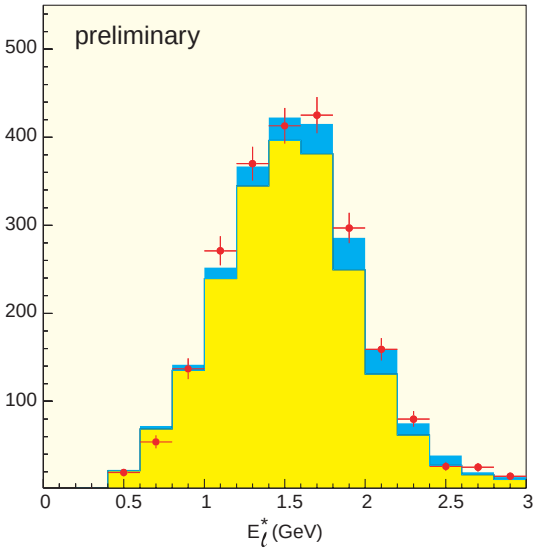

Figure 5.7: E^*_ℓ *distribution for the decays in the* $b \to u$ *enriched class with* $M_X < 1.6$ *GeV*$/c^2$. *Real data are indicated by the points with error bars, the background by the light shaded histogram and the* $b \to u\ell\nu$ *signal by the dark shaded histogram normalised to the fitted fraction of events.*

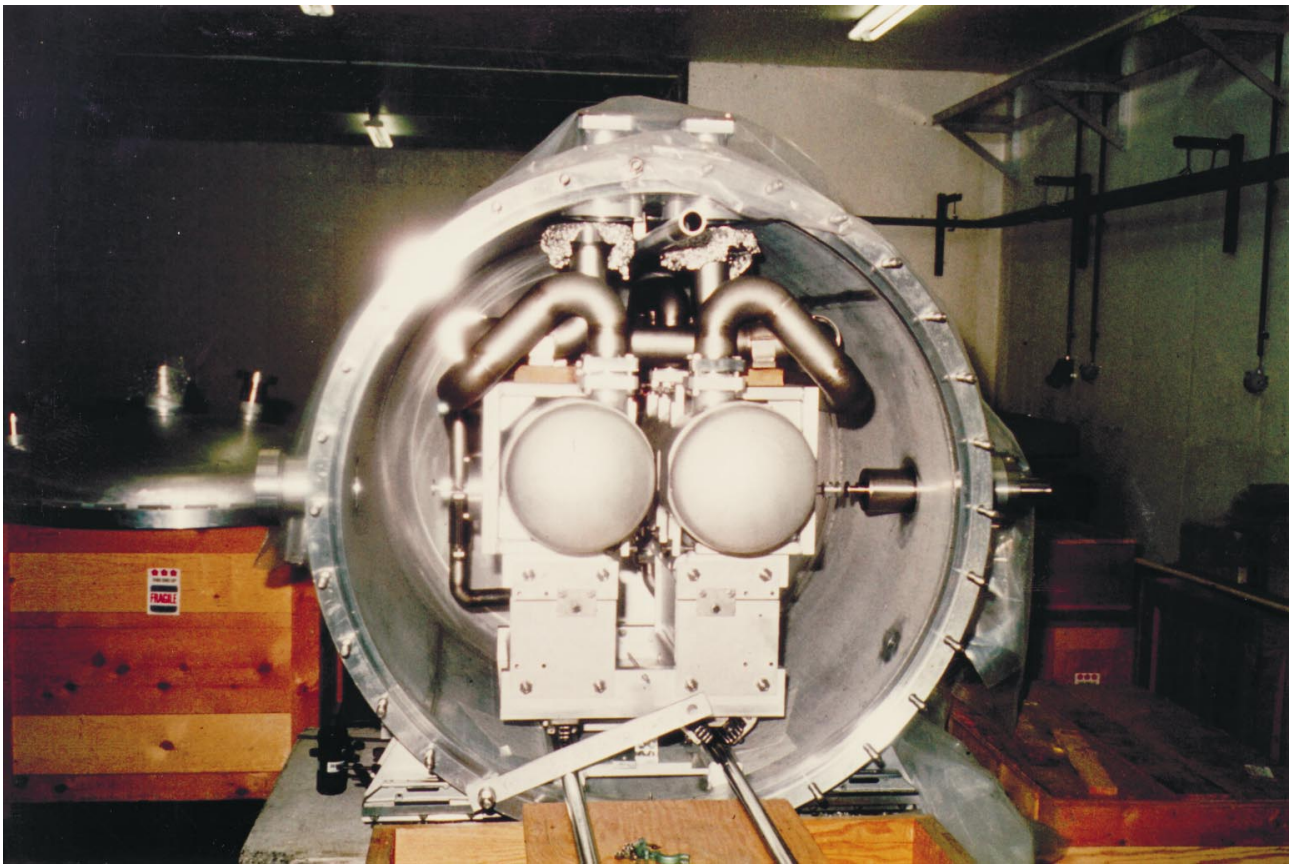

The energy defining slit (photo: NIKHEF)

6 L3

6.1 Introduction

The L3 detector is a general purpose detector with good spatial and energy resolution for the measurement of electrons, photons, muons and jets produced in e^+e^- annihilation.

During the 1997-1998 winter shutdown 32 additional superconducting RF cavities were installed bringing the total to 272. With the increased RF power a centre of mass energy of 189 GeV could be reached. For the 1999 and 2000 runs it is foreseen to install 16 more of these cavities. This, together with the increased cryogenics power that has been installed for the 1999 run will allow to operate LEP at $\sqrt{s} = 200$ GeV in order to increase the discovery potential for the Higgs boson and other as of yet unseen particles and to study the production and decay of W-bosons. With the L3 detector 177 pb^{-1} of data at $\sqrt{s} = 189$ GeV and 3 pb^{-1} of data at $\sqrt{s} = 91$ GeV (for calibration purposes) were collected and reconstructed during the 1998 run. This was the largest amount of luminosity collected by L3 in any single year. The data taking efficiency averaged 89% and detector operation was smooth with good background conditions.

In the Netherlands the participation in the L3 experiment is from the FOM institute and the universities of Amsterdam, Nijmegen and Utrecht. This year 27 papers were published; of those approximately half were based on data collected at the Z during 1991 to 1995 (see `http://l3www.cern.ch/paper/publications.html` for the L3 publications page). Furthermore the L3 collaboration contributed 62 papers to the ICHEP98 conference in Vancouver.

Some of the LEP I results are:

- The final result on τ polarisation and Michel parameters.
- The measurement of the weak dipole moment and the magnetic moments of the τ lepton.
- The measurement of an upper limit on the lifetime difference of short- and long-lived B_s mesons.
- The final result on the determination of the number of light neutrino species from single photon production.
- Measurement of the inclusive charmless semileptonic branching fraction of beauty hadrons and a determination of $|V_{ub}|$.
- Test of CP Invariance in $Z \to \mu^+\mu^-\gamma$ decay.
- Measurement of radiative Bhabha and quasi-real compton scattering.
- Measurement of the ${B_d}^0 - \bar{B}_d^0$ oscillation frequency.
- The hadronic photon structure function and the photon structure function and azimuthal correlations of lepton pairs in tagged $\gamma\gamma$ collisions.

In Nijmegen, the group has continued the simulation of e^+e^- interactions in the L3 detector. In 1998 about 22 million events were simulated in Nijmegen and made available to the pool of L3 Monte Carlo events (this corresponds to about 40% of the total, measured in CPU-time). The 12 RS6000/43P work stations accounted for most of the output, 13.5 million events. In addition, some simulation (4.3 million events) was performed on the KUN central computing facility (baserv), an IBM computer fully compatible with our RS6000 work stations. The output from the old Apollo DN10000 computers (about 2.5 million events) is coming to an end as a consequence of failing cpu's and disks. To replace the Apollos and provide some additional capacity, a new farm was put into operation in December. It consists of 17 PCs with Intel Celeron processors running the Linux operating system. This is, at present, the most cost-effective platform for our simulation. This farm went into full production on 9 December and produced about 2 million events by the end of the year.

The input and output files for the simulation are transferred from and to CERN over the network. In the first three months of the year this was over a dedicated ATM link as part of the JAMES pilot project. By the time this project ended, the normal network had been upgraded, making its use also satisfactory. The network has in general been reliable. With the increased production on the PCs, this reliability may become a problem in the near future.

In the Amsterdam group the analysis activities in 1997 were concentrated on $e^+e^- \to W^+W^-$ with both Ws decaying hadronically, τ lepton lifetime measurement using the silicon microvertex detector (SMD) and the time expansion chamber (TEC), tau-pair production at high energy, and hadron production in photon-photon collisions.

In collaboration with the UL a Monte Carlo generator for resonance production in two-photon collisions has

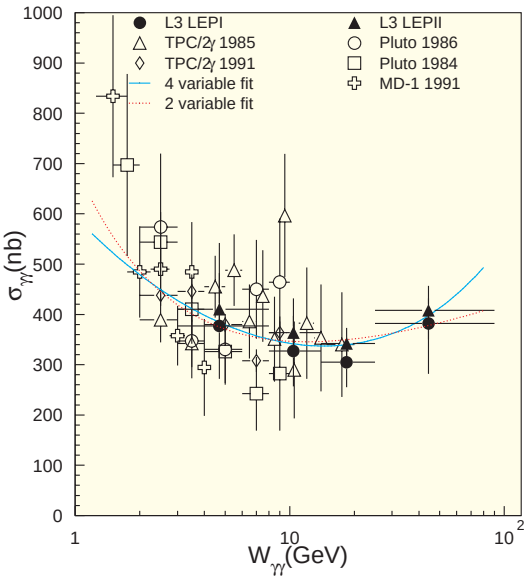

Figure 6.1: *The total hadronic cross section in $\gamma\gamma$ collisions as function of the mass, $W_{\gamma\gamma}$. The present data are indicated with full circles and triangles. The lines indicate two different parametrisations.*

been written. This Monte Carlo generator takes fully into account the Q^2 dependencies of the matrix elements and also generates the density matrices which form an essential tool for the description of the decays of the resonances. The Monte Carlo generator will be used to search for η_b resonances produced in two-photon collisions.

The analysis efforts of the Nijmegen group have concentrated on several topics in hadronic Z decays, W^+W^- production and decay (selection by minimum-spanning tree, W mass, influence from Bose-Einstein correlations), B^{**} production, and the cosmic-ray muon spectrum. Work continued on a unique investigation of Bose Einstein correlations between neutral pions using the ∼10,000 BGO crystals of the L3 electromagnetic calorimeter. Some models of particle production predict a difference between charged- and neutral-pion Bose-Einstein correlations. An analysis of Bose Einstein correlations between charged pions has been performed in three dimensions in the so-called longitudinal centre of mass system (LCMS). In this system the longitudinal component and one of the transverse components are decoupled from the time component, enabling an independent determination of spatial source size. This analysis clearly shows a larger source radius along the thrust axis of the event compared to the transverse radius.

The Utrecht L3 group studies hadron production and the formation of bound states of heavy quarks in photon-photon collisions. A Ph.D thesis with as subject the cross section and characteristics of hadron production in Two-Photon Collisions was completed in 1998. This was studied by measurements of the reaction $e^+e^- \rightarrow e^+e^-$*hadrons* at $\sqrt{s} \simeq 91$ and 131 GeV. Both of the final state electrons remain undetected, or one of these is detected at a small angle relative to the beam direction, leading to virtualities, Q^2, between 1 GeV^2 and 8 GeV^2 for the photon.

At low virtualities, the largest contribution to the two-photon interactions originates from the coupling of the photon to vector mesons. The measured cross sections for collisions between nearly real photons are shown in Fig. 6.1. There is little or no dependence on the two-photon mass up to masses of 50 GeV. At masses below 10 GeV the results can be compared with results from previous experiments, with good agreement. The measurements with one electron observed show a similar mass dependence. Their dependence on Q^2 is satisfactorily described by a generalised vector-meson dominance (GVDM) model. A simple picture emerges: the cross section is the product of a flat distribution of the mass and a strongly decreasing distribution as function of the virtuality.

To improve the study of muons produced by cosmic rays about 50 m^2 of scintillator tiles with wave length shifting fibre read-out have been installed on top of the magnet in March 1998 and a parallel read-out system for the top and bottom octant (25%) of the muon spectrometer has been added. The design and production of the electronics and the data acquisition is a joint responsibility of NIKHEF Amsterdam and Nijmegen. About 30 million cosmic muon triggers were recorded with this system. During the 1998-1999 shutdown all octants of the muon spectrometer will be equipped with this parallel read-out system and the total area of scintillator installed on top of the L3 magnet will be expanded to about 200 m^2.

6.2 The 1998 High-Energy run

In the following some of the highlights obtained in the 1998 high energy run are summarised.

- During the 1997 run at 183 GeV centre-of-mass energy, the threshold for on-shell ZZ production was reached. The dependence of the cross section with energy was studied using also the data at centre-of-mass energy of 189 GeV and good agreement with the Standard Model prediction is

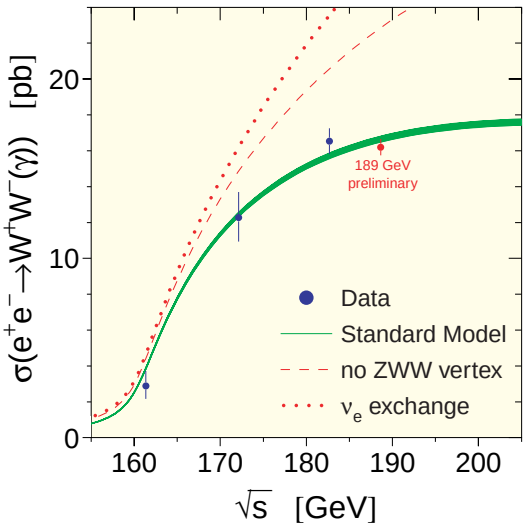

Figure 6.3: *The measured WW production cross section at $\sqrt{s} = 161$ and 172 GeV (1996) and 183 GeV (1997). Also shown are the Standard Model prediction and the predictions of two models with different W couplings.*

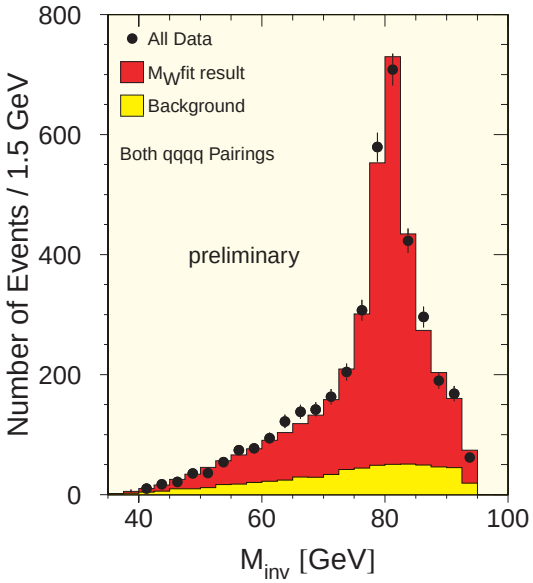

Figure 6.4: *Distribution of reconstructed invariant mass M_{inv} for W pair events selected in the 189 GeV data.*

found. The mass spectrum for $q\bar{q}\ell^+\ell^-$ and $q\bar{q}\nu\bar{\nu}$ final states is shown in Fig. 6.2.

The possible existence of anomalous couplings ZZZ or $ZZ\gamma$ is also analysed, and no evidence of them is found. L3 has been the first experiment setting limits on this kind of anomalous couplings.

- The events produced at these high energies were screened for new particles - such as the predicted Higgs boson, supersymmetric particles and new heavy leptons - and new interactions. With the statistics of the 1998 run, the high energy data improve the mass limits for the Higgs particles to more than 95 GeV. Upper limits on the production cross sections for charginos, neutralinos and sleptons were set at masses close to the beam energy.

- The large statistics of the data sample obtained in 1998 enables accurate studies of the properties of the W boson. At $\sqrt{s} \approx 189$ GeV, some 2700 $e^+e^- \to W^+W^-$ candidate events have been selected from the data, thus quadrupling the size of the total sample. The measured cross sections as a function of $\sqrt{s}$ are shown in Fig. 6.3, and are in good agreement with the Standard Model predictions.

  The events are used to determine the W mass M_W and the WWZ and $WW\gamma$ couplings. Above the WW production threshold, the W mass is measured from a fit to the invariant mass spectrum of W decay products. Combining the results at threshold and at $\sqrt{s} = 172$ and 183 GeV, the W mass is measured from the 1996 and 1997 data to be $M_W = 80.61 \pm 0.15\,(exp.) \pm 0.03$ (LEP) GeV. The invariant mass spectrum of the W decay products in the 1998 data is shown in Fig. 6.4.

  After inclusion of the 189 GeV data, the expected statistical error on the L3 measurement of the W mass will go down to 70 MeV. A thorough understanding of systematic effects influencing this measurement is thus important. Of particular importance are the effects of colour reconnection and Bose-Einstein correlations, detailed analyses making use of the energy- and charged particle flow in WW events are in progress. The differential production and decay cross sections of W bosons, as well as their total production cross section, are used in fits to determine the WWZ and $WW\gamma$ couplings. These results are combined with information on W couplings obtained from analyses of single W production and single photon production. A preliminary result for a fit to the couplings $\Delta\kappa_\gamma$ and λ_γ is shown in Fig. 6.5; the analysis of the 189 GeV data will lead to limits on anomalous contributions to these couplings that are better than the current world limits.

  Further analyses focus on the measurements of the W branching ratios and the CKM matrix element $|V_{cs}|$ from W decays.

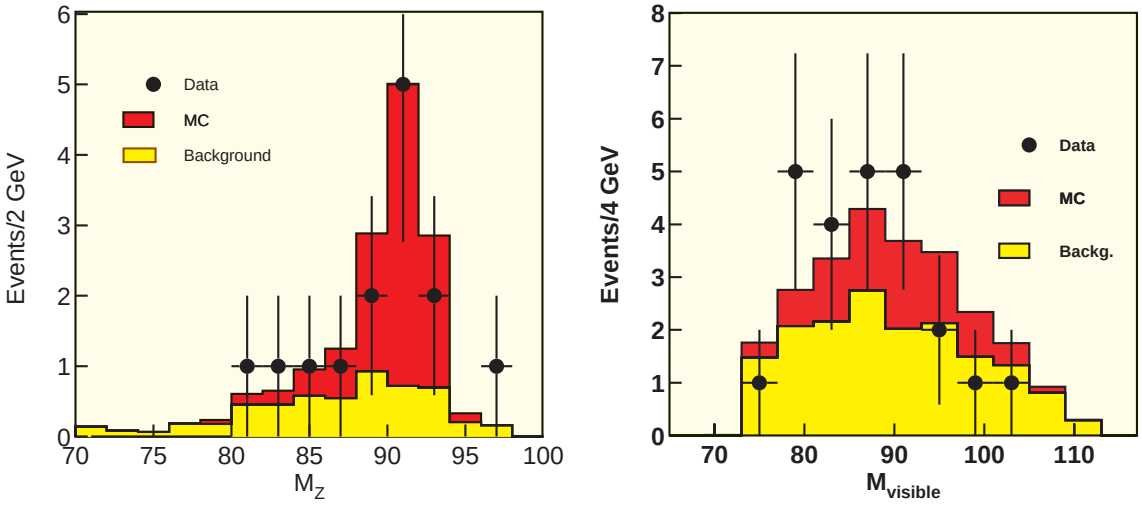

Figure 6.2: *Reconstructed Z mass in ZZ events for the $q\bar{q}\ell^+\ell^-$ (left) and $q\bar{q}\nu\bar{\nu}$ decays (right).*

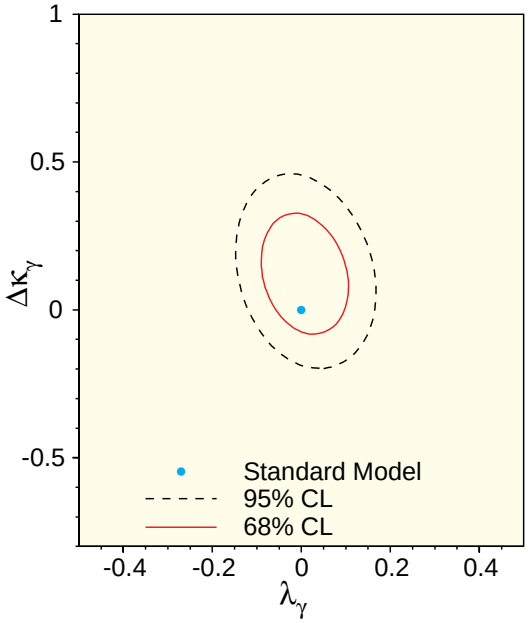

Figure 6.5: *Contours of 68% and 95% confidence level in the plane of the W couplings $\Delta\kappa_\gamma$ and λ_γ, as resulting from fits to W pair events selected in the 189 GeV data. These results are preliminary.*

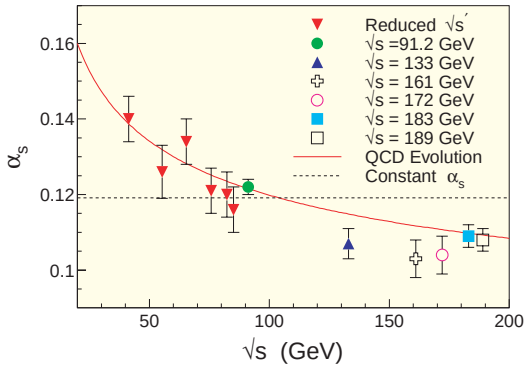

Figure 6.6: *Summary of α_s as a function of $\sqrt{s}$.*

- The event shape variables from the sample of hadronic events at high energies have been studied. The global structure of these events is well reproduced by several Monte Carlo models, based on parton shower evolution, together with string or cluster fragmentation. The preliminary measurements of the running coupling constant of the strong interaction, α_s, as a function of the centre of mass energy $\sqrt{s}$ are shown in Fig. 6.6 and in good agreement with the expected QCD evolution.

7 CHORUS

7.1 Neutrino oscillations

The quest for a proof of neutrino oscillations is one of the current challenges in particle physics. In the Europhysics Neutrino Oscillation Workshop NOW'98, held at NIKHEF in September, new results were reported and current prospects for future experiments were discussed intensively.

Strong evidence for disappearance of muon-neutrinos of atmospheric origin due to neutrino oscillations has been reported by the Japan-US Super-Kamiokande Collaboration. Earlier evidence for neutrino oscillations in a $\nu_\mu \rightarrow \nu_e$ appearance experiment at the Los Alamos low energy neutrino beam has been supported by new data. Already for decades the solar ν_e deficit problem provides a possible indication for neutrino oscillations. To reconcile the different results is difficult. Independent confirmation of the evidence so far obtained is of urgent importance.

NIKHEF participates since 1993 in the CHORUS (WA95) experiment at CERN searching for neutrino oscillations in the $\nu_\mu \rightarrow \nu_\tau$ appearance channel. The use of a nuclear emulsion target together with an electronic detector allows a background free detection of τ-decays. The τ-leptons can be produced in a ν_τ charge-current (CC) interaction, where the ν_τ emerges by flavour oscillation from ν_μ in the beam. The τ can be recognised inside the emulsion by its decay topology (kink or 3-prong). The short parent track (average length 0.8 mm) can be observed with a spatial resolution of better than 1 μm and a hit density of 300 grains/mm. Using the collected data, a flavour mixing probability $P(\nu_\mu \rightarrow \nu_\tau) < 10^{-4}$ at 90 % C.L in the region with $\Delta m^2_{\mu\tau} > 1$ eV^2, can be explored.

Charged particles from a neutrino interaction in the emulsion target are detected with electronic detectors and their momentum as well as charge are measured. The detector contains an ultra-high resolution emulsion tracker, high resolution fibre trackers with opto-electronic readout and a hexagonal air-core magnet (together forming a hadron spectrometer), a honeycomb tracker, a lead-scintillator calorimeter, and a toroidal magnetised-iron muon spectrometer.

Data from selected triggers have been recorded and stored for off-line analysis. In the analysis tracks are reconstructed pointing backward to the emulsion target, and "predicting" a track in the emulsion. Automatic scanning microscopes use the track predictions

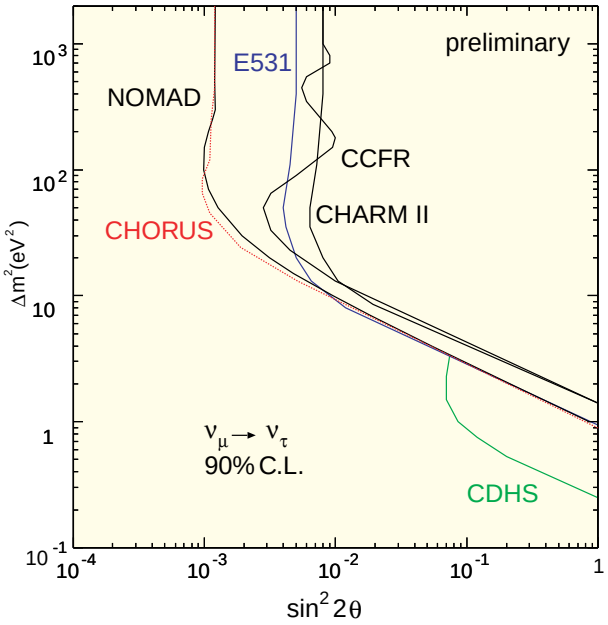

Figure 7.1: *Exclusion plot (90 % C.L.) for $\nu_\mu \rightarrow \nu_\tau$ oscillations, current state of analysis.*

to locate the tracks inside the emulsion and to follow them to the neutrino interaction vertex from which they emerge.

Last year's running period provided measurements, calibrations and tests. It marked the end of data taking of CHORUS, two periods of two years, each with 800 kg emulsion as target. No emulsion target was installed during last year's run.

The CHORUS Collaboration concentrated on finishing as early as possible the first phase of scanning and analysis of the large amount of data. A sample of about 850,000 ν_μ charged current interactions has been recorded in the emulsion plates along with accompanying data acquired from the electronic detector. Results based on a sample of about 75,000 emulsion events, consisting of two independent sets, hadronic and muonic τ decays, have been published in 1998. A new exclusion curve has been obtained, as shown in Fig. 7.1.

The present work focuses on the development and improvements of the automatic emulsion scanning technique. The major part of the scanning is performed by the Nagoya team in Japan.

Other CHORUS member institutes are on the way of

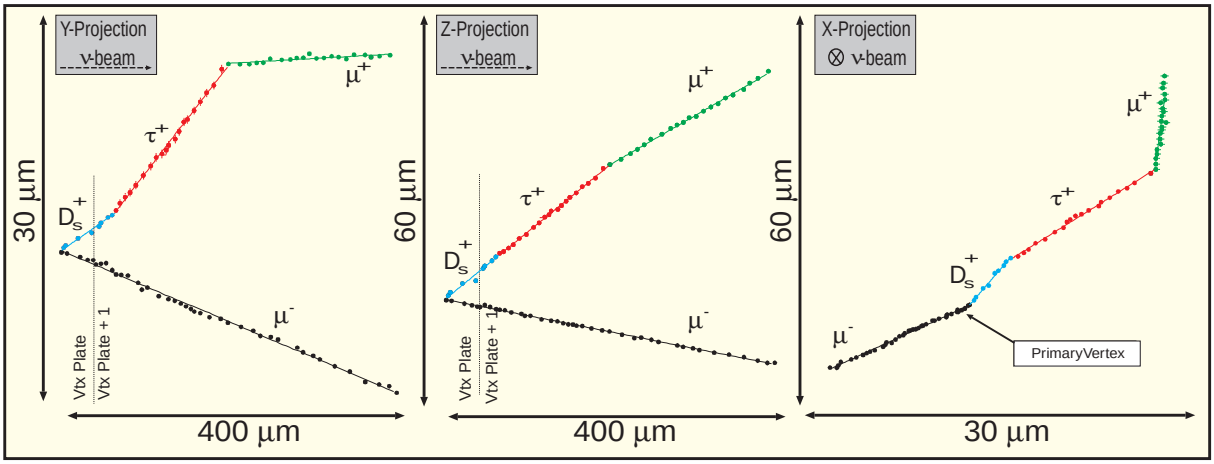

Figure 7.2: *Diffractive production of D_s^* and pure leptonic τ decay.*

increasing their scanning capabilities. A new automatic scanning facility has been set-up by CERN and NIKHEF. It contains three large microscope tables with high-performance optics and electronics.

The first phase of the analysis has been almost completed, and preparations have started for the second phase. Only after the second phase, final results in accordance with the proposal can be obtained. To fully exploit this second phase, the development of faster scanning methods has been intensified last year.

Besides the emulsion scanning for the neutrino oscillation τ search, an increasingly important part of the CHORUS programme consists of studying other subjects, such as charm production, diffractive processes, nuclear effects, and rare events.

7.2 Specific NIKHEF activities

The NIKHEF team is involved in emulsion analysis for the neutrino oscillation search as well as in studies of CC ν_μ interactions in both the emulsion target and the calorimeter.

Following extensive tracking studies and programme developments, data from the NIKHEF honeycomb tracker allowed significant improvement of the tracking precision. Through this the scanning and reconstruction efficiencies could be improved. The latter is of importance for hadronic channels of τ-decay, which have a much larger branching ratio than the muonic decay channel.

For neutrino CC interaction studies, single and double muon events in the lead calorimeter have been collected, calibrated and filtered for physics analysis. A study of deep-inelastic charm production in the calorimeter, based on the 1995 data set, was completed. This provides information on the strangeness content of the nucleon, consistent with earlier data from the CHARM-II and CCFR experiments.

An important new data sample for neutrino and anti-neutrino CC interactions in the calorimeter was obtained last year in a dedicated run. The analysis in terms of F_2 and F_3 structure functions for lead has been started. The same analysis allows to derive the neutrino beam spectrum serving also as a valuable check on the simulations of the neutrino beam.

The involvement of our team in developing scanning software has been fully committed to the automatic scanning facility at CERN. Algorithms for scanning of "predicted" tracks, general multi-track scanning, and vertex-finding, were developed and implemented.

Our team has contributed through the scanning and analysis of a single quite rare double kink event, at present the only known signature of neutrino induced diffractive production of D_s^* with purely leptonic τ decay (see Fig. 7.2).

8 WA93, WA98 and NA57

8.1 Introduction

The use of highly relativistic heavy-ion beams is well suited for studying nuclear matter under extreme conditions. Based on a statistical treatment of QCD it is expected that a deconfined state of quarks and gluons, the so called quark gluon plasma (QGP), will be created in violent collisions of heavy nuclei. The formation, detection and systematic study of such a QGP state would yield new information on strong interaction dynamics.

The various stages of the violent interaction process of two colliding heavy nuclei can be investigated separately by means of different probes. The hot early stage of the created system is probed by studying the thermal radiation of the system, by means of prompt photons. These prompt photons will provide information about the temperature evolution of the expanding system. Investigation of the production rates of particles containing heavy quarks will probe the chemical composition of the early phase as well as the final particle production process (hadronisation). The dynamical evolution of the expanding system at the last stage of the interaction is probed by investigation of the momentum spectra of the produced particles which eventually leave the system (freeze-out).

In our studies involving the probes mentioned above we investigate sulphur and lead induced collisions at the CERN-SPS accelerator complex. Within the WA93 (S+S, S+Au) and WA98 (Pb+Pb) collaborations the prompt photon production and neutral meson spectra are studied, whereas the heavy-quark production is investigated with Pb+Pb interactions within the NA57 experiment. In the future all probes will be simultaneously investigated in Pb+Pb collisions within the ALICE experiment at the CERN-LHC collider facility.

Combination of the information obtained from the different probes will yield insight in the space-time evolution of strongly interacting systems.

8.2 Neutral meson production

Within the WA93 and WA98 experiments the conditions at the freeze-out stage of the interaction process are investigated by means of the transverse momentum, (p_{T}), spectra of neutral pions. Both experiments contain large, highly segmented arrays of lead-glass calorimeter modules for photon detection through Cerenkov radiation close to mid-rapidity. To determine the impact parameter (centrality) of the collisions, calorimeters at mid-rapidity and at beam rapidity measure the transverse and longitudinal energy flow respectively. Interpretation of these energy flows with a geometrical model of the collision directly yields the centrality of the event.

The energy and spatial resolutions as well as the large phase-space coverage of the photon detector allow us to reconstruct π^0 and η mesons by means of an invariant mass analysis of photon pairs on a statistical basis. The combinatorial background is evaluated using a mixed event technique. The mixed event technique implies merging of signals from events with a different centrality of the collision.

The π^0 signal can be extracted reliably for transverse momenta above 0.4 GeV/c. For the η signal the lower limit in p_{T} amounts to 0.8 GeV/c due to the higher mass of the η and thus larger opening angle of the two decay photons. The resulting π^0 and η yields are corrected for geometrical acceptance and reconstruction efficiency of the photon detector. The reconstruction efficiency depends strongly on the particle multiplicity and hence on the centrality of the collision, due to an increased probability of several particles hitting the same detector element for larger multiplicities. The fully corrected π^0 invariant cross sections for various centralities are shown in Fig. 8.1.

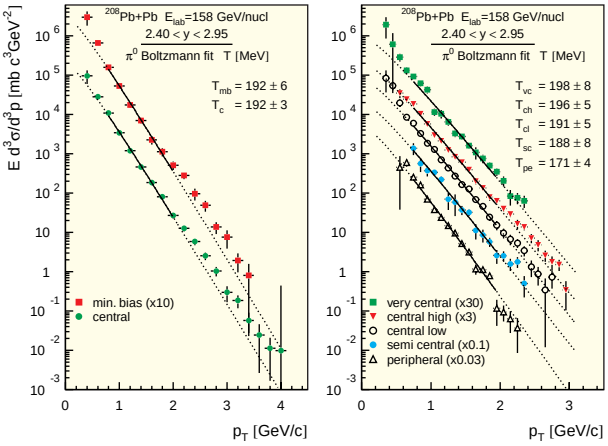

Figure 8.1: *Transverse momentum distributions of π^0 mesons in Pb+Pb collisions at 158 A GeV beam energy. The solid line represents a fit to the data of a static Boltzmann distribution. The dotted lines represent extrapolations of the fit.*

In the p_T range between 0.8 and 2 GeV/c a fit to the data has been performed using a (thermal) Boltzmann distribution for a static source. The inverse slope (T) of the fit represents the temperature of the static source at the moment the particles escape the system (freeze-out). It is observed that at low and high p_T values the spectra are described rather poorly by the fit. A similar effect is observed in the sulphur induced data of WA93. A possible explanation could be the effect of hard initial parton scattering at high p_T (Cronin effect) and resonance decays at low p_T.

If we allow for part of the collision energy to be converted into collective motion (flow) of the produced particles, we expect the p_T spectra to become flatter. This is well illustrated by a hydrodynamical model which assumes a thermal source with transverse expansion that introduces the effects of radial flow in the resulting particle spectra. The above implies that the derived freeze-out temperature T is (strongly) correlated with the flow velocity. Due to the limited statistics of the event sample a determination of the flow velocity and its correlation with the derived freeze-out temperature cannot be performed. However, using the transverse flow velocity $\beta_T = 0.43 \pm 0.15$ determined from charged pion spectra, a freeze-out temperature of $T = 121 \pm 22$ MeV is obtained, hardly depending on the centrality of the collision.

Apart from the neutral pions, the two-photon channel allows also for the reconstruction of the heavier η meson. The shape of the transverse mass (m_T) distribution of the η mesons is observed to be similar to that of the neutral pions, as can be seen in Fig. 8.2.

Comparison of the shapes of the η and π^0 spectra confirms the phenomenological concept of m_T-scaling, expected for a thermalised system. This implies that the data are consistent with a thermalised system, but it does not at all prove that the system has been in thermal equilibrium. The latter becomes clear by the observation that also the observed spectra of particles produced in high energy proton-proton collisions show a similar behaviour, whereas it is very unlikely that in these interactions a thermalised system is created. Furthermore, under the assumption of a Glauber-type multiple collision model it is seen that the π^0 yield scales with the number of participants. This would indicate that, concerning the analysis outlined above, nucleus-nucleus collisions may be regarded as a superposition of (independent) nucleon-nucleon collisions.

On the other hand, the observed ratio (extrapolated to the full phase space) $\eta/\pi^0 = 0.084 \pm 0.031(stat) \pm 0.041(syst)$ is found to agree well with the value of 0.0865 as calculated from thermodynamical models. Of course the validity of the extrapolation of the experimental results from mid-rapidity to the full phase space has yet to be quantified.

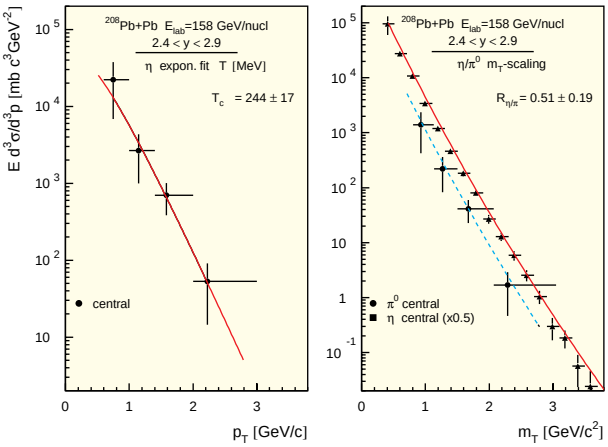

Figure 8.2: *Transverse momentum distributions of η mesons in Pb+Pb collisions at 158A GeV beam energy. In the left panel the p_T distribution for central events is fitted to an exponential. In the right panel the solid line represents a power-law fit. The dashed line shows the same power law normalised to the η distribution.*

8.3 Heavy-quark production in NA57

The production of particles containing heavy quarks ($s, c, \ldots$) has been proposed as a probe for the phase transition from a system of hadrons into a plasma of quarks and gluons. In the WA97 experiment the yields of a number of strange particles (Λ, Ξ^-, Ω^-) were measured in both p-Pb and Pb-Pb reactions at 158 A GeV/c. It was shown that the number of multi-strange hyperons per event and per participating nucleon in Pb-Pb collisions is enhanced with respect to the yield from p-Pb collisions. Furthermore, it was seen that this enhancement increases with the strangeness content. This suggests a high initial density of strangeness and could indicate the creation of a state close to the phase transition.

The purpose of the NA57 experiment is to extend the scope of WA97. It intends to determine the baryon density at central rapidity from the measurement of multiplicities of positive and negative particles, in order to study the dependence of the strangeness enhancement on nuclear stopping. Also the Pb-Pb study will be repeated at a lower beam energy of 40 GeV/c

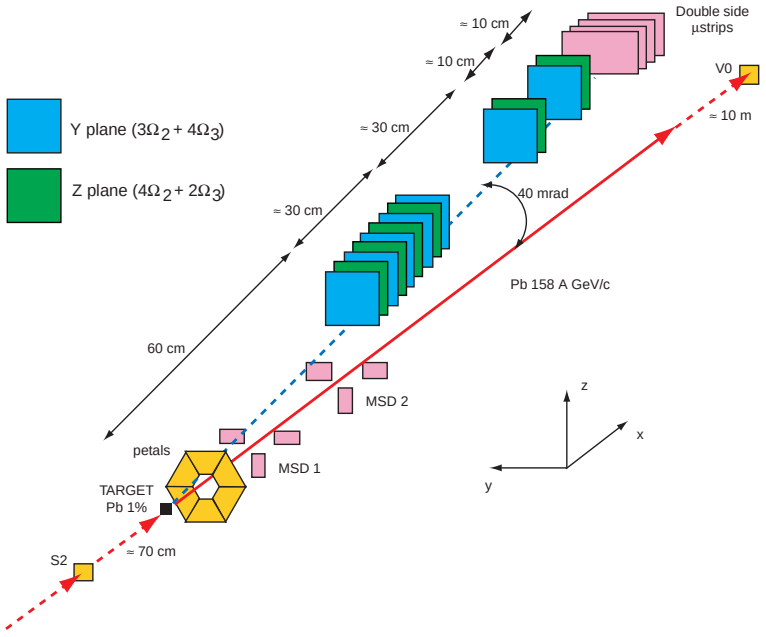

Figure 8.3: *The set-up of the NA57 experiment.*

per nucleon. In this way the collision energy lies between the old SPS value and the energy of the AGS at Brookhaven. By reducing the beam energy, a search for a possible threshold effect, indicating the onset of a new reaction mechanism, will be performed. For example, a significant drop in the Ω/Ξ ratio compared to the value at 158 A GeV/c could indicate that we have moved further away from the phase transition boundary.

8.4 Experimental setup

The experimental setup (see Fig. 8.3) is placed inside the GOLIATH magnet in the North Area of the CERN SPS ring. The setup consists of scintillators (S2, V0 and Petals) for triggering. Silicon strip detectors (MSD's) are installed for measuring the multiplicities. At an angle of 40 mrad with the beam axis a telescope is placed, which consists of 13 silicon pixel planes and four silicon micro-strip detectors. The first part of the telescope contains nine pixel detectors and is positioned at 60 cm from the target. This compact part, with a length of 30 cm, is used for track finding and momentum reconstruction. The momentum of the particles is determined from the curvature of the tracks in the magnetic field. The magnetic field has a strength of around 1.6 T and is aligned along the vertical direction, such that the tracks are curved in the horizontal plane. The remaining four pixel planes and the four micro-strip detectors serve for the improvement of the momentum determination.

The silicon micro strip detectors were developed by the department of Subatomic Physics of the Utrecht University/NIKHEF. These detectors have a size of 7.3×4.0 cm^2 in horizontal and vertical direction, respectively. The strip detectors are double sided with a stereo angle of 35 mrad and have a thickness of 300 μm. The pitch of the strips is 95 μm and the strips are oriented in vertical direction, such that the resolution is best in the bending direction of the particles. Due to the small stereo angle the vertical resolution is worse, of the order of 1 mm.

8.5 Results

In September the first data with the complete NA57 setup were taken. During this test run a 400 GeV proton beam was used on a lead target. In October and November data with a lead beam of 158 A GeV/c have been obtained. During this period a total of 220 million events were collected, which corresponds to about 3 Tbyte of data. In the future the performance of the strips will be investigated further and they will be included in the reconstruction program ORHION, after which the actual physics analysis can be started.

A view of the MEA injector and accelerator (photo: NIKHEF)

B MEA/AmPS Facility and Accelerator Physics

1.1 Introduction

The year 1998 was the last for nuclear physics experiments with AmPS. The approved proposals for these experiments exceeded by far the available beam time and therefore there was very little time for accelerator physics. Both the linac and the ring performed very well and operated at electron energies around 700 MeV for almost 5000 hours (see Table 1.1). The ratio between planned and data-taking hours is about 50%. This is lower than usual, but one has to consider the fact that experiment tuning requires both the experimental instrumentation and MEA/AmPS to be in full operation. During 9 months the facility operated in polarised electron mode with excellent performance of the polarised electron source together with the Siberian snake. A plan to continue the experiments during the first two months of 1999 had to be abandoned after a serious short circuit on December 26 in a 10 kV mains supply of AmPS.

1.2 MEA performance

Polarised electron source (PES)

The gun operated at a pulse current of 15 mA. With an injection efficiency of 35-40% it injected a current of 5-6 mA in MEA. The operational lifetime (the time during which a gun current of 15 mA could be maintained) of photocathodes in this mode was about 4-5 weeks. Strained layer InGaAsP photo-cathodes were used. The average polarisation of the electrons from the source was 70-75% yielding a polarisation in the ring of 60-70%.

Accelerator vacuum system

Several times vacuum leaks developed in the accelerator sections but could be repaired. A severe leak developed in the sections of station A12. This leak could not be repaired but additional pumps allowed resuming operation. Probably the cooling water has a connection to the vacuum part of one of the sections.

MEA Modulators and RF

Because AmPS operated in storage mode the modulators only had to pulse at a frequency of 10 Hz. This allowed air-cooling the modulators and from Fall 1998 the environmentally unfriendly coolant perchloroethane could be taken out of operation. Since the installation and test of the prototype klystron in 1990 the 12 modulators together supplied a total of 403,956 hours of high voltage and a total of 510,376 hours of cathode power to the Thomson TH2129 klystrons. These totals were accumulated with 31 klystrons. Nineteen klystrons failed since 1990. In 1998 the cathode power mean time between failure (MTBF) of the Thomson tubes increased to 27,000 hours. Two exhausted klystrons had to be replaced after 20,100 and 27,900 hours of cathode power, respectively.

1.3 AmPS performance

Magnets and Power Supplies

All magnets operated without problem including the Siberian snake. The snake was in continuous use for almost 9 months until the end of the year. On average its daily liquid He consumption was 160 litres. The total liquid He consumption in 1998 was 46650 litres. Loss of beamtime occurred due to failures in the multi-output quadrupole power supplies and in the kicker power supplies.

2856 MHz RF source

This RF source was no longer in operation because there was no stretcher mode in 1998. From the start in 1992 the source provided 16,166 hours of high voltage power to its Thomson TH 2110 50 kW c.w. klystron

476 MHz RF source

This RF transmitter was in operation for 6000 hours to enable the storage mode for ITH experiments with polarised and unpolarised electrons.

Vacuum systems

The vacuum pressure in the extraction area never dropped below 1×10^{-7} mbar. Since the operation in stretcher mode stopped in 1997 the extraction septum could be removed and replaced by a straight vacuum pipe. The pressure improved by an order of magnitude but less than expected. There were also two accidental vents of the ring vacuum because of a cracked fused silica window in one of the curves. This window transmitted the laserbeam of the Compton back-scattering measurement set-up when measuring the electron polarisation. The cracking was due to the heat load caused by the synchrotron radiation at 720 MeV with 200 mA. Since this measurement was only performed at low beam current a shutter could be installed to protect the window in normal conditions.

Activity	Beam time [h]		Tuning time [h]		Breakdown time [h]	
Experiment	**Scheduled**	**Data taking**	**MEA & AmPS**	**Experiment**	**MEA & AmPS**	**Experiment**
91-08,94-02	934	580	63	100	52	139
94-05, ^{3}He	2121	1173	71	313	525	39
97-01, ^{2}D	2466	1171	136	729	233	197
97-01, H	684	466	21	151	46	0
Maintenance						
Pes & Snake	80	—	—	—	80	—
Other systems	153	—	—	—	153	—
Total	**6483**	**3390**	**291**	**1293**	**1089**	**375**

Table 1.1: *Beam Statistics 1998.*

Beam parameters

680 MeV for [91-08] and [94-02]; target ^{4}He; thermionic electrons

720 MeV for [94-05] and [97-01]; target polarised ^{3}He, ^{2}D and H; polarised electrons and SNAKE in operation.

Remark

Maintenance: Besides scheduled repair and maintenance of equipment also the refilling of the SNAKE with liquid He is taken into account.

1.4 Accelerator physics

The design of the polarised electron source was summarised in a thesis and resulted in a PhD for Boris Militsyn.

Interruptions between the nuclear physics experiments allowed to investigate quantum efficiency and nonlinear response of the photo-cathodes with PES. The performance of a photo-cathode is usually characterised by its quantum efficiency Qe at the wavelength of maximum polarisation. However, researches aimed at obtaining a higher (pulsed) current led to the discovery that the photocurrent saturates with increasing light intensity. The saturation effect was observed at NIKHEF in 1995. Further experiments have shown that besides the saturation effect there is also a deformation of the beam pulse. While the laser pulses have a flat-top shape, the current pulses have a spike at the leading edge. The initially high current decays exponentially in time and stabilises at some lower level. It was observed as well that the difference between the spike amplitude and the pulse current (which is the total charge in the pulse divided by the pulse duration) is small at low laser power and is very significant at high power. The concept of the surface photo-voltage gives a qualitative explanation of the decay of the spike at the leading edge of the current pulse. Electrons, which are excited into the conducting band by photons partially escape the surface, providing the photocurrent, and partially are trapped in the photo-cathode's surface. After some time these electrons either recombine with the holes in the valence band or escape the crystal. If the rate of excitation is small enough (low light intensity) electrons will not be accumulated in the surface. In this case the photocathode operates in the linear mode and its current density is proportional to the light intensity. On the other hand, if the rate of excitation is high electrons will be accumulated in the surface. The corresponding accumulated charge leads to a deformation of the band structure near the photo-cathode surface, a rise of the electron affinity, and, as a result, a decrease of the escape probability. The subsequent stabilisation of the current on a low level implies that the rate of excitation of electrons into conduction band has become equal to the recombination rate. This equilibrium can be reached if the duration of the current pulse is sufficiently long. So the photocurrent depends nonlinearly of the light intensity and also depends on the length of the light pulse.

1.5 Forced stop

On December 26 at 06h55 a poor connection between a 10 kV "mains" cable and a circuitbreaker led to a short circuit and an explosion. A wall of the adjacent AmPS power supply building was literally blown away. After that part of the roof collapsed. Fortunately nobody was around at the time also because MEA/AmPS was on standby because of the Christmas holiday, but equipment racks, cables and cable trays, cooling pipes, etc. were seriously damaged. Also the short circuit "plasma" emanated a lot of soot that was deposited on and in most of the electronics. Finally the short

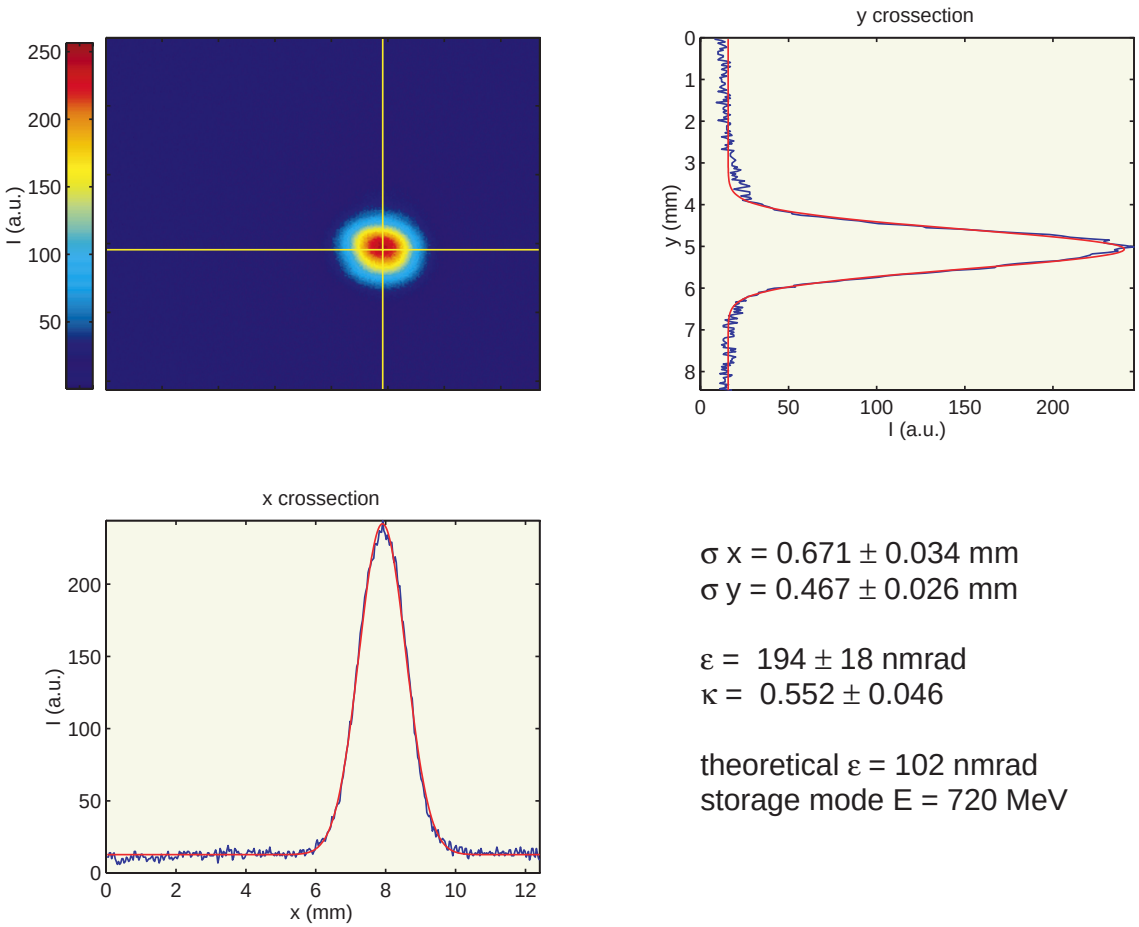

Figure 1.1: *Profile of the stored beam in AmPS before final shutdown end 1998. The beam profile was measured on the synchrotron radiation diagnostic line. The (polarised) electron energy was 720 MeV and the current was 70 mA. The internal target cell had a length of 600 mm and a diameter of 15 mm. There was no gas in the cell.*

circuit caused quite some indirect damage to the accelerator electronics and controls either because their switch off in an uncontrolled way or by voltage surge on our local power grid. The required time for a provisional repair allowing to store a beam was estimated to cost at least 8 weeks. Since both MEA and AmPS will be redeployed elsewhere it was decided to make all repairs to allow a functional test with beam prior to the shipment.

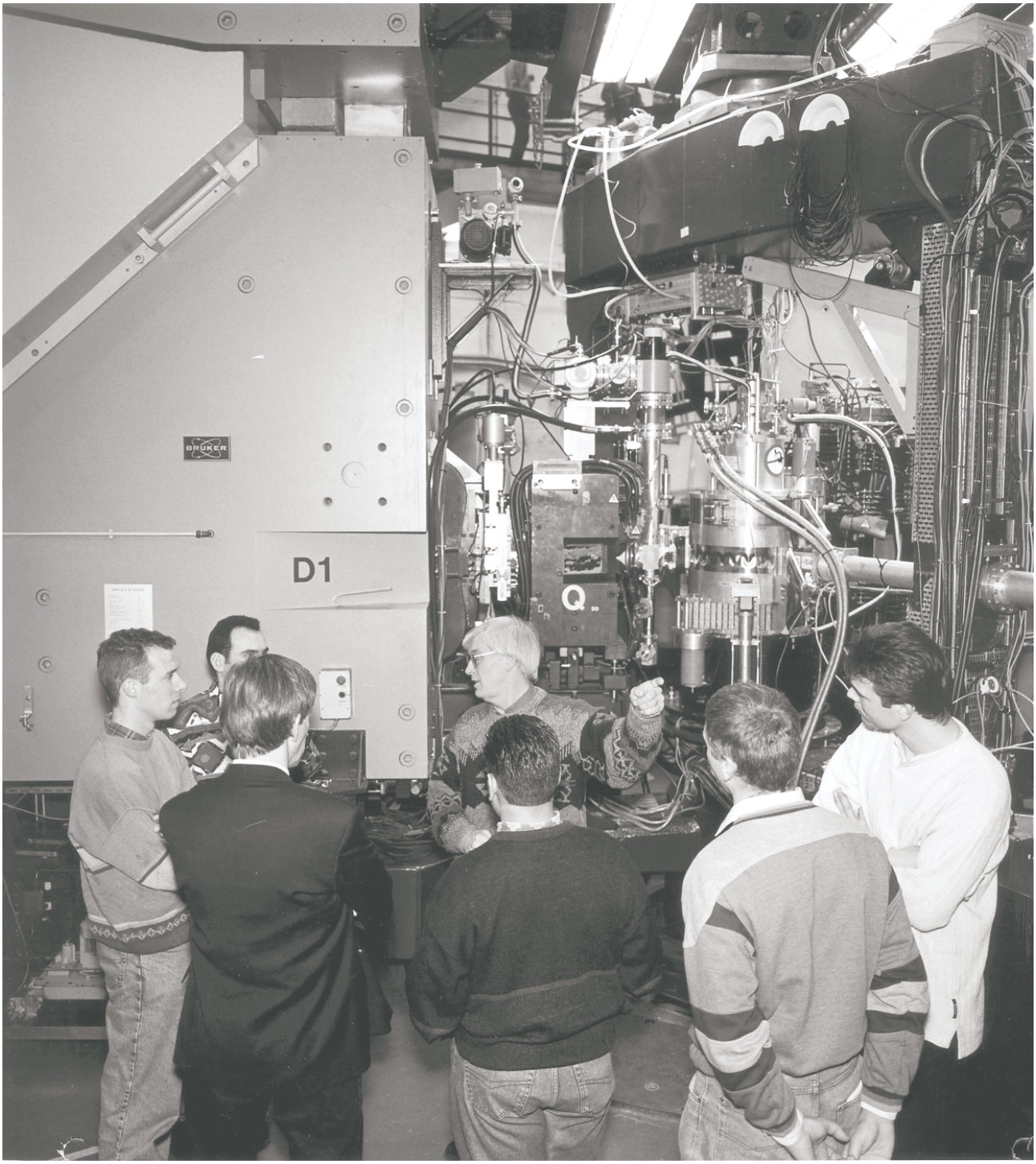

Excursion to the EMIN facility (photo: Han Singels)

C Experiments in Preparation

1 ATLAS

1.1 Introduction

One of the important steps of the Dutch ATLAS group was its official participation in the D0 experiment at FNAL (Chicago, USA). We thereby moved our involvement in exciting electro-weak physics (top quark, W boson and Higgs boson studies) backward from 2005 to 2000!

Important milestones for our contribution to ATLAS hardware have been the erection of a large cleanroom with granite table and precision mechanics for the construction of the 96 Monitored Drift Tube chambers. Important steps towards the fulfilment of the NIKHEF ATLAS contributions towards the semiconductor tracker have been the installation of a semi-automatic wire bonder and wafer probe station as well as the arrival of the large high-precision 3D coordinate measurement machine at NIKHEF.

1.2 Participation in the D0 Experiment

In July, NIKHEF groups in Amsterdam and Nijmegen have formally joined the D0 experiment at the Fermi National Accelerator Laboratory (FNAL) in the USA. The D0 detector (shown in Fig. 1.1) is one of the two general purpose detectors in the Tevatron accelerator and storage ring, in which protons and anti-protons are accelerated and collided. The Tevatron and the D0 collaboration have already had a very successful physics run (Run I) between 1991 and 1996. In the data of this run the top quark was discovered and its mass measured to a better relative precision than any other quark mass.

The Tevatron and the D0 experiment are now preparing for a new physics run (Run II), which will start in 2000. The Tevatron is being upgraded to operate at an increased centre-of-mass energy of 2 TeV (was 1.8 TeV in Run I) and a much improved luminosity. The integrated luminosity goal is set to at least 2 fb^{-1}, which is an order of magnitude more than the data collected in Run I. There is good hope that this goal will be achieved already in 2002 or 2003 and that a substantially higher integrated luminosity will be collected before the start of LHC in 2005.

To match the more demanding environment of the Run II Tevatron and to improve the abilities of the D0 detector a substantial upgrade of the detector is being performed. All the electronics and the trigger have to

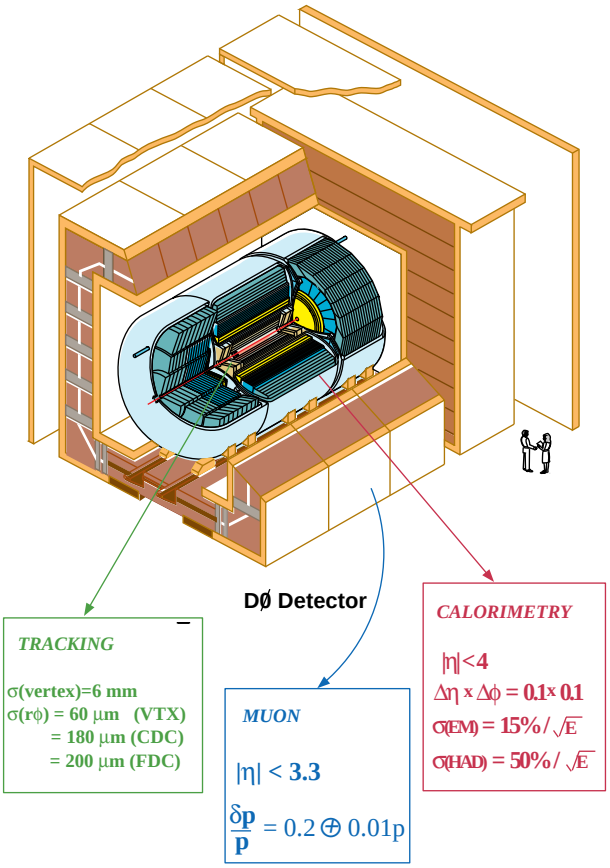

Figure 1.1: *A cutaway drawing of the D0 detector.*

be adapted to the increased bunch crossing frequency and the possibility of multiple interactions per bunch crossing. The most challenging part of the upgrade is replacing the entire inner tracker. A 2 T solenoidal superconducting magnet is added inside the calorimeter. In this field a silicon microvertex detector surrounds the interaction point. The silicon microvertex detector itself is surrounded by a scintillating fibre tracker. Both the scintillating fibre tracker and silicon microvertex tracker contain cutting-edge technology. For the scintillating fibre tracker a cryostatic visible light photon counter was developed with a quantum efficiency of 80% and a gain of about 60,000. The silicon microvertex detector has nearly an order of magnitude larger active sensor area than microvertex detectors in operation so far. It will be the first physics-grade microvertex

detector to operate in such a harsh radiation environment that the silicon bulk material properties will drastically change during operation (type inversion). The D0 calorimeter has performed extremely well in Run I and is left untouched, except for upgrading of the readout electronics. The very good muon chamber coverage from Run I is also kept, but the forward muon chamber system is being refurbished for better radiation tolerance and efficiency. In the very forward direction, proton detectors will be placed at several tens of meters from the interaction point and very close to the beam line. These new detectors allow the detection of (anti-)protons scattered under small angles and their remnants. This will allow a thorough study of the so-called rapidity gap events that have first attracted large interest at the HERA collider. Because large parts of the offline reconstruction have to be rewritten, the D0 collaboration has decided to rewrite this code entirely in an object oriented way using C++.

The Dutch groups have joined D0 in a relatively late stage of the upgrade. Nevertheless, a number of essential or important issues in the upgrade program were not or insufficiently covered. The NIKHEF groups have selected a number of projects that were most pressing to be covered. These are:

- a radiation monitoring and beam abort system to protect the silicon microvertex detector,
- a contribution to the silicon track trigger (STT),
- a system of magnetic field sensors for the inner tracker volume,
- an engineering and construction contribution to the forward proton detectors, and
- implementation of the muon reconstruction software and its subsequent implementation in the third level trigger.

The primary reason for the Dutch groups to join D0 is the expected rich physics programme. An important secondary reason is that analysing Tevatron physics is the best possible way to prepare for the LHC and the analyses of ATLAS data. Participation in D0 assures a stream of first class PhD thesis topics, offering unique possibilities for PhD students in particle physics between the end of LEP and the start of the LHC.

Radiation and beam abort system

Two systems for radiation monitoring will be made. One system consists of Beam Loss Monitors (BLM), glass tubes filled with 1 bar Argon and two concentric metal cylinders with a 2 kV potential difference. The radius of curvature of both cylinders does not allow a gas gain. These tubes constitute a current source with a current proportional to the number of ionising particles traversing the tube. These tubes are a standard item for the Tevatron, where they are used in many places as radiation monitors and also as beam abort devices for critical items, such as superconducting magnets.

The BLM are rather massive devices and as such unsuitable to be placed near the interaction point, where they would cause unwanted multiple scattering and secondary interactions. The best place that could be found for these devices is behind the electromagnetic calorimeter, near the beam pipe. However, it is unclear how the measured radiation at that point relates to the dose received by the silicon microvertex detector. Therefore, a second system of radiation monitors is integrated into the silicon microvertex detector. On some of the forward disks of this detector thin substrates will be mounted that carry large surface silicon diodes and front-end electronics. These silicon diodes will be biased and give a current proportional to the number of traversing particles, just as the BLMs. The silicon diodes are carefully selected and will be cooled in the experiment to ascertain a longer lifetime for these diodes with respect to the rest of the silicon microvertex detector. The two systems will complement each other and it will be possible to calibrate the BLMs with the real dose at the microvertex detector from the silicon diode sensors. The design of this system has started in the second half of 1998 and is ongoing. The system has to be commissioned by the end of 1999.

Silicon Track Trigger

The most important physics at the Tevatron Run II, namely Higgs search and top physics, depend heavily on the ability of the detector to select jets from bottom quarks. With the use of the new tracking system D0's abilities in this field will be greatly improved. The first hurdle to be taken though is the trigger. In order not to loose interesting events containing bottom quarks, already at the second level trigger these events will have to be recognised. The silicon track trigger (STT) uses the hit information from the silicon microvertex detector in conjunction with reconstructed tracks in the scintillating fibre tracker to improve the tracking information and to recognise tracks with large impact parameters and displaced vertices, which are so characteristic for b hadron decays. Furthermore, the STT uses the

improved track information to reconstruct the vertex position along the incoming beam axis, thereby allowing the separation of tracks from different events in the same bunch crossing. The Nijmegen group will provide financial support for part of the STT and will participate in the software and firmware developments.

Magnetic field sensors

With the advent of a strong solenoidal magnetic field, also the need arises to measure this field at regular intervals during data taking. NIKHEF has offered to supply the magnetic sensor system for the inner detector. It will consist of magnetic field sensors that measure the field in three directions, using Hall probes. The readings are converted to digital information near the sensors and the digital information is read out via a CAN field bus, a solution pioneered by NIKHEF for the ATLAS muon spectrometer.

Forward proton detector

The forward proton detector is an addition to D0 that is new for Run II. At tens of meters from the interaction point there will be several detector stations. Each station contains one or more so-called Roman pots: chambers with a very thin wall facing the beams that can be moved towards and from the beams. Inside these chambers are scintillating fibre detectors that accurately measure the position of particles traversing them. The thin walls in the chambers separating the scintillating fibre detectors and the vacuum inside the beam pipe allow the particles to pass through several stations with a minimum disturbance.

The NIKHEF group in Amsterdam makes very fruitful use of the experience in the mechanical technology department from constructing and running the MEA accelerator, by participating in the mechanical design. The Roman pots themselves, with their crucial thin windows, and the movable tables to support the entire structure and allow it to be aligned with the beam axis are being designed at NIKHEF and will be manufactured under our supervision in industry.

In 1998 the Roman pot design has been finished and the design of the support tables has started. In 1999 these items will be fabricated and shipped for installation in the Tevatron tunnel.

Muon reconstruction

The offline reconstruction for the Run II D0 detector will be completely rewritten in an object oriented way using C++. The NIKHEF group in Amsterdam has offered to participate by writing code for the muon reconstruction. This work closely relates to the same work being done for the ATLAS experiment. The muon reconstruction software is also intended to be used in the third level trigger, maybe after small modification to improve speed. In 1998 work has been done on graphical representation of the muon chambers, a work resulting in corrections to the existing data base for muon chamber positions. In 1999 the entire reconstruction software has to be written and commissioned.

Preparation for physics analysis

Preparations for physics analysis have started immediately after D0 was joined. In regular meetings of the NIKHEF groups physics topics are discussed. The NIKHEF theory department provides actively input to these discussions and there is a fruitful exchange between theory and experiment.

In November 1998 a number of NIKHEF physicists have participated in the Run II Higgs and SUSY workshop at FNAL. The Nijmegen group has the fast detector simulation for a generic Tevatron detector running and is studying the detection of Higgs events, especially through the reconstruction of tau-leptons.

1.3 ATLAS Experiment

Inner tracker

The production of the modules of the silicon central tracker (SCT) is organised in a number of production clusters, each consisting of several institutes. NIKHEF is one of the partners of the Central European Cluster (CEC), together with groups in Munich, Freiburg and Prague. We have committed ourselves to build 100 forward modules. To ensure a guaranteed performance and position accuracy, in the SCT community an extensive set of tooling is now being devised.

The positioning of the assembled forward modules onto the support disks will be done at NIKHEF for one side of the SCT. Special tooling will be devised to avoid damage during mounting of the extremely vulnerable detectors. The final detector positions on the disk will be mapped with a large 3D coordinate measuring machine which has already been installed. An automatic CCD camera system will be installed on this machine to provide contact-free measurements.

The detector modules are coupled by optical fibres to the data acquisition (DAQ) system. NIKHEF will be one of the few sites where the optical connections are made and verified. To check the modules at several stages during assembly, a DAQ system based on the DSP has been installed. Both the electronics and the

detector substrates have to be cooled, the latter to less than -10^{o}C. Preparations have been started to build a few dummy modules for cooling tests. As a contribution to the prototype testing program of the CEC, NIKHEF took the responsibility for the DAQ and the optical links to the modules. Nine prototype modules will be mounted on a partial carbon fibre disk made at NIKHEF to verify both the electrical properties and cooling operation.

Muon spectrometer

In 1998 NIKHEF continued to be the main player in the operation of the large muon spectrometer test stand (DATCHA) at CERN. The data analysis led to a revision of the mounting and calibration procedure of several components of the alignment system. The excellent performance achieved in DATCHA with the Ar-CO_2 drift gas mixture proposed by NIKHEF led the collaboration to adopt this mixture as the baseline option for LHC running. The detector control systems proposed by NIKHEF to measure the temperature and magnetic field distributions performed as expected and have hence been accepted by the collaboration.

Figure 1.2: *The prototype large muon chamber for the ATLAS detector.*

NIKHEF ideas on front-end electronics are tested presently in DATCHA and depending on the outcome these might find their way into the final layout. Most of these results have been documented in internal ATLAS notes.

In a collaboration with CERN, NIKHEF contributed to the final design of a crucial aspect of the Monitored Drift Tube system: the endplug and the way in which a single drift tube is wired in an automated and hence manpower efficient way. With this, the most important aspects of the project have been defined and the preparations towards mass production of, in the case of NIKHEF, 96 Monitored Drift Tube chambers (432 drift tubes each) have started.

Regarding the Rasnik system the radiations hardness of all components has been established and steps were taken to allow cost effective procurements of the components: masks, lens holders and CCD cameras. By mid 1999 we expect to be able to deliver to the collaboration large quantities of these systems.

A study has been started at NIKHEF of the optimal layout for data transfer from the drift tube TDCs via the Read-Out Drivers to the Read-out Buffers. NIKHEF has major responsibilities in the procurement of both the drivers (Nijmegen) and the buffers (Amsterdam). This effort is expected to come to a conclusion in 1999.

2 B Physics

2.1 Introduction

The B physics group of NIKHEF participates in LHCb at CERN and HERA-B at DESY. The goal of both experiments is the observation of CP violation in decays of heavy B mesons. Data taking at LHC is foreseen to start in the year 2005. For HERA-B, data taking is scheduled to start in 1999. The modest NIKHEF participation in HERA-B is mainly a preparation for the much larger enterprise at LHCb.

2.2 Status of LHCb

In February, the Technical Proposal has been submitted. In fall, it has been approved by CERN. At NIKHEF, we have submitted a proposal for a FOM programme "Study of Charge-Parity Violation with the LHCb Experiment at CERN". The FOM board has approved this proposal in November. With the approval of the experiment, the emphasis of the LHCb collaboration has shifted from the optimisation of the overall design of the detector to the design and R&D of the different components. Also the NIKHEF group has started to study prototype detectors in testbeams.

Besides the hardware responsibilities in tracking devices, described below, the NIKHEF group has made major contributions to the physics performance studies in the Technical Proposal. The most popular decay for the observation of CP violation is that of a B_d meson into a J/ψ meson plus a kaon, with subsequent decay of the J/ψ into a lepton pair. However, the study of one decay channel is not enough to pinpoint the sources of CP violation. At NIKHEF, we focus on the decay of B_s mesons to a charmed meson (D_s) plus a kaon. In this decay, the theoretical calculation of the CP violation can be carried out unambiguously. It is therefore very attractive for our purpose, although the measurement is rather difficult. The B_s decay products must be identified among many other particles in the final state, so a very efficient tracking system is needed. Because of the fast oscillation of the B_s meson between particle and antiparticle states, an excellent decay time resolution is needed for the measurement of the asymmetry between the B_s and its antiparticle. Our expertise in tracking will be crucial in this analysis.

LHCb detector and NIKHEF participation

The basis of a good reconstruction of B meson decays is an accurate and efficient system for measuring the tracks of charged daughter particles. Therefore, we plan to concentrate the NIKHEF involvement in LHCb hardware on the tracking system. The main tracking system of LHCb has been designed by NIKHEF. The Outer Tracker will cover 98% of its area, and is based on fast drift chambers. Design and development of the Outer Tracker are in the hands of NIKHEF. The detection of decay vertices separated by only a few millimetres from the collision point is an essential tool for B meson identification. A state-of-the-art vertex detector can measure the decay lengths with a precision of about 100 μm. NIKHEF participates in the realisation of the vertex detector. Our involvement in the tracking hardware is complemented by our responsibility for the track reconstruction software.

Outer Tracker

The Outer Tracker consists of chambers with drift cells of strawtube-like geometry. Each of the 10 tracking stations contains four planes with two staggered layers of drift cells. A plane is assembled from modules with standard width. Our experience with the Outer Tracker system of HERA-B was an essential ingredient for the choice of solutions for the LHCb detector. In the intense flux of hadrons, test chambers started to draw current. An intensive R&D program has started to investigate these aging effects. Besides participation in the HERA-B program, we have carried out aging tests at NIKHEF and at the tandem accelerator at the University of Utrecht. As a result of this program, we concentrate the module design on cathode foils from carbonised kapton. Since this material cannot easily be folded, our baseline design of the modules consists of round drift cells with strawtube geometry rather than honeycomb chambers.

A major challenge in the tracker design for LHCb lies in the fact that the proton beams in LHC may interact every 25 nanoseconds, while drift chambers are intrinsically "slow" detectors. It is crucial to find gas mixtures that allow fast transport of the ionisation signal, without loss of efficiency and without significant degradation of the measurement precision. We have carried out a dedicated research program on drift gases. We have studied prototype modules in a test beam at CERN. Figure 2.1 shows the prototype modules during set-up in Amsterdam. Main goal of the tests was the measurement of the maximum drift time in strawtube-like cells with different gas mixtures. The tests have also been carried out in magnetic fields op to 1 Tesla. The results show that our Monte Carlo simulations of the drift behaviour agree well with the measurements.

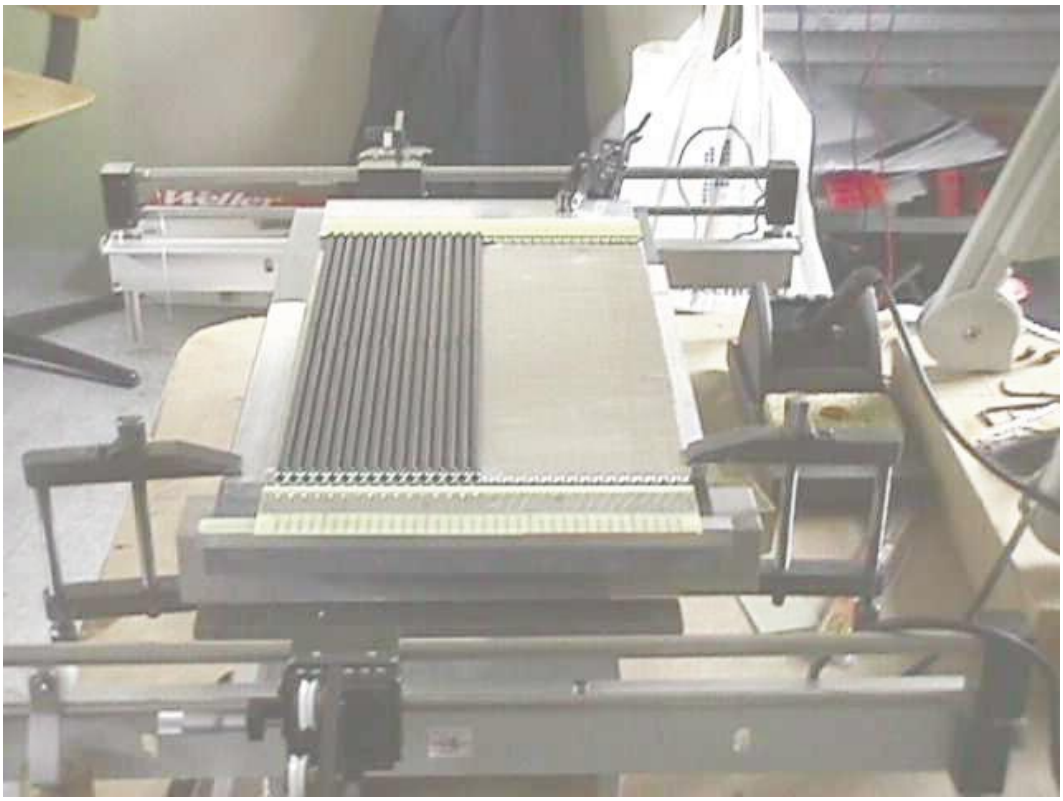

Figure 2.1: *Construction of a prototype module for the Outer Tracker for LHCb.*

In parallel to the R&D for the drift chamber modules, an engineering study of the station design has started. A full-size prototype of the frame of the middle-sized tracking station 6 has been assembled in the workshop. The aim of this enterprise is to optimise the location of the readout electronics, and to study the distribution of the services like gas, high voltage and signal cables.

Vertex Detector

The accurate measurement of the B decay vertices will be realised with an array of silicon micro-strip detectors. It is crucial to intercept the daughter particles from B decays as close as possible to the decay point, with a minimum of material between the decay point and the first point of measurement. Therefore, the silicon detectors and a part of the readout electronics will be installed inside the LHC beam pipe under ultra-high vacuum. The detectors can operate at about 8 mm from the LHC beams, once stable beam conditions are reached after filling the collider with proton bunches. During the filling process, the detectors have to be retracted by 3 cm to avoid radiation damage.

The vertex detector consists of 17 discs. Each disc is split in two halves, which are mounted in an intricate moveable support structure. The design and construction of the precision mechanics is a NIKHEF responsibility. The know-how in vacuum technology and accelerator physics in the AmPS group at NIKHEF is an important asset in this undertaking. The design needs to satisfy several requirements. The vacuum vessel and detector support must have low mass in the acceptance region and provide for precise alignment and retractability of the vertex detector. The beam-detector RF coupling must be minimised with wake-field suppressors. The design must take account of mechanical stresses induced by heat loading from leakage currents in the silicon detectors, the electronics, and remaining wake fields. It must be compatible with the LHC ultra-high vacuum, while providing feed-trough for several thousands of signal cables. Figure 2.2 shows a preliminary design of the vacuum vessel and the support structures.

One of the most critical items in the read-out electronics is the front-end chip which contains the amplifier and the pipeline buffers. One of the options the LHCb collaboration peruses is the development of a new chip, tailored to the LHCb requirements. Many components of this chip are based on similar components of HE-

LIX. The chip is designed in the new IBM 0.25 μm deep-submicron process. In parallel to the design of the chip, general R&D on radiation hardness is carried out, in particular design rules to increase radiation tolerance of CMOS structures are studied. NIKHEF participates in these activities, and is working on the design of the low-noise preamplifier of the new chip.

Next to the vertex detector proper, there will be a smaller set of silicon detectors that will be used to determine how many primary interactions occurred simultaneously within one proton bunch crossing. This will provide a measurement of the luminosity (a measure for the total interaction rate) at the LHCb interaction point. This so-called Pile-up Detector will also be used to reject events with more than one interaction. The detector was proposed by NIKHEF.

2.3 Status of HERA-B

Due to unexpected aging effects, observed in prototype chambers operating in hadron beams, the mass production of modules was interrupted in 1997. An intensive R&D program has resulted in two major changes in the design of the modules. Evidence was found for a local, permanent damage of the cathode foils. This damage can be avoided by coating the foils with a thin metal layer. After extensive tests a double layer coating with 40 nm copper and 50 nm gold has been chosen. The second important change concerns the gas mixture. The previously used mixture ($Ar/CF_4/CH_4$) was found cause aging effects. The new mixture ($Ar/CF_4/CO_2$) is not significantly slower, and no aging effects have been observed with this mixture. Module production with coated foils has been resumed. The installation of the Outer Tracker is planned for 1999, in several steps spreading over the whole year.

Since NIKHEF can not participate anymore in the restarted module production, our contribution the construction of the Outer Tracker is limited to forming of the foils. The foils are shaped with an automatic folding machine, and then tempered at about 150 degrees to remove the tensions introduced during folding.

We are also responsible for link boards between the Outer Tracker readout and the first level trigger units. These boards remap, label and serialise the wire hit data of the Outer Tracker. The data are transmitted serially via fast optical links to the trigger units. The NIKHEF design of the link boards is very flexible. It will not only be used by the Outer Tracker, as originally foreseen, but also by the Muon system. In 1998,

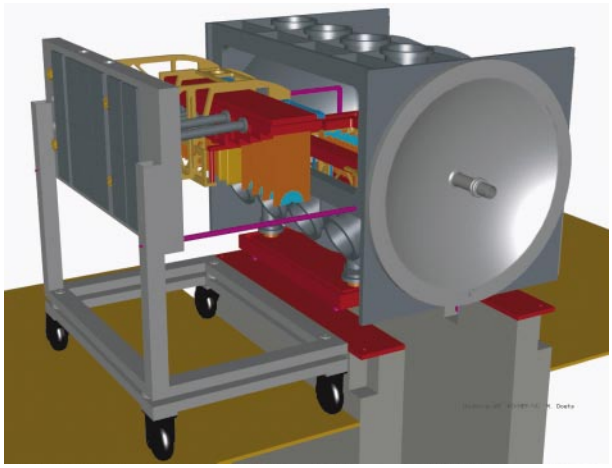

Figure 2.2: *Preliminary design of the vacuum vessel for the vertex detector in LHCb.*

prototype boards have been tested in the lab, and also in the HERA-B trigger. Unfortunately, these tests revealed some problems, which made a partial redesign of the boards necessary.

Besides our commitments in the Outer Tracker, where mainly the group from NIKHEF/FOM and UvA are involved, the Utrecht group designs and builds a silicon tracking station, located just outside the vertex tank. This complements our commitments in the Outer Tracker, where mainly the group from NIKHEF/FOM and UvA are involved. The Utrecht detector provides a third high precision measurement point for low angle tracks in the detector, and gives an online position calibration for the silicon detection planes inside the vertex detector. The detectors are located in an intense radiation environment. A part of the detector has been installed in the autumn of 1998, and is being commissioned. The full detector will be installed in the autumn of 1999.

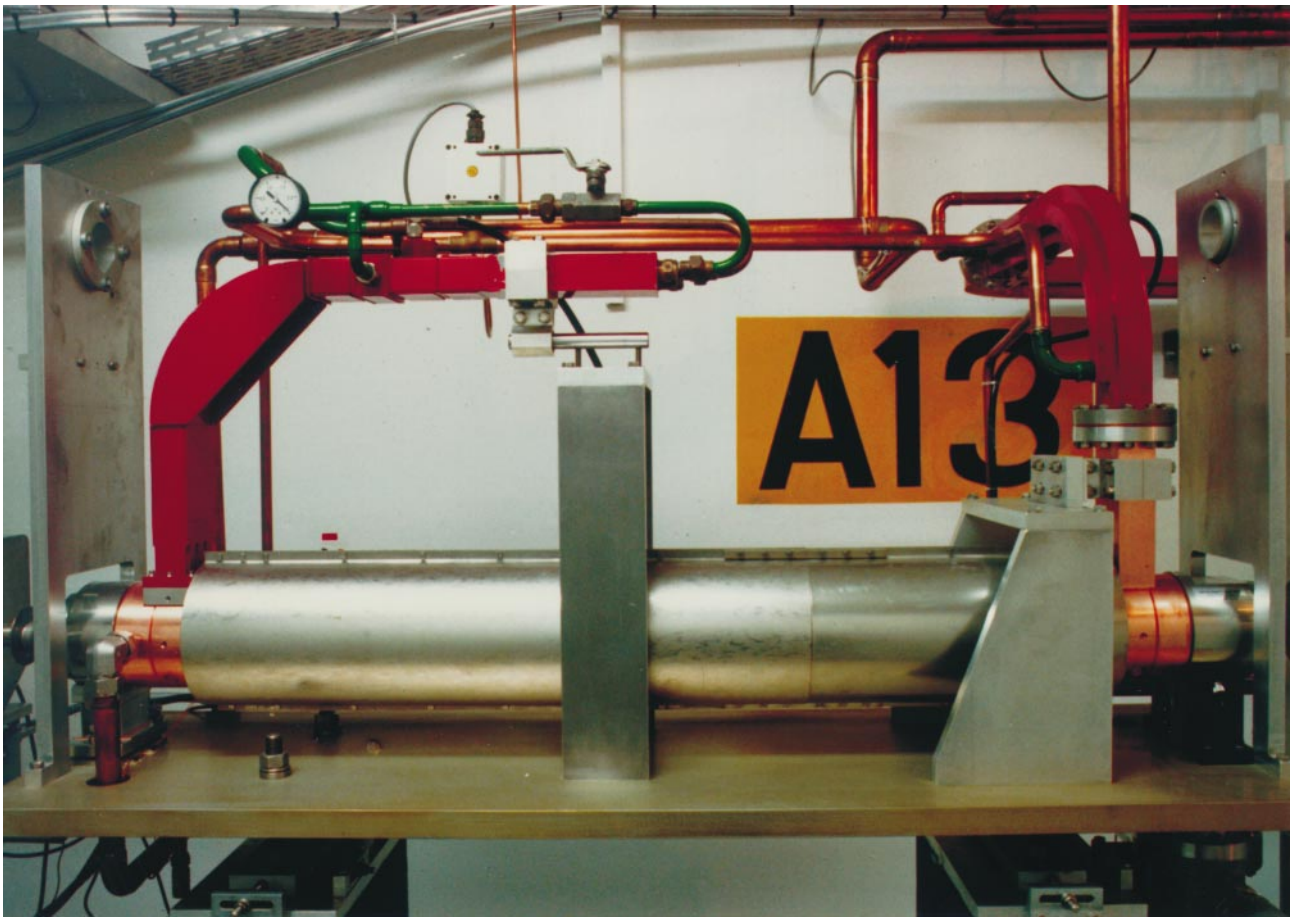

The accelerating section for the energy spectrum compressor at the end of MEA (photo: NIKHEF)

3 ALICE

3.1 The ALICE Inner Tracking System

NIKHEF has taken responsibility for the design and the integration of the silicon strip layers and the associated electronics of the ALICE inner tracking system, in cooperation with groups in Strasbourg, St. Petersburg, Kharkov, Nantes and Turin. The department of Subatomic Physics at Utrecht University, as part of the NIKHEF organisation, has played an important role in this project.

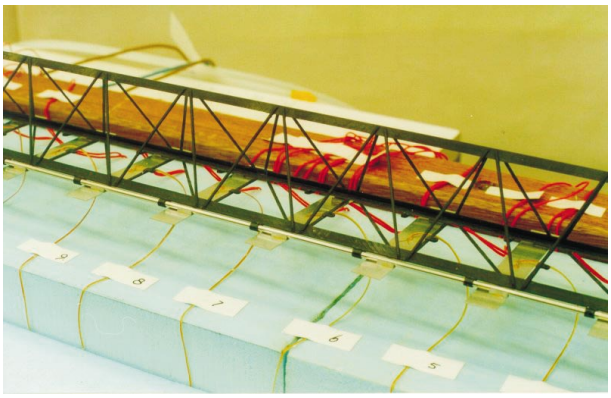

Figure 3.1: *The carbon fibre support structure prototype.*

One of the most challenging features of the silicon strip layers of the ALICE inner tracking system is the extensive use of microcables for the electronic connections near the silicon detectors. A facility has been created with which we can process the microcables and study the options for assembly of the silicon detector modules including the microcables. The Scientific Research Technological Institute of Instrument Making, Kharkov, Ukraine (SRTIIM) has produced prototype microcables which were subsequently tested in Utrecht. Using this experience we have designed new cables, together with SRTIIM. They were used in the NA57 experiment at CERN in September. It was the first application of this novel cable design in a physics experiment.

Specifications for the silicon detectors were made in close cooperation with the Strasbourg group. Detectors were ordered from two manufacturers, according to these specifications. The detectors, connected to the front-end electronics with microcables, were successfully tested in the NA57 experiment. In parallel the Strasbourg group tested detectors from the same production batch extensively in a test beam at the CERN Proton Synchrotron. The tests showed that the detectors function according to the specifications and that the microcables are a good solution for the electronics interconnection problems.

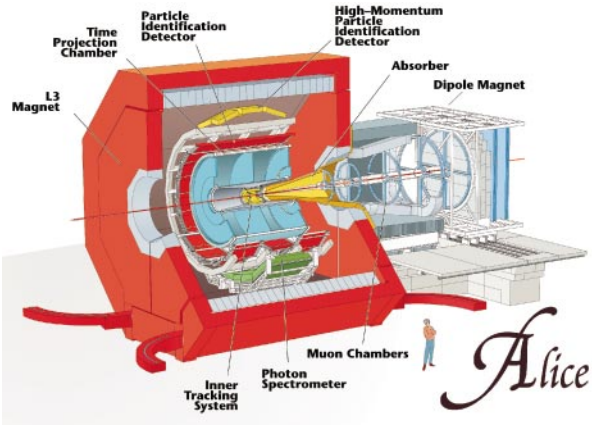

Figure 3.2: *An artists view of the ALICE detector.*

A new design for the carbon fibre support structure of the silicon strip layers (see Fig. 3.1) has been made together with the St. Petersburg group. A prototype of this support was produced in St. Petersburg, using a mould produced at the Instrumentele Groep Fysica, formerly the workshop, in Utrecht. This prototype, which includes tubes for the cooling system, is now under test in Utrecht.

More information can be found in the ALICE web pages: `http://www.phys.uu.nl/~alice`

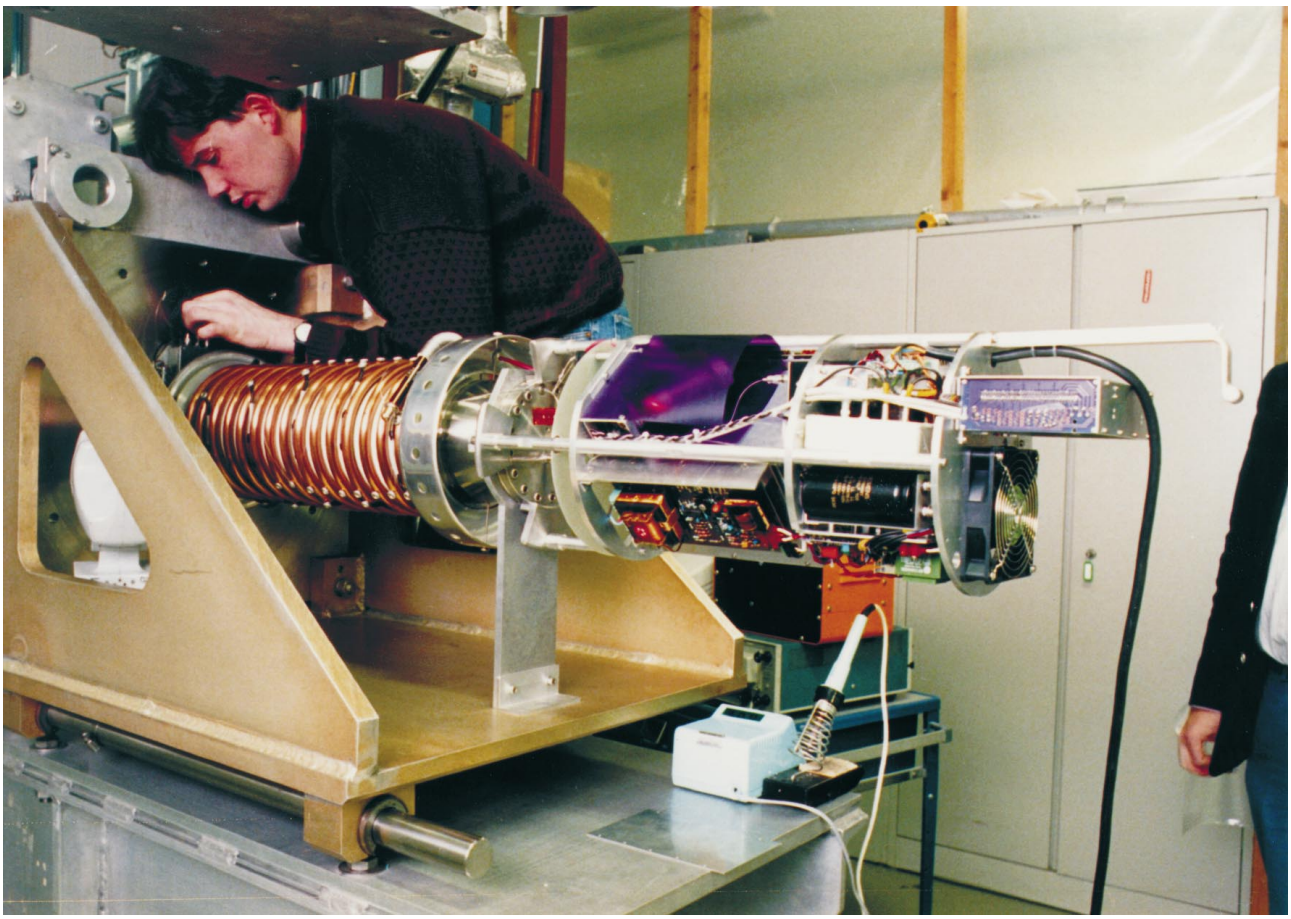

A glimpse of the inside of the MEA injector (photo: NIKHEF)

D Theoretical Physics

1 Research program Theoretical Physics

1.1 Introduction

The research program of the NIKHEF Theory Group ranges from computational work to predict and understand the outcome of specific experiments, to investigations into the mathematics of quantum field theory and its generalisations. A representative selection is described hereafter.

1.2 Hadron structure and deep-inelastic scattering

Hadrons are composite states of colour-charged objects. Usually these are interpreted as quarks and gluons. To investigate the structure of the proton experimentally, one scatters protons with very energetic colour-neutral electrons in elastic and inelastic collisions. The results of these experiments cannot be understood exclusively in terms of the perturbative formulation of QCD, i.e. in terms of local single-particle interactions between quarks and gluons. Especially in the kinematical regime of low-x, as covered by the HERA experiments, specific non-perturbative features are seen in the data. Some of these features can be modelled successfully by means of the so-called Pomeron, a concept which can only be partly understood in terms of QCD and which is supposed to be dominated by gluonic effects. In order to get information about the gluonic content of the Pomeron, Haakman, Kaidalov and Koch considered the production of charm by real and virtual photons, with special attention to diffractive charm production.

1.3 Perturbative QCD

Cross sections measured from hard scattering processes involving quarks and gluons can be computed using QCD. These computations are always done using perturbation theory, with the QCD coupling α_s as the expansion parameter. This is often a fine approach. However, if the kinematics is such that the initial state contains only slightly more energy than needed to produce the final state of interest, the effective expansion parameter actually becomes α_s times two powers of a large logarithm (the so-called Sudakov logs) which makes it much larger than α_s. To rescue the perturbative approach, one may (re)sum these logarithms to all orders, using the fact that there is a certain regularity in how they occur order by order in perturbation theory. Laenen, Oderda and Sterman have shown how this resummation technique works for single-particle inclusive kinematics, and derived resummed analytical answers for direct photon production and heavy quark production in hadronic collisions. Laenen and Moch have done the same for electroproduction of heavy quarks, a reaction measured at the HERA collider in DESY, and performed extensive numerical studies related to these resummation techniques.

To maximise the possibilities of comparing observables computed to next-to-leading order in perturbative QCD with data, it is important to have the most flexible methods to do such computations. One aims for a minimum of analytical work, and maximum ease in incorporating experimental cuts and acceptances on final state particle momenta. Keller and Laenen have devised such a method. They extended an already existing method for computation of jet cross sections in such a way as to be applicable to any reaction in which a particle (e.g. a pion, photon or heavy meson) is tagged.

1.4 Higher loops in perturbation theory

The complexity of the evaluation of diagrams in perturbative field theory increases rapidly with the order of the expansion. Hence the higher orders require enormous effort due both to the number of diagrams to be evaluated and to the mathematics involved. It seems now that certain new mathematical developments may cause some breakthroughs in this field. These diagrams are traditionally evaluated as a set of nested integrals. It turns out that the diagrams can be expressed in classes of "harmonic sums". How to do this in such a way that these sums can actually give a compact answer, is work that is currently under investigation. Related to harmonic sums is a new class of functions (harmonic polylogarithms) which should be usable to present answers of such calculations. Already, these functions provide more concise expressions for existing results. This problem has been studied by Vermaseren in collaboration with E. Remiddi (Bologna).

Another aspect of higher-loop computations concerns the group theory factors one encounters in the diagrams. A typical multi-loop diagram contains traces over quark loops, contracted with gluonic tensors. One would like to compute these factors efficiently, express them in the minimal number of group invariants, and do all this as much as possible in a group-independent way,

so that the results of for example a β-function calculation do not only apply to QCD, but also to other gauge groups that might for example appear in unified theories. Van Ritbergen, Schellekens and Vermaseren made considerable progress in this area by combining results from the literature, new results in graph combinatorics and techniques developed for studying anomaly cancellation in string theory with the power of the algebraic program FORM.

1.5 Conformal field theory

Two dimensional field theories with conformal invariance (which includes invariance under scale transformations) play an important rôle in string theory, which in its turn is a candidate theory for quantum gravity and all other interactions. Conformal invariance in two dimensions is a powerful tool, which often reduces field theory computations to algebraic problems. However, many of the required algebraic tools have only been partly developed, and much work is still needed. Furthermore the importance of non-perturbative string physics has become clear during the last few years. Although conformal field theory *a priori* only describes perturbative string theory, it still has a useful rôle to play. It was discovered that in the extreme non-perturbative limit, i.e. the limit where the coupling constant goes to infinity, an alternative, "dual" description can be used. In many cases this dual theory is again a string theory, which can be analysed with conformal field theory. The conjectured dualities are shown in Fig. 1.1. Until a few years ago, most work on conformal field theory was limited to closed strings, implying that the field theory lives on closed two-dimensional surfaces. Open strings were known, but had been neglected, until it turned out that they can appear as strong coupling duals of certain closed string theories. Now further development of conformal field theory on surfaces with boundaries has become important, and it is one of the activities being pursued in the theory group. Other activities in this area include work on fixed point resolution and work on singular vectors in $N = 2$ conformal field theories.

1.6 Supermembranes and M-theory

As explained above, strong coupling duals of string theories are often other string theories, but in some cases they are something else, new theories that are still rather poorly understood. The holy grail among them is an 11-dimensional theory often referred to as "M-theory". Evidence for the existence of such a theory has been around for years, since eleven is precisely the maximum number of dimensions in which supergravity can be formulated. Indeed, 11-dimensional supergravity has fascinated some theorists for a long time already, but it also seemed disappointing that it was outside the equally fascinating realm of string theory. Now the fields have joined, and it has become clear that 11-dimensional supergravity should be viewed as the low-energy limit of a new theory. Since string theory is not available for the description of that theory, it is much harder to get access to it. It was suggested some time ago that this theory could perhaps be described by a higher dimensional generalisation of strings, namely membranes. Unfortunately membranes are much harder to deal with than strings – partly due to the absence of conformal field theory as a tool. Furthermore early investigations of supermembrane theory revealed a continuous spectrum which was considered a disaster. However, two years ago a new theory called Matrix theory emerged from the regulating theory of the supermembranes, in which this continuous spectrum has a natural interpretation in terms of so-called "D0-particles". This matrix theory gives a concrete description in terms of the limit at large N of supersymmetric $U(N)$ Yang-Mills theory in $0 + 1$ dimensions – in other words ordinary quantum mechanics. The challenge is now to check that this theory indeed agrees with its supposed low-energy limit, 11-dimensional supergravity. For example, one may compare the scattering of gravitons in both approaches. Several such computations were done by Plefka and Waldron, in collaboration with M. Serone (U.v.A). Their conclusion,

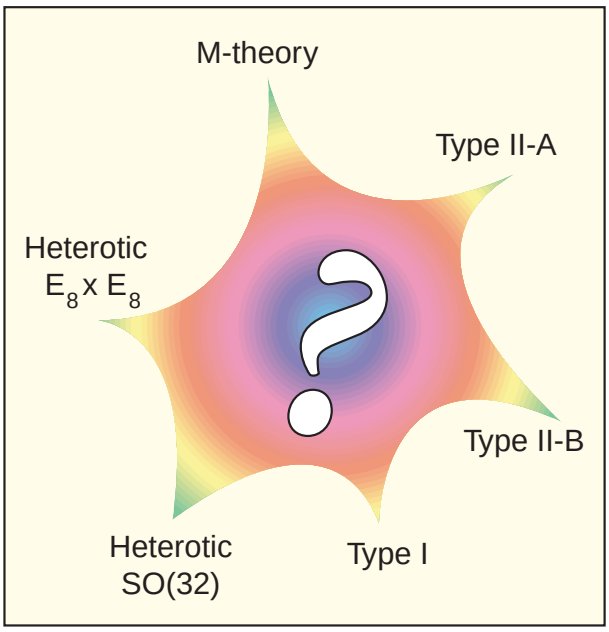

Figure 1.1: *Conjectured string dualities.*

confirmed by calculations done elsewhere, is that there is indeed agreement.

Manifestly supersymmetric versions of superparticle, superstring and supermembrane theories exhibit new fermionic symmetries. A new one is so-called local Siegel symmetry, which is important to establish the correct counting of the number of degrees of freedom in these models. Algebraic properties of this symmetry have been studied by van Holten and Jarvis, in collaboration with J. Kowalski-Glikman of the university of Wroclaw.

1.7 Supersymmetric sigma models

Supersymmetry is a symmetry connecting the properties of bosons with integral spin and those of fermions, with half-integral spin. It has attractive theoretical features, which have lead to the conjecture of a supersymmetric extension of the Standard Model of elementary particles. The search for signals of supersymmetry is on the menue of many existing and planned experiments. The origin of supersymmetry supposedly is to be sought in quantum gravity, and specifically in superstring theory. This leads one to conjecture that at scales close to the Planck scale physics is effectively described by supergravity models, theories combining gravity with local supersymmetry. There are a number of consistency requirements that such a theory has to satisfy: mathematical ones, like the absence of anomalies, and physical ones, in particular the requirement that at energies in the TeV range (hence far below the Planck scale) they reproduce the known features of the Standard Model or its supersymmetric extension.

Certain elegant models of supersymmetry, describing both massive and massless gauge bosons at equal footing, were previously thought to be inconsistent both for mathematical (anomalies) and phenomenological reasons (correct charges of particles). Groot Nibbelink and van Holten have shown that both problems can be solved in a new formulation of these theories. The class of candidate supergravity models has thereby been enlarged. Further studies will show if these models can produce the correct phenomenology to reduce to the Standard Model at low energies.

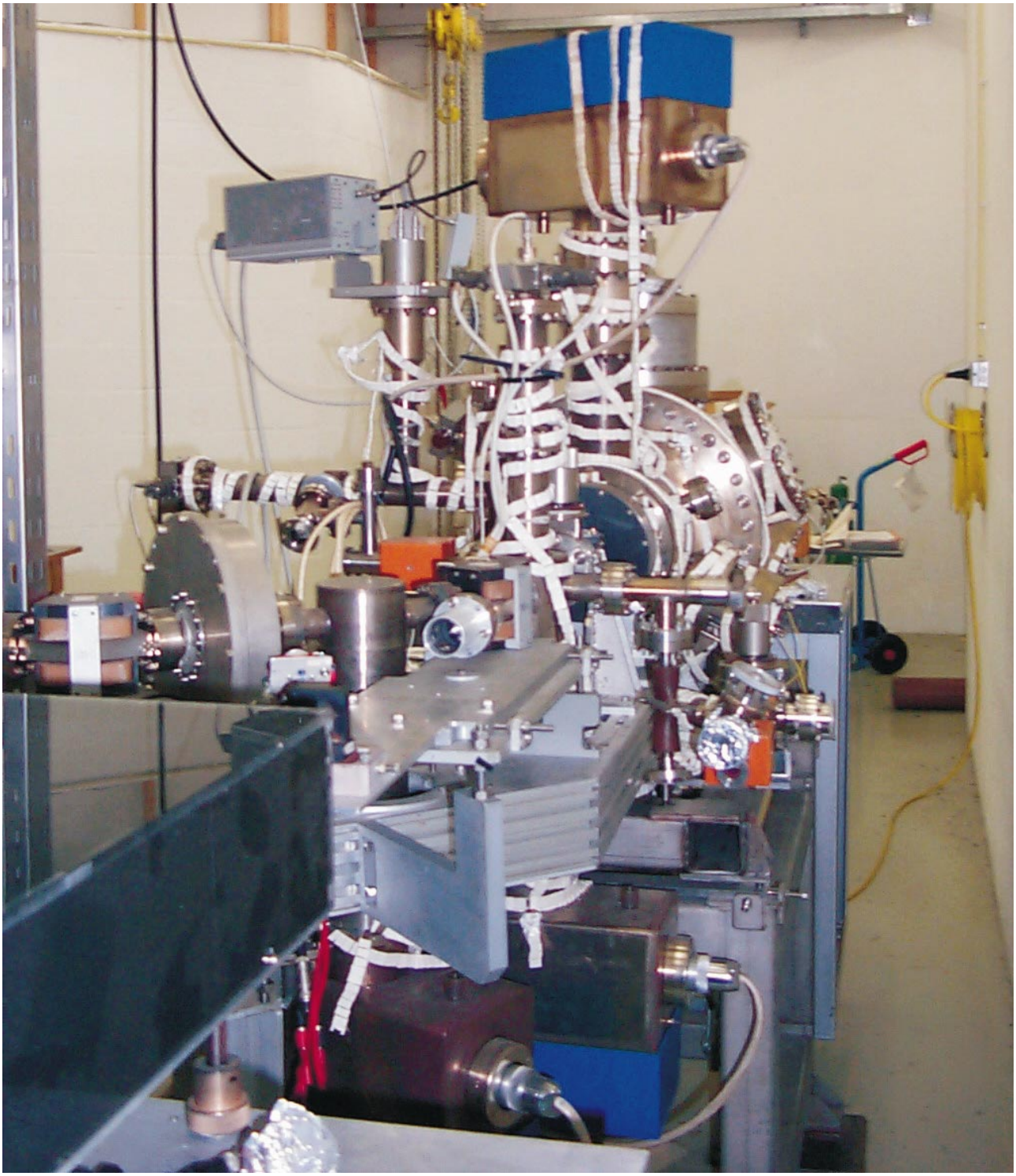

The Polarised Electron Source (PES) (photo: NIKHEF)

2 CHEAF

2.1 Introduction

This year was an extremely fruitful year for CHEAF's (Center for High Energy Astrophysics) research, with no less than three major scientific discoveries. These highlights were:

2.2 Magnetars

The discovery by the team of C. Kouveliotou and J.A. van Paradijs of the "Magnetars", neutron stars inside young supernova remnants in our Galaxy, with magnetic fields two to three orders of magnitude larger than known until then: 10^{15} Gauss (10^{11} Tesla) [1]. The existence of these neutron stars was discovered as a result of their recurrent outbursts of soft Gamma Ray emission, detected with NASA's Gamma Ray Observatory (GRO). In 1998 the Kouveliotou-Van Paradijs team discovered that the Soft Gamma Ray Repeater SGR1806-20 had a regular pulse period in Gamma Rays and X-rays of 7.476551 seconds during its outburst in November 1996, indicating that this object is a rotating magnetised neutron star. The rotation rate of such neutron stars decreases as a result of emission of magnetic dipole radiating - the rate of decrease being faster if the magnetic field strength is larger. Looking into data of its 1993 outburst the team found a pulse period of 7.4685125 seconds in 1993, indicating an extremely rapid increase of its spin period, showing that its dipole magnetic field strength must be about 10^{11} Tesla (*Nature* 393, 235, 21 May 1998). A second regular pulse period was discovered in the Soft Gamma Ray Repeater SGR1900+14, which had an enormous gamma-ray outburst on 27 August 1998. This outburst (of an object 20.000 lightyears away!) was so strong that it caused the shut-down of half a dozen satellites in orbit around the Earth (see Newsweek, October 12, 1998, p.54). Also this object is in a young supernova remnant, and has a rapidly increasing pulse period (in this case: 5.159142 sec. on 27 August 1998), again indicating a 10^{11} Tesla magnetic field strength. The very short lifetime (all of these objects are less than 3000 years old) and the fact that already half a dozen are known in our galaxy indicates that at least some 10 to 20 per cent of all neutron stars belongs to the "Magnetar"-class. It is surprising that for 32 years since the discovery of radio pulsars such a major class of neutron stars had been overlooked!

2.3 X-ray pulsar

The CHEAF graduate student Rudy Wijnands discovered, using NASA's Rossi-XTE satellite, the first millisecond X-ray pulsar, which happens to be in a close binary system. This source, SAX J1808.4-3658 is an accreting magnetised neutron star spinning some 400 times per second around its axis. Already in 1982 the existence of such millisecond X-ray pulsars had been predicted on theoretical grounds: they were theorised to be the predecessors of the millisecond radio pulsars discovered in 1982, which in many cases have been found to be members of binary systems, in which their companion stars always are "dead" stars (white dwarfs). When these companions were still active normal stars, one expects them to have been transferring mass and angular momentum to their neutron star neighbours, causing these to be X-ray sources, and at the same time causing their rotation frequently to increase to higher and higher values. The discovery by Wijnands of this "missing link" was a major breakthrough for which he was awarded –among other distinctions– with the Andreas Bonn prize (for the best Ph.D. thesis in the University of Amsterdam) of the Amsterdam Genootschap voor Natuur-, Genees- en Heelkunde. Furthermore, Wijnands was selected by NASA (from 45 candidates) for a 3-year Chandrasekhar post-doctoral fellowship (he chose to go with this Fellowship to the Massachusetts Institute of Technology). This discovery, published in *Nature* [2] received much media attention, for example from *CNN*, *"the Economist"* and many newspapers in the Netherlands and abroad.

2.4 Supernova

The CHEAF graduate student Titus Galama discovered on 25 April 1998 an extremely peculiar supernova, called "Supernova 1998 bw", occurring in a spiral galaxy 150 million lightyears away and exactly at the position on the sky of the strong Gamma Ray Burst GRB980425, discovered with the Dutch instrument aboard the Italian-Dutch Beppo SAX satellite. Follow-up of the brightness-evolution of this supernova during the subsequent weeks showed a lightcurve indicating that the moment of the supernova explosion coincided within + 1 day with the time of the Gamma Ray Burst [3]. Furthermore, the supernova showed a radio-flash, produced by relativistic electrons, indicating that matter had been accelerated here to relativistic velocities, a phenomenon never observed in a supernova before. The supernova turns out to belong to a very rare type (so-called Type Ic) and was an order of magnitude brighter than any supernova ever observed. Its brightness and spectrum (which showed the absence

of hydrogen and helium) showed that in this explosion about 0.7 solar masses of iron were ejected, over one order of magnitude more than in other supernovae produced by massive stars. Theoretical modelling showed that the exploding star was a pure Carbon-Oxygen star with a mass between 6 and 12 solar masses [4], and that the collapsing stellar core had a mass of at least 3 solar masses. Since this is larger than the upper mass limit of a neutron star, the general consensus is that here, for the first time, one has witnessed the birth of a black hole [4]. The C-O star which exploded must have been the remnant-core of an originally very massive ordinary star – with a mass over fifty times larger than that of the sun. Also this discovery received much media attention, e.g. from *Scientific American*, *Science* and many newspapers in the Netherlands and abroad. Titus Galama was offered several prestigious postdoctoral fellowships abroad, and finally decided to choose a 3-year Fairchild Fellowship offered him by the California Institute of Technology.

2.5 Top Graduate School

A further important "highlight" of this year was the selection of the Netherlands Research School for Astronomy NOVA, in which CHEAF is a partner, as a so-called "Top Graduate School", which means that for the coming 5-10 years extra funding will be available for CHEAF's research in High Energy Astrophysics (only 6 graduate schools in the country were selected for this prestigious programme of extra funding).

2.6 GRAIL funding rejected

On the other hand, an important and disappointing setback in 1998 for CHEAF's research was the fact that the Netherlands Science Foundation NWO rejected the request for funding for the GRAIL-project, aimed at constructing a large detector for gravitational waves.

For further reporting about CHEAF's activities in 1998 we refer to the annual reports of CHEAF and of the Astronomical Institute "Anton Pannekoek" of the University of Amsterdam

References

[1] C. Kouveliotou, S. Dieters, T. Strohmayer, J. van Paradijs et al.
Nature 393, 235, 1998

[2] R. Wijnands and M. van der Klis
Nature 394, 344, 1998

[3] T.J. Galama, P.M. Vreeswijk, J. van Paradijs, C. Kouveliotou et al.
Nature 395, 670, 1998

[4] K. Iwamoto, P.A. Mazzali, K. Nomoto, T.J. Galama, P.M. Vreeswijk, C. Kouveliotou, J.A. van Paradijs et al.
Nature 395, 672, 1998

E Technical Departments

1 Computer Technology

1.1 Central services

The central file service has been extended by adding a second file server *(park)* with a capacity of over 100 Gbyte of disk space for the on-line storage of physics data. Home directory services for all Unix accounts were moved to the *gandalf* file server. The Unix home directories are accessible from all clients systems (both Unix and Windows-NT) and are included in the regular daily back-up procedure. All central services in the network are implemented on servers of Sun Microsystems, with the exception of two small Windows-NT servers for dedicated services in the NIKHEF NT domain. The SAMBA protocol has been installed to connect Windows-NT (and Windows-95) clients on the desk top to the Unix file servers. Most of the Unix systems and some of the Windows systems are configured as AFS clients to be able to access the AFS servers on sites like DESY and CERN. Fig. 1.1 illustrates how client systems can be connected to the servers either inside or outside NIKHEF.

For the ATLAS scientific group a HP 9000 server system equipped with over 50 Gbyte of disk capacity has been installed as a workgroup server. This server runs with the HP-UX version 10 operating system and is comparable to the previous installed system for the Delphi/LHCb group.

On a Unix desk-top system or an X-terminal, one is not able to run typical Microsoft Office applications like *Word* and *Excel*. Obviously, alternative word processors and spreadsheets are available in the Unix world, but for compatibility reasons one often requires the functionality of the Microsoft Office tools. To fulfil this need a Windows-NT application server has been installed in the NIKHEF network. This server runs a special version of the Windows-NT system (TSE) in combination with the *MetaFrame* and *ThinConnect* packages from the Citrix company. Up to 15 users can run simultaneously Windows-NT applications like Word and Excel on this server from their Unix desk-top system or X-terminal.

Table 1.1 gives an overview of the server systems present in the NIKHEF network.

platform	OS	functionality
Sun Microsystems	Solaris	enterprise servers
Hewlett-Packard	HP-UX	workgroup servers ATLAS, LHCb
Sun Microsystems	Solaris	workgroup server EMIN/ITH
Silicon Graphics	IRIX	workgroup server ZEUS
DELL PC	Windows NT	servers Windows NT domain NIKHEF
Apple	MacOS	server Apple Macintosh domain

Table 1.1: *An overview of the server systems present in the NIKHEF network.*

1.2 Desk-top systems

Windows-NT and Linux systems running on commodity PC hardware were introduced in 1997 as an alternative on the desk top for the existing Unix platforms, X-terminals and Apple Macintoshes. This year the installation of either a Windows-NT system or a Linux system on the desk top, can be considered as a standard solution. Which system to select depends mainly on the demands of each individual user. In general non-scientific users, such as users from the administrative and technical groups, prefer a Windows-NT desk top, typically running *Office Tools* applications and specific technical software packages as *LabView*. The majority of the scientific users prefers a Unix system. Linux running on commodity PC hardware proved to be the first choice now, with the remarkable exception of the ATLAS software group, which selected Windows-NT as their preferred software development environment. Although Linux is free software and development and support are based on non-commercial agreements, the system proved to be mature, version management is well organised and Linux distributions come with a lot of free available software packages from the public domain area. Encouraging is the trend that more and more commercial software suppliers make their products available for the Linux platform in a serious attempt to prevent domination of the market by Microsoft products. Different distributions of the Linux system are available. Most likely NIKHEF will support two of them: *SUSE* for the DESY groups and *Red Hat* for the CERN related groups.

Most of the existing "traditional" Unix desk-top sys-

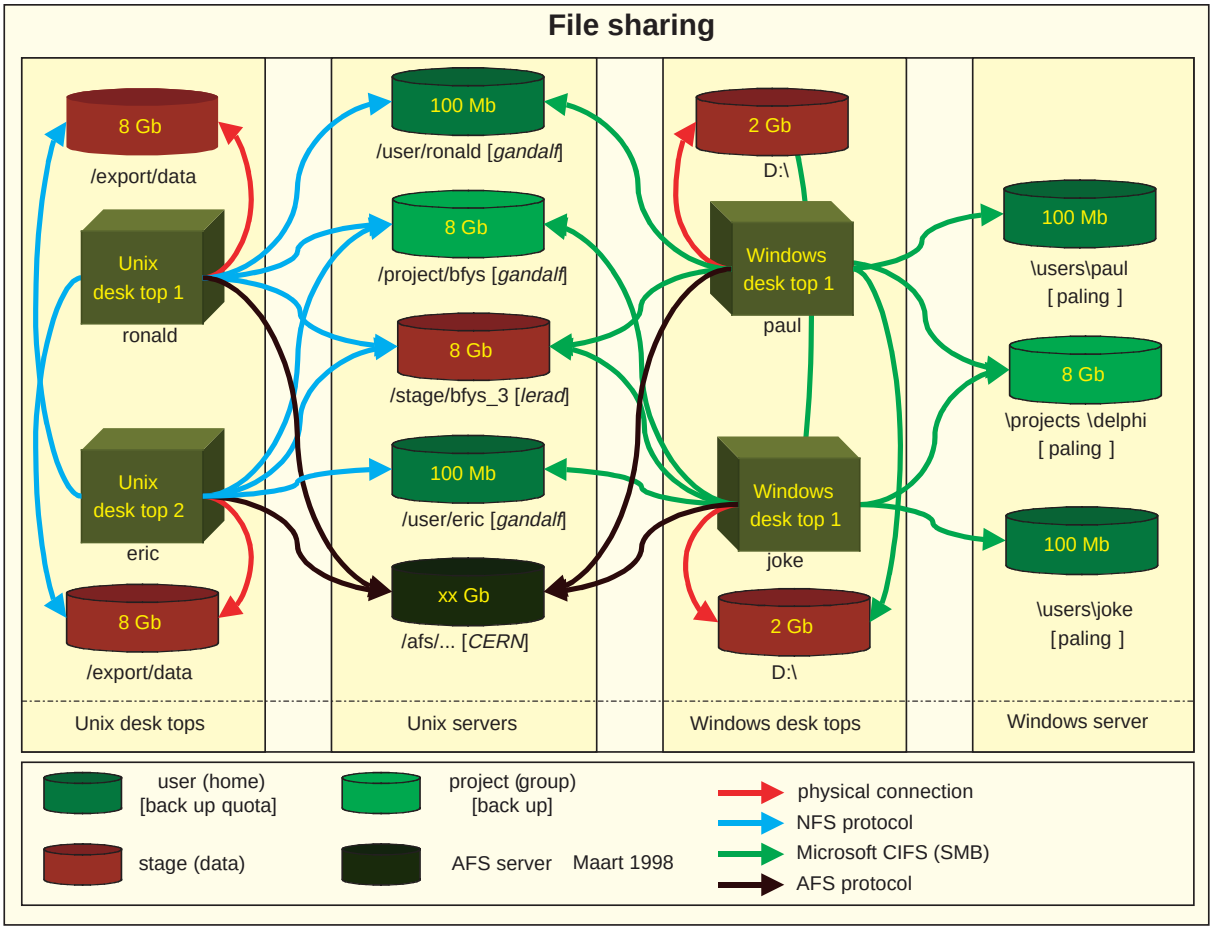

Figure 1.1: *How client systems can be connected to the servers either inside or outside NIKHEF.*

tems were either replaced by the new ones mentioned above or upgraded to newer versions of the operating system. Upgrades have been implemented for the Sun systems (from SunOS to Solaris), for the Hewlett-Packard systems (from HP-UX9 to HP-UX10) and for the SGI systems (from IRIX to IRIX 6). Table 1.2 gives an overview of the desk-top systems presently in use at NIKHEF.

1.3 Networking

The NIKHEF local area network (the *"ventweg"*) is partitioned into four segments by a CISCO 7000 router. Two segments contain mainly Unix systems, one segment is dedicated for PC and Macintosh systems, and the fourth segment,known as *guest network*, is reserved for laptops. The physical network infrastructure consists of two patch panel locations interconnected with fibre optic cables and about 700 connections from these

platform	operating system	number	trend
Sun Microsystems	Solaris/SunOS	70	∇
Hewlett-Packard	HP-UX	25	∇
Silicon Graphics	IRIX	20	∇
X-terminals	-	50	∇
DELL PC	Linux	30	Δ
DELL PC	Windows 95	50	∇
DELL PC	Windows NT	75	Δ
Apple Macintosh	MacOS	40	∇

Table 1.2: *Desk top systems at NIKHEF.*

patch panels to the end points in the NIKHEF buildings. About 30 active network components have been installed in the network. In general connections to the desk top systems are either shared or switched 10 Mbs ethernet connections.

Connection to the outside world is achieved by a shared 10 Mbps line on the WCW campus network to the SURFnet switch at SARA. Connections to CERN and DESY were improved this year by upgrading the European TEN-34 network to TEN-155 and by upgrading the academic research network (DFN) in Germany.

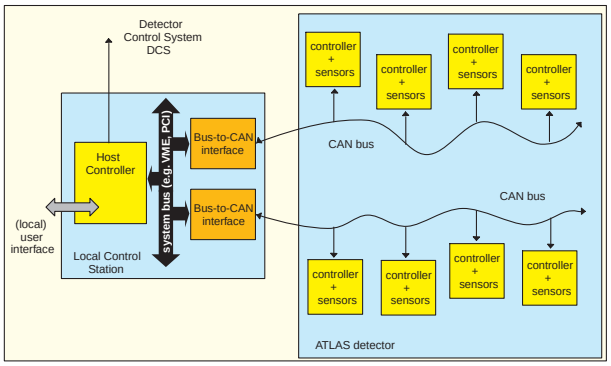

Figure 1.2: *A CAN-bus system for ATLAS sensor read-out.*

1.4 AMS-IX

SARA and NIKHEF offer housing facilities to the members of the Amsterdam Internet Exchange (AMS-IX). The AMS-IX is now one of the three largest Internet exchanges in Europe. The WCW campus location has developed into a very attractive location for telecommunication companies to concentrate their cable infrastructure and for Internet Service Providers to install network routers for the exchange of large amounts of data with each other (up to 60 Tbyte/month). At the end of 1998 five telecommunication companies and almost 30 Internet Service Providers have installed their network equipment in the central computer room of NIKHEF.

1.5 Video conferencing facility

For many years physicists at NIKHEF expressed their interest in a video-conferencing facility at NIKHEF. This facility has been realised this fall. It has been used successfully since by a number of scientists at NIKHEF for lively discussions with their colleagues at CERN, DESY and many other sites. Conferencing sessions can be set up as a point-to-point connection between two sites or as a multi-way session between more sites. The reservation and administration is organised in a professional way by the Energy Science Net (ESnet) of the Department of Energy in the U.S.A. The audio and video data can be transported by regular (ISDN) telephone lines with a maximum bandwidth of 6 x 64 Kbps, but in general sufficient bandwidth is provided by only two ISDN channels of 64 Kbps each.

1.6 Data acquisition systems

The DAQ system for the prototype tests of the LHCb Outer Tracker is derived from the DAQ system as implemented for the L3-Cosmics experiment. As data taking and environment are different in both experiments, the software running on the Motorola MVME2600 processor under the LynxOS system has been adapted to the requirements of the Outer Tracker experiment. As the event data come during spills, a read-out process has been introduced to take data from VME on high priority during these spills and to transfer it to the DAQ system for further handling between two spills. Run control and on-line event analysis are achieved by connecting the DAQ system to an HP Unix system, running a special version of the ROOT event-analysis package.

For both experiments, much effort has been put in test software to exercise the complex read-out hardware such as NIMROD's and CPC cards.

1.7 Embedded processors

Embedded processors such as digital signal processors (DSP) and fieldbus micro controllers are used for many applications in the high-energy physics instrumentation. The CT is involved in two typical areas. The first one is the on-going development for the ATLAS DAQ level-2 system. For the real-time level-2 trigger decisions a test system has been set up with SHARC DSP's from Analog Devices mounted on a PCI board. The second area where embedded and distributed intelligent processors have been implemented on a large scale are field buses. The effort put into the CAN field bus sensor read-out system for the ATLAS MDT detector (see Fig. 1.2) proved to be very valuable, because this technology could be re-used in control projects for the ZEUS and HERMES detector as well. Standardisation of the application software layer is an important requirement to achieve interoperability between different implementations. The CANopen standard, selected by CERN and NIKHEF, has been implemented for instance on temperature sensor modules by defining CANopen compliant device profiles for this type of sensors. Conforming to this type of industrial standards is very important in collaborations like ATLAS, with its many participants and its extreme long time scale.

1.8 Object-oriented analysis and design

The ATLAS back-end DAQ is not directly related to the physical read-out of the front-end crates, but it is

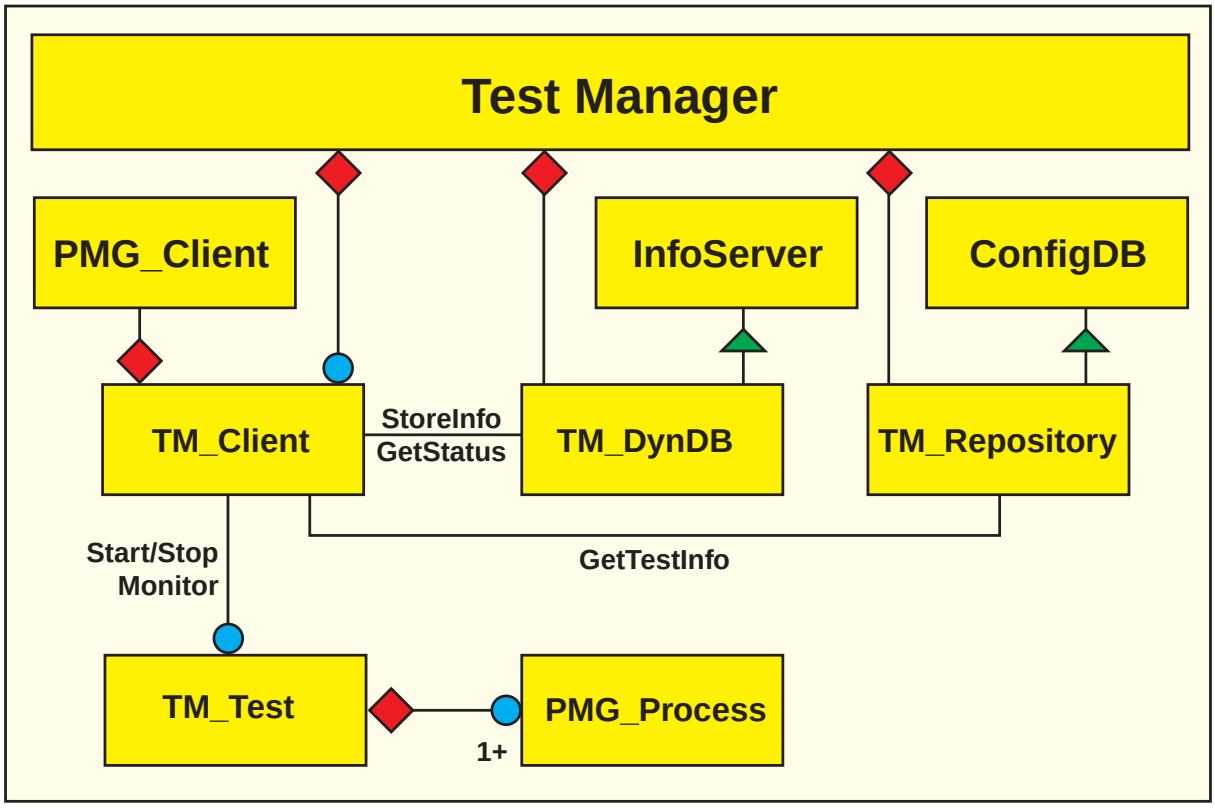

Figure 1.3: *Object model of the Test Manager (OMT notation).*

meant *to encompass the software to configure, control and monitor the DAQ but excludes the management, processing or transportation of physics data.* The CT group participates in the 'Prototype-1' DAQ project. This year the design and implementation of one component of the back-end DAQ software has been finished and this component –the test manager (see Fig. 1.3)– has been added to the DAQ system for further testing.

In close collaboration with the ATLAS software group a start has been made in gaining experience with the object-oriented database *Objectivity*. This database has been selected by the LHC community for the management of the huge amounts of event data. The software has been installed on miscellaneous platforms (HP, SGI, NT) and a small test database has been designed and implemented.

2 Electronic Department

2.1 Introduction

Design and engineering activities are considered to be the main assignment of the Electronic Technology Group. Development of the required skills is an item of continuous attention. By closing of the MEA/AmPS facility at the end of this year we are in a process of changes from accelerator related tasks to more detector related assignments. The diagram in Fig. 2.1 shows the activities of the department.

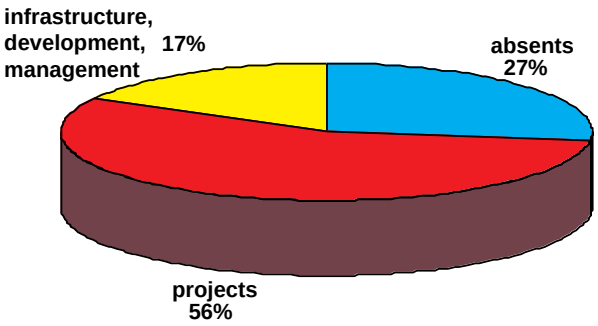

Figure 2.1: *Activities of the ET department.*

2.2 MEA/AmPS

The Electronic Technology Group supplied the MEA/AmPS facility with maintenance and operator services. Two members of the department have assisted by the cathode preparation for the polarised electron source (PES).

After closing the EMIN-hall there was only need in the beam storage mode at a 10 Hz repetition rate. Maintenance of modulators has been minimised. The spare PFN-units for the modulator were sufficient to maintain the energy of the accelerator to the end of 1998.

2.3 ATLAS

In DATCHA, the prototype test-setup of the muon drift chambers for the MDT part of ATLAS, the frontend cards, timing and data collecting and associated CAN High Voltage electronics were installed this spring for tests of the NIKHEF barrel outer layer chamber (BOL). In line with the ongoing development of MDT electronics we also designed a new frontend card for the BOL test chamber. This card, the Datimizer, uses a Cristiansen TDC32 chip for digitising the drift time of 32 channels chamber signals and an Altera FPGA based data serialiser to connect the data to a NIKHEF muon read out driver (NIMROD). Control and run parameters needed by the TDC32 and threshold settings for the input discriminators are provided via an addressable JTAG bus. Also an upgraded version of the timing and trigger module, the DDAQTv2, was designed for the NIMROD/Datimizer DAQ setup. This module accepts and selects a wide range of trigger sources to do trigger rate scaling and rate limiting, and translates the external triggers into correctly timed signals to be distributed via the read out driver to the TDCs. The NIMRODv1 is a VME64 module that collects and sorts, according to event number, data from 16 frontend cards. The Datimizers are connected to the NIMROD with 40 Mbit/s frontend-links. This frontend-link also distributes trigger and reset signals from the NIMROD to the Datimizer cards. Physically the frontend-link is a standard telecom cable. The NIMROD deserialises the incoming data and writes complete words to a fast memory. The bookkeeping section of the NIMROD keeps track of data and event numbers. The actual design of the NIMROD was almost fully made with the extensive use of the VHDL description language and simulation. Final fitting of the designed logic into FPGAs and timing verification took a major part of the total design time and resulted in the use of 10 Altera FPGAs with a total equivalent gate use of close to 300k gates.

The prototype NIMRODv1 was tested in both the L3COSMICS Phase I experiment as well as in the NIKHEF LHCb prototype tracker test setup. After several stages of bug fixing, the NIMRODv1 is now performing up to design specifications.

ATLAS Data Acquisition and Triggering

In the data acquisition and triggering chain for ATLAS several small test projects have been realised like ROB-Complex, CRUSH and Paroli-box.

ROB-Complex

The front-end electronics of the different detector parts will send their data via a read-out driver (ROD) over a 1 Gbit/s optical read-out link (ROL) to a read-out buffer (ROB). A total of 1500-2000 ROL's and ROB's are foreseen. After a positive first-level-trigger decision, the front-end electronics will send its data via a ROD to a ROB. The ROB must buffer the data during the time that the second level trigger needs to process the data. When accepted, the data is send to a event-filter for further processing. When rejected, the data in the ROB is deleted. To minimise the amount of modules

and crates a ROB-Complex module has been defined. A ROB-Complex is a module that contains multiple ROB-in parts, a ROB-controller part and a ROB-out part. Each ROB-in is connected to a ROL and performs the actual buffering of the data. The ROB-controller manages the ROB-Complex and handles requests for data or monitoring information. The ROB-out sends data over a network interface to the Level-2 trigger system or the Event-Filter. Several institutes are working on the design of a ROB-Complex and discussions are going on about the best solution to choose for the final design. Different prototype ROB-in modules are build and will be tested to measure the performance.

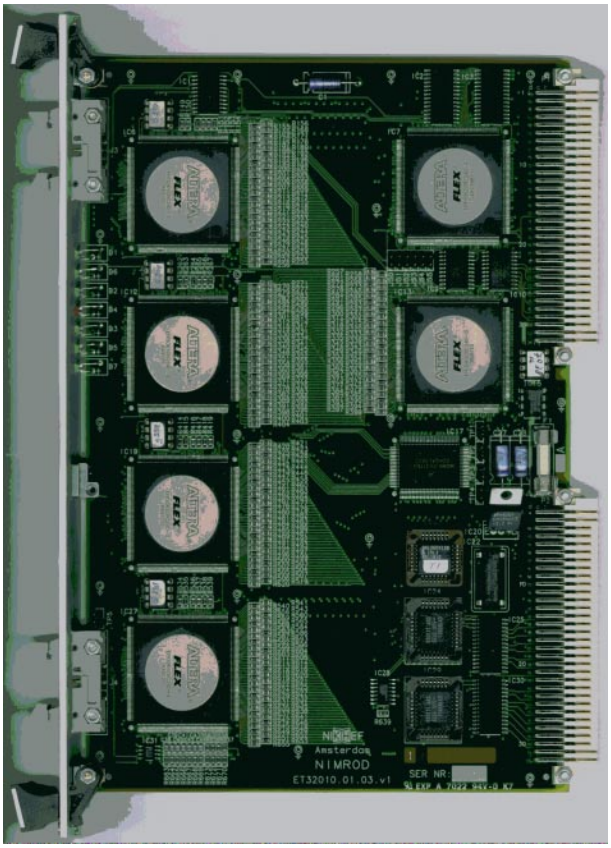

Figure 2.2: *Picture of NIMROD-topview.*

CRUSH

The Compact ROB-in using SHARC (CRUSH) is a prototype ROB-in design from NIKHEF and consists of an S-Link input-interface to the ROL, an input-FIFO, an Altera programmable logic device (FPGA), a buffer-memory and a SHARC processor (see Fig. 2.3). S-Link is a data-link specification defined by CERN,

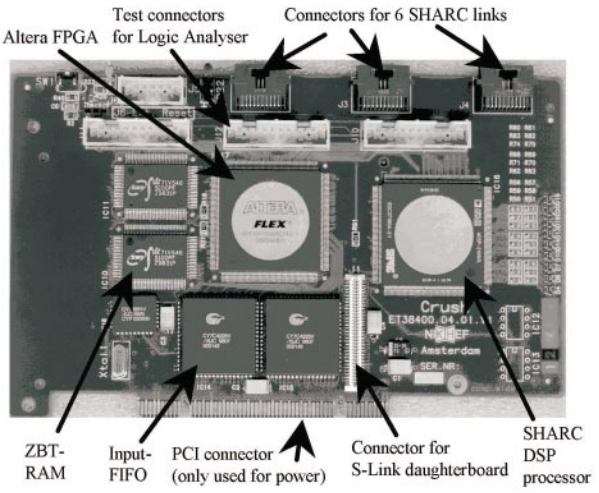

Figure 2.3: *Picture of a SHARC processor.*

intended to send data with high speed from front-end electronics to read-out electronics. The Altera FPGA autonomously writes event-data fragments from the input-FIFO in the Zero Bus Turnaround (ZBT)-buffer-memory, extracts summary information from these event fragments and writes this summary information in a paged-FIFO. The Sharc processor reads the summary information from the paged-FIFO, performs the 'bookkeeping' of the events in the buffer-memory, transfers data from the buffer-memory to the ROB-out and communicates with the ROB-controller. Via the links of the SHARC (6 links of 40 Mbytes/s each) the CRUSH connects to the ROB-out and the ROB-controller. The ZBT-buffer-memory is a high-speed synchronous memory, which runs at double the clockspeed of the CRUSH. During each 40 MHz clockcycle of the CRUSH, both the Altera FPGA and the Sharc can access the memory. The design of the CRUSH is finished and three prototypes have been produced. Tests show that they work successfully.

Paroli-box

To examine if the costs of the 1500–2000 optical 1 Gbit/s Read-Out Links between the ROD's and the ROB's can be reduced, a prototype Paroli-box has been designed and build. The intention is to use 12 short electrical gigabit-Ethernet cables to connect 12 ROD's to a Paroli-box, convert to two long optical flatcables (one for each direction) to another Paroli-box which converts the two optical flatcables back to 12 gigabit-Ethernet cables and connect to 12 ROB's. A Paroli-receiver and -transmitter device from

Siemens are used in the Paroli-box to convert electrical channels to optical channels in an optical flatcable. Because the Paroli devices use LVDS signal levels and gigabit-Ethernet uses PECL signal levels, electrical level adjustment between gigabit-ethernet signals and Paroli signals is necessary. Due to the high speed of the 1 Gbit/s signals, stripline techniques had to be used for the printed circuit board design. The Paroli box seems to work fine, but further tests must be done to see whether the device satisfies the demand of a bit error rate equal or better than 10-12.

RASNIK

RASNIK is used for the alignment of the large muon precision chambers in ATLAS. This year has seen several tests, with special emphasis on neutron radiation hardness, to select the optimum image sensor and light source for CCD-RASNIK. Also the design of an optimum multiplexing scheme for image sensor signals and light source switching has progressed to near completion. The image sensor that passed the radiation tests and meets all our requirements is a fully integrated CMOS type with serial interface for control and configuration. The infrared light source will be designed using special GaAs LEDs which also proved to be neutron radiation tolerant in our application. A test setup for system performance tests that includes prototypes of all parts of the final RASNIK system in ATLAS is near completion. The CMOS image sensor also provides an output pixel clock. Therefore the image capture can be pixel synchronous for improved and more stable video digitisation and enhanced spatial resolution.

D0

A start has been made with the design of a magnet field measurement system. It is based on the same system that is in development for ATLAS. It exists of about hundred 3D B-field sensors and a read-out with CANbus. The magnetic field sensor has to be kept within a thickness of 4mm.

L3 COSMICS

The L3 COSMICS project started in 1997. It uses the existing muon detector for a new trigger scheme and read-out. This project is also used as a pilot project for ATLAS, to test ideas about the NIMROD.

For L3 COSMICS the Phase I hardware stage was completed with the production of 60 TDC-cards (CPCv2) this spring. During the CPC test period we had assistance of two colleagues from Beijing. The CPCv2 is in essence a 96 channel TDC with Majority Trigger Logic and JTAG programming facilities. The Majority trigger Logic is used to generate pre-trigger signals on the base of hit thresholding for a section of 96 wires. The CPC uses several large programmable logic devices like a MACH466 and an Altera 10k20 to implement the highspeed logic. In November the upgraded design of the CPC was finished and ready for Phase II production of 200 pieces. In this CPCv2 the incoming 40 MHz TDC reference clock is re-synthesised with a high performance PLL to reduce clock jitter to less then 50 ps. A cosmic timing and trigger VME module (CTTv1) is used to extract an event trigger from the Majority signals of the CPC's. The CTT also distributes, via the NIMROD's, trigger, clock and reset signals to the CPCs. The master TDC clock is derived from a GPS receiver. Time-stamps can be used to correlate cosmic muon event data from several cosmic detectors. The CTT uses several large logic devices to implement a variety of possible trigger algorithms. For the Phase II of L3 COSMICS the design of a CTTv2 was almost completed by the end this year. The CTTv2 has several new trigger algorithms, a pipelined CPC like event/trigger buffer, and covers the full eight octants of L3.

The CPC data is read out with a NIMROD on a serial frontend-link at 40mbit/s using 'DS' encoding. The NIMRODv1 was installed in L3 COSMICS in September and tested extensively throughout the autumn, which, after some stages of bug fixing, ended in December with a NIMRODv1 now performing up to design specifications.

2.4 HERMES

In the beginning of the year the silicon test counter was tested in a 9 MeV proton beam from the university of Erlangen in the framework of the lambda-wheels project. In March the detector was installed in the HERMES beam vacuum and (partly) operated during the 1998 run. After that a start was made with the detailed design of the electronics for the lambda-wheels of the HERMES silicon project. The 20000 strips of two silicon wheels use the HELIX128S2.2 chips for readout. A test setup was built to obtain experience with this HELIX chip. The electronics on the hybrids inside the beamline-vacuum is minimised to fulfil the space and power requirements. The hybrids on which the HELIX chips, output amplifier and digital buffer amplifiers are mounted consist of kapton coated copper plates. This is necessary to have good thermal conductivity without degrading the vacuum specifications. Currently the first hybrids are being tested. Furthermore a control module was designed which generates all necessary control

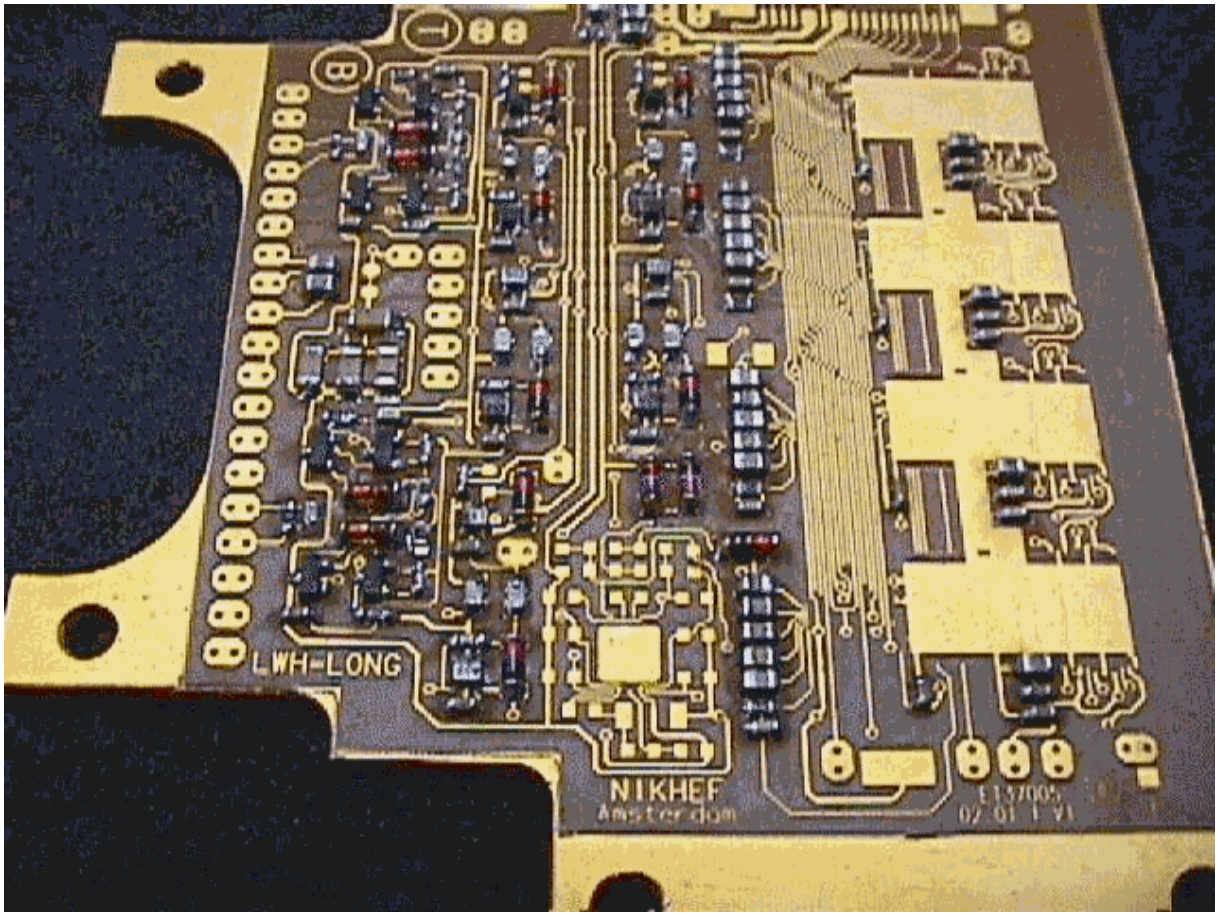

Figure 2.4: *Partly assembled hybrid for HERMES lambda-wheels (6.5x8.5 cm).*

signals for the helix chips. This module is now fabricated by industry. The design of the floating low voltage power supplies featuring output voltage and current readings via a CAN-node is finalised, the layout of the printed circuit board is in progress. The analog signals from the hybrid are digitised in 12 VME based ADC modules. Each module contains four ADC chips, pedestal tables and logic to subtract the common mode noise. The design of the ADC modules is being finalised. It was decided to test 15 wafers each containing 60 HELIX chips at NIKHEF using the newly acquired probe-station. Support electronics was built for this automated test setup.

2.5 ZEUS Micro Vertex Detector

For the readout of the Si-strip detectors the HELIX IC is used. This IC has been developed at Heidelberg University for HERA-B. In cooperation with Heidelberg the IC has been modified for ZEUS and is in production. Prototypes have been tested on electronic behaviour as well as radiation tests by NIKHEF.

A cable connection between the HELIX IC and the ADC system on a distance of $\approx$ 20 m has been developed and tested for analogue signals . A slow-control system of the Micro Vertex Detector is under development. The system can be divided into two distinct parts.

a. Monitoring the temperature of the hybrids

The Micro vertex detector consists of 32 ladders and 8 half wheels. Every ladder and half wheel is fitted with a number of hybrids. These hybrids produce about 500W of heat in total. The temperature of the ladders and the wheels is monitored with NTC's thermistors. Each ladder is monitored with one temperature sensor(NTC) and each outlet-pipe is fitted with one NTC. The NTC's are read out by a micro-controller via two NTC interfaces. The micro-controller is connected, via

a CANbus, to a host computer.

b. Cooling Control

The cooling controls are done by a Siemens PLC. This PLC has as a main objective to start up and control the cooling and do the error handling in case of a fault. The communication between the PLC and the host computer is done via a CANbus interface.

2.6 B Physics

HERA-B

For the Outer Tracker Detector for the HERA-B experiment first level trigger link boards (FLT_LB) have been tested at the HERA-B detector. Hits from the wire chambers are successfully written in the wire memories of the track finder unit (TFU) by the FLT_LB. Some minor changes were made before the mass production will start. The main purpose of the FLT_LB is to rearrange hit data from the wire chambers, add an event label to the data and transpose the data into a suitable format for the TFU. As the TFU is 30 meters away from the wire chambers the data are serialised and send to the TFU electronics. Additional hardware and software are designed and tested for the remote data upload facility in the FLT_LB. This data transforms the position dependency of the FLT_LB in the wire chambers for the appropriate hit pattern arrangement.

LHCb Outer Tracker

A lot of work has been done on prototype chamber models. The front-end electronics including the high voltage parts have been made. The front-end amplifying is based on a new ASD/BLR (Amplifier-Discriminator-Shaper / BLR) chip of the university of Pennsylvania. For timing and read-out the same system as for ATLAS is used based on TDC-32 and a NIMROD. The NIMROD module used is of an early design phase what resulted in a poor read-out. Next year the tests will be repeated with the final NIMROD, as used by L3. An extra handicap was the fact that part of the chambers have been placed inside a magnet. Special TDC-prints are designed to place just beside the magnet. The read-out system, special the TDC, has to be evaluated to a faster system for the final chambers.

2.7 Electronic Design Automation

VHSIC Hardware Description Language (VHDL)

The Electronic Design Automation environment was extended with the Spectrum logic synthesis software from Exemplar Logic. This software became available through the Europractice membership. This completes the FPGA synthesis design flow as foreseen. Now the way is open to acquire software at reasonable cost; further integrating the VHDL design environment into the Mentor Graphics PCB design flow becomes within reach. This would bridge the gap between the VHDL and the PCB design environment. Due to increasing demand for larger FPGA's (Field Programmable Gate Array) a second maxplus2 was purchased. We are investigating the possibilities to run the synthesis software on a dedicated server. Synthesis software requires large amounts of memory and consumes many hours of cpu time per run. A separate server will take the load off the desktop machines.

Very Large Scale Integration (VLSI)

VLSI plays an important role in design of modern circuits. It was indispensable in the design of the ZEUS and HERMES detectors. Within the scope of vertex R&D work has been done on more education, tools like a probe-station, bonding apparatus, T&M equipment and small projects. The goal will be to assign five members of the department who are capable to participate in VLSI developments. Under vertex R&D responsibility a second hand automatic probe-station has been purchased. This station requires intensive maintenance on the control logic. A design for a low-noise general purpose preamplifier has started. It is build in 0.6 μm CMOS IC technology. To keep VLSI knowledge up to the latest technologies, several courses have been followed.

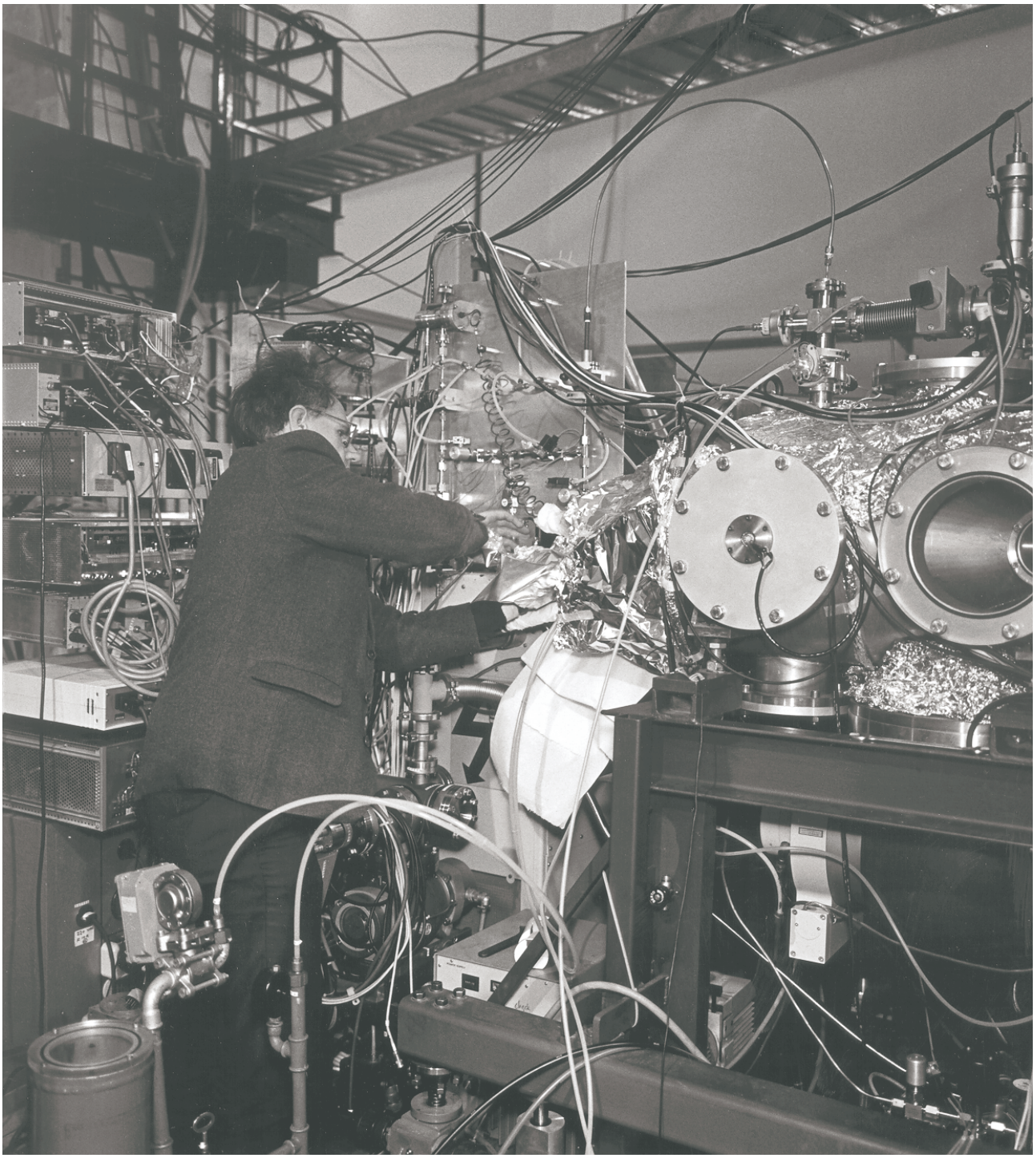

RF shielding of the Atomic Beam Source (photo: Han Singels)

3 Mechanical Technology

3.1 Introduction

The Mechanical Technology department was confronted in 1998 with severe competition in manpower from the various projects. We were again able to make an optimal balance in sharing the expertise of the group. The histogram (Fig. 3.1) shows how the manpower is distributed in 1998. The so-called "internal manpower" was to a large extend used for education of experts in the 3D survey machine, the laser interferometer and the clean-room technology. It became very clear that the extra possibilities in the form of modern equipment means that less manpower is left for producing high quality structures.

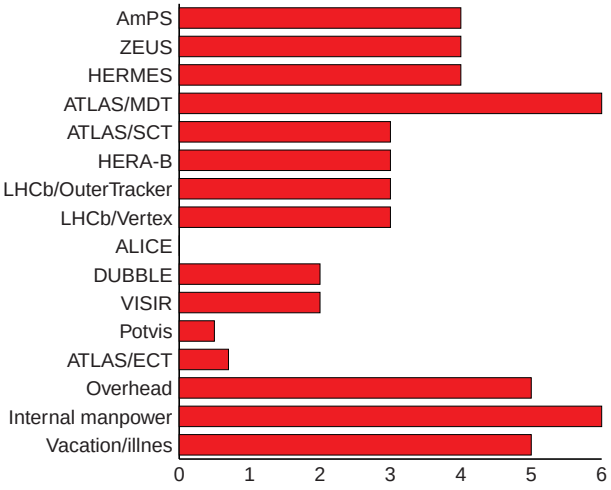

Figure 3.1: *Manpower distribution in 1998.*

3.2 ATLAS-Muonchambers

After the installation and the test of the first prototype barrel outer large (BOL) muonchamber in DATCHA, preparations were made for the production of the 96 detector units we have to deliver in the year 2005. A cleanroom with class 10.000 specifications of 17 m length, 8.4 m width and 5.5 m height has been installed and tested. A granite table, of 5.5 m x 2.5 m^2, to be used as the precision-mounting base has been installed and tested. The quality control of both items appeared to be a very manpower-consuming project. The mounting table was finally accepted with an accuracy over the total surface of about 17 μm. This has been checked with a laser interferometer in combination with electronic levelers. For assembly of the detector tubes 50 jigs with an overall accuracy of 5 μm were manufactured. Many tools like the vacuum system, the gluing equipment and the quality control setup were designed and partly manufactured. The design for the aluminium extruded spacer frame (see Fig. 3.2) has been approved by the collaboration. The parts have been ordered for the prototype at NIKHEF as well as for the Frascati module zero. Various prototype end plugs have been designed and evaluated with respect to the cost and quality. The Rasnik production type parts have been ordered for the prototypes too. Much effort was invested in the development of the procedure to do the final quality control of the tubes.

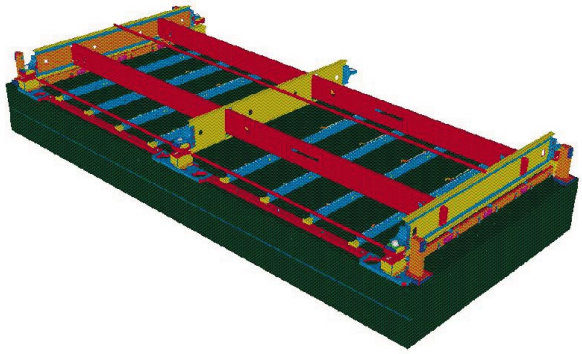

Figure 3.2: *The MDT spacer frame.*

3.3 ATLAS-SCT

Investigations in heat flow and mounting devices have been done. Carbon fibre prototype constructions have been build in order to measure stiffness and eigen frequencies. Within the collaboration discussions have lead to more clarity in the responsibilities. The fact that the final quality control of the position of the silicon detectors on the wheels will be done at NIKHEF urged us to buy and install a 3D measuring machine. The clean room specifications and the demands on quality of the apparatus itself were a major investment both in manpower as in money. Also an apparatus was build to study the heat conduction problems between the source (the electronics) and the cooling fluid. The testing equipment was used in vacuum in order to exclude the influence of convection. With this apparatus it was possible to optimise the materials for minimum multiple scattering and maximum stability.

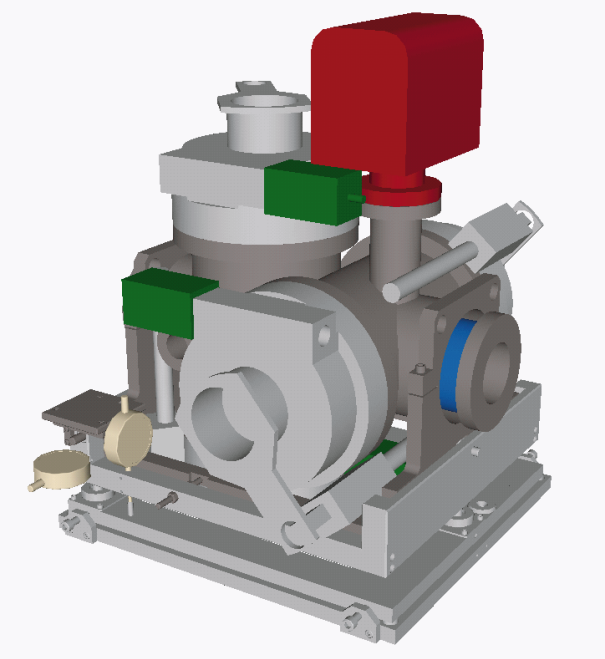

Figure 3.3: *The D0 Forward Proton Detector assembly.*

3.4 D0

Joining the D0 Forward collaboration at Fermi Lab implied for our department an important contribution in expertise concerning accelerator techniques. The tasks between the three laboratories Fermi Lab, LNLS and NIKHEF were divided. NIKHEF has produced the design and the finite element study of the thin window (0.1 mm) Roman pot and the support structure of the Forward Proton Detector (see Fig 3.3). Prototypes have been made and are being discussed. In September 1999 the final equipment must be installed in the TEVATRON.

3.5 HERA-B

This year we completed 92 % of the folding and tempering of the foils for the collaboration. The large production quantity (10.000 pieces) was possible because we were able to automate the apparatus (Fig. 3.4).

3.6 LHCb

Outer Tracker

An advanced prototype of the final Outer Tracker was build using Pokalon foil. Several problems like printed circuit boards, handling, materials have to be solved. No solution has yet been found for the production method. A real size prototype is under construction in order to study the cabling and stiffness problems.

Figure 3.4: *The HERA-B foil folding machine.*

Microvertex

A preliminary design study for the detector (see Fig. 3.5) has been presented to the collaboration. Vacuum, high frequency, cooling and a lot of mechanical problems still have to be solved. Aging of the silicon detectors is a major design criterion. Prototypes of details of the detector are being tested.

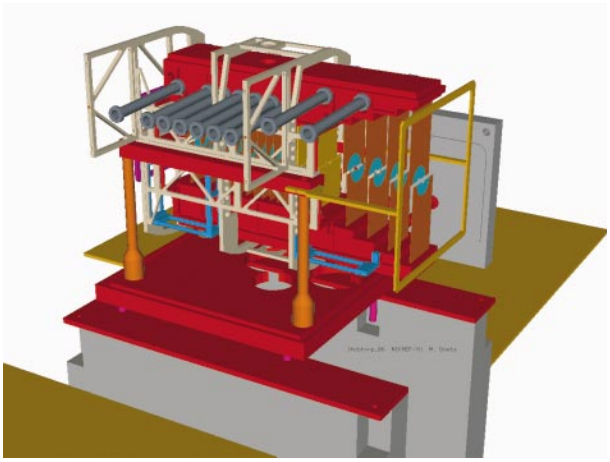

Figure 3.5: *Artist's view of the LHCb Vertex detector.*

3.7 HERMES

Within a very short time a design of the so-called Lambda wheels had to be realised. The crowded situation at the target point of HERMES is a very complicating factor in the design. Mounting and removal of the silicons out of the vacuum environment must be

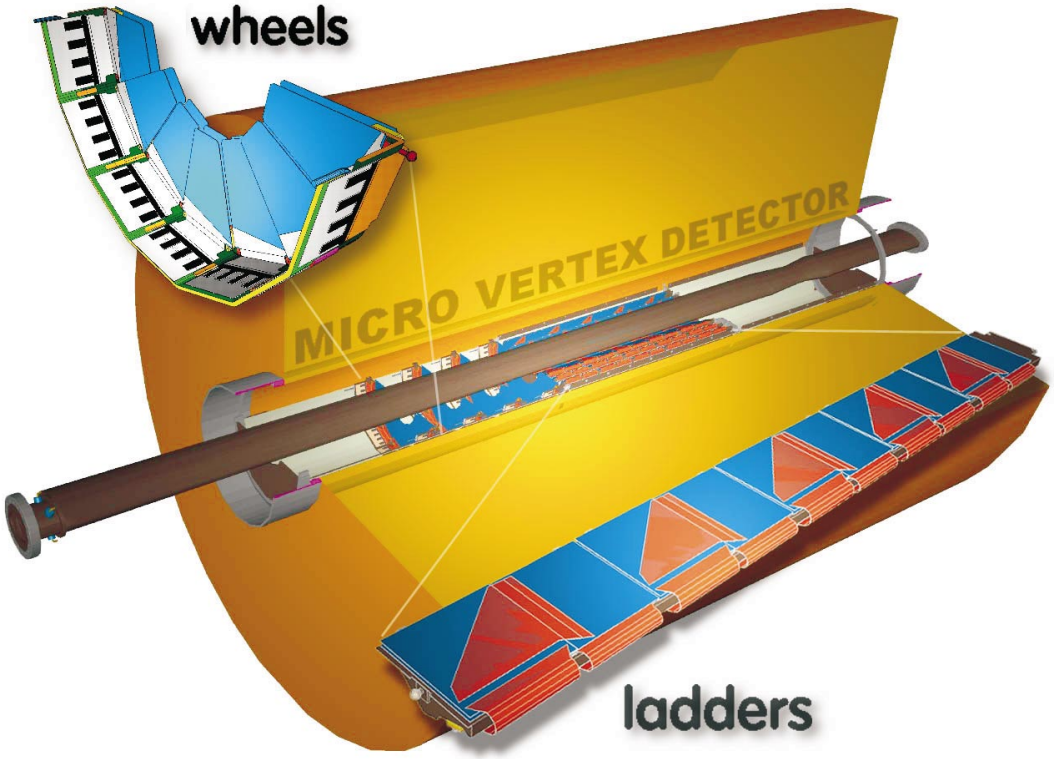

Figure 3.6: *The ZEUS Microvertex detector.*

done through a relative small flange on the vacuum system. The tools with the adequate precision, necessary for this job are under construction. In order to keep the noise level for detection low, the electronics are mounted inside the vacuum system, as close as possible to the target. Therefore the vacuum compatibility of the material is very important. We have developed, built and tested an apparatus with which we can measure outgassing rates

3.8 ZEUS microvertex

Several prototypes of details of the detector have been made in order to investigate stiffness and accessibility. Silicon layers, cooling, carbon frames have been studied in this way. Problems with carbon fibre constructions concerning form stability were experienced and solved. The final design of the detector (see Fig. 3.6) has been finished, the tools for mounting, positioning and fixation of the silicon detectors still have to be finalised. The infrastructure has been improved by creating an advanced setup for automatic bonding of chips for many of the present projects. The production of the final parts and the assembly tools has been started. The installation of the detector has to be realised before the year 2000.

3.9 ALICE

In collaboration with the University of Utrecht we are going to contribute to the ALICE detector. Especially we will deliver the design of the assembly tools. A first study has been done and resulted in accepted ideas for an automated positioning of the silicon detectors.

3.10 Projects in exploitation

AmPS

As can be seen from Fig. 3.1 the involvement from NIKHEF in the experiments in the ITH decreased because the Free University took over the responsibility. Only special expertise was delivered. The repair of the quenched solenoid of the Siberian Snake was a major activity. Some preparations have been made for the dismantling of the facility.

L3

Several repair actions have been performed in order to reactivate the so-called "dead cells" in the MM wire chambers. Carbon whiskers are growing in the detectors caused by cracking of the counting gas. By making holes in the walls of the chambers in situ and by mounting special kapton foils, the units can be repaired.

3.11 Projects for third parties

ATLAS end cap

We contributed in the optimisation of the vacuum chamber design made by Rutherford Laboratory. In combination with the Dutch industry (de Schelde and Holec) we discussed the manufacturing aspects of the vessel and the cold mass. We also did a study in order to evaluate a special temporarily sealing kit, which is to be used for the acceptance test at de Schelde. This resulted in a collaboration report.

Figure 3.7: *The COLDEX apparatus installed at CERN.*

COLDEX

The apparatus (see Fig. 3.7) needed a limited number of man months of expertise from NIKHEF in order to make changes to the beam screen. The research setup is installed as planned in EPA while the investigations for the desorption effects at 1.8 K are making progress.

DUBBLE

Various constructions for the beam line, like the SAX-WAX sample holder (see Fig. 3.8), have been designed, manufactured and tested in our department. The assembly of the mirror boxes and the monochromator is finalised; installation and alignment has been prepared. A study of the mirror bending mechanism has been done and resulted in a report with recommendations.

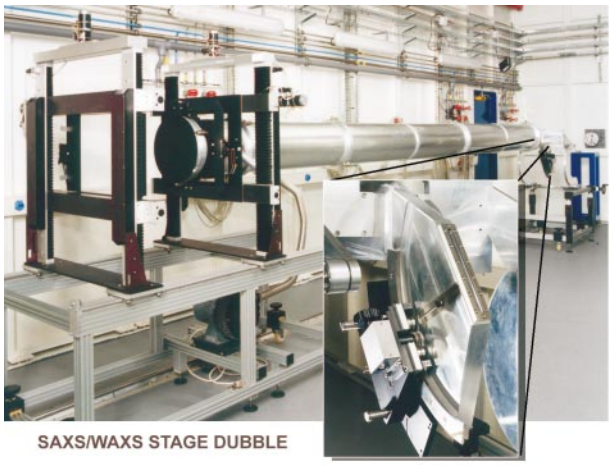

Figure 3.8: *The SAX-WAX sample holder.*

Design work on the experimental set up in Grenoble at ESRF is still ongoing.

VISIR

The tasks between NIKHEF and ASTRON were divided in such a way that NIKHEF was contributing the expertise for the temperature and stability study. The cryogenic aspects were evaluated in a model in which changes could be studied. A mechanical model was used to investigate the dimensions and material choice. The latter also delivers the option to implement the optical parameters. A project readiness review was held between SACLAY, ASTRON and NIKHEF, which resulted in the go-signal for the production of the mechanics for the detector.

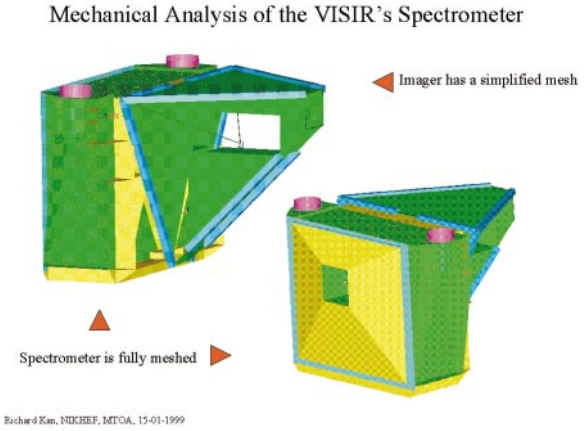

Figure 3.9: *Thermal Model.*

4 Technical Physics

4.1 Vertex Detector Technology

Virtually every particle physics experiment nowadays uses silicon detector technologies to track collision products close to the primary interaction vertex. High position resolutions are needed, combined with high event rates, high multiplicities, low mass and low power-consumption. High speed operation and low noise require close integration of the sensors with the readout electronics. Both sensor and readout chip have to withstand high radiation doses occurring near the interaction region.

These problems call for a coordinated approach and at the end of 1997 the "NIKHEF Vertex Detector Project" was instated, to stimulate activities in these fields, with a broader scope than can be the case within any specific experiment. Three main fields of attention were defined: Explorative Research and Development, Infrastructure, and Applications. Budgets for investment and explorative R&D projects were also presented.

With respect to the infrastructure, a semi-automatic wafer-probe station has been acquired (Micro Manipulator 8860). This facility can be used to probe silicon wafers up to 200 mm diameter, as well as capacity and leakage current of silicon sensors. Probe-cards to test wafers containing readout chips have been ordered and will first be used by the HERMES experiment. Also an automatic wedge-wedge bonder (Delvotec 6320) has been acquired. It can fully automatically bond wires with controlled loop length and with controlled bonding energy between sensors and readout chips, for effective pitches down to 40 μm.

An R&D project to produce large area pixel detectors in Multi-Chip Module by Deposition (MCMD) technology has been started. By bump-bonding several pixel readout chips onto one larger sensor substrate chip, hybrid assemblies of up to about 10 cm^2 can be made without the need for any wire bonding inside the assembly. All internal connections, including the output connections of the readout chips, are to be done within the same bump-bonding step. The sensor has a peripheral area where a readout bus is deposited by photolithography, leading in principle to a much improved yield and reduced cost with respect to wire bonding. Production of such assemblies must be done in industry.

Within the TMR project "Micro-Track Imaging", we have entered the Medipix Collaboration, a European consortium of institutes and university groups, based at CERN, pursuing the development of single-photon imagers in the X-ray region and in visible wavelengths. This development is a spin-off of R&D for high-energy physics, and will be useful for analytical and medical X-ray imaging and other scientific purposes. We contribute to the design of a deep-submicron (CMOS 0.25 μm technology) readout chip and to the testing of prototype Medipix detectors. We have set up an interdisciplinary collaboration with the MESA research institute at the University of Twente, who are already involved in deep-submicron design. Also we investigate, together with Delft Electronics Products (DEP), a Dutch opto-electronics company, the possibilities to integrate such Medipix detectors inside the vacuum of Image Intensifier tubes.

On the topic of radiation tolerance, we are in contact with the RD39 collaboration at CERN, to study behaviour of Silicon detectors and readout electronics at liquid nitrogen temperatures. It turns out that radiation tolerance of silicon detectors increases by many orders of magnitude by such cooling, making the use of expensive other possibilities like chemical vapour deposited (CVD) diamond less necessary. We also contribute to the RD49 collaboration at CERN, where the radiation tolerance of deep submicron CMOS circuits is increased by special layout techniques. This offers the possibility to use industry-standard fabrication methods instead of special radiation-hard CMOS technologies, with a corresponding advantage in cost and circuit density.

All these activities are oriented towards our long-term goal of creating highly granulated detector assemblies, where the electronics and an increasing part of the data processing, are integrated into the detector.

4.2 Diamond detectors

Diamond detectors measuring the track of a charged particle have been proposed for the hottest region of several experiments at the LHC. Experiments have shown that for diamond the radiation tolerance is roughly an order of magnitude better than for silicon. Because of availability and cost, we do not use natural diamond but substrates made by chemical vapour deposition (CVD). Like in a silicon detector, the diamond detector measures the collected charge that is induced in the substrate by a traversing particle. Unfortunately, part of the charge carriers is trapped by lattice defects or impurities, resulting into a reduced signal on the electrodes. The charge collection distance (CCD), the parameter characterising the average amplitude, still

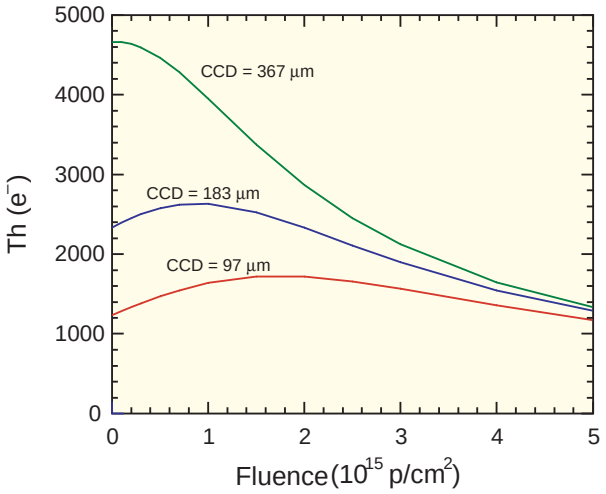

Figure 4.1: *Predicted threshold required obtaining 95% efficiency as a function of the proton fluence.*

shows a steady increase over the past years due to the combined research efforts of the physics community and industry.

The diamond research at NIKHEF is done in the framework of the RD42 collaboration. In this framework, a student took part in the RD42 beam test at CERN. Furthermore, we wrote a new analysis routine fitting a Landau curve through the distribution curve of diamond samples that were measured at the characterisation station at NIKHEF. Also a contribution to the study of radiation damage was made. This comprised the development of a new model describing the effect of proton irradiation and the characterisation of new samples for an RD42 neutron irradiation.

Modeling the effect of proton radiation on CVD diamond

Measurements of other RD42 collaborators have shown that proton irradiation has a peculiar effect on CVD diamond. Irradiation by minimum ionising protons appears not only to induce radiation damage but also invokes an annealing effect on the small pulses of the distribution. The last effect is most relevant when using CVD diamond as a track following detector, leading to a better detection efficiency. A model incorporating both effects has been developed describing the dependence on irradiation of the amplitude distribution. The model could fairly well follow the measured distribution curves. However, the limited statistics of the characterisations did not permit a refinement of the model that would be required to get a better correspondence between model and measurement. The irradiation measurements were done with moderate quality samples having a CCD of 97 μm. To get a prediction for better substrate qualities, the model was also applied for a CCD of 183 μm and 367 μm (see Fig. 4.1), representing the quality of the actual prototypes and of those in the near future. Especially for the high quality diamond, the radiation damage dominates, limiting the high quality region to fluences less than 1.5×10^{15} p/cm^2. However, one should note that this number already corresponds to the proton radiation dose obtained at a radial distance of 7 cm from the interaction point after 15 years of running at high luminosity at the LHC.

F Publications, Theses and Talks

1.1 Publications

[1] P. Abreu *et al.*; (A. Augustinus, E. Boudinov, D. Holthuizen, N.J. Kjaer, P. Kluit, M. Mulders, M. Nieuwenhuizen, J. Timmermans, D.Z. Toet, G.W. Van Apeldoorn, P. Van Dam, J. Van Eldik, DELPHI Collaboration).
Charged particle multiplicity in $e^+e^- \to q\bar{q}$ events at 161 and 172 GeV and from the decay of the W boson
Phys. Lett. **B416** (1989) 233

[2] P. Abreu *et al.*; (E. Boudinov, D. Holthuizen, N. Kjaer, P. Kluit, M. Mulders, M. Nieuwenhuizen, J. Timmermans, D.Z. Toet, G.W. van Apeldoorn, P. van Dam, J. van Eldik, I. van Vulpen, DELPHI Collaboration).
Measurement of the charged particle multiplicity of weakly decaying B hadrons
Phys. Lett. **B425** (1998) 399

[3] P. Abreu *et al.*; (E. Boudinov, D. Holthuizen, N. Kjaer, P. Kluit, M. Mulders, M. Nieuwenhuizen, J. Timmermans, D.Z. Toet, G.W. van Apeldoorn, P. van Dam, J. van Eldik, I. van Vulpen, DELPHI Collaboration).
Measurement of the inclusive charmless and double-charm B branching ratios
Phys. Lett. **B426** (1998) 193

[4] P. Abreu *et al.*; (E. Boudinov, D. Holthuizen, N. Kjaer, P. Kluit, M. Mulders, M. Nieuwenhuizen, J. Timmermans, D.Z. Toet, G.W. van Apeldoorn, P. van Dam, J. van Eldik, I. van Vulpen, DELPHI Collaboration).
First evidence for a charm radial excitation, $D^{*'}$
Phys. Lett. **B426** (1998) 231

[5] P. Abreu *et al.*; (E. Boudinov, D. Holthuizen, N. Kjaer, P. Kluit, M. Mulders, M. Nieuwenhuizen, J. Timmermans, D.Z. Toet, G.W. van Apeldoorn, P. van Dam, J. van Eldik, I. van Vulpen, DELPHI Collaboration).
Measurement of the W-pair cross-section and of the W mass in e^+e^- interactions at 172 GeV
Eur. Phys. J. **C2** (1998) 581

[6] P. Abreu *et al.*; (E. Boudinov, D. Holthuizen, N. Kjaer, P. Kluit, M. Mulders, M. Nieuwenhuizen, J. Timmermans, D.Z. Toet, G.W. van Apeldoorn, P. van Dam, J. van Eldik, I. van Vulpen, DELPHI Collaboration).
A study of the hadronic resonance structure in the decay $\tau \to 3\pi\nu_\tau$
Phys. Lett. **B426** (1998) 411

[7] P. Abreu *et al.*; (E. Boudinov, D. Holthuizen, N. Kjaer, P. Kluit, M. Mulders, M. Nieuwenhuizen, J. Timmermans, D.Z. Toet, G.W. van Apeldoorn, P. van Dam, J. van Eldik, DELPHI Collaboration).
Search for charginos, neutralinos and gravitinos at LEP
Eur. Phys. J. **C1** (1998) 1

[8] P. Abreu *et al.*; (E. Boudinov, D. Holthuizen, N. Kjaer, P. Kluit, M. Mulders, M. Nieuwenhuizen, J. Timmermans, D.Z. Toet, G.W. van Apeldoorn, P. van Dam, J. van Eldik, I. van Vulpen, DELPHI Collaboration).
Investigation of the splitting of quark and gluon jets
Eur. Phys. J. **C4** (1998) 1

[9] P. Abreu *et al.*; (E. Boudinov, D. Holthuizen, N. Kjaer, P. Kluit, M. Mulders, M. Nieuwenhuizen, J. Timmermans, D.Z. Toet, G.W. van Apeldoorn, P. van Dam, J. van Eldik, I. van Vulpen, DELPHI Collaboration).
$\pi^\pm, K^\pm, p$ and $\bar{p}$ production in $Z^0 \to q\bar{q}, Z^0 \to b\bar{b}, Z^0 \to u\bar{u}, d\bar{d}, s\bar{s}$
Eur. Phys. J. **C5** (1998) 585

[10] P. Abreu *et al.*; (E. Boudinov, D. Holthuizen, N. Kjaer, P. Kluit, M. Mulders, M. Nieuwenhuizen, J. Timmermans, D.Z. Toet, G.W. van Apeldoorn, P. van Dam, J. van Eldik, I. van Vulpen, DELPHI Collaboration).
Measurement of $|V_{cs}|$ using W decays at LEP2
Phys. Lett. **B439** (1998) 209

[11] P.Abreu *et al.*; (H.M. Blom, E. Boudinov, D. Holthuizen, N. Kjaer, P. Kluit, M. Mulders, J. Timmermans, D.Z. Toet, G.W. van Apeldoorn, P. van Dam, J. van Eldik, I. van Vulpen, DELPHI Collaboration).
Two-particle angular correlations in e^+e^- interactions compared with QCD predictions
Phys. Lett. **B440** (1998) 203

[12] P. Abreu *et al.*; (A. Augustinus, E. Boudinov, D. Holthuizen, N. Kjaer, P. Kluit, M. Mulders, M. Nieuwenhuizen, J. Timmermans, D.Z. Toet, G.W. van Apeldoorn, P. van Dam, J. van Eldik, DELPHI Collaboration).
Search for neutral and charged Higgs bosons in e^+e^- collisions at $\sqrt{s}$= 161 GeV and 172 GeV
Eur. Phys. J. **C2** (1998) 1

[13] P. Abreu *et al.*; (E. Boudinov, D. Holthuizen, N. Kjaer, P. Kluit, M. Mulders, M. Nieuwenhuizen, J. Timmermans, D.Z. Toet, G.W. van Apeldoorn, P. van Dam, J. van Eldik, I. van Vulpen, DELPHI Collaboration).
m_b at M_Z
Phys. Lett. **B418** (1998) 430

[14] P. Abreu *et al.*; (E. Boudinov, D. Holthuizen, N. Kjaer, P. Kluit, M. Mulders, M. Nieuwenhuizen, J. Timmermans, D.Z. Toet, G.W. van Apeldoorn, P. van Dam, J. van Eldik, I. van Vulpen, DELPHI Collaboration).
Search for charged Higgs bosons in e^+e^- collisions at $\sqrt{s}$ = 172 GeV
Phys. Lett. **B420** (1998) 140

[15] P. Abreu *et al.*; (E. Boudinov, D. Holthuizen, N. Kjaer, P. Kluit, M. Mulders, M. Nieuwenhuizen, J. Timmermans, D.Z. Toet, G.W. van Apeldoorn, P. van Dam, J. van Eldik, I. van Vulpen, DELPHI Collaboration).
Measurement of trilinear gauge couplings in e^+e^- collisions at 161 GeV and 172 GeV
Phys. Lett. **B423** (1998) 194

[16] P. Abreu *et al.*; (A. Augustinus, E. Boudinov, D. Holthuizen, N.J. Kjaer, P. Kluit, B. Koene, M. Merk, M. Mulders, M. Nieuwenhuizen, W. Ruckstuhl, J. Timmermans, D.Z. Toet, G.W. Van Apeldoorn, P. Van Dam, J. Van Eldik, DELPHI Collaboration).
Rapidity correlations in Λ baryon and proton production in hadronic Z^0 decays
Phys. Lett. **B416** (1998) 247

[17] P. Abreu *et al.*; (E. Boudinov, D. Holthuizen, N.J. Kjaer, P. Kluit, M. Mulders, M. Nieuwenhuizen, J. Timmermans, D.Z. Toet, G.W. van Apeldoorn, P. van Dam, J.van Eldik, I. van Vulpen, DELPHI Collaboration).
Measurement of the $e^+e^- \to \gamma\gamma(\gamma)$ cross section at the LEP energies
Phys. Lett. **B433** (1998) 429

[18] P. Abreu *et al.;* (H.M. Blom, E. Boudinov, D. Holthuizen, N.J. Kjaer, P. Kluit, M. Mulders, J. Timmermans, D.Z. Toet, G.W. van Apeldoorn, P. van Dam, J. van Eldik, I.

van Vulpen, DELPHI Collaboration.
A search for η_c' production in photon-photon fusion at LEP
Phys. Lett. **B441** (1998) 479

[19] P. Abreu *et al.;* (H.M. Blom, E. Boudinov, D. Holthuizen, N.J. Kjaer, P. Kluit, M. Mulders, J. Timmermans, D.Z. Toet, G.W. van Apeldoorn, P. van Dam, J. van Eldik, I. van Vulpen, DELPHI Collaboration.
A search for heavy stable and long-lived squarks and sleptons in e^+e^- collisions at energies from 130 to 183 GeV
Phys. Lett. **B444** (1998) 491

[20] M. Acciarri *et al.*; (G.J. Bobbink, S.V. Chekanov, A.P. Colijn, D.van Dierendonck, P. Duinker, F.C. Erné, W.C. van Hoek, W. Kittel, A.C. König, F.L. Linde, D. Mangeol, G.G.G. Massaro, W.J. Metzger, A.J.W.van Mil, A.J.M. Muijs, B. Petersen, M.P. Sanders, D.J. Schotanus, R.T. van de Walle, L3 Collaboration).
Measurement of the average lifetime of b-hadrons in Z decays
Phys. Lett. **B416** (1998) 220

[21] M. Acciarri *et al.*; (G.J. Bobbink, A. Buijs, S.V. Chekanov, A.P. Colijn, D. van Dierendonck, P. Duinker, F.C. Erné, W.C. van Hoek, W. Kittel, A.C. König, F.L. Linde, D. Mangeol, G.G.G. Massaro, W.J. Metzger, A.J.W. van Mil, A.J.M. Muijs, B. Petersen, T. van Rhee, W. van Rossum, M.P. Sanders, D.J. Schotanus, L3 Collaboration).
Measurement of the weak dipole moments of the tau lepton
Phys. Lett. **B426** (1998) 207

[22] M. Acciarri *et al.*; (G.J. Bobbink, A. Buijs, S.V. Chekanov, A.P. Colijn, D. van Dierendonck, P. Duinker, F.C. Erné, W.C. van Hoek, W. Kittel, A.C. König, F.L. Linde, D. Mangeol, G.G.G. Massaro, W.J. Metzger, A.J.W. van Mil, A.J.M. Muijs, B. Petersen, T. van Rhee, W. van Rossum, M.P. Sanders, D.J. Schotanus, L3 Collaboration).
Angular multiplicity fluctuations in hadronic Z decays and comparison to QCD models and analytical calculations
Phys. Lett. **B428** (1998) 186

[23] M. Acciarri *et al.*; (G.J. Bobbink, A. Buijs, S.V. Chekanov, A.P. Colijn, D. van Dierendonck, P. Duinker, F.C. Erné, W.C. van Hoek, W. Kittel, A.C. König, F.L. Linde, D. Mangeol, G.G.G. Massaro, W.J. Metzger, A.J.W. van Mil, A.J.M. Muijs, B. Petersen, T. van Rhee, W. van Rossum, M.P. Sanders, D.J. Schotanus, L3 Collaboration).
Search for scalar leptons, charginos and neutralinos in e^+e^- collisions at $\sqrt{s}$ = 161-172 GeV
Eur. Phys. J.**C4** (1998) 207

[24] M. Acciarri *et al.*; (G.J. Bobbink, A. Buijs, S.V. Chekanov, A.P. Colijn, D. van Dierendonck, P. Duinker, F.C. Erné, W.C. van Hoek, W. Kittel, A.C. König, F.L. Linde, D. Mangeol, G.G.G. Massaro, W.J. Metzger, A.J.W. van Mil, A.J.M. Muijs, B. Petersen, T. van Rhee, W. van Rossum, M.P. Sanders, D.J. Schotanus, L3 Collaboration).
Local multiplicity fluctuations in hadronic Z decay
Phys. Lett. **B429** (1998) 375

[25] M. Acciarri *et al.*; (G.J. Bobbink, A. Buijs, S.V. Chekanov, A.P. Colijn, D. van Dierendonck, P. Duinker, F.C. Erné, W.C. van Hoek, W. Kittel, A.C. König, F.L. Linde, D. Mangeol, G.G.G. Massaro, W.J. Metzger, A.J.W. van Mil, A.J.M. Muijs, B. Petersen, T. van Rhee, W. van Rossum, M.P. Sanders, D.J. Schotanus, L3 Collaboration).
Measurement of tau polarisation at LEP
Phys. Lett. **B429** (1998) 387

[26] M. Acciarri *et al.*; (G.J. Bobbink, A. Buijs, S.V. Chekanov, A.P. Colijn, D. van Dierendonck, P. Duinker, F.C. Erné, W.C. van Hoek, W. Kittel, A.C. König, F.L. Linde, D. Mangeol, G.G.G. Massaro, W.J. Metzger, A.J.W. van Mil, A.J.M. Muijs, B. Petersen, T. van Rhee, W. van Rossum, M.P. Sanders, D.J. Schotanus, L3 Collaboration).
Determination of the number of light neutrino species from single photon production at LEP
Phys.Lett. **B431** (1998) 199

[27] M. Acciarri *et al.*; (G.J. Bobbink, A. Buijs, S.V. Chekanov, A.P. Colijn, D. van Dierendonck, P. Duinker, F.C. Erné, R. van Gulik, W.C. van Hoek, W. Kittel, A.C. König, F.L. Linde, D. Mangeol, G.G.G. Massaro, W.J. Metzger, A.J.W. van Mil, A.J.M. Muijs, B. Petersen, T. van Rhee, M.P. Sanders, D.J. Schotanus, L3 Collaboration).
Search for the standard model Higgs boson in e^+e^- interactions at $\sqrt{s}$ = 183 GeV
Phys. Lett. **B431** (1998) 437

[28] M. Acciarri *et al.*; (G.J. Bobbink, A. Buijs, S.V. Chekanov, A.P. Colijn, D. van Dierendonck, P. Duinker, F.C. Erné, R. van Gulik, W.C. van Hoek, W. Kittel, A.C. König, F.L. Linde, D. Mangeol, G.G.G. Massaro, W.J. Metzger, A.J.W. van Mil, A.J.M. Muijs, B. Petersen, T. van Rhee, M.P. Sanders, D.J. Schotanus, L3 Collaboration).
Search for new physics phenomena in fermion-pair production at LEP
Phys. Lett. **B433** (1998) 163

[29] M. Acciarri *et al.*; (G.J. Bobbink, A. Buijs, S.V. Chekanov, A.P. Colijn, D. van Dierendonck, P. Duinker, F.C. Erné, W.C. van Hoek, W. Kittel, A.C. König, F.L. Linde, D. Mangeol, G.G.G. Massaro, W.J. Metzger, A.J.W. van Mil, A.J.M. Muijs, B. Petersen, T. van Rhee, W. van Rossum, M.P. Sanders, D.J. Schotanus, R.T. Van de Walle, L3 Collaboration).
Measurement of the $B_d^0 - \overline{B_d^0}$ oscillation frequency
Eur. Phys. J. **C5** (1998) 195

[30] M. Acciarri *et al.*; (G.J. Bobbink, A. Buijs, A.P. Colijn, D. van Dierendonck, P. Duinker, F.C. Erné, R. van Gulik, W.C. van Hoek, W. Kittel, A.C. König, F.L. Linde, D. Mangeol, G.G.G. Massaro, W.J. Metzger, A.J.W. van Mil, A.J.M. Muijs, B. Petersen, T. van Rhee, M.P. Sanders, D.J. Schotanus, C. Timmermans, L3 Collaboration).
Measurement of the inclusive charmless semileptonic branching fraction of beauty hadrons and a determinition of $|V_{ub}|$ at LEP
Phys. Lett. **B436** (1998) 174

[31] M. Acciarri *et al.*; (G.J. Bobbink, A. Buijs, A.P. Colijn, D. van Dierendonck, P. Duinker, F.C. Erné, R. van Gulik, W.C. van Hoek, W. Kittel, A.C. König, F.L. Linde, D. Mangeol, G.G.G. Massaro, W.J. Metzger, A.J.W. van Mil, A.J.M. Muijs, B. Petersen, T. van Rhee, M.P. Sanders, D.J. Schotanus, C. Timmermans, L3 Collaboration).
Study of anomalous $ZZ\gamma$ and $Z\gamma\gamma$ couplings at LEP
Phys. Lett. **B436** (1998) 187

[32] M. Acciarri *et al.*; (G.J. Bobbink, A. Buijs, A.P. Colijn, D. van Dierendonck, P. Duinker, F.C. Erné, R. van Gulik, W.C. van Hoek, W. Kittel, A.C. König, F.L. Linde, D. Mangeol, G.G.G. Massaro, W.J. Metzger, A.J.W. van Mil, A.J.M. Muijs, B. Petersen, T. van Rhee, M.P. Sanders, D.J. Schotanus, C. Timmermans, L3 Collaboration).
Measurement of W-pair cross sections in e^+e^- interactions at $\sqrt{s}$ = 183 GeV and W-decay branching fractions
Phys. Lett. **B436** (1998) 437

[33] M. Acciarri *et al.*; (G.J. Bobbink, A. Buijs, A.P. Colijn, D. van Dierendonck, P. Duinker, F.C. Erné, R. van Gulik, W.C. van Hoek, W. Kittel, A.C. König, F.L. Linde, D.

Mangeol, G.G.G. Massaro, W.J. Metzger, A.J.W. van Mil, A.J.M. Muijs, B. Petersen, T. van Rhee, M.P. Sanders, D.J. Schotanus, C. Timmermans, L3 Collaboration).
Test of CP invariance in $Z \to \mu^+\mu^-\ \gamma$ decay
Phys. Lett. **B436** (1998) 428

[34] M. Acciarri *et al.*; (G.J. Bobbink, A. Buijs, A.P. Colijn, D. van Dierendonck, P. Duinker, F.C. Erné, R. van Gulik, W.C. van Hoek, W. Kittel, A.C. König, F.L. Linde, D. Mangeol, G.G.G. Massaro, W.J. Metzger, A.J.W. van Mil, A.J.M. Muijs, B. Petersen, T. van Rhee, M.P. Sanders, D.J. Schotanus, C. Timmermans, L3 Collaboration).
Production of single W bosons in e^+e^- interactions at $130 < \sqrt{s} < 183$ GeV and limits on anomalous $WW\gamma$ couplings
Phys. Lett. **B436** (1998) 417

[35] M. Acciarri *et al.*; (G.J. Bobbink, A. Buijs, A.P. Colijn, D. van Dierendonck, P. Duinker, F.C. Erné, R. van Gulik, W.C. van Hoek, W. Kittel, A.C. König, F.L. Linde, D. Mangeol, G.G.G. Massaro, W.J. Metzger, A.J.W. van Mil, A.J.M. Muijs, B. Petersen, T. van Rhee, M.P. Sanders, D.J. Schotanus,C. Timmermans, L3 Collaboration).
Study of the hadronic photon structure function F_2^γ at LEP
Phys. Lett. **B436** (1998) 403

[36] M. Acciarri *et al.*; (G.J. Bobbink, A. Buijs, A.P. Colijn, D. van Dierendonck, P. Duinker, F.C. Erné, R. van Gulik, W.C. van Hoek, W. Kittel, A.C. König, F.L. Linde, D. Mangeol, G.G.G. Massaro, W.J. Metzger, A.J.W. van Mil, A.J.M. Muijs, B. Petersen, T. van Rhee, M.P. Sanders, D.J. Schotanus, C. Timmermans, L3 Collaboration).
Search for neutral Higgs bosons of the minimal supersymmetric standard model in e^+e^- interactions at $\sqrt{s} = 130$ - 183 GeV
Phys. Lett. **B436** (1998) 389

[37] M. Acciarri *et al.*; (G.J. Bobbink, A. Buijs, A.P. Colijn, D. van Dierendonck, P. Duinker, F.C. Erné, R. van Gulik, W.C. van Hoek, W. Kittel, A.C. König, F.L. Linde, D. Mangeol, G.G.G. Massaro, W.J. Metzger, A.J.W. van Mil, A.J.M. Muijs, B. Petersen, T. van Rhee, M.P. Sanders, D.J. Schotanus, C. Timmermans, L3 Collaboration).
Measurement of radiative Bhabha and quasi-real Compton scattering
Phys. Lett. **B439** (1998) 183

[38] M. Acciarri *et al.*; (G.J. Bobbink, A. Buijs, A.P. Colijn, D. van Dierendonck, P. Duinker, F.C. Erné, R. van Gulik, W.C. van Hoek, W. Kittel, A.C. König, F.L. Linde, D. Mangeol, G.G.G. Massaro, W.J. Metzger, A.J.W. van Mil, A.J.M. Muijs, B. Petersen, T. van Rhee, M.P. Sanders, D.J. Schotanus, C. Timmermans, L3 Collaboration).
Measurement of the effective weak mixing angle by jet-charge asymmetry in hadronic decays of the Z boson
Phys. Lett. **B439** (1998) 225

[39] M. Acciarri *et al.*; (G.J. Bobbink, A. Buijs, S.V. Chekanov, A.P. Colijn, D.van Dierendonck, P. Duinker, F.C. Erné, W.C. van Hoek, W. Kittel, A.C. König, F.L. Linde, D. Mangeol, G.G.G. Massaro, W.J. Metzger, A.J.W. van Mil, A.J.M. Muijs, B. Petersen, T. van Rhee, W.L. van Rossum, M.P. Sanders, D.J. Schotanus, R.T. van de Walle, L3 Collaboration).
Measurement of $\eta'(958)$ formation in two-photon collisions at LEP1
Phys. Lett. **B418** (1998) 399

[40] M. Acciarri *et al.*; (G.J. Bobbink, A. Buijs, A.P. Colijn, D. van Dierendonck, P. Duinker, F.C. Erné, W.C. van Hoek, W. Kittel, A.C. König, F.L. Linde, D. Mangeol, G.G.G. Massaro, W. Metzger, A.J.W. van Mil, A.J.M. Muijs, B. Petersen, T. van Rhee, W.L. van Rossum, M.P. Sanders, D.J. Schotanus, R.T. van de Walle, L3 Collaboration).
Missing mass spectra in hadronic events from e^+e^- collisions at $\sqrt{s} = 161$-172 GeV and limits on invisible Higgs decays.
Phys. Lett. **B418** (1998) 389

[41] M. Acciarri *et al*; (G.J. Bobbink, A. Buijs, S.V. Chekanov, A.P. Colijn, D. van Dierendonck, F.C. Erné, R. van Gulik, W.C. van Hoek, W. Kittel, A.C. König, F.L. Linde, G.G.G. Massaro, D. Mangeol, W.J. Metzger, A.J.W. van Mil, A.J.M. Muijs, B. Petersen, T. van Rhee, M.P. Sanders, D.J. Schotanus, L3 Collaboration).
Measurement of the anomalous magnetic and electric dipole moments of the τ lepton
Phys. Lett. **B434** (1998) 169

[42] M. Acciarri *et al*; (G.J. Bobbink, A. Buijs, S.V. Chekanov, A.P. Colijn, D. van Dierendonck, F.C. Erné, R. van Gulik, W.C. van Hoek, W. Kittel, A.C. König, F.L. Linde, G.G.G. Massaro, D. Mangeol, W.J. Metzger, A.J.W. van Mil, A.J.M. Muijs, B. Petersen, T. van Rhee, M.P. Sanders, D.J. Schotanus, L3 Collaboration).
Photon structure functions and azimuthal correlations of lepton pairs in tagged $\gamma\gamma$ collisions
Phys. Lett. **B438** (1998) 363

[43] M. Acciarri *et al.*; (G.J. Bobbink, A. Buijs, A.P. Colijn, D. van Dierendonck, F.C. Erné, R. van Gulik, W.C. van Hoek, W. Kittel, A.C. König, F.L. Linde, G.G.G. Massaro, D. Mangeol, W.J. Metzger, A.J.W. van Mil, A.J.M. Muijs, B. Petersen, T. van Rhee, M.P. Sanders, D.J. Schotanus, C. Timmermans, L3 Collaboration).
Measurement of the Michel parameters and the average τ-neutrino helicity from τ decays at LEP
Phys. Lett. **B438** (1998) 405

[44] M. Acciarri *et al.*; (G.J. Bobbink, A. Buijs, A.P. Colijn, D. van Dierendonck, F.C. Erné, R. van Gulik, W.C. van Hoek, W. Kittel, A.C. König, F.L. Linde, G.G.G. Massaro, D. Mangeol, W.J. Metzger, A.J.W. van Mil, A.J.M. Muijs, B. Petersen, T. van Rhee, M.P. Sanders, D.J. Schotanus, C. Timmermans, L3 Collaboration).
Upper limit on the lifetime difference of short and long lived B_s^0 mesons
Phys. Lett. **B438** (1998) 417

[45] M. Acciarri *et al.*; (G.J. Bobbink, A. Buijs, A.P. Colijn, D. van Dierendonck, F.C. Erné, R. van Gulik, W.C. van Hoek, W. Kittel, A.C. König, F.L. Linde, G.G.G. Massaro, D. Mangeol, W.J. Metzger, A.J.W. van Mil, A.J.M. Muijs, B. Petersen, T. van Rhee, M.P. Sanders, D.J. Schotanus, C. Timmermans, L3 Collaboration).
Single and multi-photon events with missing energy in e^+e^- collisions at $\sqrt{s} = 183$ GeV
Phys. Lett. **B444** (1998) 503

[46] M. Acciarri *et al.*; (G.J. Bobbink, A. Buijs, A.P. Colijn, D. van Dierendonck, F.C. Erné, R. van Gulik, W.C. van Hoek, W. Kittel, A.C. König, F.L. Linde, G.G.G. Massaro, D. Mangeol, W.J. Metzger, A.J.W. van Mil, A.J.M. Muijs, B. Petersen, T. van Rhee, M.P. Sanders, D.J. Schotanus, C. Timmermans, L3 Collaboration).
QCD results from studies of hadronic events produced in e^+e^- annihilations at $\sqrt{s} = 183$ GeV
Phys. Lett. **B444** (1998) 569

[47] K. Ackerstaff *et al.*; (E.C. Aschenauer, J. Blouw, H.J. Bulten, C.W. de Jager, P.K.A. de Witt Huberts, M. Doets, T.

Henkes, E. Kok, M. Kolstein, H.R. Poolman, J.F.J. van den Brand, G. van der Steenhoven, J.J. van Hunen, HERMES Collaboration).
The HERMES spectrometer
Nucl. Instr. Meth. **A417** (1998) 230

[48] K. Ackerstaff *et al.*; (M. Amarian, J. Blouw, H.J. Bulten, P.K.A. de Witt Huberts, M. Guidal, H. Ihssen, M. Kolstein, J.F.J. van den Brand, G. van der Steenhoven, J.J. van Hunen, J. Visser, HERMES Collaboration).
Measurement of the proton spin structure function g_1^p with a pure hydrogen target
Phys. Lett. **B442** (1998) 484

[49] K. Ackerstaff *et al.*; (J. Blouw, H.J. Bulten, P.K.A. de Witt Huberts, Th. Henkes, H. Ihssen, M. Kolstein, J.F.J. van den Brand, G. van der Steenhoven, J.J. van Hunen, HERMES Collaboration).
The flavor asymmetry of the light quark sea from semi-inclusive deep-inelastic scattering
Phys. Rev. Lett. **81** (1998) 5519

[50] K. Ackerstaff *et al.*; (M. Amarian, E.C. Aschenauer, J. Blouw, H.J. Bulten,P.K.A. de Witt Huberts, M.G. Guidal, Th. Henkes, H. Ihssen, M. Kolstein, H.R. Poolman, J.F.J. van den Brand, G. van der Steenhoven, J.J. van Hunen, J. Visser, HERMES Collaboration).
Determination of the Deep Inelastic Contribution to the Generalised Gerasimov- Drell-Hearn Integral for the proton and the neutron
Phys. Lett. **B444** (1998) 531

[51] B. Adeva *et al.*; (R. van Dantzig, C. Dulya, N. de Groot, T.J. Ketel, M. Litmaath, G. van Middelkoop, J.E.J. Oberski, H. Postma, E.P. Sichtermann, Spin Muon Collaboration).
Measurement of proton and nitrogen polarization in ammonia and a test of equal spin temperature
Nucl. Instr. and meth. **A419** (1998) 60

[52] B. Adeva *et al.*; (R. van Dantzig, C. Dulya, N. de Groot, T.J. Ketel, M. Litmaath, G. van Middelkoop, J.E.J. Oberski, H. Postma, E.P. Sichtermann, Spin Muon Collaboration).
Spin asymmetries A_1 and structure functions g_1 of the proton and the deuteron from polarized high energy muon scattering
Phys. Rev. **D58** (1998) 112001

[53] B. Adeva *et al.*; (R. van Dantzig, C. Dulya, N. de Groot, T.J. Ketel, M. Litmaath, G. van Middelkoop, J.E.J. Oberski, H. Postma, E.P. Sichtermann, Spin Muon Collaboration).
A Next-to-leading order QCD analysis of the spin structure function g_1
Phys. Rev. **D58** (1998) 112002

[54] B. Adeva *et al.*; (R. van Dantzig, C. Dulya, N. de Groot, T.J. Ketel, M. Litmaath, G. van Middelkoop, J.E.J. Oberski, H. Postma, E.P. Sichtermann, Spin Muon Collaboration).
Polarized quark distributions in the nucleon from semi-inclusive spin asymmetries
Phys. Lett. **B420** (1998) 180

[55] N.M. Agababyan *et al.*; (W. Kittel, EHS-NA22collaboration).
Estimation of hydrodynamical model parameters from the invariant spectrum and the Bose-Einstein correlations of π-mesons produced in $(\pi^+/K^+)p$ Interactions at 250 GeV/c
Phys. Lett. **B422** (1998) 359

[56] N.M. Agababyan *et al.*; (W. Kittel, NA22 Collaboration).
Self-affine scaling from noninteger phase-space partition in π^+p and K^+p collisions at 250 GeV/c
Phys. Lett. **B431** (1998) 451

[57] M.M. Aggarwal *et al.*; (A. Buijs, N.J.A.M. van Eijndhoven, F.J.M. Geurts, R. Kamermans, C.J.W. Twenhöfel, WA98 Collaboration).
Search for disoriented chiral condensates in 158 AGeV Pb+Pb collisions
Phys. Lett. **B420** (1998) 169

[58] M.M. Aggarwal *et al.*; (A. Buijs, N.J.A.M. van Eijndhoven, F.J.M. Geurts, R. Kamermans, C.J.W. Twenhöfel, WA98 Collaboration).
Centrality dependence of neutral pion production in 158 AGeV $^{208}Pb+^{208}Pb$ collisions
Phys. Rev. Lett. **81** (1998) 4087

[59] M.M. Aggarwal *et al*; (A. Buijs, N.J.A.M. van Eijndhoven, F.J.M. Geurts, R. Kamermans, WA93 Collaboration).
Multiplicity and pseudorapidity distributions of photons in S+Au reactions at 200 AGeV
Phys. Rev. **C58** (1998) 1146

[60] R. Albrecht *et al.*; (R. Kamermans, C.J.W. Twenhöfel, F.J.M. Geurts, WA80 Collaboration).
Transverso momentum distributions of neutral pions from nuclear collisions at 200 AGeV
Eur. Phys. J. **C5** (1998) 255

[61] P.W. van Amersfoort.
Requiem voor GRAIL
Ned. T. Nat. **64** (1998)(7) 186

[62] L. Andricek *et al.*; (E. Koffeman).
Single sided $p+n$ and double-sided silicon strip detectors exposed to fluences up to $2\times10^{14}/cm^2$ 24 GeV protons
Nucl. Instr. Meth. **A409** (1998) 184

[63] P. Annis *et al.*; (J. Konijn).
The CHORUS scintillating fiber tracker and opto-electronic readout system
Nucl. Instr. Meth. **A412** (1998) 19

[64] P. Annis *et al.*; (R. van Dantzig, M. de Jong, J. Konijn, O. Melzer, R.G.C. Oldeman, C.A.F.J. van der Poel, J.W.E. Uiterwijk, J.L. Visschers, CHORUS Collaboration).
Observation of neutrino induced diffractive D_s^{*+} production and subsequent decay $D_s^{*+}\to D_s^+\to\tau^+\to\mu^+$
Phys. Lett. **B435** (1998) 458

[65] H. Avakian *et al.*; (J.F.J. van den Brand, M. Doets, T. Henkes, M. Kolstein).
Performance of the electromagnetic calorimeter of the HERMES experiment
Nucl. Instr. Meth. **A417** (1998) 69

[66] T.C. Awes *et al.*; (A. Buijs, N.J.A.M. van Eijndhoven, F.J.M. Geurts, R. Kamermans, C.J.W. Twenhöfel, WA98 Collaboration).
Collective flow as a probe of heavy ion reaction dynamics
Nucl. Phys. **A630** (1998) 499

[67] M.G. van Beuzekom *et al.*; (M.G. Guidal, W.H.A. Hesselink, E. Kok, A. Siriphant, G. van der Steenhoven, J.J.M. Steijger, J. Visser).
A silicon micro-strip telescope for the HERMES experiment: a design study
Nucl. Instr. Meth. **A409** (1998) 255

[68] L.J. de Bever *et al.*; (I. Bobeldijk, R.L.J. van der Meer, G. van der Steenhoven).
Investigation of the $^{10}B(\gamma, p)$ reaction using tagged photons
Phys. Rev. **C58** (1998) 981

[69] L.J. de Bever *et al.*; (H.P. Blok, C.W. de Jager, L. Lapikás, G. van der Steenhoven, H. de Vries).
Radial dependence of the nucleon effective mass in ^{10}B
Phys. Rev. Lett. **80** (1998) 3924

[70] G.J. Bobbink.
Event shapes at LEP
Proceedings of the 6th International workshop on Deep Inelastic Scattering and QCD (DIS98), Brussels 4-8 April 1998
Eds. Coremans and Roosen, World Scientific (1998) 514

[71] D. Boer, P.J. Mulders.
Time-reversal odd distribution functions in leptoproduction
Phys. Rev. **D57** (1998) 5780

[72] D. Boer, R. Jakob, P.J. Mulders.
Leading asymmetries in two-hadron production in e^+e^- annihilation at the Z pole
Phys. Lett. **B424** (1998) 143

[73] D. Boer, P.J. Mulders, O.V. Teryaev.
Single spin asymmetries from a gluonic background in the Drell-Yan process
Phys. Rev. **D57** (1998) 3057

[74] Kors Bos.
The Moose project
Comput. Phys. Commun. **110** (1998) 160

[75] M. Botje, G. Wolf.
Enhancing squark/leptoquark production by increasing the HERA beam energies
DESY 98-140, hep-ex/9809027

[76] J.F.J. van den Brand *et al.*; (Th.S. Bauer, D. Boersma, T. Botto, H.J. Bulten, L. van Buuren, M. Ferro-Luzzi, D. Geurts, M. Harvey, P. Heimberg, D. Higinbotham, C.W. de Jager, I. Passchier, H.R. Poolman, M. van der Putte, E. Six, J. Steijger, D. Szczerba, H. de Vries, P.K.A. de Witt Huberts).
Spin effects in medium-energy electron-^{3}He scattering
Nucl. Instr. Meth. **A402** (1998) 268

[77] J. Breitweg *et al.*; (C. Bokel, M. Botje, N. Bruemmer, F. Chlebana, J. Engelen, E. Koffeman, P. Kooijman, A. van Sighem, H. Tiecke, N. Tuning, W. Verkerke, J. Vossebeld, M. Vreeswijk, L. Wiggers, E. de Wolf, ZEUS Collaboration).
Dijet cross-sections in photoproduction at HERA
Eur. Phys. J. **C1** (1998) 109

[78] J. Breitweg *et al.*; (C. Bokel, M. Botje, N. Bruemmer, F. Chlebana, J. Engelen, E. Koffeman, P. Kooijman, A. van Sighem, H. Tiecke, N. Tuning, W. Verkerke, J. Vossebeld, M. Vreeswijk, L. Wiggers, E. de Wolf, ZEUS Collaboration).
Measurement of the diffractive structure function $F_2^{D(4)}$ at HERA
Eur. Phys. J. **C1** (1998) 81

[79] J. Breitweg *et al.*; (C. Bokel, M. Botje, N. Bruemmer, J. Engelen, E. Koffeman, P. Kooijman, A. van Sighem, H. Tiecke, N. Tuning, W. Verkerke, J. Vossebeld, L. Wiggers, E. de Wolf, ZEUS Collaboration).
High E_T inclusive jet cross sections in photoproduction at HERA
Eur. Phys. J. **C4** (1998) 591

[80] J. Breitweg *et al.*; (C. Bokel, M. Botje, N. Bruemmer, J. Engelen, E. Koffeman, P. Kooijman, A. van Sighem, H. Tiecke, N. Tuning, W. Verkerke, J. Vossebeld, L. Wiggers, E. de Wolf, ZEUS Collaboration).
Diffractive dijet cross-sections in photoproduction at HERA
Eur. Phys. J. **C5** (1998) 41

[81] J. Breitweg *et al.*; (C. Bokel, M. Botje, N. Bruemmer, J. Engelen, E. Koffeman, P. Kooijman, A. van Sighem, H. Tiecke, N. Tuning, W. Verkerke, J. Vossebeld, L. Wiggers, E. de Wolf, ZEUS Collaboration).
Search for selectron and squark production in e^+p collisions at HERA
Phys. Lett. **B434** (1998) 214

[82] J. Breitweg *et al.*; (C. Bokel, M. Botje, N. Bruemmer, J. Engelen, E. Koffeman, P. Kooijman, A. van Sighem, H. Tiecke, N. Tuning, W. Verkerke, J. Vossebeld, L. Wiggers, E. de Wolf, ZEUS Collaboration).
Measurement of elastic upsilon photoproduction at HERA
Phys. Lett. **B437** (1998) 432

[83] J. Breitweg *et al.*; (C. Bokel, M. Botje, N. Bruemmer, F. Chlebana, J. Engelen, E. Koffeman, P. Kooijman, A. van Sighem, H. Tiecke, N. Tuning, W. Verkerke, J. Vossebeld, M. Vreeswijk, L. Wiggers, E. de Wolf, ZEUS Collaboration).
Measurement of jet shapes in photoproduction at HERA
Eur. Phys. J. **C2** (1998) 61

[84] J. Breitweg *et al.*; (C. Bokel, M. Botje, N. Bruemmer, F. Chlebana, J. Engelen, E. Koffeman, P. Kooijman, A. van Sighem, H. Tiecke, N. Tuning, W. Verkerke, J. Vossebeld, M. Vreeswijk, L. Wiggers, E. de Wolf, ZEUS Collaboration).
Charged particles and neutral kaons in photoproduced jets at HERA
Eur. Phys. J.**C2** (1998) 77

[85] J. Breitweg *et al.*; (C. Bokel, M. Botje, N. Bruemmer, F. Chlebana, J. Engelen, E. Koffeman, P. Kooijman, A. van Sighem, H. Tiecke, N. Tuning, W. Verkerke, J. Vossebeld, M. Vreeswijk, L. Wiggers, E. de Wolf, ZEUS Collaboration).
Elastic and proton-dissociative ρ_0 photoproduction at HERA
Eur. Phys. J. **C2** (1998) 247

[86] J. Breitweg *et al.*; (C. Bokel, M. Botje, N. Bruemmer, F. Chlebana, J. Engelen, E. Koffeman, P. Kooijman, A. van Sighem, H. Tiecke, N. Tuning, W. Verkerke, J. Vossebeld, M. Vreeswijk, L. Wiggers, E. de Wolf, ZEUS Collaboration).
Measurement of the t-distribution in diffractive photoproduction at HERA
Eur. Phys. J. **C2** (1998) 237

[87] J. Breitweg *et al.*; (C. Bokel, M. Botje, N. Bruemmer, F. Chlebana, J. Engelen, E. Koffeman, P. Kooijman, A. van Sighem, H. Tiecke, N. Tuning, W. Verkerke, J. Vossebeld, M. Vreeswijk, L. Wiggers, E. de Wolf, ZEUS Collaboration).
Event shape analysis of deep inelastic scattering events with a large rapidity gap at HERA
Phys. Lett. **B421** (1998) 368

[88] H.J. Bulten *et al.*; (J.F.J. van den Brand, M. Ferro-Luzzi).
Spin-exchange effects on tensor polarization of deuterium atoms
Phys. Rev. **A58** (1998) 1146

[89] M. Buza, Y. Matiounine, J. Smith, W.L. van Neerven.
Charm electroproduction viewed in the variable-flavour number scheme versus fixed-order perturbation theory
Eur. Phys. J. **C1** (1998) 301

[90] S.V. Chekanov, W. Kittel, W.C. Metzger.
Local properties of local multiplicity distributions in hadronic Z decay
Nucl. Phys. B, Proc. Suppl. **71** (1998) 146

[91] J.P. Connelly *et al.*; (H.P. Blok, L. Lapikás).
Trinicleon cluster knockout from ^6Li
Phys. Rev. **C57** (1998) 1569

[92] S. Costantini.
Search for Neutral Higgs Boson Production in the Processes $e^+e^- \to Z^*H^0$ and $e^+e^- \to H^0\gamma$ with L3, Division of Particles and Field 1996 Meeting, Minneapolis, Minesota, DPF '96: The Minneapolis Meeting, eds. K. Heller, J.K. Nelson and D. Reeder
World Scientific, Singapore, (1998) vol. 1, 246

[93] H.G. Dosch, T. Gousset, H.J. Pirner.
*Nonperturbative gamma*p interaction in the diffractive regime*
Phys. Rev. **D57** (1998) 1666

[94] J. Engelen and P. Kooijman.
Deep Inelastic Scattering at HERA: A review of experimental results in the light of Quantum Chromodynamics
Progress in Particle and Nuclear Physics **41** (1998) 1

[95] E. Eskut *et al.*; (R. van Dantzig, M. de Jong, J. Konijn, O. Melzer, R.G.C. Oldeman, C.A.F.J. van der Poel, J.W.E. Uiterwijk, J.L. Visschers, CHORUS Collaboration).
A search for $\nu_{mu} \to \nu_{tau}$ oscillation
Phys. Lett. **B424** (1998) 202

[96] E. Eskut *et al.*; (R. van Dantzig, M. de Jong, J. Konijn, O. Melzer, R.G.C. Oldeman, C.A.F.J. van der Poel, J.W.E. Uiterwijk, J.L. Visschers, CHORUS Collaboration).
Search for $\nu_{mu} \to \nu_{tau}$ oscillation using the τ decay modes into a single charged particle
Phys. Lett. **B434** (1998) 205

[97] M. Ferro-Luzzi, T. Botto, M. Bouwhuis, J.F.J. van den Brand, H.J. Bulten, C.W. de Jager, D.J. de Lange, I. Passchier, H.R. Poolman, M. van der Putte, J. Steijger, H. de Vries.
Spin-dependent electromagnetic response of few-body systems
Nucl. Phys. **A631** (1998) 190c

[98] B. Gato-Rivera.
The even and the odd spectral flows on the N=2 superconformal algebras
Nucl. Phys. **B512** (1998) 431

[99] B. Gato-Rivera and I.I. Rosade.
Subsingular vectors of the topological N=2 Superconformal Algebra
Nucl. Phys. **B514** (1998) 477

[100] H. van der Graaf, H. Dietl, P. Hendriks, F. Linde, G. Stravopoulos, M. Vreeswijk, M. Woudstra.
First system performance experience with the ATLAS high-precision muon drift chambers
Nucl. Instr. and Meth. Physics Research **A419** (1998) 336

[101] S. Groot Nibbelink and J.W. van Holten.
Matter coupling and anomaly cancellation in supersymmetric sigma models
Phys. Lett. **B442** (1998) 185

[102] L.P.A. Haakman, J.H. Koch.
The BFKL Pomeron with running coupling constant: how much of its hard nature survives?
Nucl. Phys. **B518** (1998) 275

[103] L.P.A. Haakman, A.B. Kaidalov, J.H. Koch.
Charm production in deep inelastic and diffractive scattering
Eur. Phys. J. **C1** (1998) 547

[104] A.W. van Halderen *et al.*; (R. van Dantzig).
Hierarchical resource management in the Polder Metacomputing Initiative
Parallel Computing **24** (1998) 1807

[105] J.W. van Holten.
Stability and mass of point particles
Nucl. Phys. **B529** (1998) 525

[106] Jan-Willem van Holten.
Bericht uit het veld
Ned. T. Nat. **64** (1998) 204

[107] J.W. van Holten.
Theories de jauge et unification des interactions fondamentales
Le Vide, Univers du Tout et du Rien, eds. E. Gunzig and S. Diner; Revue de l'Universite de Bruxelles (1998)

[108] J.W. van Holten, P. Jarvis and J. Kowalski-Glikman.
Off-shell kappa-invariance of the superparticle and spinning superparticle
Phys. Lett. **B427** (1998) 47

[109] J.J. van Hunen.
Performance of the HERMES micro-strip gas chamber
Nucl. Instr. Meth. **A409** (1998) 95

[110] W-J. Kasdorp, W.H.A. Hesselink, D.L. Groep, E. Jans, N. Kalantar-Nayestanaki, L. Lapikás, J.J. van Leeuwe, A. Misiejuk, G.J.L. Nooren, C.J.G. Onderwater, A.R. Pellegrino, C.M. Spaltro, R. Starink, G. van der Steenhoven, J.J.M. Steijger, J.A. Templon.
Deuteron electrodisintegration at high missing momenta
Few Body Systems **25** (1998) 115

[111] T.J. Ketel (Spin Muon Collaboration).
Experimental results on polarized nucleon structure functions
Proceedings of the Cracow Epiphany Conference on Spin effects in Particle Physics, Cracow (Poland), Ed. K. Fialkowski and M. Jezabek,
Acta Phys. Polonica **B29** (1998) 1265

[112] W. Kittel, S.V. Chekanov, D. Mangeol, W.J. Metzger.
Multiplicities, fluctuations and QCD: Interplay between soft and hard physics?
Nucl. Phys. B, Proc. Suppl. **71** (1998) 90

[113] Justus H. Koch, Hubertus R. Mall, Stefan Lenz.
Stochastic methods for zero energy quantum scattering
Comput. Phys. Commun. **108** (1998) 115

[114] Machiel Kolstein (for the HERMES Collaboration).
Diffractive ρ^0 production at HERMES
Proceedings of the PHOTON'97 Conference, Egmond aan Zee, 10-15 May 1997, Eds. A. Buijs and F.C. Erné (1998) p.314

[115] Eric Laenen, Gianluca Oderda, George Sterman.
Resummation of threshold corrections for single particle inclusive cross-sections
Phys. Lett.**B438** (1998) 173

[116] D.J.J. de Lange, H.P. Blok, D.J. Boersma, T. Botto, P. Heimberg, D.W. Higinbotham, I. Passchier, M.J.M. van Sambeek, E. Six, M.F.M. Steenbakkers, J.J.M. Steijger, H. de Vries.

The optical properties of the BigBite spectrometer at NIKHEF
Nucl. Instr. Meth. **A412** (1998) 254

[117] D.J.J. de Lange *et al.*; (D.W. Higinbotham, J.J.M. Steijger, H. de Vries).
A large acceptance spectrometer for the internal target facility at NIKHEF
Nucl. Instr. Meth. **A406** (1998) 182

[118] J.J. van Leeuwe *et al.*; (H.P. Blok, J.F.J. van den Brand, H.J. Bulten, G.E. Dodge, R. Ent, E. Jans, W.H.A. Hesselink, L. Lapikás, W.-J. Kasdorp, S.I. Nagorny, A. Pellegrino, C.J.G. Onderwater, C.M. Spaltro, J.J.M. Steijger, J.A. Templon, O. Unal).
High missing-momentum components in $^4He(e,e'p)^3H$ reaction
Phys. Rev. Lett. **80** (1998) 2543

[119] J.J. van Leeuwe *et al.*; (H.P. Blok, J.F.J. van den Brand, H.J. Bulten, G.E. Dodge, R. Ent, W.H.A. Hesselink, E. Jans, W.J. Kasdorp, L. Lapikás, C.J.G. Onderwater, A.R. Pellegrino, C.M. Spaltro, J.J.M. Steijger, J.A. Templon, O. Unal).
The $^4He(e,e'p)$ cross section at large missing energy
Nucl. Phys. **A631** (1998) 593c

[120] T. Nayak *et al.*; (A. Buijs, N.J.A.M. van Eijndhoven, F.J.M. Geurts, R. Kamermans, C.J.W. Twenhöfel, WA98 Collaboration).
Present status and future of DCC analysis
Nucl. Phys. **A368** (1998) 249

[121] J. Oberski.
Neutrino-oscillatie of platvloerse interpretatie?
Ned. T. Nat. **64** (1998) 202

[122] C.J.G. Onderwater *et al.*; (E.C. Aschenauer, Th.S. Bauer, D.J. Boersma, D.L. Groep, W.H.A. Hesselink, E. Jans, W.-J. Kasdorp, L. Lapikás, J.J. van Leeuwe, A. Misiejuk, A.R. Pellegrino, R. Starink, M. Steenbakkers, G. van der Steenhoven, J.J.M. Steijger, M.A. van Uden, H.W. Willering).
Signatures for short-range correlations in ^{16}O observed in the reaction $^{16}O(e,e'pp)^{14}C$
Phys. Rev. Lett. **81** (1998) 2213

[123] I. Passchier *et al.*; (D.W. Higinbotham, C.W. de Jager, B.E. Norum, N.H. Papadakis, N.P. Vodinas).
A Compton backscattering polarimeter for measuring longitudinal electron polarization
Nucl. Instr. Meth. **A414** (1998) 446

[124] J.C. Plefka, A.K. Waldron.
On the quantum mechanics of M(atrix) theory
Nucl. Phys. **B512** (1998) 460

[125] J.C. Plefka, M. Serone, A.K. Waldron.
The matrix theory S matrix
Phys. Rev. Lett. **81** (1998) 2866

[126] Jan C. Plefka, Stuart Samuel.
Monte Carlo simulations of the CP3 model and U(1) gauge theory in the presence of a theta term
Nucl. Phys.**B63** (Proc. Suppl.) (1998) 715

[127] Jan Plefka, Marco Serone and Andrew Waldron.
D=11 SUGRA as the low–energy effective action of Matrix theory: Three Form Scattering
J. High Energy Phys.**9811** (1998) 010

[128] Jan Plefka and Andrew Waldron.
Asymptotic supergraviton states in Matrix theory
Theory of elementary particles, Buckow (1997), p.130

[129] M.J.J. van den Putte, C.W. de Jager, B.L. Militsyn, Yu.M. Shatunov, Yu.F. Tokarev.
Photocathode lifetime improvement by using a pulsed high voltage on the photocathode gun of the polarized electron source at NIKHEF
Nucl. Instr. and Meth. **A406** (1998) 50

[130] T. van Rhee.
Meson Formation in photon-photon collisions at LEP with the L3 detector
Proceedings of The Meson98 and Conference on the structure of Mesons, Baryon and Nuclei, Cracow Poland, May 26 - June 2, 1998
Acta Physica Polonica **B29** (1998) 3401

[131] W.L. van Rossum (for the L3 Collaboration).
Cross section for hadron production in two photon events at LEP
Proceedings of the PHOTON'97 Conference, Egmond aan Zee, 10-15 May 1997, Eds. A. Buijs and F.C. Erné (1998), p.80

[132] M.J.M. van Sambeek *et al.* (M.G. van Beuzekom, H.P. Blok, G.E. Dodge, P. Heimberg, P.P.M. Jansweijer, M.F.M. Steenbakkers, J.J.M. Steijger, J.C. Verkooijen).
A recoil detector for the internal target facility of AmPS (NIKHEF)
Nucl. Instr. Meth. **A409** (1998) 443

[133] M.J.M. van Sambeek, Th.S. Bauer, T. Botto, H.P. Blok, D.J. Boersma, D.L. Groep, W.H.A. Hesselink, C.W. de Jager, E. Jans, T.J. Ketel, D.J.J. de Lange, L. Lapikás, I. Passchier, M.F.M. Steenbakkers, J.J.M. Steijger, H. de Vries.
Coherent π^0 electroproduction on ^4He in the Δ region
Nucl. Phys. **A631** (1998) 545c

[134] A.N. Schellekens.
Naar een waardig slot, oratie KUN, 16-09-1998
ISBN Nr. 90-9012073-4

[135] E.P. Sichtermann (Spin Muon Collaboration).
A NLO QCD analysis of the spin structure function g_1
Proceedings of the 6th Int. Workshop on Deep Inelastic Scattering and QCD (DIS98) 4-8 April 1998
Ed. Coremans and Roosen, World Scientific (1998), p.661

[136] R.J.M. Snellings, A. van den Brink, A.P. de Haas, J.J.L.M. Habets, W. Hulsbergen, R. Kamermans, P.G. Kuijer, C.T.A.M. de Laat, R.W. Ostendorf, A. Péghaire, E.P. Prendergas.
IMF-IMF azimuthal correlations as a tool to probe reaction dynamics in $^{36}Ar + ^{48}Ti$ at 45 AMeV
Phys. Lett. **B426** (1998) 263

[137] C.M. Spaltro *et al.*;(Th.S. Bauer, H.P. Blok, T. Botto, G.E. Dodge, M.N. Harakeh, E. Jans, W-J. Kasdorp, C. Kormanyos, L. Lapikás, A. Misiejuk, S.I. Nagorny, G.J. Nooren, C.J.G. Onderwater, M. van Sambeek, R. Starink, G. van der Steenhoven, J. Tjon, M.A. van Uden, H. de Vries, M. Yeomans).
q and p_m dependence of the $^3He(e,e'd)p$ reaction
Phys. Rev. Lett. **81** (1998) 2870

[138] G. van der Steenhoven (for the HERMES Collaboration).
Diffractive ρ^0 production at HERMES
Proceedings of the Workshop on Colour Transparency (CT97), Grenoble, 25-27 June 1997, Ed. E. Voutier (1998) 23

[139] J. Timmerman.
Precision Tests of the Electroweak Interaction from e^+e^-

Colliders
in Proceedings of the XVIII International Symposium on Lepton-Photon Interactions LP'97, Hamburg (Germany), July 28 - August 1, 1997, eds. A. De Roeck and A. Wagner, Publ. World Scientific 0(1998), p.465

[140] M.A. van Uden *et al.*; (E.C. Aschenauer, L.J. de Bever, H.L. Castricum, D.L. Groep, W-J. Kasdorp, L. Lapikás, C.J.G. Onderwater, M. Schroevers, C.M. Spaltro, R. Starink, G. van der Steenhoven, J.J.M. Steijger).
High resolution $^{16}O(\gamma^*,\pi^- p)$ experiment
Phys. Rev. **C58** (1998) 3462

[141] J.W.E. Uiterwijk *et al.*; (M.G. van Beuzekom, R. van Dantzig, H. van der Graaf, M. de Jong E. Kok, J. Konijn, J.P.M. Metselaar, R.G.C. Oldeman, C.A.F.J. van der Poel, J.L. Visschers).
The CHORUS honeycomb tracker and its bitstream electronics
Nucl. Instr. Meth. **A409** (1998) 682

[142] J.A.M. Vermaseren.
Some problems in high loop calculations
Acta Phys. Pol. **B29** (1998) 2599

[143] J. Vermaseren *et al.*
Pomerons and jet events at HERA
Phys. Lett. **B418** (1998) 363

[144] J.C. Vermeulen *et al.*
Discrete Event Simulation of the ATLAS Second Level Trigger
IEEE Trans. on Nucl. Sci. **45** (1998) 1989

[145] A.H. Wapstra.
Geruzie over de namen van nieuwe elementen
Ned. T. Nat. **64** (1998) 139 (erratum p.204)

[146] B. de Wit, K. Peeters, J.C. Plefka.
The supermembrane with winding
Nucl. Phys. **B62** (Proc. Suppl.) (1998) 405

[147] B. de Wit, K. Peeters, J.C. Plefka.
Open and closed supermembranes with winding
Nucl. Phys. **B68** (Proc. Suppl.) (1998) 206

[148] B. de Wit, K. Peeters, J.C. Plefka.
Superspace geometry for supermembrane backgrounds
Nucl. Phys. **B532** (1998) 99

[149] B. de Wit, K. Peeters, J.C. Plefka and A. Sevrin.
The M theory two-brane in $Ads_4 \times S^7$ and $AdS_7 \times S^4$
Phys. Lett. **B443** (1998) 153

[150] F.J. Yndurain.
Pure QCD bounds and estimates for light quark masses
Nucl. Phys. **B517** (1998) 324

1.2 Ph.D. Theses

[1] Wim van Rossum
'Hadron production in two-photon collisions at LEP'
Universiteit Utrecht, March 1998

[2] Maurice Bouwhuis
'Tensor polarization observables in electron deuteron scattering'
Universiteit Utrecht, March 1998

[3] Dirk-Jan Jeroen de Lange
'A study of collective aspects of ^{4}He electro disintegration with the BigBite spectrometer'
Universiteit Utrecht, April 1998

[4] Cornelis Johannes Gerardus Onderwater
'Investigation of short-range correlations using the $^{16}O(e,e'pp)$ reaction'
Vrije Universiteit Amsterdam, April 1998

[5] Leonard Peter Anton Haakman
'QCD aspects of the Pomeron: from soft to hard scales'
Universiteit van Amsterdam, June 1998

[6] Kasper Peeters
'Geometrical aspects of supersymmetry: spinning particles, string dualities and the eleven-dimensional supermembrane'
Universiteit Utrecht, June 1998

[7] Wouter Verkerke
'Measurement of Charm production in deep inelastic scattering'
Universiteit van Amsterdam, June 1998

[8] Tulay Cuhadar
'Measurements of the spin structure functions g_1^p and g_1^d in deep inelastic scattering'
Vrije Universiteit Amsterdam, June 1998

[9] Daniel Boer
'Azimuthal asymmetries in hard scattering processes'
Vrije Universiteit Amsterdam, September 1998

[10] F.J.M. Geurts
'Neutral meson production in hot matter'
Universiteit Utrecht, October 1998

[11] Machiel Kolstein
'Exclusive ρ^0 - meson electroproduction at HERMES'
Vrije Universiteit Amsterdam, October 1998

[12] Reinier Joseph Dankers
'The physics performance of and level 2 trigger for the inner detector of ATLAS'
Universiteit Twente, October 1998

[13] Johan Blouw
'Spin-dependent deep-inelastic positron scattering from polarized ^{3}He'
Vrije Universiteit Amsterdam, October 1998

[14] Boris Leonidovich Militsyn
'A pulsed polarized electron source for nuclear physics experiments'
Technische Universiteit Eindhoven, December 1998

1.3 Invited Talks

[1] P.W. van Amersfoort
'The GRAIL project'
11e CPS/NNV Symposium 'Plasmafysica en Stralingstechnologie', Lunteren (The Netherlands), March 17, 1998

[2] H.P. Blok
'Coherent and quasi-free π^0 production on ^{4}He studied by recoil detection'
KVI, Groningen (The Netherlands), April 21, 1998

[3] H.P. Blok
Lectures on '(e,e'x) coincidence reactions'
13th Annual Hampton University Graduate Studies (HUGS), CEBAF (USA), May 26-June 12, 1998

[4] H.P. Blok
Lectures on 'Electron scattering and nucleon and nuclear structure'
Hampton University, June 2-5, 1998

[5] H.P. Blok
'Pion electroproduction on $^{1,2}H$ and the pion form factor'
Workshop on Structure functions and hadronic wave functions, Bad Honnef (Germany), December 14-18, 1998

[6] G.J. Bobbink
'Event shapes at LEP'
6th International Workshop on Deep Inelastic Scattering and QCD (DIS98), Brussels (Belgium), April 4-8, 1998

[7] G.J. Bobbink
'Tests of lepton universality in τ decays'
XXIX International Conference on High Energy Physics (ICHEP98), Vancouver (Canada), July 23-29, 1998

[8] D. Boer
'Gluonic poles and the Drell-Yan process'
Workshop Deep Inelastic Nonforward and Forward Lepton-Nucleon Scattering, Regensburg (Germany), June 29 - July 10, 1998

[9] D. Boer
'Transverse spin and transverse momentum'
Brookhaven National Laboratory, Upton, New York (USA), November 20, 1998

[10] D. Boer
'Origins of transverse spin asymmetries in hadron-hadron collisions'
Center of Theoretical Physics, MIT, Cambridge (USA), December 8, 1998

[11] M. Botje
'ZEUS QCD fits'
Aspects of deep-inelastic scattering, DESY Zeuthen (Germany), June 3-6, 1998

[12] T. Botto
'Cohorent neutral pion production from ^4He'
1998 Gordon Research Conference on Photonuclear Reactions, Tilton School, Tilton (USA), July 26-31, 1998

[13] N. Brummer
'The Standard Model and beyond in ep physics'
Hadron Structure98, Stara Lesna (Slovakia), September 7-13, 1998

[14] A. Buijs
'The study of heavy ion collisions with the ALICE detector at the LHC'
Xth International Symposium on Very High Energy Cosmic Ray Interactions,
Laboratori Nazionali Del Gran Sasso, Assergi (Italy), July 12-17 1998

[15] A.P. Colijn
'L3 analysis of tau lifetime'
Workshop on tau lepton physics (TAU98), Santander (Spain), September 14-17, 1998

[16] J. van Dalen
'Pion interferometry of the pion source in e^+e^- collisions in L3'
8th Int. Workshop on Multiparticle Production, Matrahaza (Hungary), June 14-21, 1998

[17] S. Duensing
'W-Physik bei LEP II'
Deutsche Physikerinnen Tagung, Hamburg (Germany), November 12-15, 1998

[18] B. van Eijk
'Tracking through Physics, Physics through Tracking'
Katholieke Universiteit Nijmegen, Nijmegen (The Netherlands), January 19, 1998

[19] B. van Eijk
'Symmetries in Nature' ('Science as Culture')
Leerstoel presentatie Universiteit Twente, Eindhoven (The Netherlands), June 5, 1998

[20] J.J. Engelen
'Electron-proton scattering at High Energy'
Algemeen Colloquium Vrije Universiteit, Amsterdam (The Netherlands), March, 1998

[21] J.J. Engelen
'Results from the first six years at HERA'
NNV Annual Meeting Subatomic Physics, Petten (The Netherlands), October 30 1998

[22] S. Groot Nibbelink
'Summary of Workshop of LHC processes'
Globe meeting 98, NIKHEF, Amsterdam (The Netherlands), March 17, 1998

[23] S. Groot Nibbelink
'Consistent Grassmannian Models'
Bergische Universitaet Gesamthochschule Wuppertal, Wuppertal (Germany), October 28, 1998

[24] P. Heimberg
'Recent results from the Internal Target Hall at NIKHEF'
Mesons and Light Nuclei, Prague, 1998

[25] W.H.A. Hesselink
'Short-range-correlations in ^{16}O studied with the reaction ^{16}O(e,e'pp)^{14}C'
Nuclear Physics Spring Meeting, Bochum (Germany), March 16-20, 1998

[26] W.H.A. Hesselink
'Short Range Correlations in ^3He and ^{16}O investigated with the reaction (e,e'pp)'
1998 Gordon Research Conference on Photonuclear Reactions, Tilton School, Tilton (USA), July 26-31, 1998

[27] N. Hessey
'The precision drift chambers for the ATLAS Muon Spectrometer'
The Vienna Wire Chamber Conference, Vienna (Austria), February 23-27, 1998

[28] J.W. van Holten
'Gravitational Waves: the harmony of spheres'
Rijksuniversiteit Leiden, Leiden (The Netherlands), February 5, 1998
Einstein Institute, Potsdam (Germany), February 24, 1998

[29] J.W. van Holten
'Killing-Yano tensors and Killing dualities'
National Seminar on Theoretical HEF, NIKHEF, Amsterdam (The Netherlands), May 8, 1998
Institute of Theoretical Physics, University of Wroclaw, Wroclaw (Poland), September 21, 1998

[30] J.W. van Holten
'Kaehler geometry and supersymetric sigma models'
Bergische Universität, Wuppertal (Germany), October 28, 1998

[31] J.W. van Holten
'Gravitational Waves'
Universität Mainz, Mainz (Germany), November 4, 1998

[32] J.W. van Holten
'Physics and detection of gravitational waves'
Annual Meeting on Theoretical Physics, Rutherford Laboratory, Didcot (United Kingdom), December 18, 1998

[33] J.J. van Hunen
'Hadronization in a nuclear environment'
Winter Institute Chateau Lake Louise, Quantum Chromodynamics, Lake Louise (Canada), February 15-21, 1998

[34] J.J. van Hunen
'Semi-inclusive hadron production from ^{14}N'
Workshop on Coherent QCD Processes with nucleons and nuclei, ECT*, Trento (Italy), September 1-11, 1998

[35] J.J. van Hunen
'Semi-inclusive hadron production at HERMES'
MPI-Heidelberg, Department for theoretical physics, Heidelberg (Germany), November 24, 1998

[36] H. Ihssen
'Extraction of fragmentation functions at HERMES'
Mid Term Review Meeting of the TMR network Hadronic Physics with High Energy Electromagnetic Probes, Pavia, March 19-21, 1998

[37] H. Ihssen
'Flavour asymmetry of the light quark sea'
Rencontres de Moriond on QCD and High Energy Hadronic Interactions, Les Arcs 1800 (France), March 20-27, 1998

[38] H. Ihssen
'Nucleon spin structure measurement at DESY'
QCD 98 Euroconference, Montpellier (France), July 7-13, 1998

[39] H. Ihssen
'Nucleon spin structure measurement at HERMES'
3rd UK Phenomenology Workshop on HERA Physics, St. John's College, Durham (Great Brittain) September 20-25, 1998

[40] E. Jans
'NN-correlations studied with electron-induced knockout reactions'
KVI, Groningen (The Netherlands), June 23, 1998

[41] M. de Jong
'Neutrino: masses, mixing and oscillations'
Technische Universiteit Twente, Eindhoven (The Netherlands), September 29, 1998

[42] M. de Jong
'Neutrino: masses, mixing and oscillations'
AMOLF, Amsterdam (The Netherlands), January 11 1999

[43] P. de Jong
'W production at LEP: cross sections and W properties'
Moriond electroweak, Les Arcs (France), March 14-21, 1998

[44] P. de Jong
'Reconnection and Bose-Einstein effects in WW Decay'
XXVIII International Symposium on Multiparticle Dynamics, Delphi (Greece), September 6-11, 1998

[45] S. de Jong
'Workshop Summary'
VERTEX98, Santorini (Greece), October 3, 1998

[46] S. de Jong
'The D0 expertiment at Fermilab'
Katholieke Universiteit Nijmegen, Nijmegen (The Netherlands), October 6, 1998

[47] S. de Jong
'How to proceed the experimental Higgs programme'
DESY/ECFA Linear Collider Workshop, Frascati (Italy), November 9, 1998

[48] S. de Jong
'LC98 Higgs WG: Report and outlook'
DESY/ECFA Linear Collider Workshop, Frascati (Italy), November 10, 1998

[49] T.J. Ketel
'Experimental results on polarized nucleon structure functions'
Cracow Epiphany Conference on Spin effects in Particle Physics, Cracow (Poland), January 10, 1998

[50] W. Kittel
'Multiplicity fluctuations in L3 and QCD'
Lake Louise Winter Institute, Lake Louise (Canada), February 15-21, 1998
Workshop on Density Fluctuations in Multiparticle Production, Wuhan (China), May 15-16, 1998

[51] W. Kittel
'Angular multiplicity fluctuations in hadronic Z decays and QCD'
8th Int. Workshop on Multiparticle Production, Matrahaza (Hungary), June 14-21, 1998

[52] W. Kittel
'4 Lectures on 3 Experiments at CERN (Past, Present and Future)'
Huazhong Normal University, Wuhan (China), May 11-14, 1998

[53] W. Kittel
'2 Seminars on Correlations and Fluctuations in High Energy Physics'
Huazhong Normal University, Wuhan (China), May 7 and 10, 1998

[54] W. Kittel
'High Energy Physics'
Jingzhou Teachers College, Jingzhou (China), May 9, 1998

[55] W. Kittel
'Particle physics in the Universe and on Earth'
Hubei University, Wuhan (China), May, 1998

[56] W. Kittel
'Multiplicity fluctuations'
IHEP, Academia Sinica, Beijing (China), May 22, 1998

[57] P. Klok
'4 Lectures 'Introduction to UNIX' and 'UNIX system management'
Huazong Normal University, Wuhan (China), November, 1998

[58] P. Klok
'Lecture 'Computers'
Jingzhou Teachers College, Jingzhou (China), November, 1998

[59] P. Kluit
'Particle identification using the DELPHI RICH detectors'
RICH98, Third Int. Workshop on Ring Imaging Cherenkov Detectors, Ein-Gedi, Dead Sea (Israel), November 15-20, 1998

[60] J. Koch
'The Pomeron'
University of Erlangen, Erlangen (Germany), February 4, 1998

[61] J. Koch
'The use of formfactors in intermediate energy reactions'
University of Gent, Gent (Belgium), February 18, 1998

[62] J. Koch
'The description of hadron structure in electromagnetic reactions'
KVI, Groningen (The Netherlands), March 31, 1998

[63] J. Koch
'Stochastic methods for quantum scattering'
KVI, Groningen (The Netherlands), June 19, 1998

[64] E. Koffeman
'Radiation hard vertex detectors'
Universiteit Utrecht, Utrecht (The Netherlands), April 27, 1998

[65] J. Konijn
'Does the neutrino have mass and how can we measure it?'
Physics Institute of Uppsala University (Sweden), June 12, 1998

[66] N. Kjaer
'W mass measurement at LEP2'
XXXIII'rd Rencontres de Moriond "Electroweak Interactions and Unified Theories", Les Arcs (France), March 14-21, 1998

[67] E. Laenen
'10 Lectures on Renormalons'
AIO/OIO School of Theoretical High energy Physics, Nijmegen (The Netherlands), February, 1998

[68] E. Laenen
'8 Lectures on QCD'
10th Joint Belgian-Dutch-German Annual Graduate School of Particle Physics, Ysermonde (Belgium), September 7-18, 1998

[69] E. Laenen
'QCD Aspects of Heavy Qark Production in Hadronic Collisions'
Universiteit Utrecht, Utrecht (The Netherlands), June, 1998

[70] E. Laenen
'Aspects of Resummation in QCD Sections'
University Freiburg, Freiburg (Germany), June, 1998

[71] E. Laenen
'Electroproduction of Heavy Quarks'
DESY, Hamburg (Germany), November, 1998

[72] L. Lapikás
'Nucleons and nucleon pairs in nuclei'
Workshop on Electron-Nucleus scattering, Elba (Italy), June 25, 1998

[73] W. Lavrijsen
'Combined Muon Fit Using Geane'
ATLAS Physics Workshop, Grenoble (France), March 30, 1998

[74] F.L. Linde
'The ATLAS muon Spectrometer and its Physics'
Katholieke Universiteit Nijmegen, Nijmegen (The Netherlands), May, 1998

[75] D. Mangeol
'Analysis of the charged particle multiplicity distribution using the ratio of cumulant factorial moments at L3'
8th Int. Workshop on Multiparticle Production, Matrahaza (Hungary), June 14-21, 1998

[76] D. Mangeol
'QCD studies with the L3 detectors'
Int. High-Energy Physics Euroconference in Quantum Chromodynamics (QCD98), Montpellier (France), July 2-8, 1998

[77] O. Melzer
'Charm production by neutrinos'
DELPHI seminar, CERN, Geneva (Switzerland), August 18, 1998
Hyperons, charm and beauty hadrons 98, Genova (Italy), June 2, 1998

[78] O. Melzer
'Diffractive production of D_s^* by neutrinos'
XXIXth International Conference on High Energy Physics (ICHEP 98), Vancouver (Canada), July 23-29, 1998

[79] W. Metzger
'Multiplicity fluctuations and multiparticle correlations'
XXIX Int. Conference on High Energy Physics (ICHEP 98), Vancouver (Canada), July 23-29, 1998

[80] W. Metzger
'Oscillation of H_q moments as not a test of QCD'
XXVII Int. Symposium on Multiparticle Dynamics, Delphi (Greece), September 9, 1998

[81] W. Metzger
'QCD (Experimental)'
3 Lectures at the 10th Joint Belgian-Dutch-German Annual Graduate School of Particle Physics, Ysermonde (Belgium), September 7-18, 1998

[82] S. Moch
'QCD-Instantons in Deep-Inelastic Scattering'
Ruhr Universität, Bochum (Germany), February 2, 1998
10th Workshop on Theory beyond the Standard Model, Bad Honnef (Germany), March 11, 1998

[83] S. Moch
'Sudakov resummation for heavy-quark electroproduction'
DIS98, Brussels (Belgium), April 5, 1998
RWTH, Aachen (Germany), April 30, 1998

[84] S. Moch
'Soft gluon resummation for heavy quark electroproduction'
Third UK Phenomenology Workshop on HERA Physics, Durham (United Kingdom), September 21, 1998

[85] S. Moch
'General aspects of renormalization'
Seminar on Effective Field Theories, NIKHEF, Amsterdam (The Netherlands), December 15, 1998

[86] M. Mulders
'Direct measurement of the W boson mass in DELPHI'
NATO Advanced Study Institute (ASI) on Techniques and Concepts of High Energy Physics, Christiansted, St. Croix, US Virgin Islands (USA), June 18-29, 1998

[87] K. Peeters
'Geometry of supermembrane backgrounds'
National Seminar Theoretical HEF, NIKHEF, Amsterdam (The Netherlands), March 6 1998
X. Arbeitstreffen Theoretische Ansätze jenseits des Standardmodells, Bad Honnef (Germany), March 11, 1998

[88] B. Petersen
'The L3+cosmics experiment'
Xth Int. Symp. on Very High Energy Cosmic Ray Interaction (ISVHECRI), Gran Sasso (Italy), July 14, 1998

[89] T. van Rhee
'Meson formation in photon-photon collisions at LEP with the L3 detector'
Workshop on the structure of Mesons, Baryons and Nuclei (MESON 98), Cracow (Poland), May 30-June 2, 1998

[90] A.N. Schellekens
'Modular properties of WZW-models'
Technische Universiteit Eindhoven (TUE), Eindhoven (The Netherlands), April, 1998

[91] A.N. Schellekens
'Naar een waardig slot'
Oratie Katholieke Universiteit Nijmegen, Nijmegen (The Netherlands), September 16, 1998

[92] E.P. Sichtermann
'A NLO QCD analysis of the spin structure function g_1'
6th International Workshop on Deep Inelastic Scattering and QCD (DIS 98), Brussels (Belgium), April 4-8, 1998

[93] A. van Sighem
'High x, high Q^2 cross sections at HERA'
Lake Louise Winter Institute, Lake Louise (Canada), February 15-21, 1998

[94] J. da Silva Marcos
'Neutrino masses'
Bergische Universität, Wuppertal (Germany), October 28, 1998

[95] G. van der Steenhoven
'Het proton: waar draait 't om?'
Technische Universiteit Eindhoven (TUE), Eindhoven (The Netherlands), February 17, 1998

[96] G. van der Steenhoven
'Deep Inelastic Scattering on internal (nuclear) targets at HERMES'
Nuclear Physics Spring Meeting, Bochum (Germany), March 16-20, 1998

[97] G. van der Steenhoven
'Probing the spin-flavour structure of nucleons at HERMES'
Institut de Physique Nucleaire (IPN), Orsay (France), June 15, 1998

[98] G. van der Steenhoven
'Search for coherence effects in quasi-elastic process at J-Lab, HERMES, SLAC and FNAL'
Workshop on Exclusive Processes in QCD, ECT*, Trento (Italy), September 1, 1998

[99] G. van der Steenhoven
'Coherence-length effects observed at HERMES'
Kernfysisch Versneller Instituut (KVI), Groningen (The Netherlands), September 29, 1998

[100] J. Timmermans
'Electroweak results from LEP II'
Wuppertal (Germany), June 18, 1998

[101] C. Timmermans
'E821, A measurement of the muon anomalous magnetic moment at BNL'
XXIX Int. Conference on High Energy Physics (ICHEP 98), Vancouver (Canada), July 23-29, 1998

[102] W. Verkerke
'Measurement of the charm structure function of the proton from D production and semileptonic charm decay'*
ICHEP98, Vancouver (Canada), July 23-29, 1998

[103] J.A.M. Vermaseren
'Some problems in loop calculations'
Loops and Legs in gauge theories, Rheinsberg (Germany), April, 1998

[104] J.A.M. Vermaseren
'Techniques for loop integrals'
Karlsruhe (Germany), August, 1998

[105] J. Vossebeld
'Photon structure in $\gamma - p$ interactions'
6th International Workshop on Deep Inelastic Scattering and QCD (DIS 98), Brussels (Belgium), April 4-8, 1998

[106] A. Waldron
'The Quantum Mechanics of Matrix theory'
Bergische Universität Wuppertal, Wuppertal (Germany), March, 1998

[107] A. Waldron
'The d=11 SUGRA S Matrix from Matrix theory'
Institute for Theoretical Physics, SUNY, Stony Brook (USA), June, 1998

[108] A. Waldron
'Gravitation and antisymmetric tensor scattering in Matrix theory and d=11 SUGRA'
Institute for Theoretical Physics, Brown University (USA), October, 1998
Center for Theoretical Phyisics, MIT, Cambridge (USA), October, 1998
City College, CUNY, New York (USA), October, 1998

[109] A. Waldron
'D=11 SUGRA as the low energy effective action of Matrix theory: Three Form Scattering'
Spinoza Instituut, Utrecht (The Netherlands), November, 1998

1.4 Internal Talks

[1] January 14, 1998, Amsterdam
Prof. Tomokazu Fukuda (KEK)
'Physics with the Japan Hadron Facility (JHF)'

[2] January 16, 1998, Nijmegen
Prof. Tomokazu Fukuda (KEK)
'Physics with the Japan Hadron Facility (JFH)'

[3] January 23, 1998, Amsterdam
Prof. H. Meyer (Wuppertal)
'Precision Measurement of Newton's Constant'

[4] February 6, 1998, Amsterdam
M. Seymour (Rutherford Lab)
'Jets in Hadronic Collisions'

[5] February 12, 1998, Amsterdam
Oliver Melzer (NIKHEF/CHORUS)
'Search for neutrino induced diffractive D_s production and decay'

[6] February 13, 1998, Amsterdam
Ioanis Giomataris
'MICROMEGAS: a new very high-rate position sensitive detector'

[7] February 20, 1998, Amsterdam
Dr J. Pretz (University of Mainz)
'Spin Structure of the Nucleon from Semi-Inclusive Deep Inelastic Scattering'

[8] February 26, 1998, Amsterdam
Joop Konijn (NIKHEF)
'Current status of the Solar Neutrino Problem'

[9] March 5, 1998, Amsterdam
C. Weinheimer (Mainz University)
'Neutrino mass from tritium beta decay and other direct neutrino mass measurements'

[10] March 6, 1998, Amsterdam
National seminar theoretical HEF
Prof. W. Buchmuller (DESY)
'Cosmological Baryon Asymmetry and Neutrino Mixing'

[11] March 20, 1998, Amsterdam
Prof. H. Weerts (Michigan State University and D0 spokesperson)
'Current and future results from the Tevatron'

[12] March 24, 1998, Nijmegen
Dr. H. Drevermann (CERN)
'Event Viewing'

[13] March 26, 1998, Amsterdam
L. Moscoso (DAPNIA-CEA/SPP, Saclay) and P. Payre (CPPM, Marseille)
'Simulation and event reconstruction in a sub-oceanic neutrino detector: the case for ANTARES'

[14] March 27, 1998, Amsterdam
J.M. Laget (DAPNIA-Saclay)
'Hard and soft processes in the electro production of mesons'

[15] April 2, 1998, Amsterdam
J. Yu (Fermilab)
'Recent QCD and Electroweak Results from NuTeV/CCFR'

[16] April 3, 1998, Amsterdam
National seminar theoretical HEF
D. Kosower (Saclay)
'At the cutting edge of QCD'

[17] April 9, 1998, Amsterdam
Andreas Vogt (Wuerzburg)
'Deep Inelastic Scattering at Small x'

[18] April 9, 1998, Amsterdam
Nikolaos Kidonakis
'Resummation for Di-Jet Cross Sections'

[19] April 24, 1998, Amsterdam
L. Mankiewicz
'Gluon Polarization in the Nucleon'

[20] April 28, 1998, Amsterdam
H. Dreiner (Rutherford)
'Higgs $\rightarrow$ WW $\rightarrow$ $l\nu l\nu$ as a Higgs Discovery Mode in the SM and the MSSM at the LHC'

[21] May 8, 1998, Amsterdam
National seminar theoretical HEF
H.-P. Nilles (Bonn)
'M-theory: Unification and Supersymmetry Breakdown'

[22] May 12, 1998, Amsterdam
F. Wilczek (Princeton/Leiden)
'Quantum field theory'

[23] May 20, 1998, Amsterdam
Nicolo de Groot (SLAC)
'Charm Physics Results from SLD'

[24] May 25, 1998, Amsterdam
J. Golak (Jagellonian University/Krakow)
'Electromagnetic probes interacting with ^3He'

[25] May 27, 1998, Utrecht
E.W. Kittel (Katholieke Universiteit Nijmegen)
'Correlations and Fluctuations'

[26] May 28, 1998, Amsterdam
G. Veneziano (CERN)
'String Cosmology'

[27] May 28, 1998, Amsterdam
J. Uiterwijk (NIKHEF)
'Nuclear Track Emulsion: Technique of the past or of the future?'

[28] May 29, 1998, Amsterdam
P. de Jong (CERN)
'W production at LEP'

[29] June 5, 1998, Amsterdam
B. Holstein (Univ. of Massachusetts)
'Low Energy Tests of Chiral Invariance'

[30] June 8, 1998, Amsterdam
Frank Filthaut
'Physics with Fermion Pairs above the Z'

[31] June 8, 1998, Amsterdam
Els Koffeman (NIKHEF)
'ZEUS 2000'

[32] June 12, 1998, Amsterdam
Lucio Ludovici (CERN)
'Prospects for a high sensitivity search for $\nu_\mu \rightarrow \nu_e$ oscillation'

[33] June 19, 1998, Amsterdam
M. Harakeh (KVI)
'AGOR: A versatile facility for Nuclear Physics research at low and intermediate energies'

[34] June 22, 1998, Amsterdam
Massimiliano Ferro-Luzzi
'Nuclear and Nucleon Spin Structure Studied at AmPS'

[35] June 23, 1998, Amsterdam
Olaf Steinkamp (NIKHEF)
'B Physics at HERA - Status and Perspectives'

[36] June 26, 1998, Amsterdam
Antonio Ereditato (Naples University)
'Search for $\nu_\mu \rightarrow \nu_\tau$ oscillation with the long-baseline OPERA experiment at Gran Sasso'

[37] June 29, 1998, Amsterdam
E. Remiddi (Bologna)
'Master Differential Equations for Master Feynman Amplitudes'

[38] July 2, 1998, Amsterdam
Stan Bentvelsen
'Recent developments in QCD at LEP'

[39] July 2, 1998, Amsterdam
Nichol Brummer
'High Q^2 deep inelastic scattering at HERA'

[40] July 24, 1998, Amsterdam
Prof.R. Akhoury (Univ. of Michigan)
'An Operator Expansion in the Elastic Limit'

[41] August 21, 1998, Amsterdam
Prof. H.P. Paar (UC San Diego)
'Experimentele Resultaten aangaande de Gluebal Struktuur van de fJ(2220)'

[42] August 31, 1998, Amsterdam
Nigel Hessey (CERN)
'The Precision Drift Chambers of the ATLAS Muon Spectrometer'

[43] August 31, 1998, Amsterdam
W. Burger (CERN)
'The AMS Experiment'

[44] October 2, 1998, Amsterdam
K. Braune (CERN)
'Exotic physics with the Crystall Barrel at LEAR'

[45] October 6, 1998, Amsterdam
H. Morita (Perugia, Italy)
'Realistic calculations of nuclear transparency and nucleon momentum distributions in ^4He'

[46] October 8, 1998, Nijmegen
L. Drndarski
'Minimal spanning tree approach to W-pair selection'

[47] October 9, 1998, Amsterdam
Marnix van der Wiel (TUE)
'The all-plasma table top X-ray free electron laser'

[48] October 12, 1998, Amsterdam
Open Presentation SAC; R. van Dantzig
'NOW98 and future neutrino physics at NIKHEF'

[49] October 15, 1998, Nijmegen
D. Zer-Zion (CERN)
'Bose-Einstein condensation in OPAL'

[50] October 16, 1998,Amsterdam
National seminar theoretical HEF
Daniel Zer-zion (CERN)
'Detection of Gravitational Waves with Storage Rings'

[51] October 22, 1998, Nijmegen
W.C. van Hoek
'Excited beauty in L3'

[52] October 23, 1998, Amsterdam
I. Hofmann (GSI/Darmstadt)
'Prospects of Inertial Fusion'

[53] October 28, 1998, Amsterdam
V. Smirnov (Moscow State University)
'Asymptotic expansions of Feynman integrals in limits of large momenta and masses and near threshold'

[54] October 29, 1998, Nijmegen
P. Draggiotis
'On the computation of multiparticle amplitudes'

[55] November 5, 1998, Nijmegen
S. Duensing
'Measurement of Triple Gauge Boson Couplings with W-pair events at LEP II'

[56] November 6, 1998, Amsterdam
Prof.A.H.M. Verkooijen (TU Delft)
'Research at IRI and the European Spallation Source'

[57] November 10, 1998, Amsterdam
C. Spiering (DESY-Zeuthen)
'Status of Amanda and Baikal'

[58] November 11, 1998, Amsterdam
Dr. G.J. Bobbink (NIKHEF/CERN)
'Highlights from ICHEP 98- XXIX International Conference in High Energy Physics in Vancouver'

[59] November 13, 1998, Amsterdam
Dr. E. Aschenauer (DESY)
'The HERMES Dual Radiator RICH Which particle is which, to know build/use a RICH'

[60] November 19, 1998, Nijmegen
R. Hakobyan
'Three-dimensional Bose-Einstein analysis and the space-time distribution of the pion source'

[61] November 25, 1998, Amsterdam
Special Seminars on the Prospects of LEP

[62] November 26, 1998, Nijmegen
T. Csörgo
'Hydrodynamics for particle correlations and spectra in high energy physics'

[63] November 27, 1998, Amsterdam
Dr. F. de Boer (NIKHEF)
'Search for a short-lived neutral boson with a mass around 9 MeV/c^2'

[64] December 3, 1998, Nijmegen
A. van Hameren
'Quantum field theory for discrepancies'

[65] December 4, 1998, Amsterdam
National seminar theoretical HEF
N. Manton (Cambridge)
'Moduli Space Dynamics of Vortices'

[66] December 9, 1998, Nijmegen
K. Eggert (CERN)
'Cosmic Muons at LEP'

[67] December 10, 1998, Nijmegen
J. Valks
'Het principe van Mach'

1.5 NIKHEF Annual Scientific Meeting

December 17-18, 1998, Amsterdam

[1] D. Read
LEP Overview

[2] M. Mulders
W-pair production in DELPHI

[3] T. van Rhee
Charm production in two-photon collissions in L3

[4] H. de Vries
AmPS Overview

[5] I. Passchier
The charge form factor of the neutron

[6] D. Groep
Electron induced two-proton knockout from ^{3}He

[7] P. Kooijman
ZEUS overview (+HERA status)

[8] A. van Sighem
Measurement of deep-inelastic ep scattering at very high Q^2

[9] G. van der Steenhoven
HERMES Overview

[10] B. Schellekens
Developments in string theory

[11] S.O. Moch
Soft gluon resummation for heavy quark production

[12] E. Heijne
The NIKHEF vertex project

[13] A.P. Kaan
Mechanical engineering

[14] E. Heine
Electronic engineering

[15] W. Heubers
Computer technology

[16] R. van Dantzig
Neutrino physics: CHORUS, NOW and prospects

[17] R. Oldeman
Neutrino structure functions, CHORUS '98 run

[18] A. Buijs
Introduction Heavy-Ion physics

[19] F. Geurts
Meson production in hot matter

[20] P. van de Ven
The NA57 experiment

[21] F. Linde
ATLAS overview

[22] B. van Eijk
Forward silicon tracker

[23] S. de Jong
D0 experiment

[24] W. Ruckstuhl
B-physics overview

[25] O. Steinkamp
Status of the Outer Trackers for HERA-B and LHCb

[26] N. Zaitsev
Results of the LHCb silicon test beam experiment

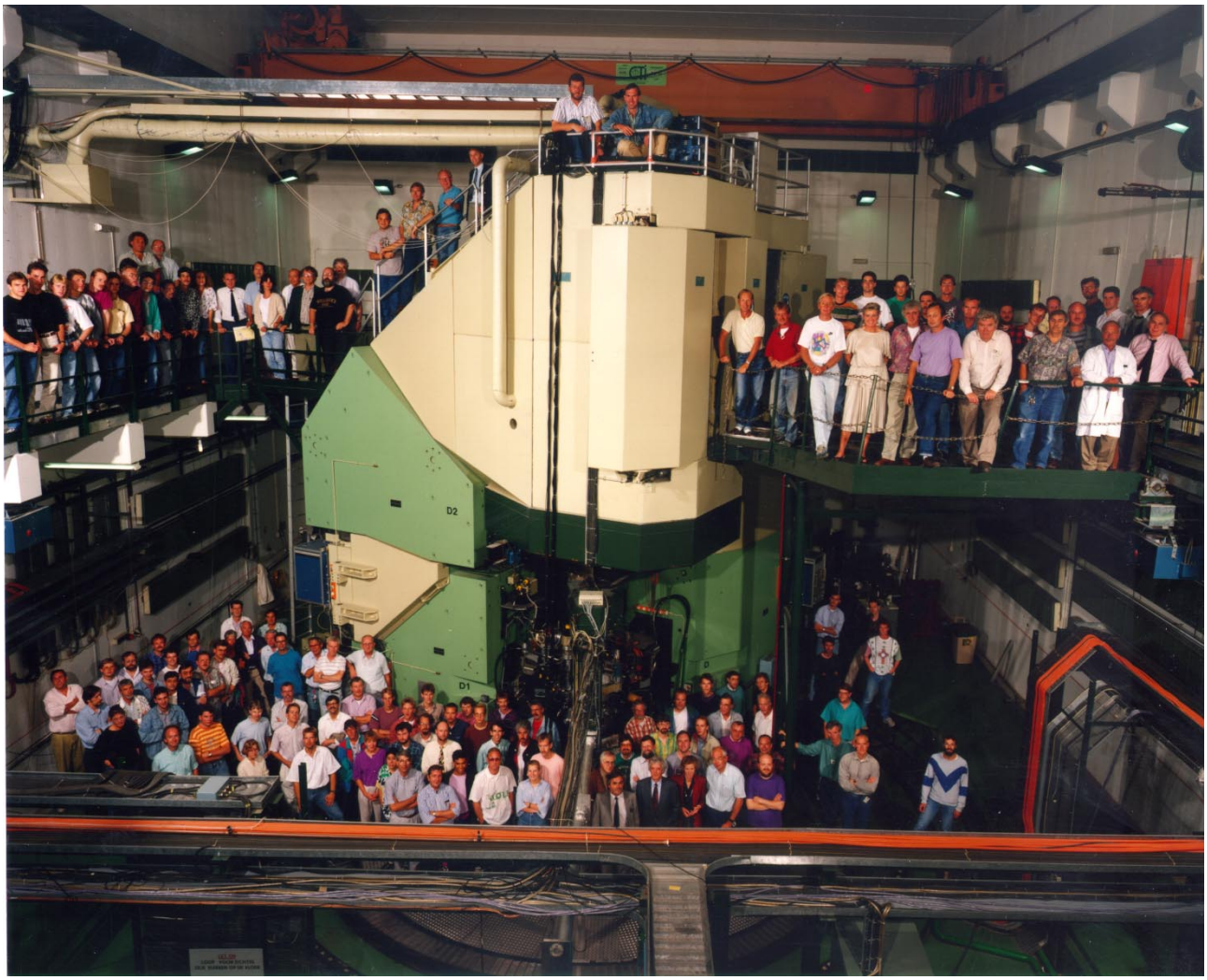

A few of those who made MEA/AmPS possible (photo: NIKHEF)

G Resources and Personnel

1 Resources

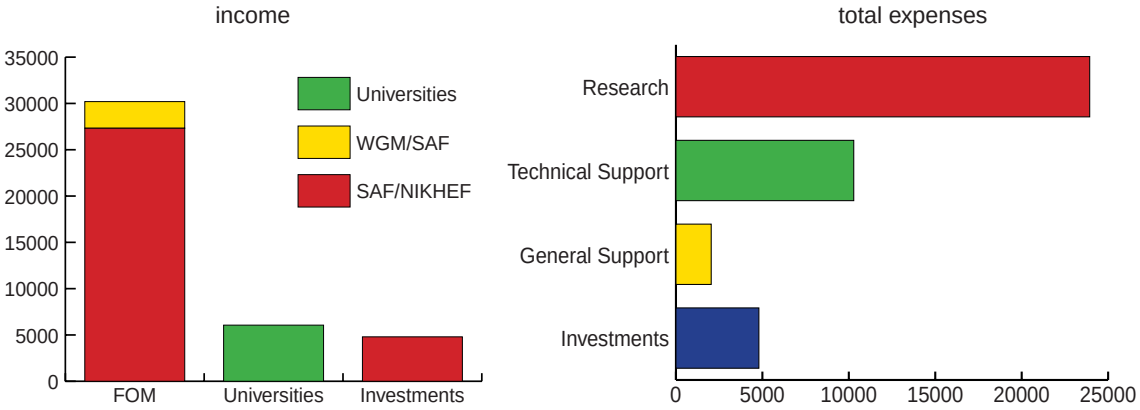

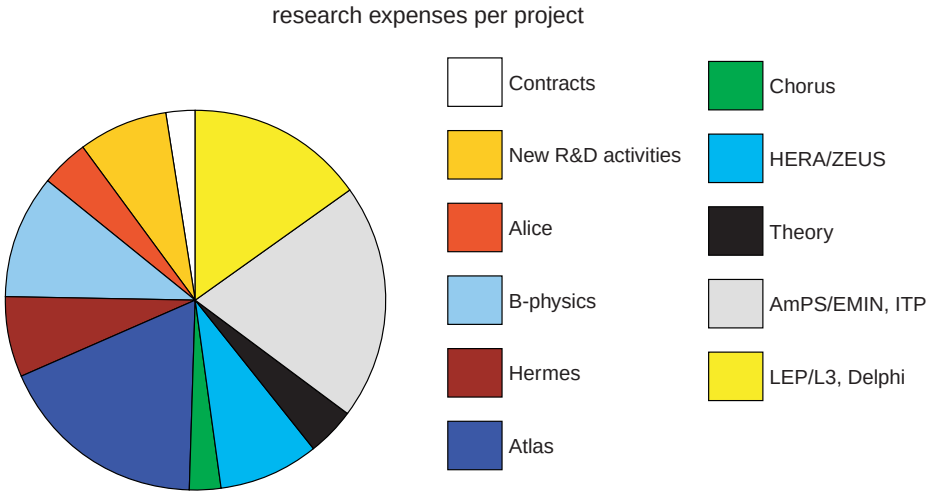

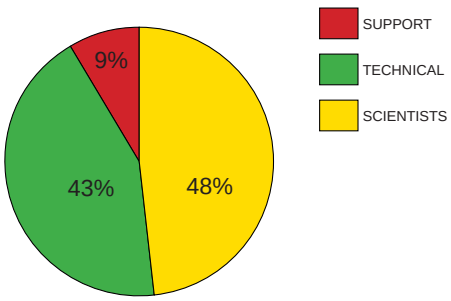

personel NIKHEF: 280

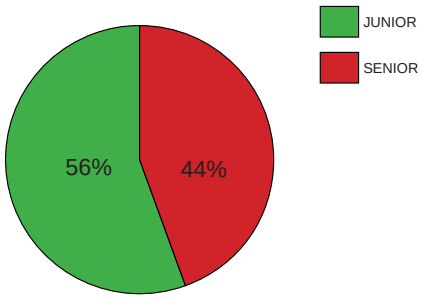

scientists

2 Membership of Councils and Committees during 1998

NIKHEF Board
J.K.M. Gevers (UvA, chairman), †August 5th, 1998
K.H. Chang (FOM)
A.R. de Monchy (FOM)
G.W. Noomen (VU)
Th.H.J. Stoelinga (KUN)
J.G.F. Veldhuis (UU)
H.M. van Pinxteren (secretary, FOM)

Scientific Advisory Committee NIKHEF
P. Darriulat (CERN, Chairman)
B. Frois (CEA Saclay)
D. von Harrach (Univ. Mainz)
B. Mecking (Jefferson Lab.)
I. Sick (Univ. Basel)
P. Söding (DESY)

NIKHEF Works Council
J.B. van der Laan (chairman)
R.G.K. Hart (1st secretary)
J.H.G. Dokter (2nd secretary)
H. Boer Rookhuizen
R.P. de Boer
P.H.A. van Dam
J.J. Hogenbirk
G.J.L. Nooren
P.J.M. Werneke
L.W. Wiggers

FOM Board
J.J. Engelen

Fund for Scientific Research Flanders, Belgium
G. van Middelkoop

Schwerpunktprogramm, Advisory Commission DFG, Bonn
J.H. Koch

SPC-CERN
J.J. Engelen
K.J.F. Gaemers

LHCC-CERN
J.J. Engelen (chairman as from July 1998)

SPSC-CERN
B. Koene

Extended Scientific Council, DESY
K.J.F. Gaemers

ECFA
J.J. Engelen, K.J.F. Gaemers, R. Kamermans, E.W. Kittel, G. van Middelkoop (also in Restricted ECFA)

NuPECC
G. van Middelkoop

HEP Board EPS
J.J. Engelen

EPAC
P.W. van Amersfoort
G. Luijckx

Scientific Advisory Committee, Physique Nucleaire, Orsay
P.K.A. de Witt Huberts

Scientific Advisory Committee, DFG 'Hadronen Physik'
P.K.A. de Witt Huberts

Other committees
ASP Board J. Langelaar
ASTRON Board W. Hoogland
DS Board J. Langelaar
DS Liaison J. Geerinck
EPCS W. Heubers
ESRF G. Luijckx
HEP CCC W. Hoogland
HTASK K. Bos
IRI J.H. Koch
IUPAP, C11 committee W. Hoogland
OECD Megascience Forum Working Groups W. Hoogland, G. van Middelkoop
SURF W. Hoogland
RIPE R. Blokzijl
SCTF W. van Amersfoort
WCW Board J. Langelaar

3 Personnel as of December 31, 1998

1. Experimental Physicists:

Agasi, Drs. E.E.	GST	DELPHI
Amersfoort, Dr.Ir. P.W. van	FOM	TF/INSTR
Apeldoorn, Dr. G.W. van	UVA	DELPHI
Bakel, Drs. N.A. van	FOM	B–Phys.
Baldew, Drs. S.V.	UVA	L-3
Batenburg, Drs. M.F. van	FOM	AmPS-Phys.
Bauer, Dr. T.S.	FOM-UU	AmPS-Phys.
Blok, Dr. H.P.	VU	AmPS-Phys.
Blom, Drs. H.M.	FOM	DELPHI
Blouw, Dr. J.	GST	HERMES
Bobbink, Dr. G.J.	FOM	L-3
Boer, Dr. F.W.N. de	GST	ALGEMEEN
Boersma, Drs. D.J.	FOM	AmPS-Phys.
Bokel, Drs. C.H.	FOM	ZEUS
Bos, Dr. K.	FOM	ATLAS
Botje, Dr. M.A.J.	FOM	ZEUS
Botto, Drs. T.	GST	AmPS-Phys.
Boudinov, Drs. E.	FOM	DELPHI
Brand, Prof.Dr. J.F.J. van den	FOM	AmPS-Phys.
Bruinsma, Drs. M.	FOM	B–Phys.
Brümmer, Dr. N.C.	FOM	ZEUS
Buis, Drs. E.J.	FOM	ATLAS
Buijs, Prof.Dr. A.	UU	ALICE
Bulten, Dr. H.J.	FOM-VU	HERMES
Buuren, Drs. L.D. van	FOM	AmPS-Phys.
Chekanov, Drs. S.	KUN	L-3
Colijn, Drs. A.P.	FOM-BR	L-3
Crijns, Dipl.Phys.F.J.G.H.	FOM-KUN	ATLAS
Dalen, Drs. J. van	FOM-KUN	L-3
Dam, Dr. P.H.A. van	UVA	DELPHI
Dantzig, Dr. R. van	FOM	CHORUS
Daum, Prof.Dr. C.	GST	ATLAS
Diddens, Prof.Dr. A.N.	GST	DELPHI
Dierendonck, Drs. D.N. van	FOM	L-3
Duensing, Drs. Mw. S.	KUN	ATLAS
Duinker, Prof.Dr. P.	FOM	L-3
Eijk, Prof.Dr. B. van	FOM	ATLAS
Eijk, Ir. R.M. van der	FOM	B–Phys.
Eldik, Drs. J.E. van	GST	DELPHI
Engelen, Prof.Dr. J.J.	UVA	ZEUS
Erné, Prof.Dr.Ir F.C.	GST	L-3
Ferro-Luzzi, Dr. M.M.E.	FOM-VU	AmPS-Phys.
Fiedler, Dr. K.	GST	HERMES
Graaf, Dr.Ir. H. van der	FOM	TF/INSTR
Gracia Abril, Dr. G.	FOM	B–Phys.
Groep, Drs. D.L.	FOM	AmPS-Phys.
Gulik, Drs. R.C.W.	UL	L-3
Hartjes, Dr. F.G.	FOM	TF/INSTR
Heesbeen, Drs. D.	FOM	HERMES
Heijne, Dr. H.M.	GST	TF/INSTR
Hendriks, Drs. P.J.	FOM	ATLAS
Hesselink, Dr. W.H.A.	VU	AmPS-Phys.
Hierck, Drs. R.H.	FOM-VU	B–Phys.
Hoek, Drs. Mw. M.	GST	L-3
Hoffmann-Rothe, Dr. P.	FOM-HCM	HERMES
Hoogland, Prof.Dr. W.	UVA	B–Phys.
Hulsbergen, Drs. W.D.	FOM	B–Phys.
Hunen, Ir. J.J. van	FOM	HERMES
Ihssen, Dr. H	GST	HERMES
Jans, Dr. E.	FOM	AmPS-Phys.
Jong, Dr. M. de	FOM	CHORUS
Jong, Prof.Dr. S.J.	KUN	ATLAS
Kamermans, Prof.Dr. R.	FOM-UU	WA93/98
Ketel, Dr. T.J.	FOM-VU	SMC
Kittel, Prof.Dr. E.W.	KUN	L-3
Kjaer, Dr. N.J.	FOM	DELPHI
Klok, Drs. P.F.	FOM-KUN	ATLAS
Kluit, Dr. P.M.	FOM	DELPHI
Koene, Dr. B.K.S.	FOM	DELPHI
Koffeman, Dr.Ir. Mw. E.N.	UVA	ZEUS
Kolster, Dr. H.	FOM	HERMES
Konijn, Dr.Ir. J.	GST	CHORUS
König, Dr. A.C.	KUN	ATLAS
Kooijman, Dr. P.M.	UVA	ZEUS
Kroes, Ir. F.B.	FOM	TF/INSTR
Kuijer, Dr. P.G.	FOM	WA93/98
Kuur, Dr.Ir. J. van der	FOM	B–Phys
Laan, Dr. J.B. van der	FOM	TF/INSTR
Lapikás, Dr. L.	FOM	AmPS-Phys.
Lavrijsen, Drs. W.T.L.P.	FOM-KUN	ATLAS
Linde, Prof.Dr. F.L.	UVA	ATLAS
Luijckx, Ir. G.	FOM	TF/INSTR
Lutterot, Drs. M.	FOM	ALICE
Maas, Dr. R.	FOM	TF/INSTR
Mangeol, Drs. D	FOM	L-3
Massaro, Dr. G.G.G.	FOM	L-3
Melzer, Dipl.Phys. O.	FOM	CHORUS
Merk, Dr. M.H.M.	UU	DELPHI
Metzger, Dr. W.J.	KUN	L-3
Mevius, Drs. Mw. M.	UU	B–Phys.
Middelkoop, Prof.Dr. G. van	VU	DIR
Militsyn, Dr. B.L	FOM	TF/INSTR
Mill, Drs. A. van	KUN	L-3
Muijs, Drs. Mw. A.J.M.	FOM	L-3
Mulders, Ir. M.P.	FOM-BR	DELPHI
Nagorny, Dr. S.I.	FOM	AmPS-Phys.
Noomen, Ir. J.G.	FOM	TF/INSTR
Nooren, Dr.Ir. G.J.L.	FOM	TF/INSTR
Oberski, Dr. J.E.J.	FOM	SMC
Oldeman, Ir. R.G.C.	FOM	CHORUS
Passchier, Drs. I.	FOM	AmPS-Phys.
Peeters, Ir. S.J.M.	FOM	ATLAS
Peters, Drs. O.	UVA	ATLAS
Petersen, Drs. B.	KUN	L-3
Pijll Drs. E.C. van der	FOM-UU	WA93/98
Poel, Drs. C.A.F.J. van der	GST	CHORUS
Pols, Dr. C.L.A.	KUN	ATLAS
Poolman, Dr. H.R.	FOM-VU	AmPS-Phys.
Reid, Dr. D.W.	FOM	DELPHI
Rhee, Drs. Mw. T. van	FOM	L-3
Ruckstuhl, Dr. W.	FOM	DELPHI
San Segundo Bello, Drs. D.	FOM-HCM	TF/INSTR

Sanders, Drs. M.	KUN	L-3
Schillings, Drs. E.	FOM-UU	NA57
Schotanus, Dr. D. J.	KUN	L-3
Sichtermann, Drs. E.P.	GST	SMC
Sighem, Drs. A.I. van	FOM	ZEUS
Simani Drs. Mw. M.C.	VU	HERMES
Starink, Drs. R.	VU	AmPS-Phys.
Steenbakkers, Drs. M.F.M.	FOM-VU	AmPS-Phys.
Steenhoven, Dr. G. van der	FOM	HERMES
Steijger, Dr. J.J.M.	FOM	TF/INSTR
Steinkamp, Dr. O.	FOM	B–Phys.
Tiecke, Dr. H.G.J.M.	FOM	ZEUS
Timmermans, Dr. J.J.M.	FOM	DELPHI
Toet, Dr. D.Z.	GST	DELPHI
Tuning, Drs. N.	UVA	ZEUS
Uiterwijk, Ir. J.W.E.	FOM	CHORUS
Veenhof, Dr. R.J.	FOM	ATLAS
Velthuis, Ir. J.J.	FOM	ZEUS
Ven, Drs. P.A.G. van de	FOM-UU	WA93/98
Vermeulen, Dr.Ir. J.C.	UVA	ATLAS
Visschers, Dr. J.L.	FOM	TF/INSTR
Visser, Drs. E.	KUN	ATLAS
Visser, Drs. J.	FOM	HERMES
Volmer, Dipl.Phys. J.	FOM	AmPS-Phys.
Vossebeld, Drs. J.H.	FOM	ZEUS
Vries, Dr. H. de	FOM	AmPS-Phys.
Vulpen, Drs. I.B. van	FOM	DELPHI
Wiggers, Dr. L.W.	FOM	ZEUS
Wilkens, Drs. H.	FOM-KUN	L-3
Witt Huberts, Prof.Dr. P.K.A.	FOM	HERMES
Wijngaarden, Drs. D.A.	KUN	ATLAS
Wolf, Dr. Mw. E. de	UVA	ZEUS
Woudstra, Ir. M.J.	FOM	ATLAS
Zaitsev, Drs. N.U.	UVA	B–Phys.

2. Theoretical Physicist:

Boglione, Drs. Mw. M.	FOM-HCM
Eynck, Dipl.Phys. T.O.	FOM
Gaemers, Prof.Dr. K.J.F.	UVA
Gato-Rivera, Dr. Mw. B.	GST
Groot Nibbelink, Drs. S.	FOM
Henneman, Drs. A.	VU
Holten, Dr. J.W. van	FOM
Huiszoon, Drs. L.R.	FOM
Kleiss, Prof.Dr. R.H.P.	KUN
Koch, Prof.Dr. J.H.	FOM
Laenen, Dr. E.	FOM
Marques de Sousa, Drs. N.M.	GST
Moch, Dr. S.O.	FOM
Mulders, Prof.Dr. P.J.G.	VU
Pascalutsa, Dr. V.V.	FOM
Schellekens, Prof.Dr. A.N.J.J.	FOM
Silva Marcos, Dr. J.T. da	GST
Vermaseren, Dr. J.A.M.	FOM
Waldron, Dr. A.K.	FOM
Weinzierl, Dr. S.D.	FOM
Wit, Prof.Dr. B.Q.P.J. de	UU
Wolters, Dr. G.F.	FOM

3. Computer Technology Group:

Blokzijl, Dr. R.	FOM
Boontje, Ing. R.	FOM
Boterenbrood, Ir. H.	FOM
Damen, Ing. A.C.M.	FOM
Hart, Ing. R.G.K.	FOM
Heubers, Ing. W.P.J.	FOM
Huyser, K.	FOM
Kruszynska, Drs. Mw. M.N.	FOM
Kuipers, Drs. P.	FOM
Leeuwen, Drs. W.M. van	FOM
Oudolf, J.D.	QUADO
Schimmel, Ing. A.	FOM
Tierie, Mw. J.J.E.	FOM
Wassenaar, Drs. E.	FOM
Wijk, R.F. van	FOM

4. Electronics Technology Group:

Akker, T.G.M. van den	FOM
Berkien, A.W.M.	FOM
Beuzekom, Ing. M.G.van	FOM
Boer, J. de	FOM
Boerkamp, A.L.J.	FOM
Born, E.A. van den	FOM
Es, J.T. van	FOM
Evers, G.J.	FOM
Gotink, G.W.	FOM
Groen, P.J.M. de	FOM
Groenstege, Ing. H.L.	FOM
Harmsen, C.J.	FOM
Heine, Ing. E.	FOM
Heutenik, B.	FOM
Hogenbirk, Ing. J.J.	FOM
Jansen, L.W.A.	FOM
Jansweijer, Ing. P.P.M.	FOM
Kieft, Ing. G.N.M.	FOM
Kluit, Ing. R.	FOM
Kok, Ing. E.	FOM
Koopstra, J.	UVA
Kruijer, A.H.	FOM
Kuijt, Ing. J.J.	FOM
Peek, Ing. H.Z.	FOM
Reen, A.T.H. van	FOM
Rewiersma, Ing. P.A.M.	FOM
Schipper, Ing. J.D.	FOM
Sluijk, Ing. T.G.B.W.	FOM
Stolte, J.	FOM
Timmer, P.F.	FOM
Trigt, J.H. van	FOM
Verkooijen, Ing. J.C.	FOM
Wieten, P.	FOM
Zwart, Ing. A.N.M.	FOM
Zwart, F. de	FOM

5. Mechanical Technology Group:

Arink, R.P.J.	FOM
Band, H.A.	FOM
Beumer, H.	FOM

Boer, R.P. de	FOM
Boomgaard-Hilferink, Mw. J.G.	FOM
Boucher, A.	FOM
Bron, M.	FOM
Brouwer, G.R.	FOM
Buis, R.	FOM
Buskens, J.P.M.	UVA
Buskop, Ir. J.J.F.	FOM
Ceelie, L.	UVA
Dernison, Ing. P.J.H.	FOM
Doets, M.	FOM
Groot, J.I. de	FOM
Haster, Mw. S.M.A.	FOM
Homma, J.	FOM
Jaspers, M.J.F.	UVA
Kaan, Ir. A.P.	FOM
Kan, Ing. R.P.	FOM
Kok, J.W.	FOM
Korporaal, A.	FOM
Kraan, Ing. M.J.	FOM
Kuilman, W.C.	FOM
Langedijk, J.S.	FOM
Lassing, P.	FOM
Lefévere, Y.	FOM
Leguyt, R.	FOM
Mul, F.A.	FOM-VU
Munneke, Ing. B.	FOM
Petten, O.R. van	FOM
Postma, Ing. O.	FOM
Rietmeijer, A.A.	FOM
Rövekamp, J.C.D.F.	UVA
Schuijlenburg, Ing. H.W.A.	FOM
Sijpheer, Ing. N.C.S.	FOM
Thobe, P.H.	FOM
Veen, J. van	FOM
Verlaat, Ing. B.A.	FOM
Werneke, Ing. P.J.M.	FOM
Zegers, Ing. A.J.M.	FOM

6. AmPS Management Project:

Heuvel, Mw. G.A. van den	FOM
Kuijer, L.H.	FOM
Steman, W.A.	FOM
Stoffelen, A.C.	FOM

7. AmPS Optics Project:

Boer Rookhuizen, H.	FOM

8. Management and Administration

Backerra, Drs. Mw. F.E.H.M.	FOM
Bakker, C.N.M.	FOM
Berg, A. van den	FOM
Bruinsma, Ir. P.J.T.	FOM
Buitenhuis, W.E.J.	FOM
Bulten, F.	FOM
Dokter, J.H.G.	FOM
Echtelt, Ing. H.J.B. van	FOM
Egdom, T. van	FOM
Geerinck, Ir. J.	FOM
Gerritsen-Visser, Mw. J.	FOM
Greven-v.Beusekom, Mw. E.C.L.	FOM
Heyselaar van 't Hof, Mw. M.J	FOM
Kerkhoff, Mw. E.H.M. van	FOM
Kesgin-Boonstra, Drs. Mw. M.J.	FOM
Kolkman, J.	FOM
Kranenburg, Drs. Mw. M.E.L.	FOM
Kwakkel, Ir. E.	FOM
La Rooij, Mw. T.J.	QUADO
Langelaar, Dr. J.	UVA
Langenhorst, A.	FOM
Lemaire-Vonk, Mw. M.C.	FOM
Louwrier, Dr. P.W.F.	FOM
Mors, A.G.S.	UVA
Mur, Drs. Mw. L.	FOM
Ploeg, F.	FOM
Post, Mw. E.C.	FOM
Post, Dr. J.C.	GST
Schäfer-v.d.Weijden, Mw. W.	FOM
Schenkelaars, Mw. Drs. E.M.	FOM
Schoemaker - Weltevreden, Mw. S.	FOM
Spelt, Ing. J.B.	FOM
Visser, J.	FOM
Vos, R.A.	UITZEND
Vries, W. de	FOM
Wielenga, Mw. M.	FOM
Zelst, W. van	FOM

Apprentices in 1998:

Addens, D.G.	MT
Babaei Gaven, K.	MT
Bakel, N.A. van	AmPS-Phys
Balm, P.	ATLAS
Bar, E.N.	ET
Bommel, H. van	ET
Bouwmeester, N.	ET
Broers, G.W.	MT
Coskan, H.	MT
Eijk, Q. van	ET
El Azhari, M.	ET
Es, Mw. M. van	ZEUS
Geelhoed, B.	HERMES
Geest, B.G.H. van der	ET
Geest, J.W. van der	MT
Grijpink, S.J.L.A.	ZEUS
Hagen, C. van der	MT
Heijboer, A.J.	THEORIE
Helm, S.	MT
Hierck, R.H.	B–Phys
Hover, E.P.	MT
Hulsbergen D.G.	MT
Kaaij, J.S.	MT
Koelewijn, D.	CT
Kooij, T.A.P. van der	MT
Köper, D.	ATLAS
Langelaar, D.G.	MT
Leeuwen, S.A.	MT
Pannekoek, J.B.	MT

Peters, O.	ATLAS
Salzmann, I.S.	ATLAS
Schagen, S.E.S.	ZEUS
Scholte, R.	ATLAS
Terbonssen, Mw. H.H.V.	MT
Tjon A Meeuw, R.C.	MT
Trapman, J.P.	TF/INSTR
Veld, N.F.	MT
Velthuis, J.J.	ATLAS
Wijngaard, J.H.J.	ET
Wijngaarden, D.A.	B–Phys

They left us in 1998:

Alarcon, Dr. R.	AmPS-Phys
Bakker, M.	ABG
Berkulo, S.J.M.	FA
Boer, Dr. D.	THEORIE
Bordes, Mw. Dr. G.	THEORIE
Boreskov, Dr. K.	THEORIE
Bouwhuis, Dr. M.	AmPS-Phys
Cuhadar, Dr. T.	SMC
Daal, H.J.M.	ABG
Dankers, Dr. Ir. R.J.	ATLAS
De Natris, Mw. Y.S.	ABG
Erné, Prof.Dr.Ir F.C.	L-3
Fiedler, Dr. K.	HERMES
Genee, J.	THD
Gracia Abril, Dr. G.	B–Phys.
Haakman, Dr. L.P.A.	THEORIE
Heide, Ing. G. van der	MT
Heimberg, Dr. P.A.	AmPS-Phys
Highinbotham, Drs. D.W.	AmPS-Phys
Holthuizen, Dr. D.J.	DELPHI
Jager, S.W. de	ABG
Kappert, Ing. E.	ET
Kapteyn, Mw. J.C.	VD
Klimine, P.	TF/INSTR
Kolstein, Dr. M.	HERMES
Koop, Dr. I.	TF/INST
Lange, Dr. D.J.J. de	AmPS-Phys
Langelaar, Dr. J.	DIR
Langerveld-Tuyp, Mw. A.M.M.	FA
Larin, Dr. S.	THEORIE
Leeuwen, Ing. E.P. van	MT
Leurs, Ing. G.A.J.	CT
Militsyn, Dr. B.L.	TF/INSTR
Munneke, Mw. C.C.	INKOOP
Nieuwenhuizen, Drs. M.	DELPHI
Nikolenko, Dr. D.	AmPS-Phys
Noteboom, C.W.J.	MT
Oskam-Tamboezer, Mw. Mr. M.	DIR/ADM
Onderwater, Dr. C.J.G.	AmPS-Phys
Paulich, Dr. A.G.	TF/INSTR
Peeters, Dr. Ir. K.	THEORIE
Peperkamp, Ing. J.A.M.	VD
Plefka, Dr. J.C.	THEORIE
Pols, G.J.	MT
Poolman, Dr. H.R.	AmPS-Phys
Prins, E.	MT
Putte, Dr. Ir. M.J.J.	AmPS-Phys
Rachek, dr. I.	AmPS-Phys
Reichold, Dr. A.J.H.	ATLAS
Rodriques, Drs. J.M.	THEORIE
Rossum, Dr. W. van	L-3
Schäfer, J.S.E.	CT
Schmitz, H.	ABG
Sichtermann, Drs. E.P.	SMC
Siriphant, A.J.	MT
Six III, Drs. E.	AmPS-Phys
Spallici, Dr. A.	THEORIE
Stulens, Mw. Drs. V.L.	DIR/ADM
Szczerba, Dr. D.	AmPS-Phys
Tabaux, Drs. P.	CT
Tummers, B.J.	CT
Uithuisje, D.	MT
Veenhof, Dr. R.J.	ATLAS
Verkerke, Dr. W.	ZEUS
Wang, X.W.	L-3
Xu, Dr. Y.	L-3
Yang, Dr. X.	L-3